C–H FUNCTIONALIZATION OF HETEROCYCLIC MOIETIES USING TRANSITION METAL CATALYST FOR EVALUATION OF ANTICANCER ACTIVITY

A thesis submitted for the award of the degree of

Doctor of Philosophy

Submitted by:

Dinesh Singla

(**Regn. No. 901709004**)

Under the Supervision of

Dr. Kamaldeep Paul

Professor

SCHOOL OF CHEMISTRY AND BIOCHEMISTRY

THAPAR INSTITUTE OF ENGINEERING AND TECHNOLOGY

PATIALA-147004

PUNJAB

January 2023

THAPAR INSTITUTE
OF ENGINEERING & TECHNOLOGY
(Deemed to be University)

Thapar Institute of Engineering and Technology
Patiala

School of Chemistry and Biochemistry

STATEMENT

I hereby declare that matter embodied in this thesis is the result of investigations carried out by me in the School of Chemistry and Biochemistry, Thapar Institute of Engineering and Technology, Patiala, India, under the supervision of Prof. Kamaldeep Paul. This thesis has been submitted by me to the School of Chemistry and Biochemistry, TIET, for the award of the degree of Doctor of Philosophy

In keeping with the general practice of reporting scientific observations, due acknowledgments have been made wherever the work described is based on the findings of other investigations. I further declare that this work has not been submitted anywhere else for any degree, diploma, associateship, etc., of any Institute or University to the best of my knowledge.

Dinesh Singla
Reg. No. 901709004
School of Chemistry and Biochemistry,
Thapar Institute of Engineering and Technology
Patiala-147004, Punjab, India

Dr. Kamaldeep Paul
Professor
School of Chemistry and Biochemistry,
Thapar Institute of Engineering and Technology,
Patiala-147004, Punjab, India

THAPAR INSTITUTE
OF ENGINEERING & TECHNOLOGY
(Deemed to be University)

Thapar Institute of Engineering and Technology
Patiala

School of Chemistry and Biochemistry

CERTIFICATE

It is certified that the work contained in the thesis entitled "**C–H Functionalization of Heterocyclic Moieties Using Transition Metal Catalyst for Evaluation of Anticancer Activity** " by Dinesh Singla in fulfillment of the degree of Doctor of Philosophy is an authentic record of the candidate's own independent and original research work carried out under my supervision in the School of Chemistry and Biochemistry, Thapar Institute of Engineering and Technology, Patiala, Punjab, India. The material embodied in this thesis has not been submitted in part or full to any other University or Institute for the award of any degree.

Dr. Kamaldeep Paul
Professor
School of Chemistry and Biochemistry,
Thapar Institute of Engineering and Technology
Patiala-147004, Punjab, India

11/5/23

Prof. Satnam Singh
(Head, SCBC)
School of Chemistry and Biochemistry,
Thapar Institute of Engineering and Technology
Patiala-147004, Punjab, India

ii

DEDICATED TO MY BELOVED

FAMILY

Acknowledgment

Completing this thesis would not have been possible without the support and encouragement of several notable people. Hence, I would like to take this opportunity to show my gratitude to those who have assisted me in completing my thesis.

First, I would like to extend my appreciation to my respected supervisor Prof. Kamaldeep Paul
allowing me to do a Ph.D. with his research group. This study would not have been feasible without his inspired leadership, academic support, encouragement, and determination to tackle new scientific challenges. He also formed effective collaborations, allowing me to gain experience with various research issues. I appreciate his assistance in the composition of this dissertation and previous research pieces and for helping me improve my scientific communication and approach. I express my gratitude to the Director, Thapar Institute of Engineering & Technology, Patiala (TIET), Dr. Rafat Siddique, Dean of Research and Development Centre (DRDC), Dr. N. Tejo Prakash, Associate Dean RDC, Prof. Satnam Singh (Head, SCBC) for all facilities which have been immensely helpful in completing my work.

I am also thankful to all my respected teachers at the School of Chemistry and Biochemistry (SCBC) and my doctoral committee members, Prof. Satnam Singh, Dr. Vikas Tyagi and Dr. Manoj Baranwal, who were involved in the validation survey for this research project. Their valuable suggestions and endless encouragement help me to represent my research work in a better way. My sincere thanks also go to Mr. Mayank Sharma, the office staff, Mr. Chander Singh Thakur, Hemant Sharma, Chandar Shekher, and Vishwanath Dass Thakur technical staff for their cooperation, support, and help.

During my Ph.D. studies, I had the opportunity to work in close collaborations with other research groups. I sincerely thank Dr. Vijay Luxami for initiating collaboration and inspiring me to learn spectroscopy studies. I thank her group members, especially Dr. Gulshan Kumar and Aastha Palta, for their support and discussion. Time flew by in the company of good friends, and therefore, a special thanks to Iqubal Singh, Sudesh Rani, Richa Bansal, Ruhi Mehta, Gulshan Kumar, Aastha Palta, Rekha Thakur, Saurabh Gupta, Rohini Gupta, Palak Sharma, Shifali, Geetika Rani, Nandan Sarkar, Sonia Wadwa. I would also like to express my gratitude to other colleagues for creating a great work atmosphere and helping at different stages during my course study. I appreciate other research scholars, Santosh Kumar Rath,

Aadil Bathla, Nirmalya Haider, Deepika, Priyanka Gautam, and others who are not mentioned by name, for their support and encouragement. I express my warm thanks to my colleagues and friends with whom I spent and enjoyed scientific and social activities. I now have a forever collection of stories and a lot of everlasting memories to tell, and thanks to my best friends Mohd Zeeshan Ala Ansari, Pankhuri Sein, Sunil Dutt, Ranjit Jha, Yogesh Saini and Ashok Kumar for scientific and non-scientific help during the Ph.D. studies. I extend my thankful acknowledgment to SAI Labs (TIET); SAIF Lab, Panjab University, Chandigarh; I extend my gratitude to Mr. Mukesh Aggarwal, SAI Labs (TIET) for their cooperation during NMR/CHN data collection. I thankfully acknowledge DST-SERB (CRG/ 2018/002159), CSIR, New Delhi, [02(0310)/17/EMR-II] for financial support. for financial assistant during my course. Finally, none of this would have been possible without all my family members' constant love, support, guidance, and patience.

I owe my gratitude to my respected parents, whose blessings, beliefs, and encouragement have shown me the path to pursue my goals in life. One strong person in my life is my mother, Mrs. Saroj Bala. She has been a constant source of support and encouragement and made countless sacrifices for the entire family, especially me. She is a great inspiration to me. I show my deep gratitude to my sister and my wife for everything they have done for me for the completion of this work.

Besides this, I am thankful to the persons who knowingly and unknowingly helped me during the successful completion of this work.

…….

Dinesh Singla

Abbreviations and Acronyms

α	Alpha
Å	Angström
Ac	Acetyl
AcOH	Acetic acid
Ar	Aryl
β	Beta
Bu	Butyl
°C	Celsius degrees
C	Carbon
^{13}C NMR	Carbon nuclear magnetic resonance
CDC	Cross-dehydrogenative coupling
Cp	Cyclopentadienyl
Cy	Cyclohexyl
δ	NMR chemical shift
d	Doublet
D	Dimensional
DABCO	1,4-Diazabicyclo[2.2.2]octane
DBU	1,8-Diazabicyclo[5.4.0]undec-7-ene
DCE	Dichloroethane
DCM	Dichloromethane
dd	Doublet of doublets
ddd	Doublet of doublets of doublets
deg	Degree
DEPT	Distortionless enhancement by polarisation transfer
DFT	Density functional theory
DMA	Dimethylacetamide
DMAP	4-Dimethylaminopyridine
DMF	Dimethylformamide
DMSO	Dimethylsulfoxide

dt	Doublet of triplets
ESI	Electrospray ionization
EWG	Electron withdrawing group
FDA	Food and Drug Administration
g	Gram(s)
h	Hour(s)
^{1}H NMR	Proton nuclear magnetic resonance
HetAr	Heteroaryl
HRMS	High-resolution mass spectrometry
Hz	Hertz
HFIP	Hexafluoroisoproponol
IR	Infrared
J	Coupling constant
KIE	Kinetic isotope effect
m	Multiplet
m	Meta
M	Molar
m/z	Mass-to-charge ratio
max	Maximum
***m*-CPBA**	*m*-Chloroperoxybenzoic acid
mol%	Mole percent
m.p.	Melting point
MS	Mass spectrometry
NBS	*N*-bromosuccinimide
NMP	*N*-methyl-2-pyrrolidone
NMR	Nuclear magnetic resonance
Ph	Phenyl
PivOH	Pivalic acid
PivO-	Pivalate
ppm	Parts per million
td	Triplet of doublets
tert	Tertiary
TFA	Trifluoroacetic acid, trifluoroacetate

μM	Micro molar
AR	Analytical reagents
ArH	Aromatic hydrogen
$B(OH)_2$	Boronic acid
$CDCl_3$	Deuterated chloroform
ct	Calf thymus
DHFR	Dihydrofolate reductase
DNA	Deoxyribonucleic acid
EB	Ethidium bromide
EGFR	Epidermal growth factor receptor
GI%	Percentage growth inhibition
GI_{50}	Median growth inhibition concentration
H_2SO_4	Sulphuric acid
H-bonding	Hydrogen bonding
IC_{50}	Median inhibition concentration
IPA	Isopropanol
K_2CO_3	Potassium carbonate
LC_{50}	Median lethal concentration
MG-MID	Mean graph mid-point
MTT	3-(4,5-Dimethylthiazol-2-yl)-2,5-diphenyl tetrazolium bromide
NCI	National cancer institute
NT	Not treated
SAR	Structure-activity relationship
TGI	Total growth inhibition concentration
TPSA	Total polar surface area
Trp	Tryptophan
Tyr	Tyrosine
USA	United States America

Contents

CHAPTER 1

Introduction and Literature Review

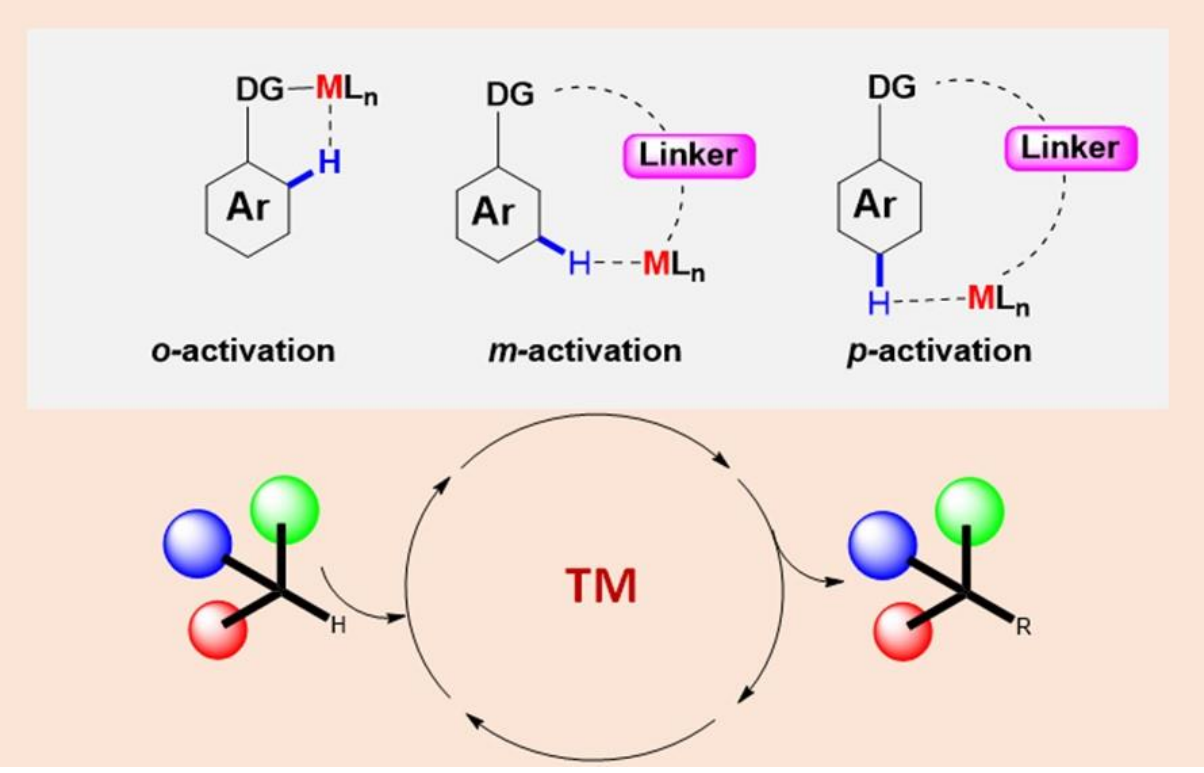

CHAPTER 1

1.1. Cancer is Most Challenging Disease

During the last decades, cancer has been a major worldwide health problem.[1] Cancer is a lethal disease,[2] second leading cause of mortality exceeding cardiovascular disease. Despite many therapeutic successes, cancer remains one of the most promising challenges of the 21st century.[3] The American Cancer Society (ACS) statistics estimated that in 2022, over 19,18,030 cases were diagnosed in the United States alone, and over 6,90,360 people died from this disease.[4] Cancer is characterized by aberrations in cellular growth and proliferation pathways, resulting in an uncontrolled division of abnormal cells to form lumps or masses of tissue called a tumor.[5] It can release a hormone that can alter the body's function and affects the digestive, nervous, circulatory, and many other systems. Cancer can be found in any organ, such as the lung, pancreas, brain, colon, breast, skin, bones, ovarian, blood, or nervous tissue (**Figure 1.1**).[6]

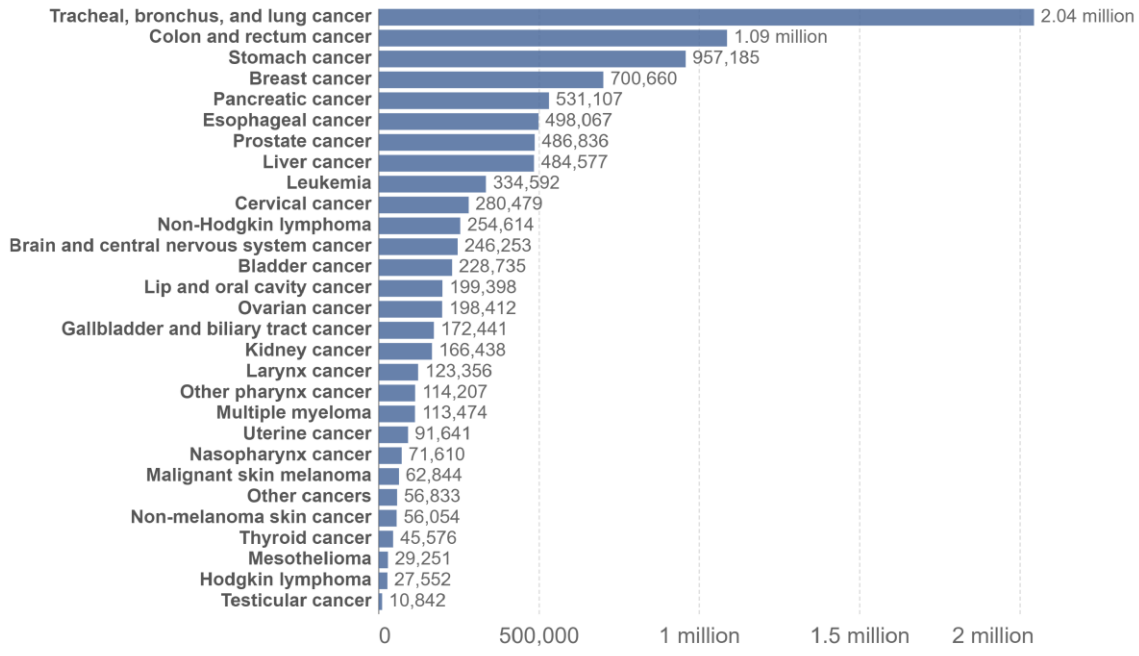

Figure 1.1. Cancer deaths by type in the World

Currently, chemotherapy[7] is the most effective way to cure metastatic cancer. A chemotherapeutic agent targets particular cellular DNA and inhibits DNA replication and transcription by intercalation or blocking various enzymes used in DNA synthesis, such as

topoisomerase, which causes cell cycle arrest and leads to programmed cell death called apoptosis.[8] The discovery and synthesis of high-potential and low-toxic anticancer drugs continue to be a tremendous challenge for medicinal chemistry.[9] Synthesis of potential drug involves various types of reaction such as asymmetric synthesis, C-H functionalization, Grignard reaction etc. Among all C-H functionalization has claimed incessant attention for the synthesis of these types of moieties. The potency of chemotherapeutic agents has also improved by late-stage modification through C-H functionalization. It is noteworthy that anticancer drugs may have various fluorophores having interesting photophysical properties and thus have wide applications in the pharmaceutical industry and material sciences. Hence, synthesis and late-stage modification of heterocyclic organic compounds using different pharmacophores and fluorophores through various methodologies such as C-H functionalization[10], one-pot synthesis, etc., are fascinating topics and claimed constant attention from an organic community in last two decades.

Here, I have synthesized various heterocyclic moieties using coumarin, quinazoline, benzimidazole, pyrazole, etc., as pharmacophores and fluorophores *via* the methodology mentioned above and performed regioselective C-H functionalization using transition metal catalysts. After that, these synthesized compounds were evaluated for their anticancer activity against 60 human cancer cell lines. In addition, these compounds were also assessed for their photophysical behavior.

1.2. Molecular Hybridization of Heterocycles

Hybrid drugs combine two pharmacophores into a single molecule. These are primarily meant to interact with numerous targets, enhance their effects on another bio target as a single entity, or mitigate the known adverse effects of the other hybrid portion. Researchers worldwide have been working on ligands to eliminate the issues involved with combination therapy by combining two pharmacophores in a single biological molecule and modulating several targets. Hybridization of pharmacophores is similar to traditional combination therapy, except that the two moieties are covalently bonded and available as a single entity.[11]

Singla and coworkers reported the synthesis of benzimidazole-triazine conjugates and anticancer studies (**1** and **2**; **Figure 1.2**) against the cancer cell lines. Four hybrids, **1.1a** and **1.2a-1.2c,** exhibited remarkable activity against leukemia cancer cell lines (SR) with GI_{50} values of 731, 125, 539, and 31 μM, respectively. Moreover, these compounds also showed

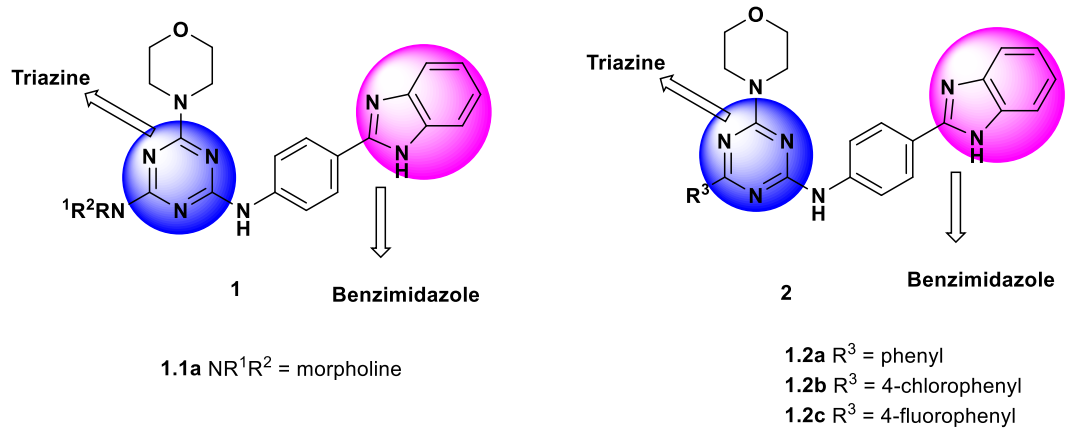

Figure 1.2. Benzimidazole-triazine hybrids (**1.1** and **1.2**) with potent anticancer activities

promising activity against renal cancer cell lines RXF393 (GI_{50} < 750 μM). The presence of an aryl moiety on the triazine ring positively influenced the anticancer activity of the hybrids.[12]

Galayev *et al.* performed the conjugation of 7-hydroxy-8-methyl-coumarin with indole (**3**) and tested their cytotoxicity against the NCI-60 cell panel. SAR studies recognized indole-coumarin hybrid **1.3a** with fluoro substituent at C-6 position of indole ring, revealed high anti-mitotic activity against leukemia (GI_{50} = 3.08 μM) and melanoma (TGI = 9.71 μM) cancer cell lines (**Figure 1.3**).[13]

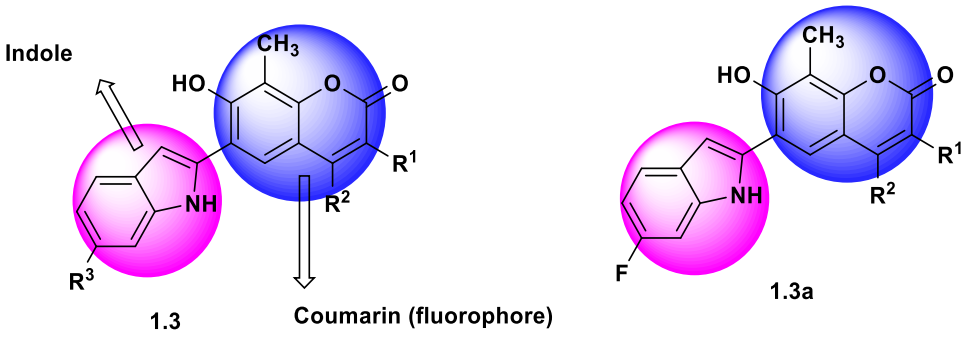

Figure 1.3. Coumarin-indole hybrids (**1.3**) with potent anticancer activity

The coumarin-triazole hybrids (**4, Figure 1.4)**, synthesized by Kraljevic and coworkers,[14] emerged as prospective anti-proliferating hybrids against A-549 (lung) and HeLa (cervical) carcinoma cell lines with IC_{50} < 30 μM. 7-Methylcoumarin-1*H*-1,2,3-triazole-2-ethyl-benzimidazole **1.4a** displayed better cytotoxicity among synthesized hybrids with IC_{50}

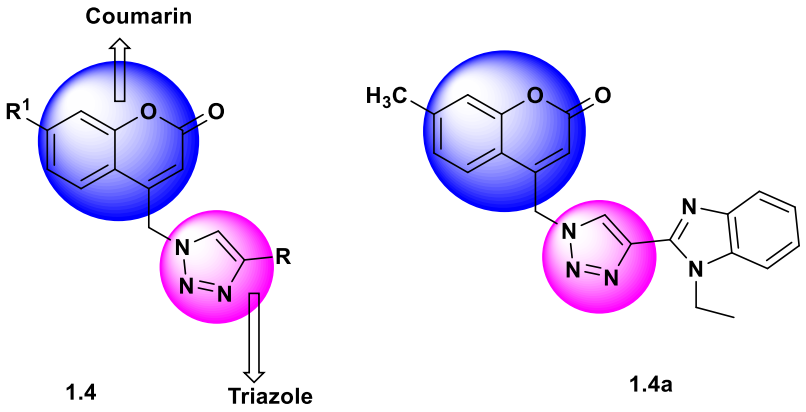

Figure 1.4. Coumarin-triazole hybrids (**1.4**) with potent anticancer activity

value of 0.90 μM against HepG2 (hepatocellular) cell line with a selectivity index of 50, but somewhat toxic to normal fibroblasts WI38 and 3T3 (IC_{50} = 45.33 μM).

Chen *et al*. synthesized chalcone-based hybrids (**1.5**) that displayed moderate to good antiproliferative activities in the micromolar to sub-micromolar range. SAR studies suggested that the hybrids synthesized from 4,5,6,7-tetramethoxy indanone with different indole carbaldehydes usually gave more potent antiproliferative activities than the corresponding 5,6,7-trimethoxy indanone derivatives. Representative compound **1.5a** displayed impressive anticancer activity (GI_{50} = 0.026-0.035 μM) against the A549 (lung), HeLa (cervical), Bel-7402 (liver carcinoma), PC-3 (prostate), and K562 (gastric) cell lines. Mechanistic studies established that **1.5a** effectively inhibited *in vitro* cellular tubulin polymerization and caused cell cycle arrest in the G2/M cell cycle (**Figure 1.5**).[15]

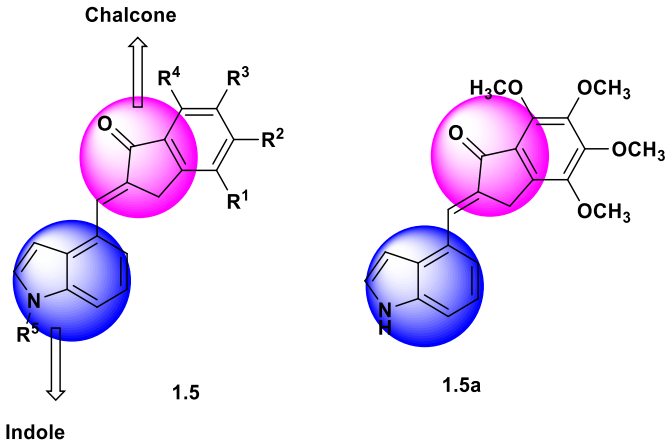

Figure 1.5. Chalcone-indole hybrids (**1.5**) with potent antiproliferative activity

1.3. C-H Functionalization of Heterocycles

C-H functionalization is a process in which ubiquitous C-H bonds can be transformed into valuable moieties. C-H functionalization is found to be site specific.[16] For synthesizing new heterocyclic medicinally important compounds and natural products, the catalytic activation of C-H bonds has brought a revolution.[17] As C-H functionalization is established on industrial level also for the synthesis of various API and help in cost reducing by decreasing number of step, this approach has turned out to be a novel methodology for constructing the core structure of new pharmaceuticals. Negishi *et al.* developed Suzuki cross-coupling using palladium catalysis, for which they were awarded the Nobel prize in 2010.[18] However, this approach required pre-functionalized substrates, but with the advancement in transition metal-catalyzed C-H functionalization, pre-functionalization can be avoided. The regioselective functionalization of C-H bonds replaces various classical cross-coupling reactions of alkyl halides/aryl halides. Burgeoning research for designing new strategies for C-H functionalization can be grouped into two major categories: (i) Directing Group (DG) assisted C-H bond activation and (ii) Cross-Dehydrogenative Coupling (CDC) reaction (**Scheme 1.1**). Here I will discuss only directing group-assisted C-H functionalization.

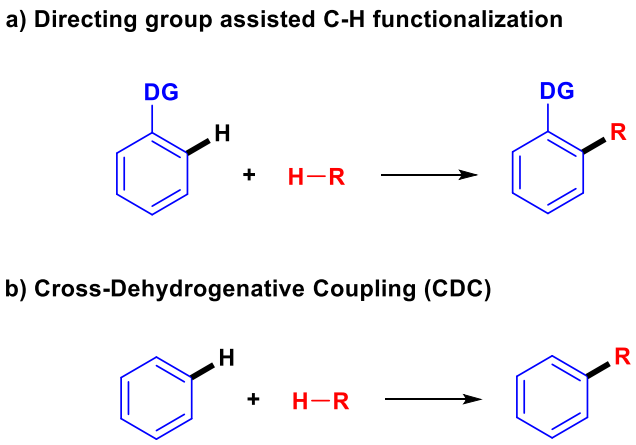

Scheme 1.1. Different routes to C-H functionalization

1.3.1. Directing Group-assisted C-H Functionalization

Heterocyclic scaffolds have several C-H bonds having nearly the same reactivity; hence it is quite challenging to perform selective functionalization of the desired C-H bond. The chosen functionalization can be achieved by installing the directing group with at least one heteroatom (such as N, O, and S). The hetero atom of directing group tends to chelate with

transition metal ions such as Ru, Rh, Pd, Ir, Pt, Co, or Cu and direct it to a proximal C-H bond to form resourceful intermediate (usually a five-member or six-member metallacycle) for the formation of new C-C or C-X (X = N, S, O) bond through activation of sp^2 or sp^3 C-H bond.[19] However, installing and removing the hetero atom-containing directing group is a difficult task which causes a significant drawback with this methodology. C-H functionalization using several directing groups has been widely explored for constructing valuable C-C or C-X bond. Directed C-H activation affords alkenyl, alkynyl, aryl, and trifluoromethyl products at the *ortho*, *para*, *or meta* position of aromatic ring. Various functional groups and heterocyclic moieties, such as amide, imine, aldehyde, ketone, benzimidazole, etc., are widely used as directing groups.[20]

1.3.1.1. Amide as a Directing Group

In 2014, Zhao and coworkers demonstrated highly site-selective palladium-catalyzed alkenylation using amide as a weak directing group. They used $Pd(OAc)_2$ as a catalyst and Ag_2CO_3 as an oxidant in the presence of $(n\text{-BuO})_2POOH$ as an additive in DCE at 120 °C. The developed methodology showed wide substrate scope and broad functional group tolerance to give corresponding compound **1.8** in 70% to 88% yield (**Scheme 1.2**). Furthermore, complex alkenylated arenes were also constructed by sequential alkenylation. In addition, the removal of directing group under mild conditions was also demonstrated.[21]

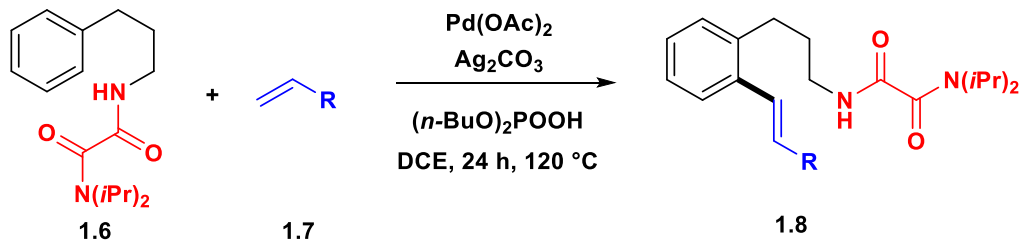

Scheme 1.2. Regioselective alkenylation using amide as a weak directing group

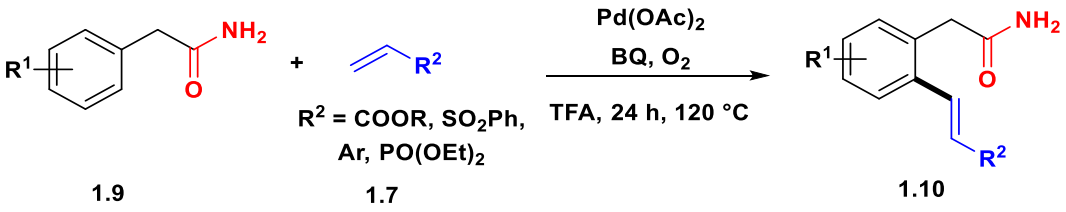

Scheme 1.3. C-H alkenylation of arylacetamide

Similarly, in 2018, Kumar and coworkers also disclosed regioselective alkenylation of arylacetamide (**1.9**) using amide as a weak directing group (**Scheme 1.3**). They performed the reaction using $Pd(OAc)_2$ as a catalyst; benzoquinone (BQ) was used as an oxidant in the atmosphere of oxygen using TFA as solvent. Using a developed methodology, the author incorporated different alkenyl groups (**7**) at the *ortho*-position of arylacetamides and gave the corresponding product in upto 82% yield.[22]

1.3.1.2. Imine as a Directing Group

An imine, a functional group with a double bond between carbon and nitrogen, is a weakly coordinating directing group. However, after intensive research on directed C-H functionalization, imine has shown great potential as the directing group. In addition, there are some reports where the imine group is used as a transient directing group.

In 2017, Chen *et al*. showed imine as directing group for the *ortho*-arylation of benzaldehyde (**1.11**) under palladium catalysis. They used anthranilic acid as a ligand (**L1**) that generated imine, through which palladium formed palladacycle, and showed acid as the second directing group. This complex underwent migratory insertion on imine carbon followed by *β*-hydride elimination, afforded the desired product **1.13**. Several substituted fluorenones were obtained using different benzaldehyde and aryl iodide in 60% to 90 % yields (**Scheme 1.4**).[23]

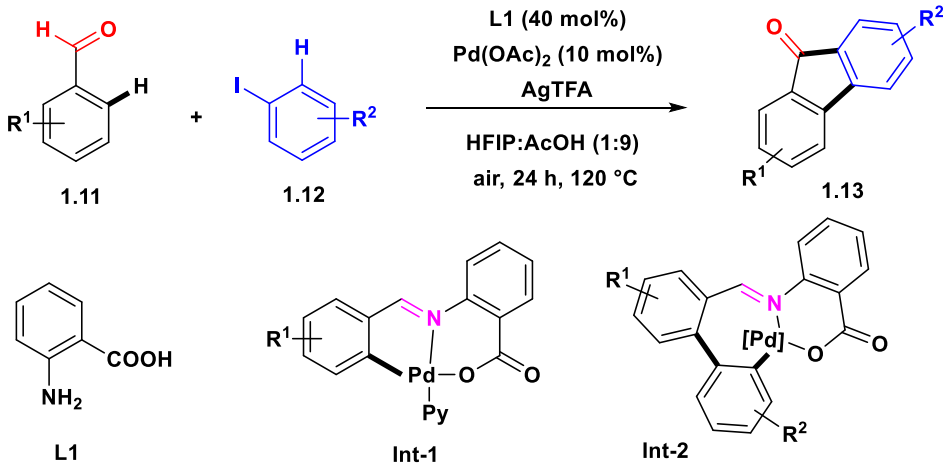

Scheme 1.4. *ortho*-Arylation of benzaldehyde

Recently, Cheng group disclosed C-H activation/annulation of salicylaldehyde (**1.14**) with 4-diazoisochroman-3-imines (**1.15**) *via* rhodium catalysis. The reaction was carried out

using a rhodium catalyst in the presence of CsOAc in dioxane in an air atmosphere. The author also proposed that the reaction proceeded through the sequential activation and carbene migration process, followed by intramolecular annulation. They designed several scaffolds (**1.16**) in upto 90% yield (**Scheme 1.5**).[24]

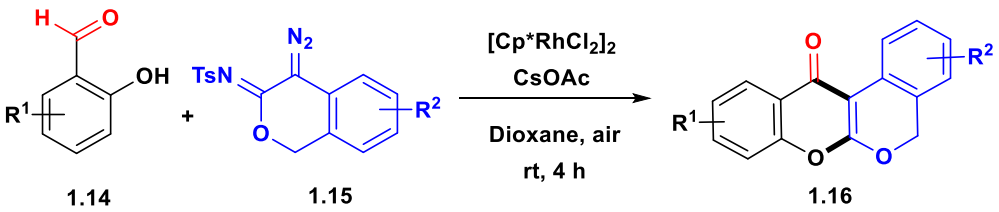

Scheme 1.5. Rhodium catalyzed C-H activation/annulation

1.3.1.3. Aldehyde and Ketone as Directing Groups

The carbonyl group in aldehyde and ketone were widely used as directing groups in the C-H functionalization process. Pioneering development in this context was made by Murai *et al.* in 1993.[18] This tremendous contribution of highly effective and regioselective C-C bond formation using ruthenium complex on different substrates such as furan and thiophene were accomplished. However, this field is still active even after the publication of significant reports.

Prabhu group in 2015 used ketone as a directing group and carried out C-H functionalization of acetophenone (**1.17**) under ruthenium catalysis with maleimide (**1.18**). They used a ruthenium catalyst with $Cu(OAc)_2.H_2O$ as an oxidant in $AgSbF_6$ as an additive in DCE at 120 °C under the atmosphere of argon (**Scheme 1.6**). The reaction was undergone *via* a Concerted Metalation-Deprotonation (CMD) mechanism, where alkene insertion occurred in an *endo* manner.[25]

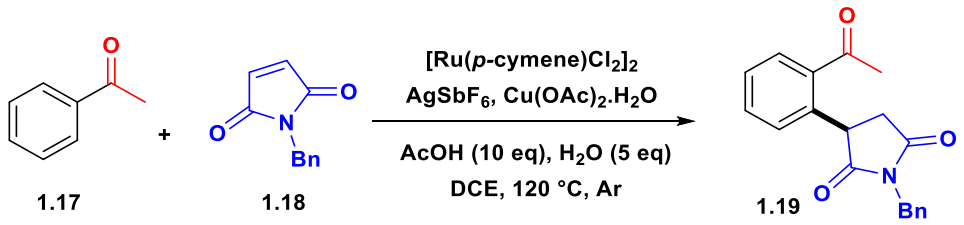

Scheme 1.6. Ketone-directed C-H functionalization of acetophenone with maleimide

You group, in 2015, developed a strategy to use aldehyde as a traceless directing group for the regioselective C-H functionalization followed by proto-deformylation under Rh(III) catalysis. They performed the reaction between indolyl aldehydes (**1.20**) and alkynes (**1.21**) using $[Cp^*RhCl_2]_2$ as a catalyst and $Cu(OAc)_2$ as an oxidant in the presence of CsOPiv in dioxane (**Scheme 1.7**). Here, the reaction was compatible with a broad range of functional groups such as -Cl, -F, OR, -CN, and RCO_2R' and gave corresponding compounds (**1.22**) in 60% to 88% yields. Various control experiments suggested that the reaction proceeded through chelation assistance followed by migratory insertion and protodemetalation process.[26]

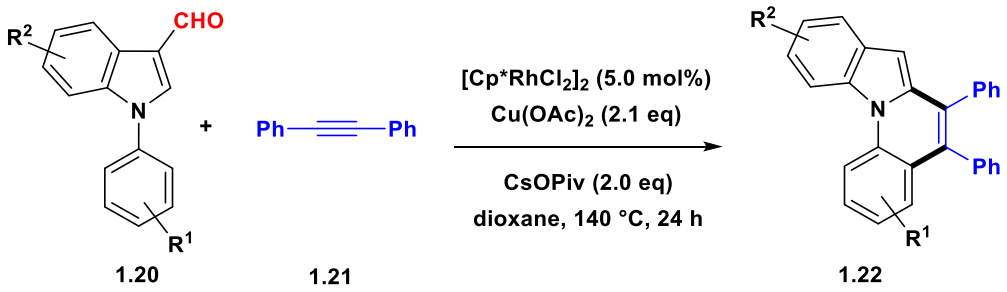

Scheme 1.7. Facile synthesis of versatile indolo[1,2-*a*]quinolines

After two years, the same group showed C4-functionalization of indole (**1.23**) using aldehyde as directing group under Ir-catalysis. They disclosed the C4-amidation of indoles using sulfonyl azides (**1.24**) in the presence of $AgNTf_2$ as an additive or catalyst activator. Here, not only *N*-unprotected indoles were obtained, but these also showed tunning with various functional groups such as carboxyl, amide and acetyl at C3 position (**Scheme 1.8**).[27]

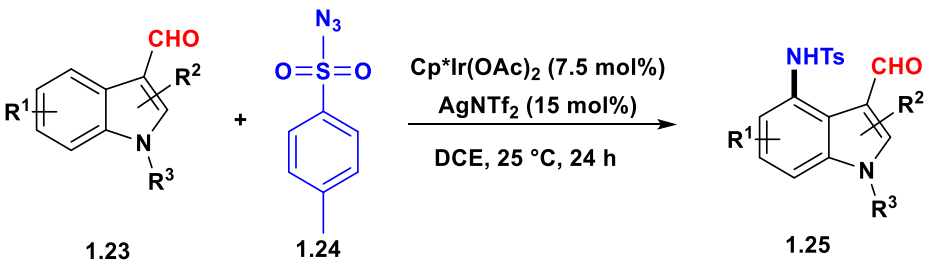

Scheme 1.8. Regioselective C4-amidation of indoles

1.3.1.4. Benzimidazole or Benzothiazole as Directing Group

Chakraborti and his coworkers displayed alkenylation of heteroarenes using ruthenium catalysis directed by biological active heterocyclic moiety benzimidazole. They proposed that the reaction proceeded through chelation assistance and was carried out using a ruthenium catalyst in the presence of $AgBF_4$ and PhCOOH in DCE at 85 °C for 5 h (**Scheme 1.9**). In addition, the reaction exhibited broad substrate scope in heteroarene and alkyne scaffolds and afforded corresponding compounds (**1.27**) in upto 80% yields. During mechanistic studies, the role of carboxylic acid was significant for generating a ruthenium complex that could activate the proximal C-H bond *via* proton abstraction.[28]

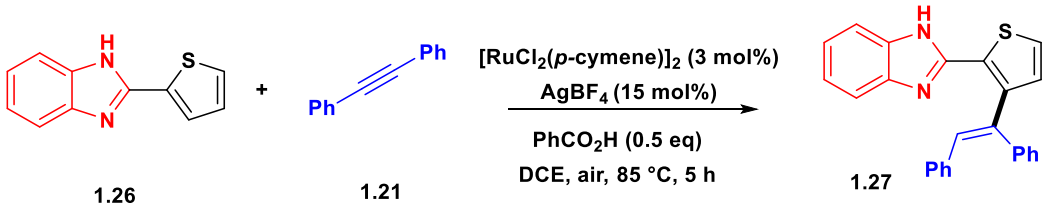

Scheme 1.9. Alkenylation of heteroarene using alkynes

Wang *et al.*, in 2021, demonstrated the C-H functionalization of diverse fused polycyclic benzimidazole using rhodium catalysis. They synthesized a novel fused heterocyclic scaffold **30** by the reaction between substituted 2-phenoxy-1*H*-benzimidazole (**1.28**) and various alkynoate (**29**) in the presence of the catalytic amount of rhodium catalyst in DCE. They used AgOTf as a catalyst activator and NaOAc as well as AcOH as oxidants. The developed protocol was compatible with several substrates and gave corresponding compounds (**1.30**) in 80% yields (**Scheme 1.10**).[29]

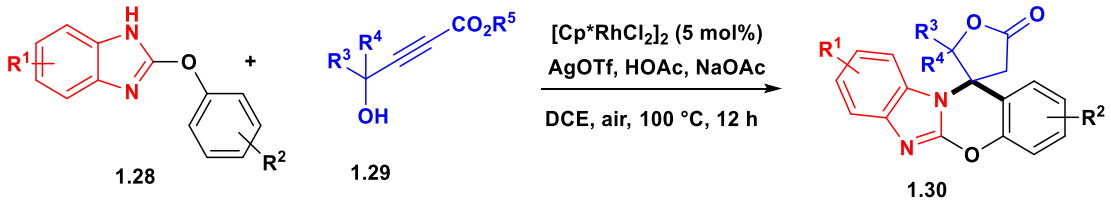

Scheme 1.10. Synthesis of fused polycyclic benzimidazole

1.4. Biological Significance of Targeted Heterocycles

Hetero atoms containing scaffolds and their analogues have a profound prevalence as an active structural motif in biologically active compounds, natural products, material science, and pharmaceuticals. Most drugs in their skeleton hold at least one heterocyclic motif. Some targeted heterocyclic compounds are quinazolinone, coumarin, pyrazole, and pyridine as shown in **Figure 1.6**.

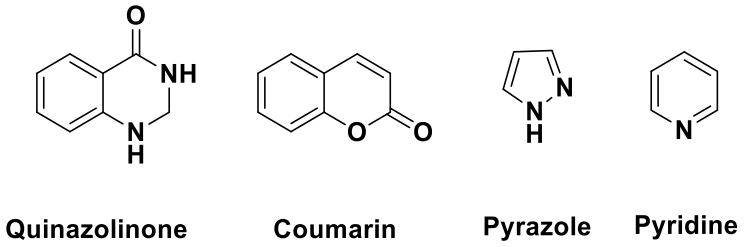

Figure 1.6. Biologically active heterocycles

Quinazolinone and its analogs are the most active structural motifs in numerous naturally occurring alkaloids isolated from different families of the plant kingdom. Raltitrexed drug (**1.31**) contains quinazolinone heterocyclic nucleus (**Figure 1.7**) and is widely used as an anti-tumor. In addition, this motif also possesses several other biological functions, such as GABA receptors, cellular phosphorylation inhibitors, etc. and also used as DNA-binding agents.[30]

Coumarins are oxygen-containing heterocyclic scaffolds broadly distributed in the plant kingdom. Coumarin-containing compounds are obtained from roots (*Ferulago campestris*), fruits (*Aegle marmelos*), and leaves (*Murraya paniculata*), which have a tremendous role in the treatment of cancer. In addition, coumarin derivatives can potentially trigger cell cycle arrest, kinase inhibition, and angiogenesis inhibition in several cancer cells.[31]

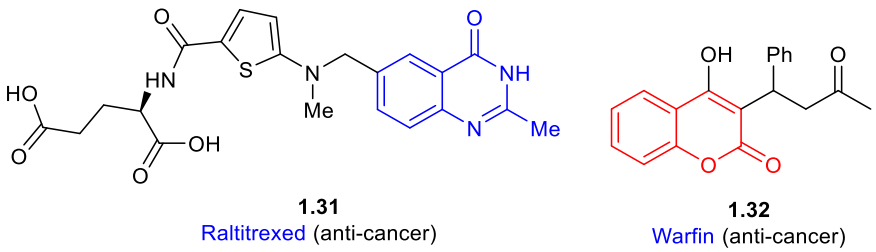

Figure 1.7. Importance of targeted heterocycles in pharmaceuticals

Both synthetically and naturally derived compounds show pharmacological properties. Due to these reasons, the synthesis and isolation of coumarin-based motifs have gained constant attention from organic chemists. Recently, warfin (**1.32**) (**Figure 1.7**) exhibited cytotoxicity against the human ovarian cancer cell and hence considered a potent drug in cancer chemotherapy.

Similarly, pyrazole belongs to the azole family, a five-membered heterocyclic ring with two nitrogen atoms at adjacent positions. Various therapeutic agents incorporate the pyrazole nucleus, which has a broad spectrum of biological activities. Hence, developing pyrazole-like scaffolds has gained significant interest among organic chemists. Noteworthy, crizotinib[31] (**1.33**) and pyrazofurin[32] (**1.34**) (**Figure 1.8**) are two drugs having a pyrazole nucleus and are commonly used for the treatment of breast cancer.[32]

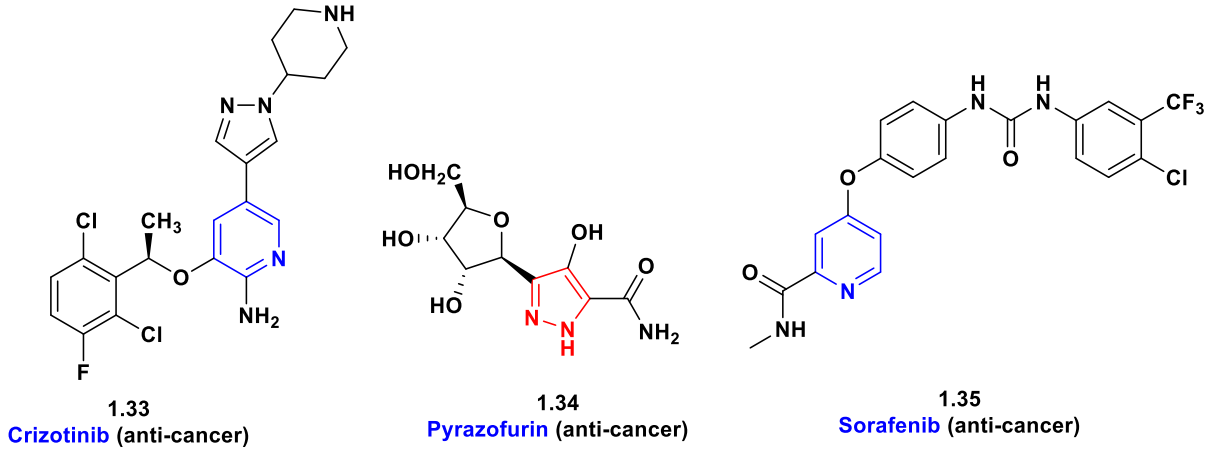

Figure 1.8. Pharmaceutically active drugs

Pyridine is another important heterocyclic compound endowed with versatile biological activities, especially anticancer activity. Various motifs with a pyridine nucleus have been approved as potential drug candidates in chemotherapy for cancer treatment. Sorafenib (**35**) is among the diverse endorsed pyridine-based drug candidates; it has very low toxicity and inhibits several kinases involving cell proliferation.[33]

1.5. C-H Functionalization of Quinazolinone

Several methodologies have been developed for the regioselective C-H functionalization of quinazolinone, including arylation, alkylation, and alkenylation. Most of the reactions have been performed for C-2 functionalization of quinazolinone. Subsequently, reaction at unreactive positions of quinazolinone is still a great challenge for organic chemists.

In 2015, Xuan group demonstrated a unique one-pot cascade approach for the functionalization of quinazolinone (**1.36**) *via* Ru(II)-catalyzed oxidative C-H activation followed by aza-Michael addition to access pyrrolo[2,1-*b*]quinazolin-9(1*H*)-one scaffolds (**1.37**). They performed the reaction using $[RuCl_2(p\text{-cymene})]_2$ (5 mol%), $Cu(OAc)_2.H_2O$ (2.2 eq) in DCE at 100 °C for 12 h (**Scheme 1.11**). Initially, various substituted 2-arylquinazolinone were subjected to the standard reaction conditions and obtained related products in 88% yields. This protocol has significant compatibility with acrylamides, styrenes and acrylate.[34]

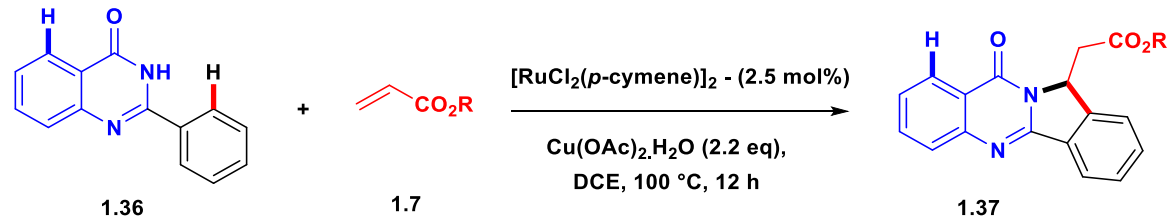

Scheme 1.11. Ru(II)-catalyzed oxidative C-H activation of quinazolinone

Samanta *et al*. in 2016 disclosed an effective and highly selective C-2 alkylation of various substituted quinazolinone (**1.38**) under rhodium catalysis with *α*-diazo carbonyl compound (**1.39**). They used rhodium catalyst (1 mol%) in the presence of silver additives in DCE at 80 °C for 24 h. The reaction was assisted with 2-pyridyl, directing the group to afford 78% yield of final alkylated product **1.40** (**Scheme 1.12**).[35]

Inspired by Xuan group, Mhaske and his colleagues outlined the straightforward method for C-H bond alkenylation of quinazolinones (**1.36**) with terminal alkynes *via* ruthenium

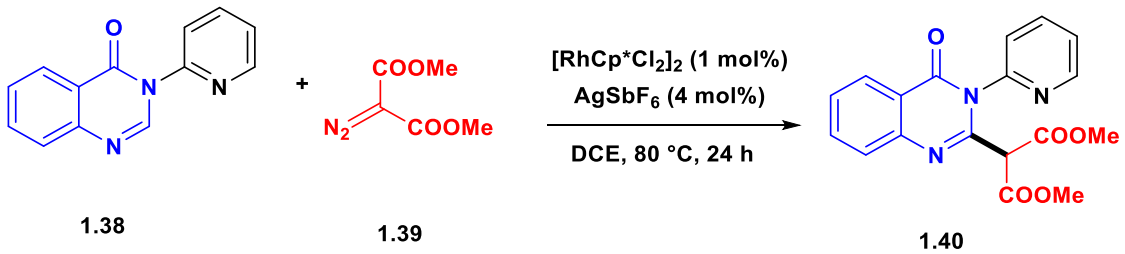

Scheme 1.12. C-2 alkylation of quinazolinone

catalyst to generate various mono or dialkenylated derivatives with excellent yields (**Scheme 1.13**). Here, ruthenium-catalyzed alkenylation was assisted by amide as a weak directing group through nitrogen atom and followed the oxidative addition pathway. Notably, this catalytic system was compatible with a wide range of electron-donating, electron-withdrawing, and halogen functionalities in the arene ring of quinazolinone. Various substituted terminal alkynes (-Me, -OMe, -Cl) showed valuable tunning in generating the alkenylated products in satisfactory yields, but aliphatic terminal alkyne stayed sterile under conventional reaction conditions, even though the increased reaction time of 48 h and temperature increase allowed mono C-H alkenylation in inadequate yield.[36]

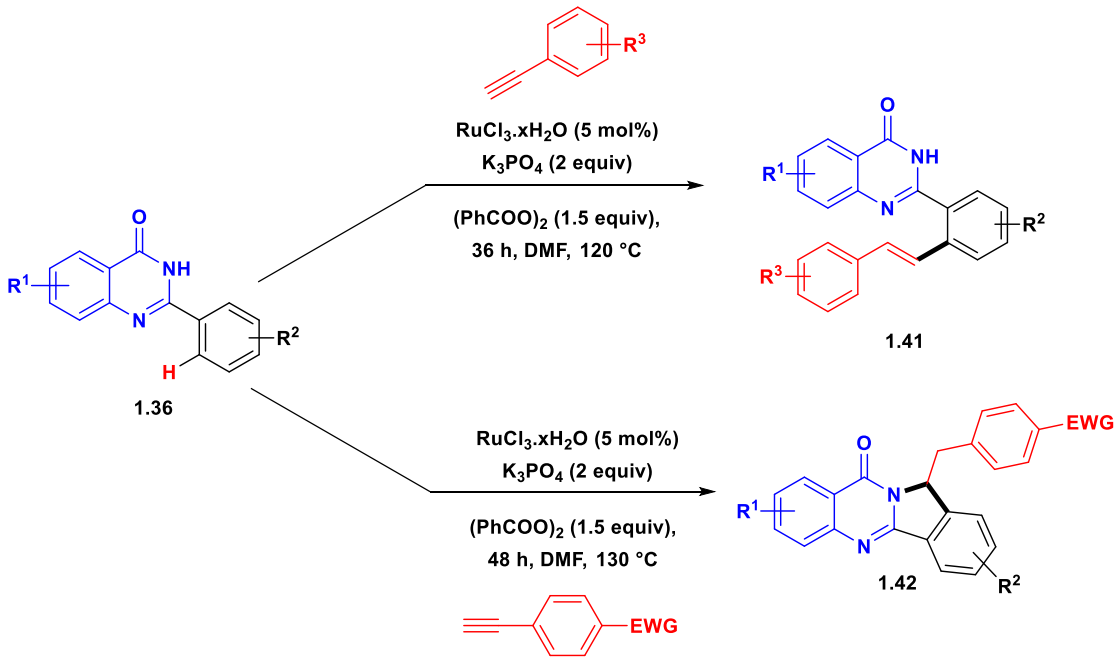

Scheme 1.13. Alkenylation of quinazolinones with terminal alkynes

In the same year, Peng group demonstrated an unprecedented approach to access isoquinolino[1,2-*b*]quinazolin-10-one (**1.43**) using rhodium catalysis *via* cascade annulation of unveiling 2-arylquinazolin-4(3*H*)-ones (**1.36**) and several vinyl acetates (**1.7**). They performed the reaction using $[RhCp^*Cl_2]_2$ (2.5 mol%) as catalyst and $AgSbF_6$ (10 mol%) as co-catalyst in the presence 2 equiv. of oxidant (AgTFA) in chlorobenzene (**Scheme 1.14**). The reaction was completed by sequential operations of C-H alkenylation followed by intramolecular aza-Heck cyclization. Several electron-donating and -withdrawing groups were employed and afforded corresponding compounds in 70% to 84% yields.[37]

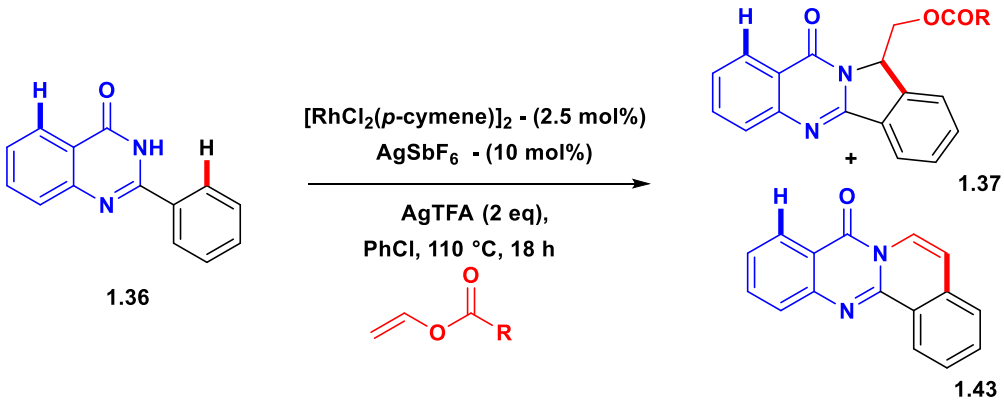

Scheme 1.14. Rhodium-catalyzed cascade annulation 2-arylquinazolinone

In 2018, Jana *et al.* reported the first distinctive and easy redox-neutral methodology to synthesize dihydroisoquinoline-fused quinazolinone moiety (**1.44**) *via* Ru(II)-catalyzed regioselective C-H bond functionalization and subsequently intermolecular cascade hydroamination of 2-arylquinazolinone (**1.36**). The reaction was carried out using [Ru(*p*-cymene)$_2$Cl$_2$]$_2$ as a catalyst in the presence of silver-based co-catalyst $AgSbF_6$ using AdCOOH as an additive in DCE. Substitution with various groups on the aryl ring of quinazolinone at different positions gave compounds in upto 90% yields **(Scheme 1.15)**. However, *para*-

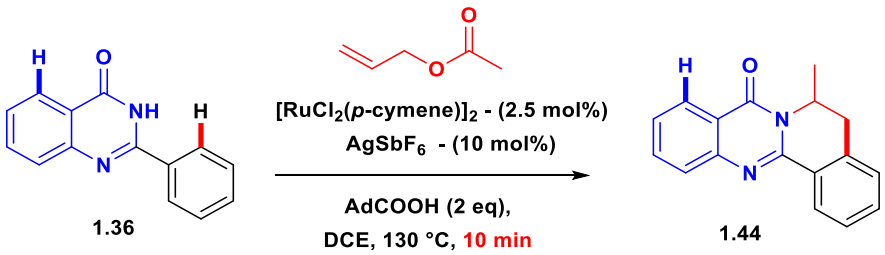

Scheme 1.15. Hydroamination of 2-arylquinazolinone

substituted substrates showed low compatibility compared to *ortho*- and *meta*-substituted quinazolinone. In addition, several heterocyclic congeners at the C-2 position also showed good compatibility to afford respective compounds. Again, the reaction was assisted using

amide as a weak directing group through nitrogen atom that formed a five-membered ruthenacycle.[38]

1.6. C-H Functionalization of 1-Phenyl Pyrazole

Several groups have reported C-H functionalization of 1-phenylpyrzole; they performed various reactions under transition metal catalysis to explore the regioselectivity and late-stage modification. Though multiple methodologies have been developed, synthesis of starting materials and pre-functionalizations are still required.

In 2011, the Miura group demonstrated Ru(II)-catalyzed oxidative alkenylation of 1-phenylpyrazole (**1.45**). The reaction was carried out using [Ru(*p*-cymene)$_2$Cl$_2$] as a catalyst in the presence of Cu(OAc)$_2$.H$_2$O in DMF at 100 °C. Numerous mono-alkenylated products (**1.46**) were obtained in 60% to 92% yields (**Scheme 1.16**).[39]

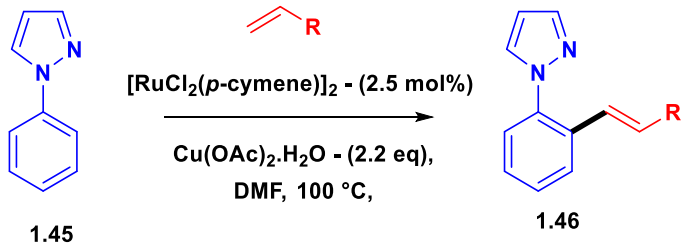

Scheme 1.16. Ru(II)-catalyzed monoalkenylation of 1-phenylpyrazole

In 2013, Wu group developed a strategy to access substituted alkenylated *N*-phenyl pyrazoles. They demonstrated a straightforward, direct method for C4-H activation of substituted pyrazole using palladium catalysis. They used Pd(OAc)$_2$ in the presence of Ag_2CO_3 as an oxidant in

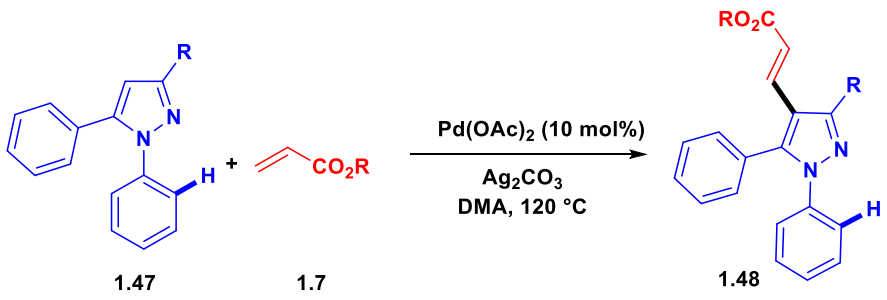

Scheme 1.17. Palladium-catalyzed C4-H activation of substituted pyrazole using

DMA at 120 °C (**Scheme 1.17**). Substitution with electron-donating and -withdrawing groups at different positions of arene ring and pyrazole ring obtained the corresponding compound (**1.48**) in upto 90% yield. However, the electron-withdrawing groups showed better tolerance compared to the electron-donating groups. In addition, various alkenes also showed compatibility to afford respective compounds in upto 84% yields.[40]

Zhu and coworkers, in 2020, reported rhodium-catalyzed switchable C-H functionalization of 2-(1*H*-pyrazole-1-yl)pyridine (**1.49**) using internal alkynes (**1.21**). The reaction used *N*,*N*-bidentate chelating substrates with alkynes, which gave rapid access to diverse alkenylation. Various control experiments suggested the engrossment of a rollover mechanism. The reaction was performed using $[Cp^*RhCl_2]_2$ as a catalyst and $Cu(OAc)_2.H_2O$ as an oxidant in DMF at 85 °C for 24 h (**Scheme 1.18**). Several diarylalkynes and dialkylalkynes were employed to afford the corresponding compound (**1.50**) in 60% to 80% yields. In addition, substitutions with electron-donating and -withdrawing groups at different positions of the aromatic ring also showed satisfactory results. However, halogen-substituted substrates have better compatibility among all other reactions.[41]

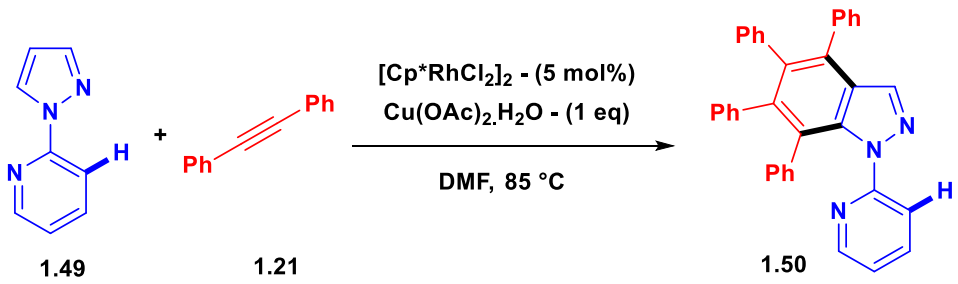

Scheme 1.18. Rhodium-catalyzed switchable C-H functionalization

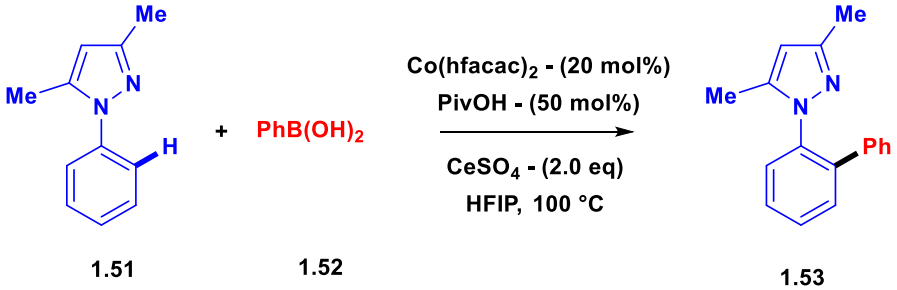

Scheme 1.19. Direct arylation of *N*-aryl pyrazole

Phan and coworkers, in 2021, displayed cobalt-catalyzed direct arylation of *N*-aryl pyrazole (**1.51**). They performed a reaction using $Co(hfacac)_2$, PivOH in the presence of $CeSO_4$ in HFIP at 100 °C. The reaction has broad substrate scope and wide functional group tolerance to afford the final compound (**1.53**) in good yield (**Scheme 1.19**).[42]

1.7. C-H Functionalization of Coumarin

Coumarin is a privileged motif in several pharmaceutical drugs and natural products. Coumarin-containing scaffolds have broad applications in medicinal and material sciences. Different medicinal and bioactivities of coumarin-based motifs are dependent on substitution patterns. Hence, the functionalization of the coumarin nucleus has claimed continual attention from organic chemists.

Hong group in 2012 gave a facile approach for C4-arylation of coumarin (**1.54**) in the presence of palladium catalysis. The reaction was carried out with phenylboronic acid (**1.52**) as the starting substrate using $Pd(OAc)_2$ catalyst in the presence of 1,10-phenanthroline in DMF under the atmosphere of oxygen at 100 °C for 24 h. No external oxidant was used; only oxygen atmosphere was used as an oxidant. The reaction showed broad substrate scope and wide functional group tolerance bearing electron-withdrawing and -donating groups and afforded corresponding compound 1.**55** in good yield (**Scheme 1.20**).[43]

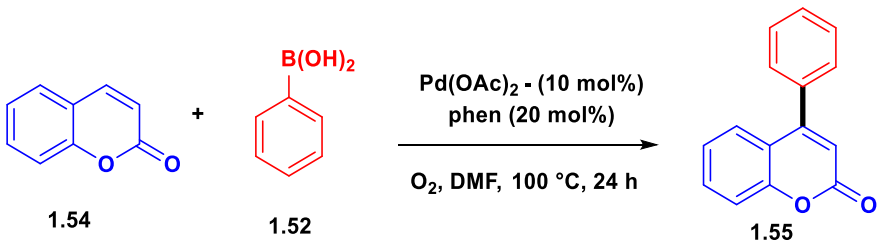

Scheme 1.20. C4-arylation of coumarin using palladium catalysis

After one year, they explored regioselective palladium-catalyzed alkenylation of coumarin (1.**54**) through the Heck reaction. The reaction was performed using $Pd(OPiv)_2$ as a catalyst in the presence of a mild base and an oxygen atmosphere without using any external oxidant at 80 °C. Various ligands were also employed during optimization, leading to lower yield. The reaction showed broad substrate scope and wide functional group tolerance to afford final compound 1.**56** in upto 85% yield (**Scheme 1.21**). In addition, several electron-

donating and -withdrawing groups were tested to afford the corresponding compounds. Furthermore, the reaction was proposed to proceed through reductive elimination pathway.[44]

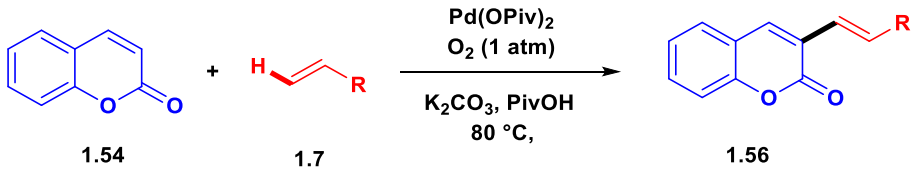

Scheme 1.21. Palladium-catalyzed alkenylation of coumarin

Inspired by the pioneering developments of Shafiee's group, Zhao and coworkers demonstrated a unique approach by utilizing ketone as a directing group to access exclusive C4-alkenylated coumarin (1.**58**) under ruthenium catalysis. Directing group-assisted cross-dehydrogenative coupling technique was used to perform the C4 functionalization of coumarin. The reaction was carried out using 3-acetyl-2*H*-chromen-2-one (1.**57**) and alkene (1.**7**) as starting substrate in the presence of $[RuCl_2(p\text{-cymene})]_2$ catalyst, while $AgSbF_6$ was used as an additive and $Cu(OAc)_2.H_2O$ as an oxidant in DCE for 12 h. The reaction showed compatibility with a broad range of substrates and gave corresponding compound 1.**58** in good yield (**Scheme 1.22**).[45]

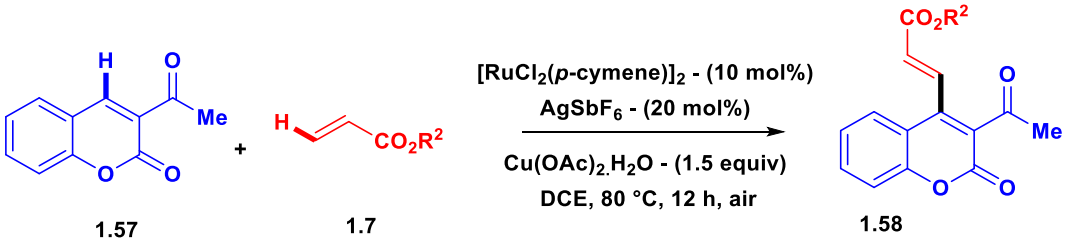

Scheme 1.22. Directing group-assisted cross-dehydrogenative coupling

Hu group, in 2019, showed C4-arylation of coumarin using -COOH as a traceless directing group using rhodium catalysis. As -COOH is an electron-withdrawing group, thus, increasing electron deficiency at C4-position and making this site more electrophilic for the reaction. The reaction was performed between coumarin-3-carboxylic acid (**1.59**) and 2-arylpyridine (**1.60**) in the presence of $[Cp^*RhCl_2]_2$ catalyst, $AgNTf_2$ co-catalyst and $AdCO_2H$ as an additive in toluene at 120 °C for 24 h (**Scheme 1.23**). The reaction showed significant tunning with electron-withdrawing and -donating groups to afford respective compound **1.61**

in good yield. Here, the author also revealed the crucial role of carboxylic acid at C3-position of coumarins.[46]

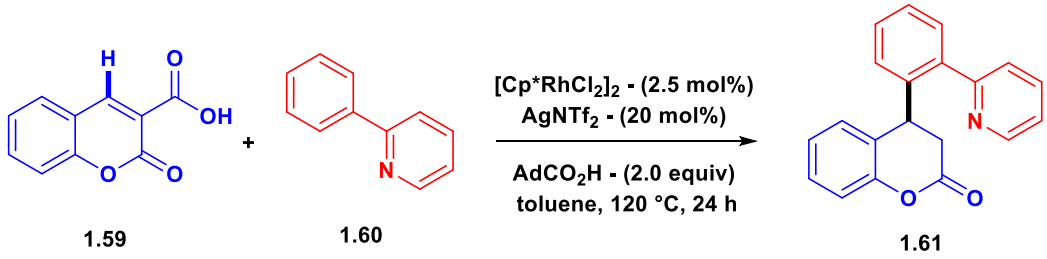

Scheme 1.23. C4-arylation of coumarin using traceless directing group

In 2016 Gogoi group performed a cascade reaction using a palladium catalyst of 4-hydroxycoumarin (**1.62**) with *in-situ* arynes for the synthesis of coumestans (**1.63**) in upto 84% yield. This approach involved C-H activation and further formation of C-C and C-O bonds (**Scheme 1.24a**).[47]

After three years, they again functionalized 4-hydroxycoumarin (**1.62**) at C3 position with aryl carboxylic acid and demonstrated oxidative annulation *via* palladium catalyst for the synthesis of bis-coumarins (**1.64**). Various substituted bis-coumarins with broad functional group tolerance were synthesized in upto 80% yield (**Scheme 1.24b**).[48]

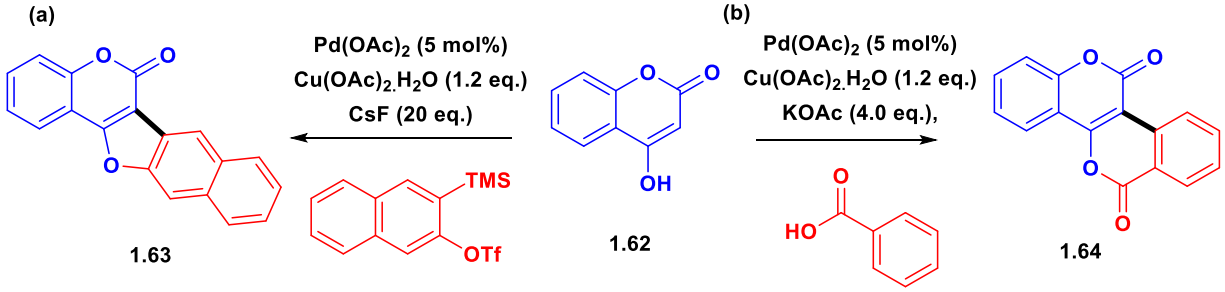

Scheme 1.24. Synthesis of coumestans and bis-coumarins

1.8. Mechanisms of C-H Functionalization

In C-H bond activation, the primary discussion is limited to forming the C-C bond of C-H bond and transition metal, as C-H activation occurs at metal centers. Sanford has proposed two mechanistic pathways for C-H activation: (i) inner-sphere and (ii) outer sphere.[49] In the 'inner-sphere' mechanism, the insertion of transition metal into C-H bond forms a well-

defined carbon metal (C-M) bond, subsequently, conversion of *in situ* generated reacting species into a new functional group through an external reagent. However, in the 'outer-sphere' pathway, the C-H bond of the substrate reacts with the transition metal actively to form a coordinate bond.[50] Notably, both 'inner-sphere' and 'outer sphere' mechanistic pathways were limited to saturated alkane only. Later after myriad developments, the reactions were conveniently categorized from a broader perspective. Bercaw gave a more comprehensive classification for C-H bond functionalization:[51] (i) oxidative addition, (ii) electrophilic activation, (iii) σ-bond metathesis, (iv) 1,2-addition, and (v) metalloradical activation.

1.8.1. Oxidative Addition

In the oxidative addition pathway, the coordination of heavy transition metal to C-H σ-bond and transfer of the electron density to empty σ^* orbital of C-H bond forms complex **A** (**Scheme 1.25**). Subsequently, bond order reduces and weakens the C-H bond; as a result, a new C-M bond formation takes place to give complex **B.** Thus, C-H bond cleavage occurs when the transition metal oxidation state increases.

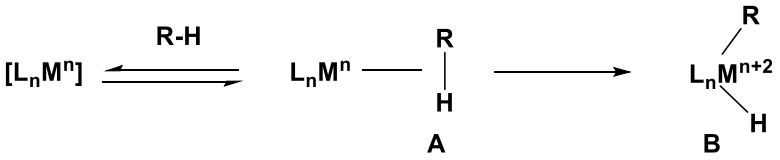

Scheme 1.25. Mechanism of oxidative addition

Figure 1.9a shows the molecular orbital diagram and C-H-M π interactions. Low valent complexes having high electron density of late transition metals (including Re, Fe, Ru, Rh, and Ir) are involved in the oxidative addition pathway.

1.8.2. Electrophilic Activation

Late transition metals involve electrophilic activation in their higher oxidation state. Electrophilic activation of the π-conjugated system or aromatic nucleus has mainly two stages

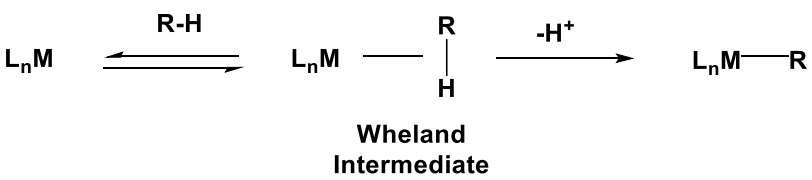

Scheme 1.26. Mechanism of electrophilic activation

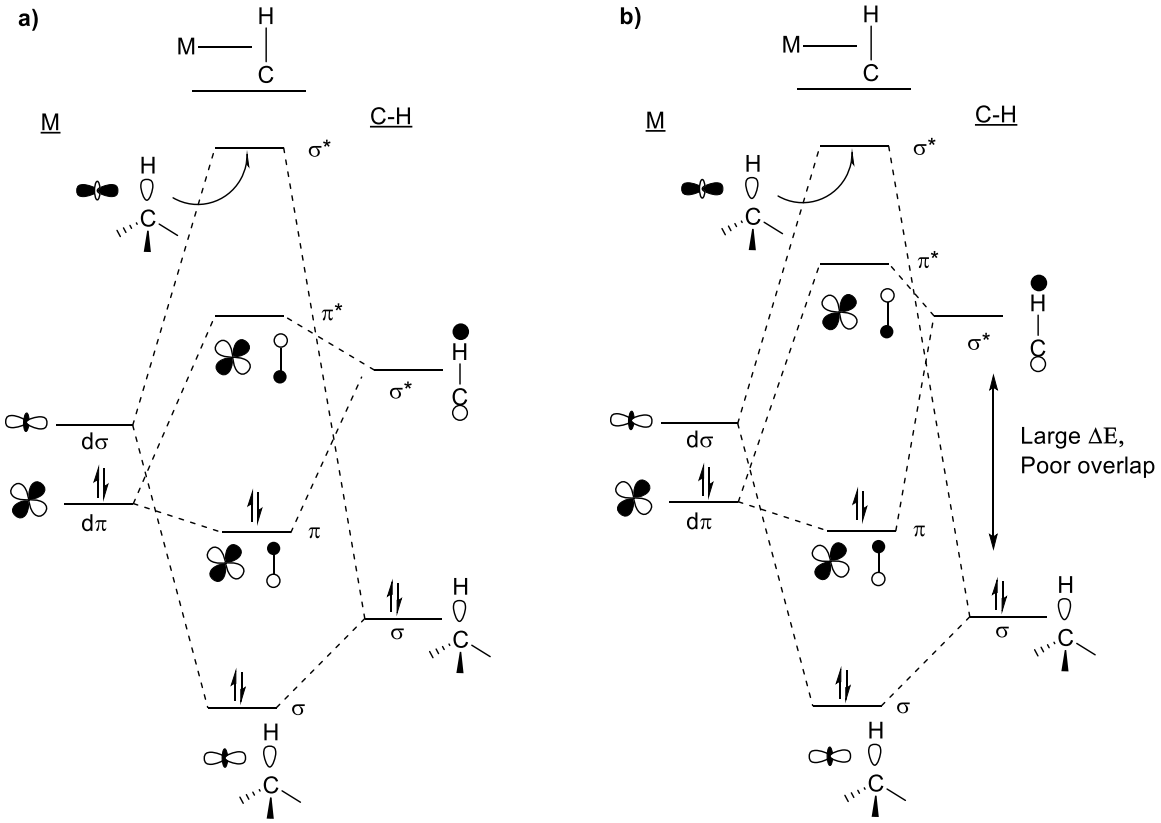

Figure 1.9. Molecular orbital diagrams of (a) oxidative addition and (b) electrophilic activation

attack of electrophilic species to arene to give Wheland intermediate, subsequently *σ*-organyl complex forms by loss of proton (**Scheme 1.26**). **Figure 1.9b** shows the molecular orbital diagram to show electrophilic activation involved by transition metals where d orbital energy dropped (Pd^{2+}, Ti^{3+}, $Pt^{2+/4+}$, and Hg^{2+}).

1.8.3. σ-Bond Metathesis

In this mechanism, σ-bond cleavage is catalyzed by complexes of early transition metals having d^0 orbital. These mainly involve four center transition states (**Scheme 1.27**). As there are no d-electrons, these have no π interactions, as shown in **Figure 1.10**.

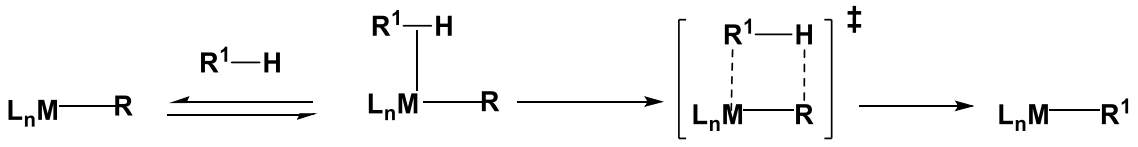

Scheme 1.27. Mechanism of σ-bond metathesis

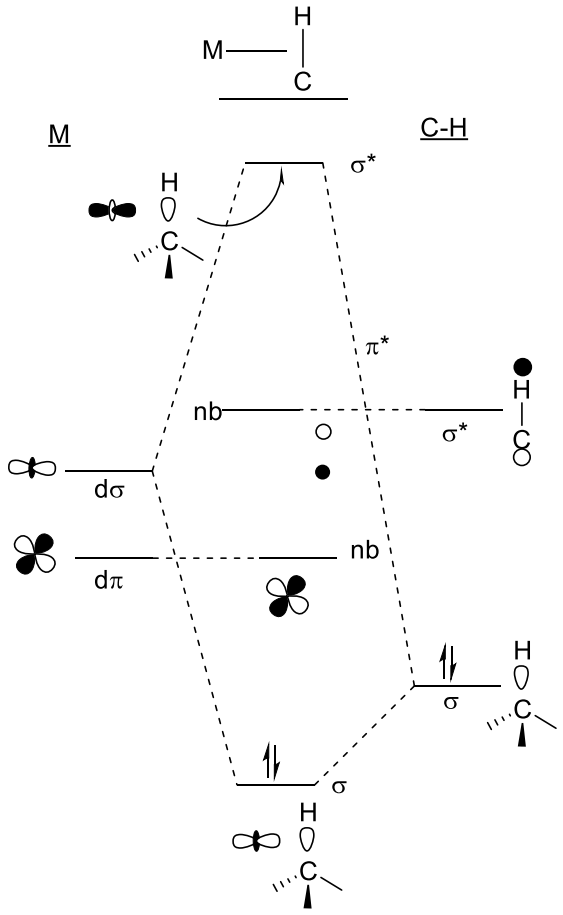

Figure 1.10. Molecular orbital diagram of σ-bond metathesis

1.8.4. 1,2-Addition Reaction

1,2-Addition involves the generation of 4-membered transition state *via* inserting an alkane C- H bond to the metal-nonmetal double bond (**Scheme 1.28**). Most commonly, additions of these bonds to metal-nitrogen or metal-carbon double bonds are known.

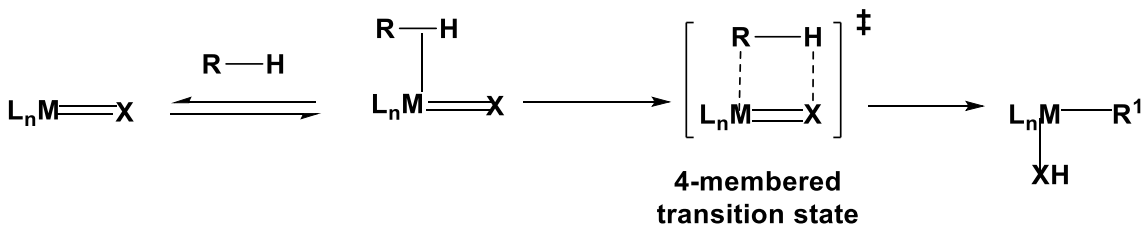

Scheme 1.28. Mechanism of 1,2-addition reaction

1.8.5. Metalloradical Activation

C-H activation of alkanes involves metalloradical activation mechanistic pathway. Here, a complex of transition metal exists in monomer-dimer equilibrium and has the potential to break C-H bond into two fragments. These fragments are added to two halves of the complex (**Scheme 1.29**). Generally, rhodium and ruthenium complexes are used for this type of reaction.

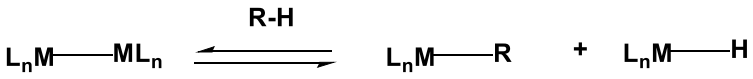

Scheme 1.29. Mechanism of metalloradical activation

1.9. Gaps in the Present Study

The literature was reviewed in detail to find the gaps in the present study. It has been found that the following areas have not been much explored till now:

- C-H bond activations or C-H functionalization using transition metal catalysts on coumarin-based heterocyclic moieties are rare.
- The evaluation of C-H functionalized heterocyclic compounds for anti-tumor activities is rare.
- C-H activation on molecular hybrids of various heterocyclic compounds, such as coumarin, pyrazole, benzimidazole/benzothiazole, etc., has not been explored much.
- Anti-tumor activity on C-H functionalized hybrid molecules is not explained.

1.10. Objectives

1. To functionalize on biological active heterocyclic moieties with C-H activation by using transition metals catalyst.
2. To synthesize and characterize hybrids of biologically active moieties, *viz.*, coumarin, pyrazole, benzimidazole, naphthalimide, indole, etc.
3. To functionalize hybrids of two pharmacophores with C-H activation using a transition metal catalyst.
4. *In vitro* evaluation of C-H functionalized compounds for anticancer activity and to develop their structure-activity relationship.

CHAPTER 2

C(5)–H Functionalization of Quinazolinone-Coumarin Conjugates

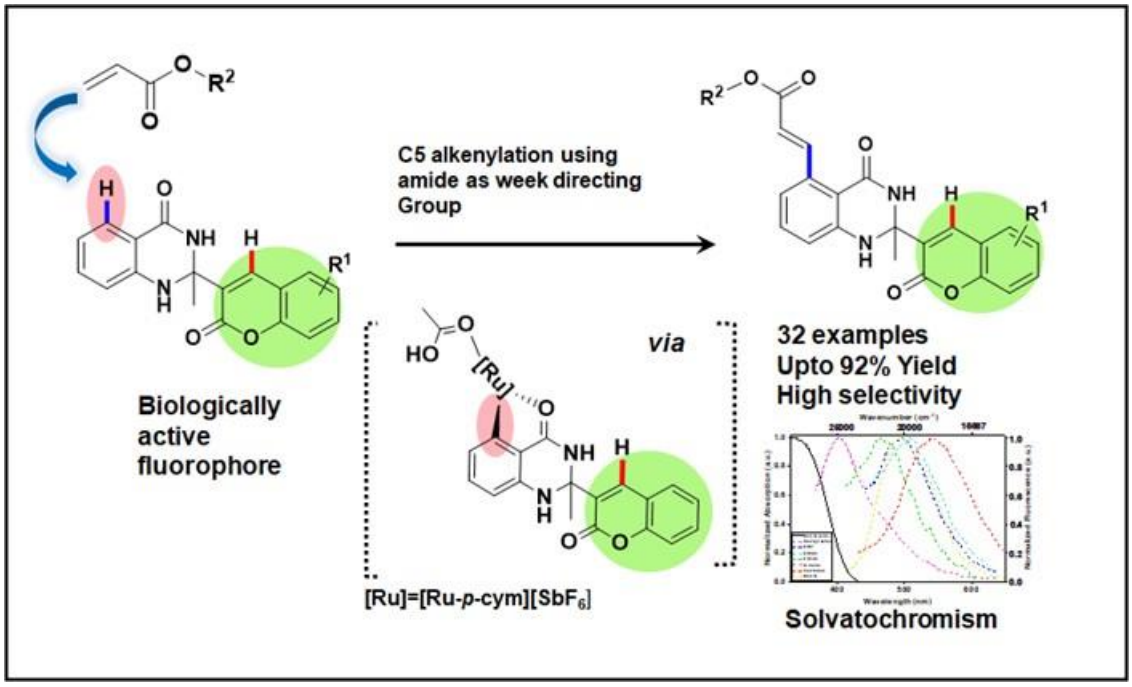

CHAPTER 2

2.1. Introduction

Quinazolinone is a prevalent heterocyclic scaffold in pharmaceutically active compounds with significant bioactivity.[52] These biologically active moieties have either alkylation or arylation at C–2 position of an aromatic ring; these derivatives are prime targets in C–C bond formation through expedient late-stage modification to synthesize analogs of novel drugs. In addition, 2*H*-coumarin also constitutes a particular class of bioactive compounds. 2*H*-coumarin motif has a distinctive structure, remarkable photophysical properties, significant Stokes shift, and high quantum yield. It has excellent application in live-cell imaging and is widely used in material science.[53] Consequently, the construction of quinazolinone and coumarin moieties, and their modification has claimed incessant attention from organic society in recent years.[54] C–H functionalization using transition metal-catalyst has emerged as an efficient synthetic approach for forming functional C–C bonds and late-stage modification by transforming ubiquitous C–H bonds selectively into more reactive groups.[55] Utilizing this strategy to modify bioactive heterocycles such as quinazolinone is a vital synthetic tool to access the synthesis of new drug molecules.[56] Ruthenium-catalyzed C–H bond alkenylation is prevalent in organic synthesis due to pioneering developments by several groups.[57] Methodology using weakly coordinating amide groups to access reactive functional groups has engrossed rapidly.[58] Despite the burgeoning research in this context of regio-selective alkylation or arylation of quinazolinone, this motif has not been used earlier for functionalization at C–5 position governing ruthenium catalysis. Although early work reporting C–2 functionalization of quinazolinone,[59] includes C–2 acetoxylation-methoxylation using palladium catalysis by the Reddy group (**Figure 2.1**).[60] In 2017, the Mhaske group unveiled the mono-arylation of 2-arylquinazolinone using diaryliodonium triflates under palladium catalysis.[61] In 2018, they gave a unique approach for regioselective alkenylation/tandem hydroamination cyclization of 2-arylquinazolinone using alkynes under ruthenium catalysis.[56] Still, reactivity at the unreactive C–5 position of quinazolinone has been rarely observed.[55] In the past few years, the catalytic community has faced a significant hurdle to access unreactive C–H bonds.[62]

2.2. Objective

Herein, the utility of a weakly coordinating amide group of quinazolinone and focus on alkene insertion at C–5 position of quinazolinone *via* chelation assistance is examined. It is

proposed to proceed with this transformation through the cyclometallation activation pathway utilizing a weak directing group. Additionally, photophysical studies of C–H functionalized conjugates are also discussed.

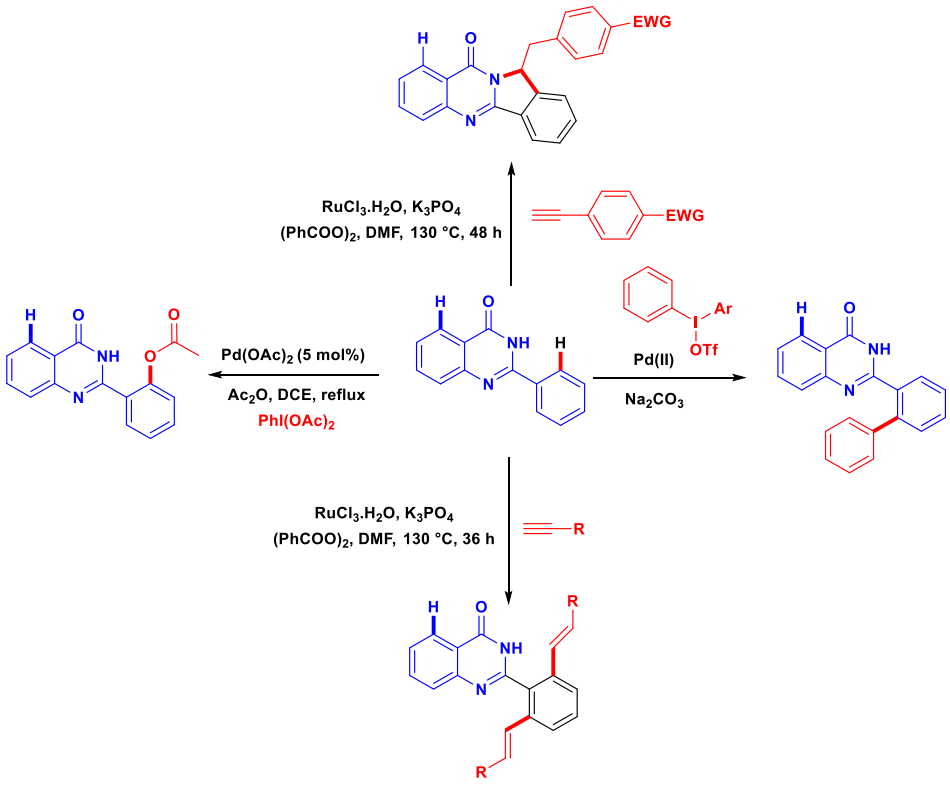

Figure 2.1. C-H functionalization of 2-arylquinazolinone

2.3. Results and Discussion

2.3.1. Synthesis of Coumarin-Quinazolinone Hybrid

To evaluate the envisioned reaction hypothesis, first synthesis of coumarin-quinazolinone conjugates is done (**Scheme 2.1**). Initially, Knoevenagel condensation was performed by reacting salicylaldehyde (**2.1**) with ethyl acetoacetate (**2.2**) using piperidine as a weak base in ethanol and gave 3-acetyl-2*H*-chromen-2-one (**2.3**).[63-67] Compound **3a** was confirmed by ^{1}H NMR spectrum as the compound showed 1H singlet at δ 8.58 ppm, three 1H doublets at δ 7.88, 7.69 and 7.40 ppm, 1H multiplet at δ 7.37 – 7.34 ppm in the aromatic region, and 3H singlet at δ 2.53 due to CH_3 group in the aliphatic region. Then, 3-acetyl-2*H*-chromen-2-one (**2.3**) was reacted with 2-aminobenzamide (**2.4**) in the presence of iodine in DMF to afford the desired hybrid **2.5a** having two active biological pharmacophores such as quinazolinone and coumarin.

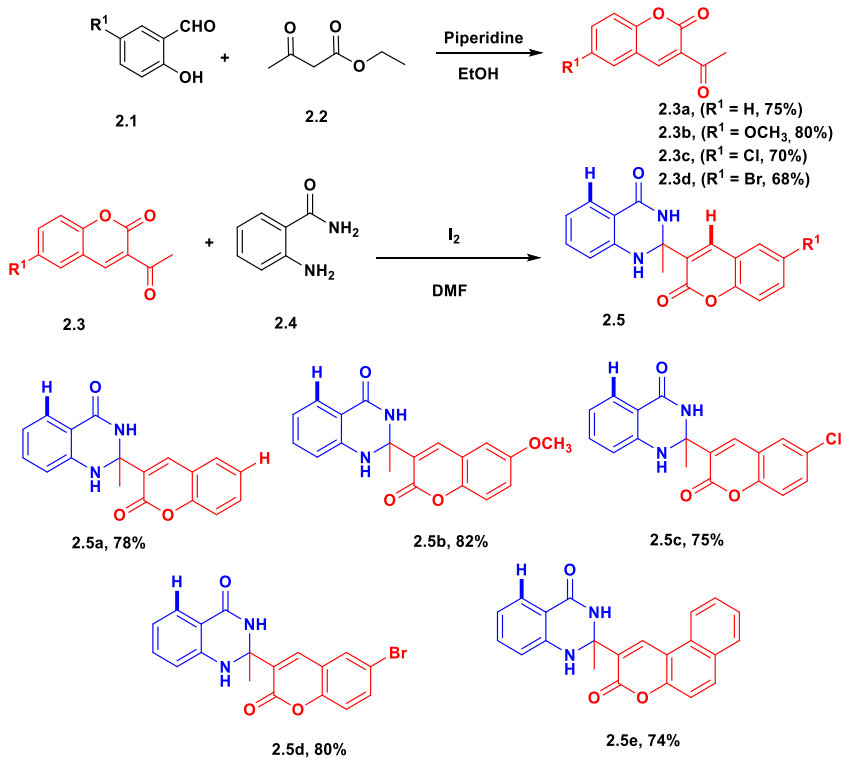

Scheme 2.1. Synthesis of coumarin-quinazolinone hybrid

Compound **2.5a** showed characteristic signals in ^{1}H NMR and ^{13}C NMR, as 1H doublet at δ 8.43 ppm due to CH, 1H singlet at δ 7.77 ppm, two 1H double doublets at δ 7.56 ppm and 7.52 ppm, 1H multiplet at δ 7.50-7.44 ppm, 1H double doublet at δ 7.24 ppm, 2H multiplet at δ 7.22-7.17 ppm and 1H multiplet at δ 6.83-6.78 ppm in aromatic region, two 1H singlets at δ 7.14 and 6.63 ppm due to two NH groups and further 3H singlet at δ 1.76 ppm due to CH_3 group of aliphatic in ^{1}H NMR and signals at δ 69.7 and 26.9 ppm due to methine and methyl groups, respectively in ^{13}C NMR confirmed the structure of compound **2.5a**. Similarly, compounds **5b-5e** were synthesized and characterized with the same methodology.

2.3.2. Optimization for C5-H Alkenylation

I chose 2-methyl-2-(2-oxo-2*H*-chromen-3-yl)-2,3-dihydroquinazolin-4(1*H*)-one (**2.5a**)[68] and *tert*-butyl acrylate (**2.6a**) as the starting substrates for the optimization of reaction condition (**Table 2.1).** Due to electron deficiency, acrylates are more compatible with rhodium, ruthenium, and palladium-catalyzed C–H alkenylation.[69] Initially, the reaction was carried out in NMP using $[RuCl_2(p\text{-cymene})]_2$ as the catalyst at 100 °C, $AgSbF_6$ (10 mol%) as the catalyst activator, and $Cu(OAc)_2.H_2O$ (1.0 equiv) as an oxidant, low conversion was observed under these presuming conditions (entry 1). However, a slight increase in yield of alkenylated product

Table 2.1. Representative optimization of reaction conditions

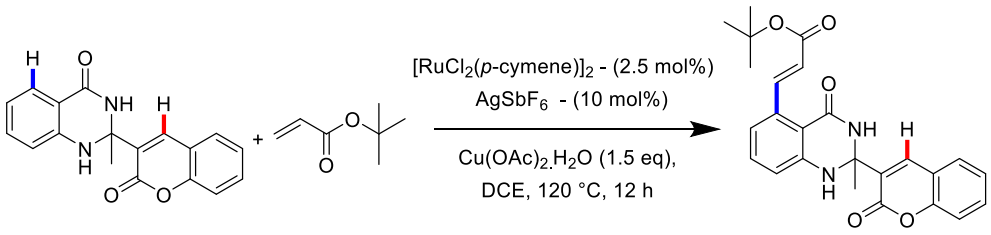

2.5a **2.6a** **2.7aa**

Entry	Solvent	Oxidant	Additive	Yield **2.7aa** (%)[b]
1	NMP	$Cu(OAc)_2.H_2O$	$AgSbF_6$	20
2[c]	1,4-dioxane	$Cu(OAc)_2.H_2O$	$AgSbF_6$	25
3	1,4-dioxane	$Cu(OAc)_2.H_2O$	$AgSbF_6$	30
4	THF	$Cu(OAc)_2.H_2O$	$AgSbF_6$	Traces
5	DMF	$Cu(OAc)_2.H_2O$	$AgSbF_6$	Traces
6	Toluene	$Cu(OAc)_2.H_2O$	$AgSbF_6$	Traces
7[d]	DCE	$Cu(OAc)_2.H_2O$	$AgSbF_6$	65
8	DCE	AgOAc	$AgSbF_6$	60
9	DCE	$Cu(OAc)_2.H_2O$	NaOAc	--
10	DCE	$AgNO_3$	$AgSbF_6$	42
11	DCE	Ag_2CO_3	$AgSbF_6$	25
12[e]	DCE	$Cu(OAc)_2.H_2O$	$AgSbF_6$	82
13[f]	DCE	$Cu(OAc)_2.H_2O$	$AgSbF_6$	--
14	DCE	…….	$AgSbF_6$	--
15	DCE	$Cu(OAc)_2.H_2O$	$NaSbF_6$	Traces
16	DCE	$Cu(OAc)_2.H_2O$	$AgNTf_2$	--

[a]General reaction condition: **2.5a** (1 mmol), **2.6a** (3 mmol), $[RuCl_2(p\text{-cymene})]_2$ (2.5 mol %), $AgSbF_6$ (10 mol %), $Cu(OAc)_2.H_2O$ (1.5 equiv), solvent (2 ml), [b]Isolated yields after purification, [c]temperature = 100 °C, [d]$Cu(OAc)_2.H_2O$ (1 equiv), [e]$Cu(OAc)_2.H_2O$ (1.5 equiv), [f]In absence of $[RuCl_2(p\text{-cymene})]_2$.

2.7aa was observed in 1,4-dioxane at higher temperatures along with the homocoupled byproduct of **2.6a** (entries 2 and 3). Subsequent reactions were carried out in THF, DMF and toluene, but only traces were obtained in these solvents (entries 4-6, respectively), while significant transformation was observed in DCE (entry 7). Hence, DCE was used here as the solvent to facilitate further alkenylation.[70] Intensive screening of oxidants was carried out,

and $Cu(OAc)_2.H_2O$ showed superior activity over other oxidants (entries 7-12). Carboxylate ions of the oxidants were more compatible toward concerted metalation-deprotonation and metal-ligand activation of C–H functionalization. It is worth noting that no efficacy was maintained either in the absence of catalyst $[RuCl_2(p\text{-cymene})]_2$ or oxidant $Cu(OAc)_2.H_2O$ (entries 13 and 14). Multiple additives were examined, but none showed better activity than $AgSbF_6$ (entries 15 and 16). The striking feature of the reaction is high regio-selectivity throughout the optimization. It was significant that only C–5 alkenylations of quinazolinone were obtained; neither C–4 alkenylation of coumarin nor dialkenylated product was observed in TLC or NMR.

Compound **2.7aa** was confirmed by ^1H and ^{13}C NMR spectra as compound showed characteristic signals of aromatic protons in 1H NMR of doublet at δ 8.61 ppm with *J* = 15.9 Hz of 1H, singlet of 1H at δ 7.95 ppm, doublet at δ 7.53 ppm with *J* = 8.1 Hz of 1H, multiplet at δ 7.51-7.48 ppm of 1H, doublet at δ 7.28 ppm with *J* = 8.1 Hz of 2H, doublet at δ 7.20 ppm with *J* = 4.4 Hz of 1H, singlet at δ 7.19 ppm of NH, doublet at δ 6.89 ppm with *J* = 7.3 Hz of 1H, doublet at δ 6.69 ppm with *J* = 8.1 Hz, doublet at δ 6.10 ppm with *J* = 15.9 Hz of 1H and singlet at δ 6.03 ppm of NH. Notably, two vinylic protons have same *J* values of 15.9 Hz ruling out any cyclization. In addition, in aliphatic region, signals as singlet at δ 1.95 Hz of 3H of CH_3 and singlet of 9H of *tert*-butyl acrylate at δ 1.48 Hz confirmed the incorporation of acrylate to the starting substrate. Furthermore, characteristic signals in ^{13}C NMR at δ 69.6 ppm showed methine group, and at δ 28.2 ppm of methyl group confirmed the structure.

2.3.3. Substrate Scope for C5-H Alkenylation

After optimization of the feasible reaction condition, then turned to examine the scope of this catalytic conversion by reacting 2-methyl-2-(2-oxo-2*H*-chromen-3-yl)-2,3-dihydroquinazolin-4(1*H*)-one (**2.5a**) with various acrylates (**Scheme 2.2**). Methyl, ethyl, and *n*-butyl acrylates (**2.6b-d**) reacted well with **2.5a** to give corresponding alkenylated products **2.7ab-2.7ad** up to 90% yields. Phenyl vinyl sulfone, which has dienophilic properties, was also employed, and this substrate provides desired product **2.7ae** in 78% yield.

Furthermore, 2-ethyl hexyl acrylate (**2.6f**), having a long aliphatic side chain, and isobornyl acrylate (**2.6g**) bearing cyclic side chain were also well-compatible reactants for this catalytic transformation (**2.7af-2.7ag**). Moreover, to show the catalytic activity, various electron-deficient alkenes, such as propargyl acrylate, methyl vinyl ketone, acrylonitrile, acrylic acid, etc., having low volatility and low reactivity, were employed under the same conditions. Among these substrates, only methyl vinyl ketone has shown a good yield of

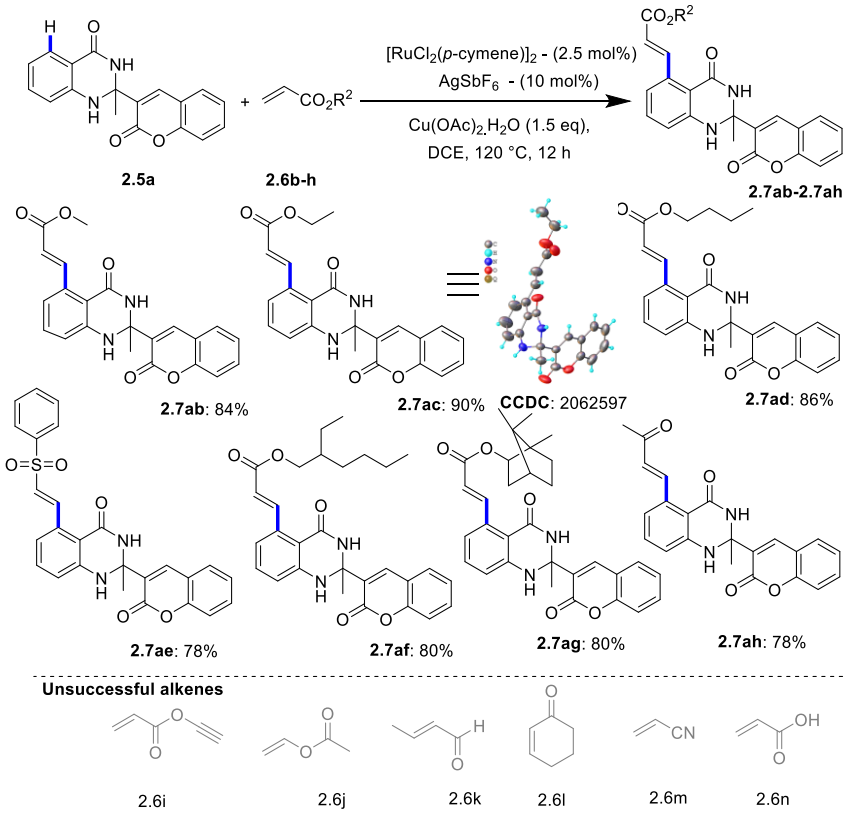

Scheme 2.2. Alkene scope for the alkenylation of conjugates

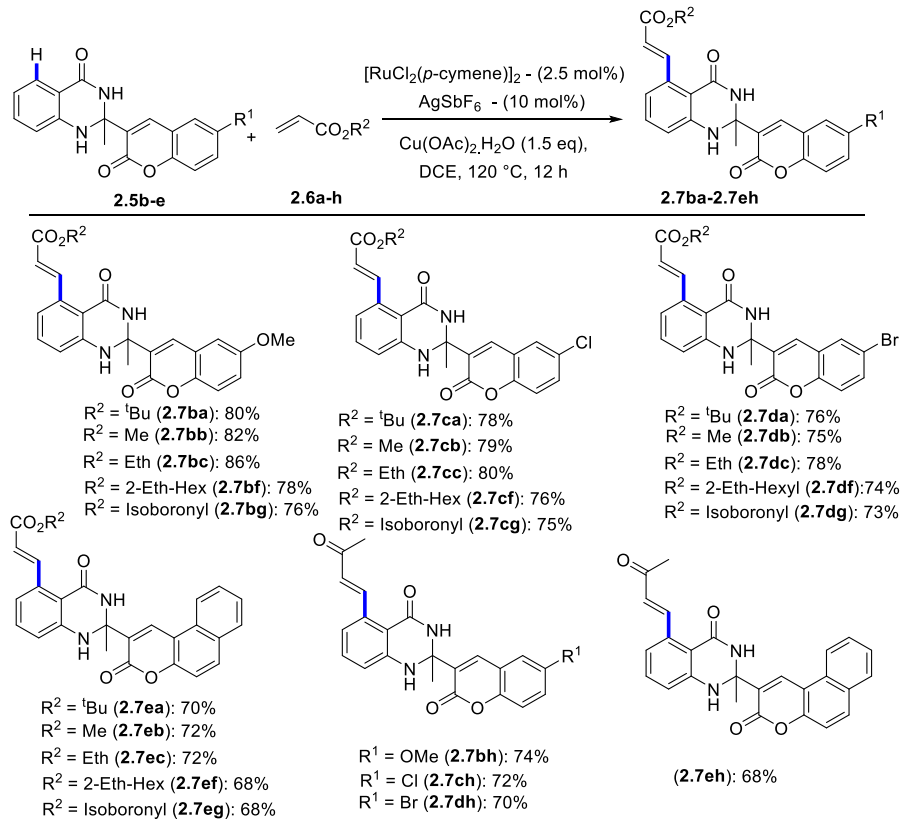

Scheme 2.3. Substrate scope of Ru(II) catalyzed C–H alkenylation

compound **2.7ah** (78%). As coumarin has significant photophysical properties, I have primarily substituted the coumarin nucleus with electron-withdrawing and -donating groups to check the reaction scope and photophysical behaviour. Initially, the electron-donating effect was investigated using a methoxy group on coumarin nucleus (**2.5b**) with various alkenes; the corresponding compounds were obtained in excellent yields.

Similarly, electron-withdrawing groups on coumarin nuclei, such as Br, Cl and aryl (**2.5c-2.5e**), were also investigated with the same alkenes and gave the desired products (**2.7ca-2.7eg**) in good yield, shown in **Scheme 2.3**. In addition to acrylates, methyl vinyl ketone as the reacting partner also tested having different electronic properties and terminal functions with substituted conjugates of coumarin and quinazolinone (**2.5b-2.5e**) to give corresponding compounds **2.7bh-2.7eh** in 68% to 90% yields. In selectivity and mono-alkenylation, compound **2.7ac** gave an excellent yield of 90%. Compound **2.7ac** was further characterized by single-crystal X-ray crystallography (**CCDC no.** 2062597) to provide more insights into regioselectivity alkenylation. Compound **2.7ac** comprises three planar fragments, coumarin, quinazolinone, and ethyl acrylate, which are in conjugation with each other. Compound **2.7ac**, has Z = 4 and exhibits monoclinic structure in the space group P21/c (**Table 2.2**).

Table 2.2. X-ray analysis of compound **2.7ac**

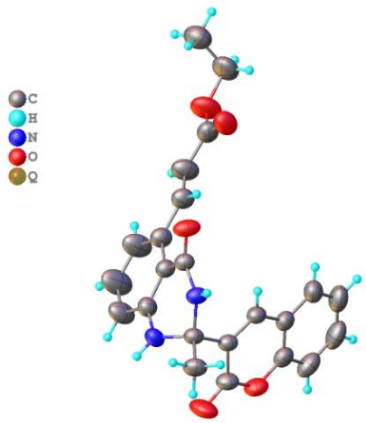

Identification code	**Pat-1**
Empirical formula	$C_{23}H_{20}N_2O_5$
Formula weight	404.41
Temperature/K	293(2)
Crystal system	monoclinic

Space group	P21/c
a/Å	12.2737(4)
b/Å	13.4317(3)
c/Å	12.8708(4)
α/°	90
β/°	106.481(3)
γ/°	90
Volume/Å3	2034.66(11)
Z	4
ρcalcg/cm3	1.320
μ/mm-1	0.094
F(000)	848.0
Crystal size/mm3	0.08 × 0.06 × 0.055
Radiation	MoKα (λ = 0.71073)
2Θ range for data collection/° 6.528 to 54.786	
Index ranges	-15 ≤ h ≤ 15, -17 ≤ k ≤ 16, -15 ≤ l ≤ 16
Reflections collected	26160
Independent reflections	4407
Data/restraints/parameters	1.093
Goodness-of-fit on F2	R1 = 0.0669, wR2 = 0.1404

2.3.4. Gram Scale and Further Transformation

A scale-up experiment was set up to examine the efficacy of the present methodology and industrial utility, giving 88% yield of the alkenylated product (**Scheme 2.4a**) and reducing the catalyst and co-catalyst loads gave **2.7aa** in 70% yield along with recovery of 25% of starting material (**Scheme 2.4b**). The compound has ester and alkene groups, allowing further transformation to form highly decorated scaffolds. Alkaline hydrolysis of ester allowed access to the corresponding compound **2.8a** (60%) without interacting with other heterocycles (**Scheme 2.4c**).

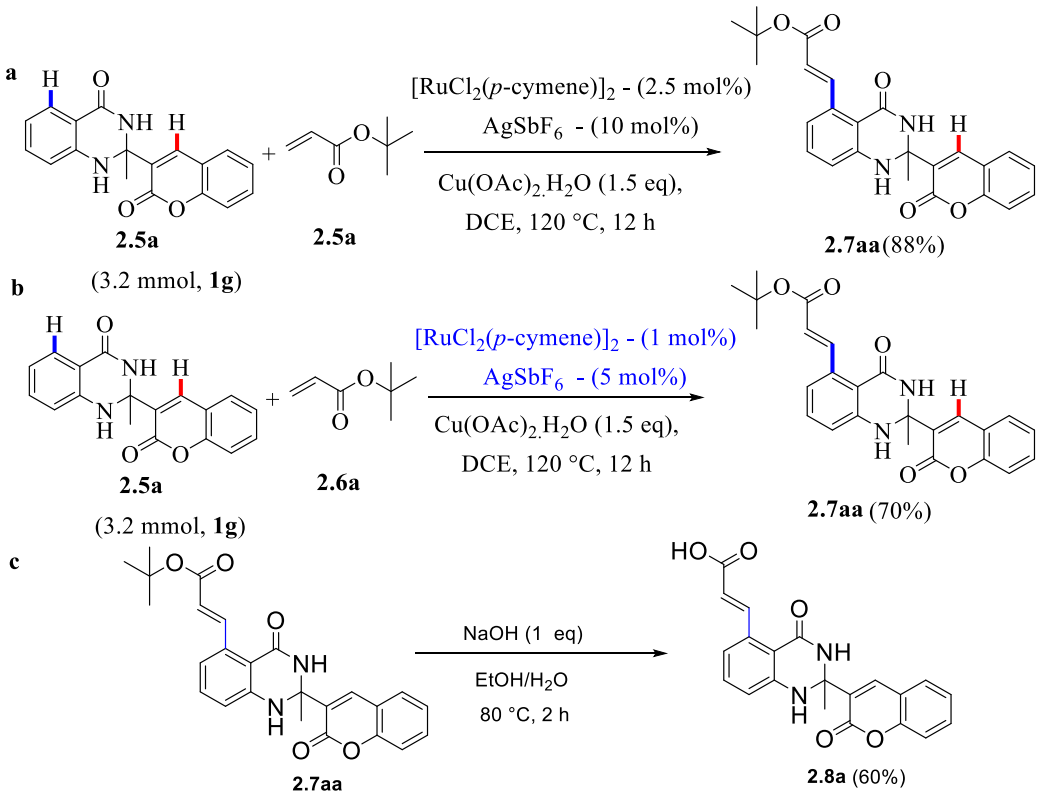

Scheme 2.4. Gram scale and further transformation

2.3.5. Amide Selectivity

To check the role of an amide as a directing group, I carried out chlorination[71] with $POCl_3$ and performed C–H alkenylation using optimized conditions on chlorinated reactant **2.5f**, but no product was observed. Thus, the amide-directing group is essential for quinazolinone's C–5 alkenylation (**Scheme 2.5**).

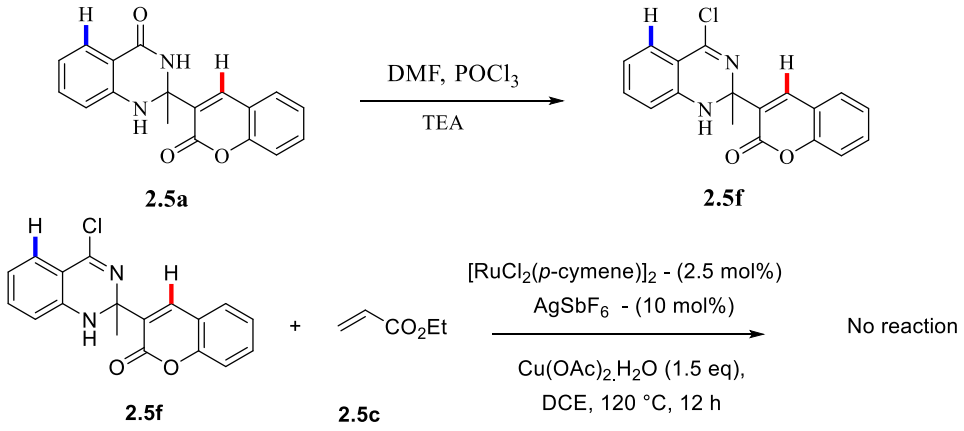

Scheme 2.5. To check the selectivity of an amide group

2.3.6. Deuterium Labeled and Control Experiments

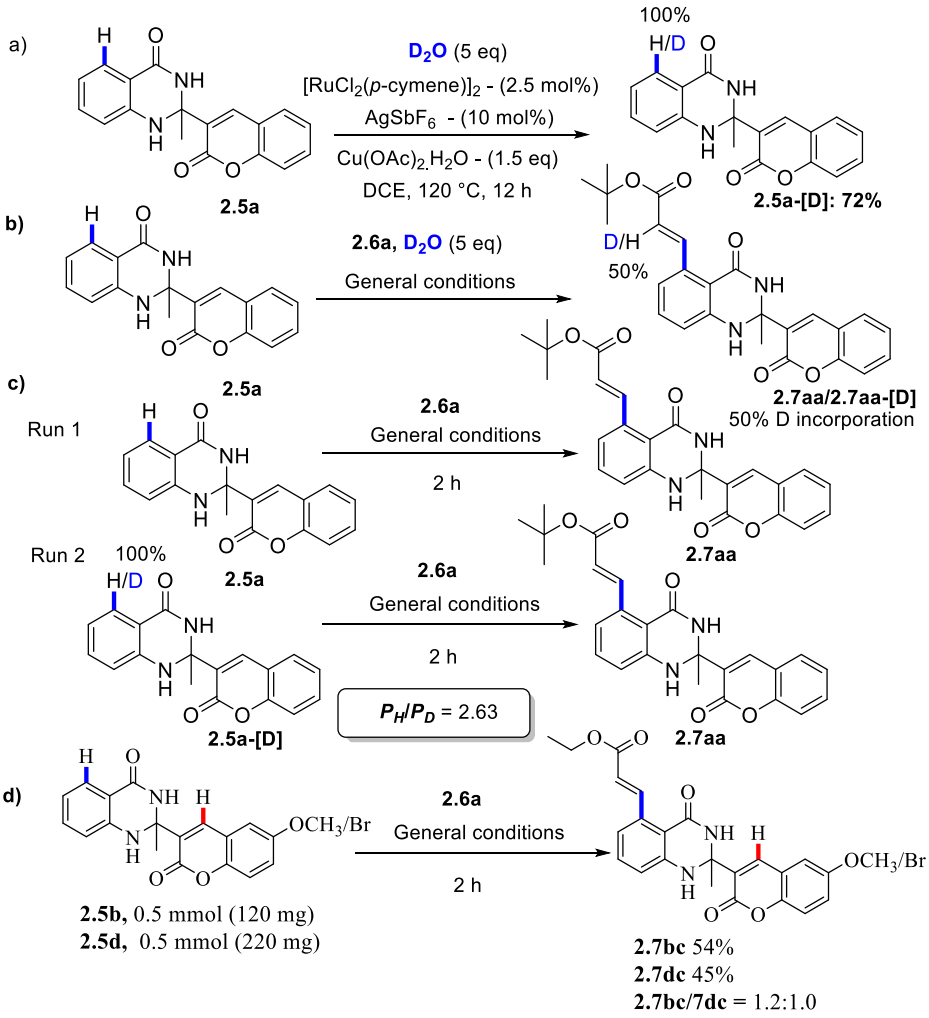

Scheme 2.6. Deuterium labeled and control experiments

To get more mechanistic knowledge, substrate **2.5a** was treated with optimized reaction conditions without **2.6a** using 5 equiv of D_2O, 100% H–D exchange was observed at reactive site in isotopically labeled structure **2.5a-[D]**, which indicates reversibility of C–H activation step (**Scheme 2.6a**).[72] When **2.5a** was exposed to optimal conditions of deuterium source and acrylate **2.6a**, 50% deuterium incorporation was seen at one of the vinylic hydrogen, indicating that catalytic cycle may include a protodemetalation phase (**Scheme 2.6b**).[55] To examine the kinetic isotope effect (KIE), parallel reactions between **2.5a** and deuterated substrate **2.5a-[D]** (**Scheme 2.6c**) were carried out using general procedure C with the following reactants: 2-Methyl-2-(2-oxo-2*H*-chromen-3-yl)-2,3-dihydroquinazolin-4(1*H*)-one, **2.1a** (0.30 g, 1 mmol, 1.0 eq) or **2.1a-[D]** (0.30 g, 1.0 mmol, 1.0 eq), *tert*-butyl acrylate (0.44 mL, 0.38 g, 3.0 mmol, 3.0 eq), $[RuCl_2(p\text{-cymene})]_2$ (0.025 mmol), $AgSbF_6$ (0.035 g, 0.1

mmol), $Cu(OAc)_2.H_2O$ (0.27 g, 1.5 mmol, 1.5 eq). The crudes were purified using column chromatography and analyzed using NMR. This experiment showed a relevant *KIE* as P_H/P_D = 2.63, suggesting that C–H cleavage is in or near the rate-determining step.[73] In the intermolecular competition experiment between **2.5b** and **2.5d** in an oven-dried 50 ml round bottom flask was performed, a solution was made of **2.1b** (0.17 g, 0.5 mmol, 0.5 eq), **2.1d** (0.19 g, 0.5 mmol, 0.5 eq), acrylate **2.2c** (3 mmol, 3.0 eq) in 2 ml DCE in an inert atmosphere of nitrogen followed by the addition of $Cu(OAc)_2.H_2O$ (0.27 g, 1.5 mmol, 1.5 eq), then loaded the catalytic system: $[RuCl_2(p\text{-cymene})]_2$ (2.5 mol%) and $AgSbF_6$ (10 mol%). The resulting reaction mixture was refluxed under nitrogen at 120 °C (using an oil bath) for 12 h. NMR analysis was carried out on a crude sample gave **2.7bc/2.7dc** as 1.2:1.0 ratio, which indicates, electron-donating groups have more compatibility for this reaction **(Scheme 2.6d)**.

2.4. Proposed Mechanism

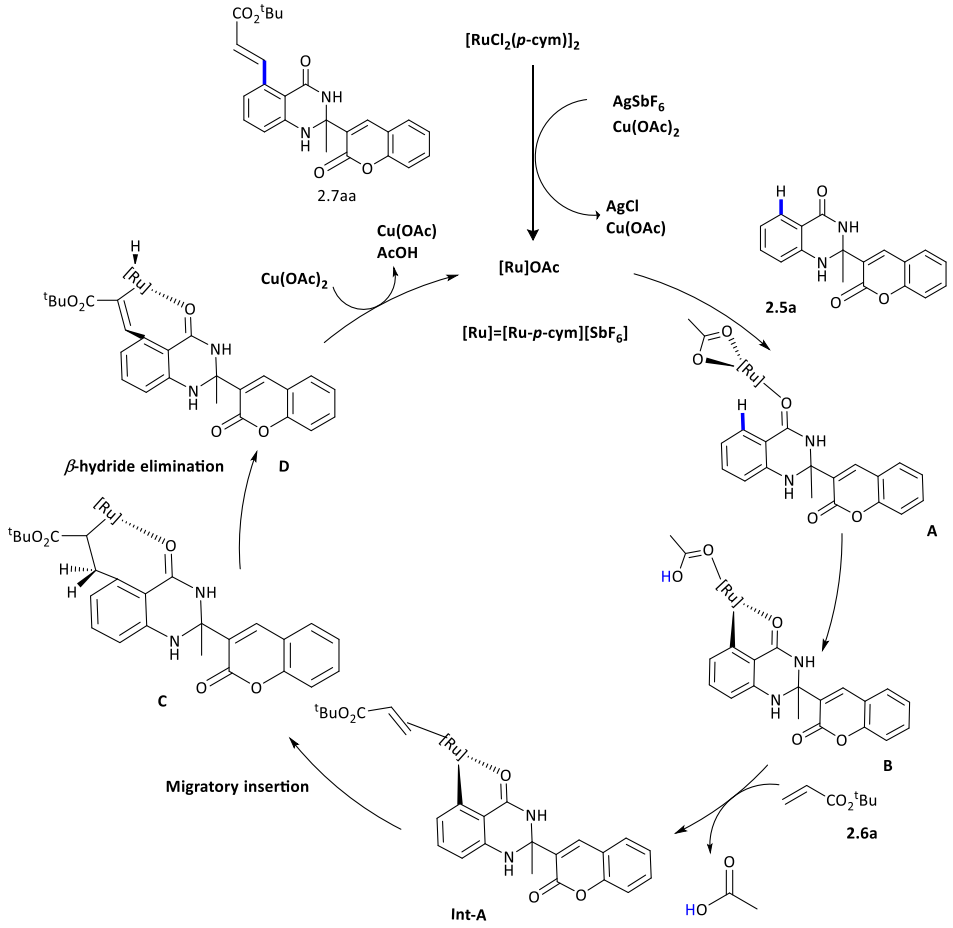

Scheme 2.7. Catalytic cycle

Based on the above studies and literature precedent, I proposed a plausible mechanism for Ru(II) catalyzed C–5 alkenylations of **2.5a** based on experimental analysis, computational studies, and literature precedent. Coordination of amide's oxygen atom of substrate **2.5a** with active catalyst gives complex **A** and forms a five-membered ruthenacycle *via* sp^2 C_5–H insertion to give complex **B** that undergoes alkene insertion to generate **Int-A**, which readily converts into complex **C** after migratory alkene insertion. Complex **C** undergoes *β*-hydride elimination followed by protodemetalation to obtain desired compound **2.7aa** (**Scheme 2.7**).[72]

2.5. Photophysical Studies

Further, photophysical studies of synthesized compounds have been performed. To better understand and investigate the substitution effect on the coumarin nucleus of conjugates, I have chosen compounds **2.7ah-2.7eh**. The parent compound **2.7ah** has absorption maxima at 328 nm, while methoxy-substituted compound **2.7bh** has absorption maxima at 345 nm. Compounds substituted with chloro (**2.7ch**) and bromo (**2.7dh**) have absorption maxima at 326 nm **(Figure 2.2),** while increasing π conjugation on the coumarin nucleus, compound **2.7eh** has an absorption band at 316 nm. These compounds have shown hypsochromic shift with electron-withdrawing groups in the absorption band. On the other hand, the parent compound **2.7ah** has emission maxima lying at 451 nm with a Stokes shift of 8300 cm^{-1}. On substitution, using electron-donating group (methoxy) corresponding derivative **2.7bh** led to significant bathochromic shift to 485 nm with Stokes shift 8400 cm^{-1}. However, on the introduction of chloro and bromo, respective derivatives **2.7ch** and **2.7dh** have emission wavelengths at 405 nm with Stokes shift 6000 cm^{-1} and 428 nm with Stokes shift 7300 cm^{-1} (**Table 2.3**). On increasing the π conjugation on the coumarin nucleus, the derivative **2.7eh** has emission maxima at 407 nm with Stokes shift 7100 cm^{-1}. Relative quantum yields,[74] were calculated with hymecromone as standard (Φ_F = 0.74).[75] The determination of the fluorescence quantum yield of a fluorophore using a relative optical method consists of the following steps: (i) measurement of the absorption and emission spectrum of the sample, (ii) choice of a suitable fluorescence quantum yield standard absorbing and emitting within a similar wavelength region as the sample the quantum yield of which should be reliably known for the measurement conditions to be used (e.g., solvent/matrix, excitation wavelength, temperature, chromophore concentration), (iii) choice of measurement conditions (e.g., excitation wavelength λ_{ex} and absorbance at λ_{ex}, identical instrument settings

for sample and standard) and measurement of the corresponding absorption and emission spectra of sample and standard and the emission spectra of the corresponding solvents, that must be subtracted from the emission spectra of sample and standard to remove possible background signals (scattering and fluorescence from the solvent; dark counts at the detector), and (iv) data evaluation and calculation of the relative fluorescence quantum yield according to **formula 1**. It has been found that electron-withdrawing groups and extended π conjugation appeared to have low quantum yields.

$$\boldsymbol{\Phi(f,x)} = \Phi(f,st).\frac{F(x)}{F(st)} \cdot \frac{F(st).\Lambda ex}{F(st)\Lambda ex}.\frac{nx^2}{nst2} \quad \textbf{(formula 1)}$$

Table 2.3. Photophysical properties of 2.7ah-2.7eh

Structure	$\lambda_{max,Abs}$(nm)[a]	ε (M^{-1} cm^{-1})	$\lambda_{max,Em}$(nm)[b,c]	(Φ_F)	Stokes Shift (cm^{-1})
2.7ah	328	7150	451	0.08	8300
2.7bh	345	3450	485	0.27	8400
2.7ch	326	5050	405	0.18	6000
2.7dh	326	6250	428	0.10	7300
2.7eh	316	15150	407	0.30	7100

[a]Absorption maxima in acetonitrile (20 × 10^{-6} M). [b]Emission maxima in acetonitrile (20 × 10^{-6} M). [c]Fluorescence quantum yields determined by hymecromone (Φ_F = 0.74 in acetonitrile).

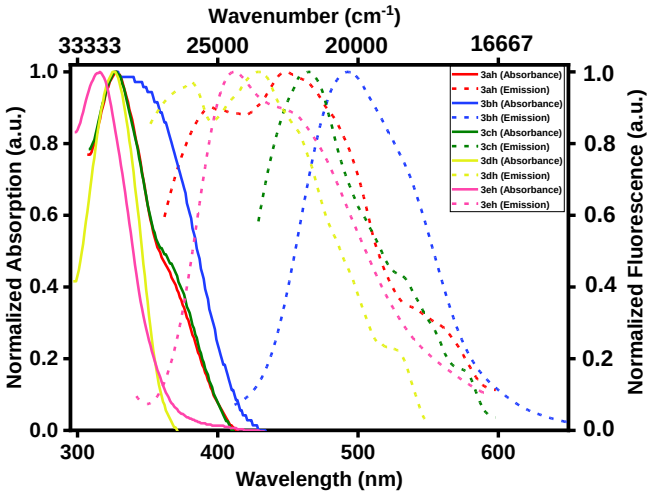

Figure 2.2. Absorption maxima (solid lines) and emission maxima (dashed lines) of **2.7ah-2.7eh** in acetonitrile.

In contrast, the electron-donating group has a significant effect and increases fluorescence efficiency. Fascinated by increased absorption and emission efficiency, I performed solvatochromic studies using **2.7bh** to investigate the solvent effect by recording its absorption and emission spectra in different solvents of different polarities (**Figure 2.3a**).

Table 2.4. Photophysical properties of 2.7bh in different solvents

Solvent	$\lambda_{max,Abs}$ (nm)	$\lambda_{max,Em}$ (nm)	Stokes Shift (cm^{-1})
Toluene	342	404	4500
diethyl ether	340	404	4700
ethyl acetate	338	466	8100
Acetonitrile	345	485	8400
dimethylformamide	345	497	8900
dimethylsulphoxide	345	507	9300
Methanol	350	541	10100

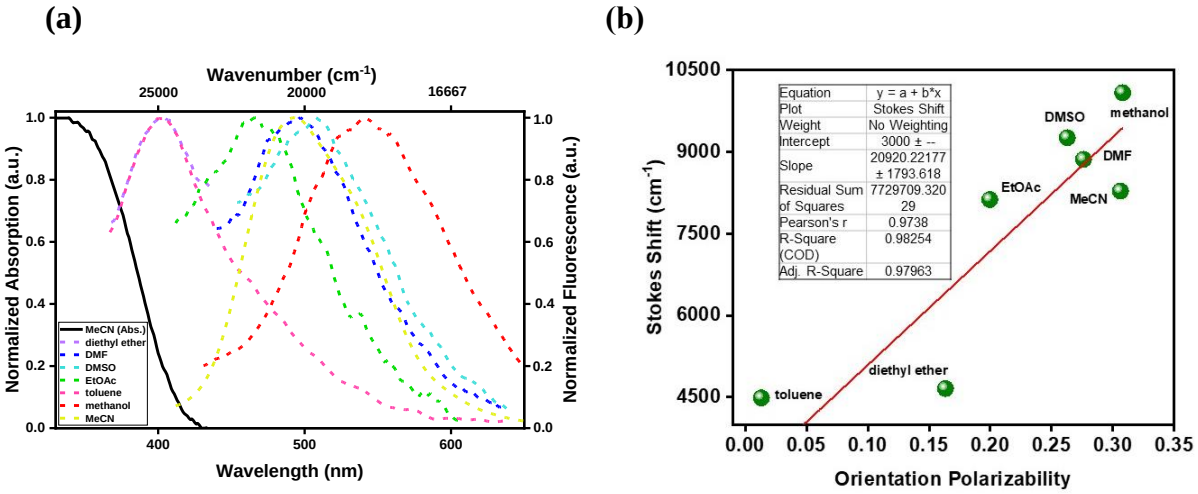

Figure 2.3. (**a**) Absorption maxima (solid line) in acetonitrile and emission maxima (dashed lines) of **7bh** in different solvents and (**b**) Lippert plot of compound **2.7bh**

Notably, no solvatochromic is observed in absorption maxima, as it remains almost the same between 338 to 350 nm. However, solvent polarity significantly impacts emission maxima, ranging from 404 nm in toluene to 541 nm in methanol (**Table 2.4**). Lippert plot[16] between Stokes shift against orientation polarizability of respective solvent gave satisfactory linear correlation (**Figure 2.3b**). Orientation polarizability for each solvent was computed

using eq 2.1,[74,] where ε_r is the electrical permittivity, and *n* is the refractive index of the respective solvent.

$$\Delta f = \frac{\varepsilon_r - 1}{2\varepsilon_r + 1} - \frac{n^2 - 1}{2n^2 + 1} \qquad (\text{eq } 2.1)$$

2.6. Conclusion

In summary, I am able to synthesize the hybrid of two heterocyclic moieties (coumarin and quinazolinone) *via* molecular hybridization technique. Followed by, I have developed the first ruthenium-catalyzed regioselective C–5 alkenylation of quinazolinone-coumarin conjugates using amide as the weak directing group. This was accomplished using the concept of cyclometallation. This methodology has led to the synthesis of 32 novel alkenylated quinazolinone conjugates with absolute regioselectivity and up to 90% yield that allowed access to late-stage functionalization. In addition, gram scale and further transformation experiments have been performed successfully to examine the utility at large scale. Moreover, photophysical properties such as relative quantum yield, molar extinction coefficient, and Stokes shifts have been calculated. In addition, various substitution patterns and their effects on photophysical properties of interesting fluorophores have been studied, and subsequently, these compounds have shown positive solvatochromism.

2.7. Experimental Section

General Information. All the reactions were performed under an inert atmosphere of N_2 in oven-dried glassware. Commercially available reagents were obtained from Sigma-Aldrich, Alfa Aesar, and Spectrochem Pvt. Ltd., India, and used without any purification unless stated. Anhydrous solvents such as 1,2-dichloroethane (DCE) and *N,N*-dimethylformamide (DMF) were used. Anhydrous solvents and other chemicals were transferred to the dried glassware using syringes purged with N_2 before use. Reactions were monitored using thin-layer chromatography (TLC) on silica plates coated with silica gel HF-254. TLCs were seen with UV light (254 or 365 nm) or I_2 staining. Purifications were carried out by column chromatography using SiO_2 (60-120 mesh). Samples were loaded on a small amount of silica gel and transferred to a silica bed. ^1H and ^{13}C NMR spectra were recorded on Jeol-400 MHz or Jeol-500 MHz spectrometer (^1H NMR at 400 MHz or 500 MHz, $^{13}C\{^1H\}$ NMR at 101 MHz or 126 MHz). Chemical Shifts were expressed in parts per million with TMS as an internal reference, and residual peaks for deuterated solvents are $CDCl_3$ at 7.26 ppm, D_2O at 4.79 ppm, and DMSO-d_6 at 3.33 ppm or 2.50 ppm. The following abbreviations represent the

NMR data (s, singlet; d, doublet; t, triplet; q, quartet; dd, doublet of doublets; dt, doublet of triplets, m, multiplet). Electrospray ionization high-resolution mass spectrometry was performed on a Bruker micrOTOF spectrometer. The SuperNova system for single-crystal X-ray diffraction was used for crystal analysis manufactured by Oxford-Rigaku Analytical X-ray Systems. The system consists of a four-axis KAPPA goniometer module with a HyPix3000 detector with a micro-focus Mo source. For absorption spectra 'Shimadzu-2600' UV-visible spectrophotometer was used whereas for emission studies 'Agilent carry eclipse fluorescence spectrophotometer' was used.

General procedure A, involved the synthesis of 3-acetyl-2*H*-chromen-2-one through Knoevenagel condensation. Initially, in an oven-dried 50 ml round bottom flask, salicylaldehyde (5 mmol, 1.0 eq) was taken in ethanol (2 ml).[10b-10e] The solution was stirred at room temperature for 15 min, followed by adding a catalytic amount of piperidine (10 mol%), and ethyl acetoacetate (7.5 mmol, 1.5 eq). The resulting solution was stirred at room temperature for 2 h. The reaction mixture was diluted using water and stirred further for 15 min; the white solid was separated which was filtered off. The resulting crude was purified using column chromatography (EtOAc: Hexane 10:90) to **2.3a** yield 3-acetyl-2*H*-chromen-2-one.

General procedure B for the synthesis of quinazolinone-coumarin conjugates, the sealed tube was charged with 3-acetyl-2*H*-chromen-2-one (188 mg, 1 mmol, 1.0 eq), iodine (63 mg, 0.5 mmol, 0.5 eq), and DMF (2 ml). The reaction mixture was heated at 110 °C in an oil bath for 30 min and then added 2-aminobenzamide (135 mg, 1 mmol, 1.0 eq) and heated again at the same temperature for next 16 h until complete conversion of 3-acetyl-2*H*-chromen-2-one (monitored by TLC). The reaction was diluted with water (20 ml), and the solid was separated, which was filtered off. The crude was purified using column chromatography (EtOAc: Hexane 30:70) to yield **2.5a** as a pure white compound (239 mg, 78%).

General procedure C for the synthesis of alkenylated products. In an oven-dried 50 ml round bottom flask, a solution was made of the coumarin-quinazolinone conjugate (1 mmol, 1 eq), acrylate (3 mmol, 3.0 eq) in 2 ml DCE in an inert atmosphere of nitrogen followed by the addition of $Cu(OAc)_2.H_2O$ (1.5 mmol, 1.5 eq), then loaded the catalytic system: $[RuCl_2(p\text{-cymene})]_2$ (2.5 mol%) and $AgSbF_6$ (10 mol%). The resulting reaction mixture was refluxed under nitrogen at 120 °C (using an oil bath) for 12 h. The reaction was quenched with DCM (10 ml) and then passed through the celite pad followed by the

extraction with DCM (3 × 50 ml); the combined organic layers were washed with brine solution and dried over sodium sulfate, and then concentrated under reduced pressure. The crude product was purified using column chromatography (EtOAc: Hexane 30:70 to 70:30) to yield the desired compound.

3-Acetyl-2*H*-chromen-2-one (**2.3a**)

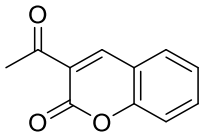

3-Acetyl-2*H*-chromen-2-one was synthesized using general procedure A and obtained as white solid compound, 75% (410 mg); R_f = 0.5 (10% EtOAc + Hexane); **mp** 110-112 °C. **^{1}H NMR** (400 MHz, DMSO-d_6) δ 8.58 (s, 1H), 7.88 (dd, *J* = 7.7, 1.6 Hz, 1H), 7.69 (dd, *J* = 8.4, 7.3 Hz, 1H), 7.40 (d, *J* = 6.4 Hz, 1H), 7.37 – 7.34 (m, 1H), 2.53 (s, 3H).

3-Acetyl-6-methoxy-2*H*-chromen-2-one (**2.3b**)

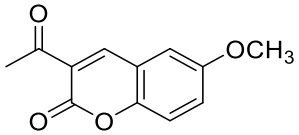

3-Acetyl-6-methoxy-2*H*-chromen-2-one was synthesized using general procedure A and obtained as white solid compound, 80% (510 mg); R_f = 0.5 (20% EtOAc + Hexane); **mp** 170-172 °C. **^{1}H NMR** (400 MHz, DMSO-d_6) δ 8.54 (s, 1H), 7.41 (dd, *J* = 7.7, 1.5 Hz, 1H), 7.36 (dd, *J* = 8.2, 1.5 Hz, 1H), 7.29 (d, *J* = 7.7 Hz, 1H), 2.52 (s, 3H).

3-Acetyl-6-chloro-2*H*-chromen-2-one (2.3c)

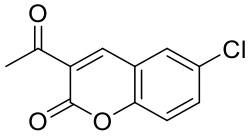

3-Acetyl-6-chloro-2*H*-chromen-2-one was synthesized using general procedure A and obtained as white solid compound, 70% (390 mg); R_f = 0.5 (30% EtOAc + Hexane); **mp** 217-219 °C. **^{1}H NMR** (400 MHz, DMSO-d_6) δ 8.40 (s, 1H), 7.62 (d, *J* = 2.4 Hz, 1H), 7.58 (dd, *J* = 8.8, 2.5 Hz, 1H), 7.32 (d, *J* = 8.9 Hz, 1H), 1.57 (s, 3H).

3-Acetyl-6-bromo-2*H*-chromen-2-one (2.3d)

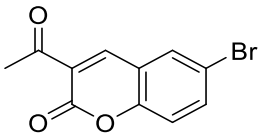

3-Acetyl-6-bromo-2*H*-chromen-2-one was synthesized using general procedure A and obtained as white solid compound, 68% (390 mg); R_f = 0.5 (30% EtOAc + Hexane); mp 220-223 °C. ^{1}H NMR (400 MHz, DMSO-d_6) δ 8.54 (s, 1H), 8.14 (d, *J* = 21.8 Hz, 1H), 7.79 (dd, *J* = 8.9, 2.5 Hz, 1H), 7.35 (d, *J* = 8.8 Hz, 1H), 2.53 (s, 3H).

2-Acetyl-3*H*-benzo[*f*]chromen-3-one (**2.3e**)

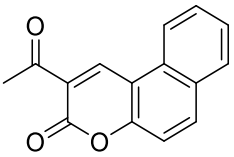

2-Acetyl-3*H*-benzo[*f*]chromen-3-one was synthesized using general procedure A and obtained as white solid compound, 68% (390 mg); R_f = 0.5 (30% EtOAc + Hexane); **mp** 190-193 °C. **^{1}H NMR** (400 MHz, $CDCl_3$) δ 8.76 (s, 1H), 8.29 (d, *J* = 8.9 Hz, 1H), 7.97 (d, *J* = 9.4 Hz, 1H), 7.76 (dd, *J* = 9.6, 1.7 Hz, 1H), 7.67 (td, *J* = 8.6, 1.7 Hz, 1H), 7.57 (d, *J* = 2.7 Hz, 1H), 7.56 (s, 1H), 1.98 (s, 3H).

2-Methyl-2-(2-oxo-2*H*-chromen-3-*yl*)-2,3-dihydroquinazolin-4(1*H*)-one (2.5a).

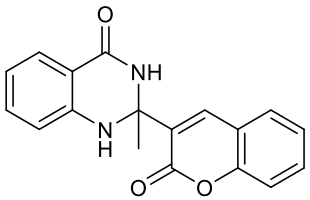

Compound **2.5a** was synthesized using general procedure B and obtained as white solid **2.5a** in 78% (0.24 g); R_f = 0.5 (30% EtOAc + Hexane); **mp** 178-182 °C. **^{1}H NMR** (400 MHz, DMSO-d_6) δ 8.43 (d, *J* = 1.1 Hz, 1H), 7.77 (s, 1H), 7.56 (dd, *J* = 7.8, 1.5 Hz, 1H), 7.52 (dd, *J* = 7.8, 1.5 Hz, 1H), 7.50 – 7.44 (m, 1H), 7.24 (dd, *J* = 4.1, 0.7 Hz, 1H), 7.22 – 7.17 (m, 2H), 7.14 (s, 1H), 6.83 – 6.78 (m, 1H), 6.63 (s, 1H), 1.76 (s, 3H). **^{13}C{^{1}H} NMR** (101 MHz, DMSO-d_6) δ 164.0 (s), 159.6 (s), 153.1 (s), 146.6 (s), 139.2 (s), 134.3 (s), 132.6 (s), 131.3 (s), 129.1 (s), 127.8 (s), 125.3 (s), 118.4 (s), 118.2 (s), 116.3 (s), 115.1 (s), 114.4 (s), 69.7 (s), 26.9 (s). **HRMS** (ESI-TOF): m/z $[M+H]^+$ calcd for $C_{18}H_{15}N_2O_3$ 307.1038; found 307.1043.

2-(6-Methoxy-2-oxo-2*H*-chromen-3-*yl*)-2-methyl-2,3-dihydroquinazolin-4(1*H*)-one (**2.5b**).

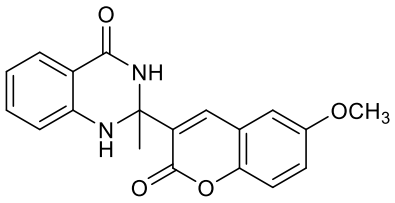

The compound **2.5b** was synthesized using general procedure B and obtained as white solid **2.5b,** in 82% (0.34 g); R_f = 0.5 (30% EtOAc + Hexane); **mp** 182-185 °C. **^{1}H NMR** (400 MHz, $CDCl_3$) δ 7.88 (s, 1H), 7.78 (dd, *J* = 7.8, 1.4 Hz, 1H), 7.66 (s, 1H), 7.21 (dd, *J* = 7.2, 1.3 Hz, 1H), 7.12 (d, *J* = 8.0 Hz, 1H), 6.98 (dd, *J* = 5.0, 3.2 Hz, 1H), 6.72 (t, *J* = 7.6 Hz, 1H), 6.67 (d, *J* = 8.0 Hz, 1H), 6.04 (d, *J* = 1.1 Hz, 1H), 3.89 (s, 3H), 1.98 (s, 3H). **^{13}C{^{1}H} NMR** (101 MHz, $CDCl_3$) δ 165.3 (s), 160.1 (s), 146.8 (s), 146.3 (s), 142.9 (s), 139.8 (s), 134.5 (s), 131.0 (s), 128.2 (s), 124.7 (s), 119.9 (s), 119.4 (s), 119.1 (s), 115.1 (s), 114.3 (s), 113.7 (s), 70.3 (s), 56.2 (s), 27.4 (s). **HRMS** (ESI-TOF): m/z $[M+H]^+$ calcd for $C_{19}H_{17}N_2O_4$ 337.1144; found 337.1154.

2-(6-Chloro-2-oxo-2*H*-chromen-3-*yl*)-2-methyl-2,3-dihydroquinazolin-4(1*H*)-one (2.5c).

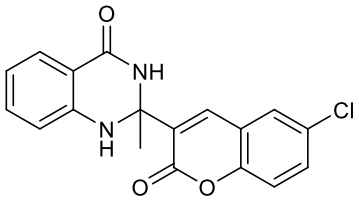

The compound **5c** was synthesized using general procedure B and obtained as white solid **2.5c** in 75% (0.29 g); R_f = 0.5 (40% EtOAc + Hexane); **mp** 174-178 °C. **^{1}H NMR** (400 MHz, $CDCl_3$) δ 7.87 (s, 1H), 7.81 – 7.74 (m, 2H), 7.46 (d, *J* = 2.3 Hz, 1H), 7.43 – 7.40 (m, 1H), 7.21 (s, 1H), 6.75 (d, *J* = 7.5 Hz, 1H), 6.67 (d, *J* = 8.2 Hz, 1H), 5.94 (s, 1H), 1.98 (s, 3H). **^{13}C{^{1}H} NMR** (101 MHz, $CDCl_3$) δ 165.2 (s), 160.1 (s), 151.7 (s), 146.0 (s), 138.6 (s), 134.6 (s), 132.1 (s), 132.0 (s), 130.2 (s), 128.3 (s), 127.8 (s), 119.7 (s), 119.6 (s), 117.7 (s), 115.0 (s), 114.3 (s), 70.2 (s), 27.5 (s). **HRMS** (ESI-TOF): m/z $[M+H]^+$ calcd for $C_{18}H_{14}ClN_2O_3$ 340.0615; found 340.0625.

2-(6-Bromo-2-oxo-2*H*-chromen-3-*yl*)-2-methyl-2,3-dihydroquinazolin-4(1*H*)-one (2.5d).

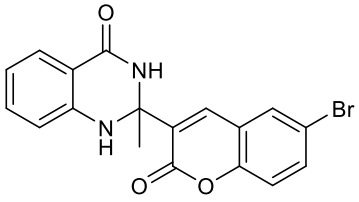

The compound **2.5d** was synthesized using general procedure B and obtained as white solid **2.5d** in 80% (0.39 g); R_f = 0.5 (40% EtOAc + Hexane); **mp** 180-184 °C. **^{1}H NMR** (400 MHz, $CDCl_3$) δ 7.88 (s, 1H), 7.78 (d, *J* = 6.3 Hz, 1H), 7.66 (d, *J* = 6.0 Hz, 1H), 7.22 (dd, *J* = 4.9, 3.3 Hz, 1H), 7.12 (d, *J* = 8.0 Hz, 1H), 7.00 – 6.97 (m, 2H), 6.72 (t, *J* = 7.6 Hz, 1H), 6.67 (d, *J* = 8.0 Hz, 1H), 6.04 (d, *J* = 1.2 Hz, 1H), 1.98 (s, 3H). **^{13}C{^{1}H} NMR** (101 MHz, $CDCl_3$) δ 165.2 (s), 160.1 (s), 151.7 (s), 146.0 (s), 138.6 (s), 134.6 (s), 132.1 (s), 132.0 (s), 130.2 (s), 128.3 (s), 127.8 (s), 119.7 (s), 119.6 (s), 117.7 (s), 115.0 (s), 114.3 (s), 70.2 (s), 27.5 (s). **HRMS** (ESI-TOF): m/z $[M+H]^+$ calcd for $C_{18}H_{14}{}^{79}BrN_2O_3$ 385.2170; found 385.2190. calcd for $C_{18}H_{14}{}^{81}BrN_2O_3$ 387.0089; found 387.0078.

2-Methyl-2-(3-oxo-3*H*-benzo[*f*]chromen-2-*yl*)-2,3-dihydroquinazolin-4(1*H*)-one (2.5e).

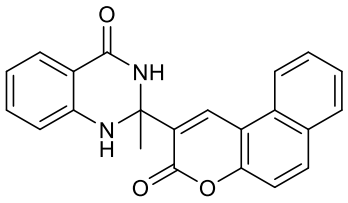

Compound **5e** was synthesized using general procedure B and obtained as white solid **2.5e** in 74% (0.41 g); R_f = 0.5 (30% EtOAc + Hexane); **mp** 184-188 °C. **^{1}H NMR** (400 MHz, $CDCl_3$) δ 8.76 (s, 1H), 8.29 (d, *J* = 8.9 Hz, 1H), 8.21 (s, 1H), 7.98 (s, 1H), 7.88 (d, *J* = 8.2 Hz, 1H), 7.76 (dd, *J* = 9.7, 1.6 Hz, 1H), 7.67 (td, *J* = 8.5, 1.6 Hz, 1H), 7.56 (d, *J* = 2.0 Hz, 2H), 7.40 (d, *J* = 9.1 Hz, 1H), 6.83 (d, *J* = 8.5 Hz, 1H), 6.72 (t, *J* = 7.8 Hz, 1H), 6.59 (s, 1H), 1.98 (s, 3H). **^{13}C{^{1}H} NMR** (101 MHz, $CDCl_3$) δ 165.5 (s), 160.5 (s), 153.1 (s), 147.7 (s), 135.6 (s), 133.7 (s), 133.4 (s), 130.2 (s), 129.8 (s), 129.5 (s), 128.9 (s), 128.4 (s), 128.3 (s), 126.3 (s), 121.5 (s), 119.5 (s), 117.1 (s), 116.2 (s), 112.7 (s), 111.9 (s), 70.0 (s), 27.8 (s). **HRMS** (ESI-TOF): m/z $[M+H]^+$ calcd for $C_{22}H_{17}N_2O_3$ 357.1194; found 357.1203.

***tert*-Butyl(*E*)-3-(2-methyl-4-oxo-2-(2-oxo-2*H*-chromen-3-*yl*)-1,2,3,4-tetrahydroquinazolin-5-*yl*) acrylate (2.7aa)**.

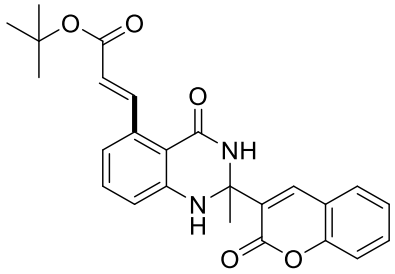

The compound **2.7aa** was synthesized using general procedure C and obtained as white solid **2.7aa** in 82% (0.35 g); R_f = 0.5 (30% EtOAc + Hexane); **mp** 182-184 °C. **^{1}H**

NMR (400 MHz, $CDCl_3$) δ 8.61 (d, *J* = 15.9 Hz, 1H), 7.95 (s, 1H), 7.53 (d, *J* = 8.1 Hz, 1H), 7.51 – 7.48 (m, 1H), 7.28 (d, *J* = 8.1 Hz, 2H), 7.20 (d, *J* = 4.4 Hz, 1H), 7.19 (s, 1H), 6.89 (d, *J* = 7.3 Hz, 1H), 6.69 (d, *J* = 8.1 Hz, 1H), 6.10 (d, *J* = 15.9 Hz, 1H), 6.03 (s, 1H), 1.95 (s, 3H), 1.48 (s, 9H). **$^{13}C\{^1H\}$ NMR** (101 MHz, $CDCl_3$) δ 166.2 (s), 165.0 (s), 160.7 (s), 153.3 (s), 147.5 (s), 143.8 (s), 140.0 (s), 138.1 (s), 133.6 (s), 132.2 (s), 130.6 (s), 128.8 (s), 124.9 (s), 122.1 (s), 119.6 (s), 118.5 (s), 116.6 (s), 116.3 (s), 112.4 (s), 80.3 (s), 69.6 (s), 28.2 (s). **HRMS** (ESI-TOF): m/z $[M+H]^+$ calcd for $C_{25}H_{25}N_2O_5$ 433.1719; found 433.1733.

Methyl (*E*)-3-(2-methyl-4-oxo-2-(2-oxo-2*H*-chromen-3-*yl*)-1,2,3,4-tetrahydroquinazolin-5-*yl*) acrylate (2.7ab).

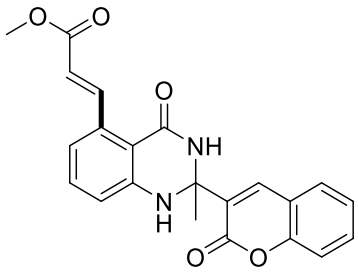

The compound **2.7ab** was synthesized using general procedure C and obtained as yellow solid compound **2.7ab**, 84% (0.32 g); R_f = 0.5 (30% EtOAc + Hexane); **mp** 184-188 °C. **^1H NMR** (400 MHz, $CDCl_3$) δ 8.73 (d, *J* = 16.0 Hz, 1H), 8.37 (d, *J* =12.0 Hz, 1H), 7.98 (s, 1H), 7.51 (dd, *J* = 7.5, 1.2 Hz, 1H), 7.49 – 7.46 (m, 1H), 7.28 – 7.24 (m, 2H), 7.23 – 7.21 (m, 1H), 6.87 (d, *J* = 8.0 Hz, 1H), 6.73 (d, *J* = 8.1 Hz, 1H), 6.16 – 6.12 (m, 2H), 3.69 (s, 3H), 1.99 (s, 3H). **$^{13}C\{^1H\}$ NMR** (101 MHz, $CDCl_3$) δ 167.2 (s), 164.9 (s), 160.5 (s), 153.3 (s), 147.4 (s), 145.1 (s), 139.9 (s), 137.7 (s), 133.6 (s), 132.1 (s), 130.5 (s), 128.7 (s), 124.8 (s), 119.7 (s), 119.4 (s), 118.5 (s), 116.8 (s), 116.2 (s), 112.3 (s), 69.6 (s), 51.6 (s), 27.3 (s). **HRMS** (ESI-TOF): m/z $[M+H]^+$ calcd for $C_{22}H_{19}N_2O_5$ requires 391.1249 for found 391.1260.

Ethyl (*E*)-3-(2-methyl-4-oxo-2-(2-oxo-2*H*-chromen-3-*yl*)-1,2,3,4-tetrahydroquinazolin-5-*yl*) acrylate (2.7ac).

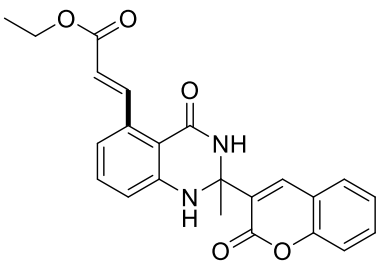

The compound **2.7ac** was synthesized using general procedure C and obtained as white solid compound, **2.7ac**, 90% (0.36 g); R_f = 0.5 (40% EtOAc + Hexane); **mp** 188-192

°C. **^{1}H NMR** (400 MHz, $CDCl_3$) δ 8.71 (d, *J* = 16.1 Hz, 1H), 7.99 (s, 1H), 7.53 – 7.50 (m, 1H), 7.48 – 7.46 (m, 1H), 7.28 – 7.25 (m, 2H), 7.23 – 7.21 (m, 1H), 7.20 – 7.18 (m, 1H), 6.87 (d, *J* = 7.8 Hz, 1H), 6.73 (dd, *J* = 8.3, 1.0 Hz, 1H), 6.14 (dd, *J* = 11.2, 5.9 Hz, 2H), 4.19 – 4.13 (m, 2H), 1.99 (s, 3H), 1.24 (t, *J* = 7.1 Hz, 3H). **^{13}C{^{1}H} NMR** (101 MHz, $CDCl_3$) δ 166.9 (s), 165.3 (s), 160.7 (s), 153.3 (s), 147.6 (s), 144.9 (s), 140.1 (s), 137.8 (s), 133.7 (s), 132.1 (s), 130.6 (s), 128.8 (s), 124.9 (s), 120.1 (s), 119.5 (s), 118.6 (s), 116.9 (s), 116.3 (s), 112.3 (s), 69.7 (s), 60.5 (s), 27.3 (s), 14.3 (s). **HRMS** (ESI-TOF): m/z $[M+H]^+$ calcd for $C_{23}H_{21}N_2O_5$ 405.1406; found 405.1441.

Butyl (*E*)-3-(2-methyl-4-oxo-2-(2-oxo-2*H*-chromen-3-*yl*)-1,2,3,4-tetrahydroquinazolin-5-*yl*) acrylate (**2.7ad**).

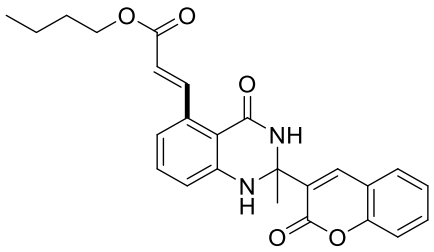

The compound **2.7ad** was synthesized using general procedure C and obtained as light-yellow solid compound, **2.7ad**, 86% (0.37 g); R_f = 0.5 (30% EtOAc + Hexane); **mp** 182-186 °C. **^{1}H NMR** (500 MHz, $CDCl_3$) δ 8.74 (d, *J* = 16.0 Hz, 1H), 8.22 (s, 1H), 8.00 (s, 1H), 7.53 (d, *J* = 10 Hz, 2H), 7.49 (d, *J* = 10 Hz, 1H), 7.24 (dd, *J* = 5.6, 4.7 Hz, 1H), 7.21 (d, *J* = 7.9 Hz, 1H), 6.90 (d, *J* = 7.6 Hz, 1H), 6.74 (d, *J* = 8.0 Hz, 1H), 6.16 (d, *J* = 10 Hz, 1H), 6.13 (s, 1H), 4.12 (t, *J* = 6.8 Hz, 2H), 2.01 (s, 3H), 1.62 (dt, *J* = 14.6, 6.9 Hz, 2H), 1.37 (dd, *J* = 15.0, 7.5 Hz, 2H), 0.91 (t, *J* = 7.4 Hz, 3H). **^{13}C{^{1}H} NMR** (126 MHz, $CDCl_3$) δ 166.8 (s), 165.0 (s), 160.6 (s), 153.3 (s), 147.5 (s), 144.8 (s), 139.9 (s), 137.8 (s), 133.5 (s), 132.0 (s), 130.6 (s), 128.7 (s), 124.8 (s), 120.1 (s), 119.4 (s), 118.5 (s), 116.7 (s), 116.2 (s), 112.3 (s), 69.6 (s), 64.3 (s), 30.7 (s), 27.3 (s), 19.1 (s), 13.7 (s). **HRMS** (ESI-TOF): m/z $[M+H]^+$ calcd for $C_{25}H_{25}N_2O_5$ 433.1719; found 433.1746.

(*E*)-2-Methyl-2-(2-oxo-2*H*-chromen-3-*yl*)-5-(2-(phenylsulfonyl)vinyl)-2,3-dihydroquinazolin-4(1*H*)-one (**2.7ae**).

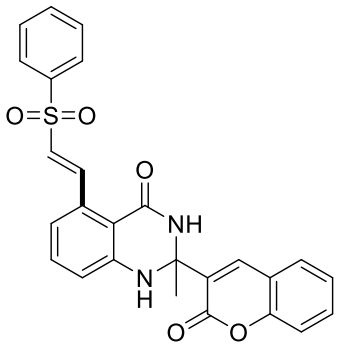

The compound **2.7ae** was synthesized using general procedure C and obtained as light-yellow solid compound, **2.7ae**, 78% (0.36 g); R_f = 0.6 (40% EtOAc + Hexane); **mp** 194-198 °C. **^{1}H NMR** (400 MHz, $CDCl_3$) δ 8.76 (d, *J* = 15.3 Hz, 1H), 8.22 (s, 1H), 7.99 (s, 1H), 7.93 (d, *J* = 7.2 Hz, 2H), 7.58 (d, *J* = 6.6 Hz, 1H), 7.52 (d, *J* = 7.3 Hz, 2H), 7.44 (t, *J* = 7.6 Hz, 2H), 7.28 (d, *J* = 5.1 Hz, 2H), 7.20 (t, *J* = 7.9 Hz, 1H), 6.76 (dd, *J* = 11.4, 7.8 Hz, 2H), 6.58 (d, *J* = 15.3 Hz, 1H), 6.16 (s, 1H), 2.00 (s, 3H). **^{13}C{^{1}H} NMR** (101 MHz $CDCl_3$) δ 164.8 (s), 160.6 (s), 153.4 (s), 147.6 (s), 144.1 (s), 140.9 (s), 140.0 (s), 135.5 (s), 133.8 (s), 133.2 (s), 132.3 (s), 130.4 (s), 129.2 (s), 128.9 (s), 128.2 (s), 127.7 (s), 125.0 (s), 119.6 (s), 118.5 (s), 117.6 (s), 116.3 (s), 112.4 (s), 69.6 (s), 27.4 (s). **HRMS** (ESI-TOF): m/z $[M+H]^+$ calcd for $C_{26}H_{21}N_2O_5S$ 473.1126; found 473.1166.

2-Ethylhexyl(*E*)-3-(2-methyl-4-oxo-2-(2-oxo-2*H*-chromen-3-*yl*)-1,2,3,4-tetrahydroquinazolin-5-*yl*) acrylate (**2.7af**).

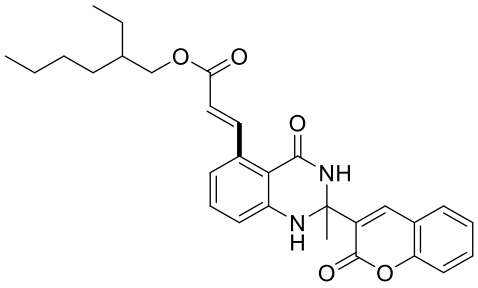

The compound **2.7af** was synthesized using general procedure C and obtained as light-yellow solid compound, **2.7af**, 80% (0.39 g); R_f = 0.5 (30% EtOAc + Hexane); **mp** 202-206 °C. **^{1}H NMR** (400 MHz, $CDCl_3$) δ 8.73 (d, *J* = 16.2 Hz, 1H), 8.00 (s, 1H), 7.51 (dd, *J* = 11.8, 10.7 Hz, 2H), 7.27 (s, 1H), 7.25 (t, *J* = 2.0 Hz, 1H), 7.24 – 7.21 (m, 1H), 7.20 (s, 1H), 6.89 (d, *J* = 7.9 Hz, 1H), 6.73 (d, *J* = 8.4 Hz, 1H), 6.18 – 6.14 (m, 2H), 4.03 – 3.99 (m, 2H), 2.00 (s, 3H), 1.35 – 1.31 (m, 2H), 1.29 (d, *J* = 7.6 Hz, 1H), 1.24 (d, *J* = 4.0 Hz, 6H), 0.84 (t, *J* = 7.1, 6H). **^{13}C{^{1}H} NMR** (101 MHz, $CDCl_3$) δ 167.1 (s), 165.3 (s), 160.7 (s), 153.3 (s), 147.6 (s), 145.0 (s), 140.1 (s), 137.8 (s), 133.6 (s), 132.1 (s), 130.6 (s), 128.8 (s), 120.1 (s), 119.5 (s), 118.6 (s), 116.8 (s), 116.2 (s), 112.4 (s), 69.7 (s), 66.9 (s), 38.8 (s), 30.4 (s), 28.9

(s), 27.3 (s), 23.8 (s), 23.0 (s), 14.1 (s), 11.0 (s). **HRMS** (ESI-TOF): m/z $[M+H]^+$ calcd for $C_{29}H_{33}N_2O_5$ 489.2345; found 489.2375.

(1*R*,2*R*,4*R*)-1,7,7-Trimethylbicyclo [2.2.1] heptan-2-*yl* (*E*)-3-(2-methyl-4-oxo-2-(2-oxo-2*H*-chromen-3-*yl*)-1,2,3,4 tetrahydroquinazolin-5-yl) acrylate (**2.7ag**).

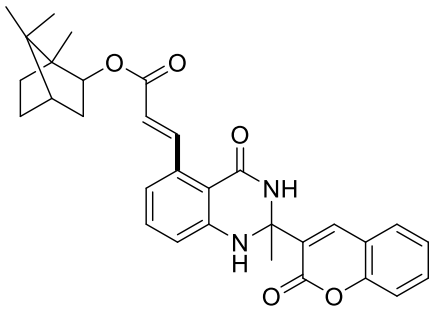

The compound **2.7ag** was synthesized using general procedure C and obtained as light-yellow solid compound, **2.7ag**, 80% (0.41 g); R_f = 0.6 (30% EtOAc + Hexane); **mp** 198-202 °C. **^{1}H NMR** (500 MHz, $CDCl_3$) δ 8.72 (dd, *J* = 15.9, 7.1 Hz, 1H), 7.98 (s, 1H), 7.90 (d, *J* = 8.4 Hz, 1H), 7.55 – 7.49 (m, 2H), 7.28 (dd, *J* = 8.0, 3.1 Hz, 2H), 7.21 (t, *J* = 7.9 Hz, 1H), 6.91 (dd, *J* = 7.5, 3.8 Hz, 1H), 6.73 (d, *J* = 7.9 Hz, 1H), 6.17 – 6.12 (m, 1H), 6.09 (s, 1H), 4.74 (td, *J* = 7.7, 4.0 Hz, 1H), 1.98 (t, *J* = 3.0 Hz, 3H), 1.86 – 1.74 (m, 3H), 1.73 – 1.66 (m, 2H), 1.57 – 1.51 (m, 1H), 1.17 (m, 3H), 1.01 (s, 3H), 0.86 (s, 2H), 0.82 (d, *J* = 2.5 Hz, 2H). **^{13}C{^{1}H} NMR** (126 MHz, $CDCl_3$) δ 166.3 (s), 164.7 (s), 160.5 (s), 153.3 (s), 147.4 (s), 144.6 (s), 139.8 (s), 137.9 (s), 133.5 (s), 132.1 (s), 130.6 (s), 128.7 (s), 124.8 (s), 120.7 (s), 119.5 (s), 118.5 (s), 116.7 (s), 116.2 (s), 80.9 (s), 69.6 (s), 48.8 (s), 46.9 (s), 45.0 (s), 38.8 (s), 33.7 (s), 27.4 (s), 27.0 (s), 20.2 (s), 11.5 (s). **HRMS** (ESI-TOF): m/z $[M+H]^+$ calcd for $C_{31}H_{33}N_2O_5$ 513.2345; found 513.2385.

(*E*)-2-Methyl-2-(2-oxo-2*H*-chromen-3-*yl*)-5-(3-oxobut-1-en-1-*yl*)-2,3-dihydroquinazolin-4(1*H*)-one (**2.7ah**).

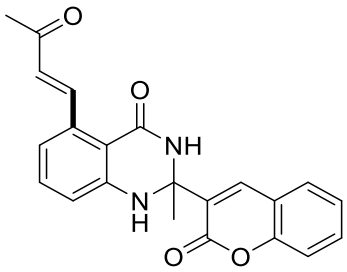

The crude was purified using column chromatography to give yellow solid compound, **2.7ah**, 78% (0.29 g); R_f = 0.5 (50% EtOAc + Hexane); **mp** 172-176 °C. **^{1}H NMR** (400 MHz, $CDCl_3$) δ 8.66 (d, *J* = 16.4 Hz, 1H), 7.94 (s, 1H), 7.55 – 7.53 (m, 1H), 7.52 – 7.49

(m, 1H), 7.30 (d, *J* = 2.0 Hz, 1H), 7.28 (d, *J* = 0.9 Hz, 2H), 7.23 (d, *J* = 8.0 Hz, 1H), 6.92 (d, *J* = 7.6 Hz, 1H), 6.74 (d, *J* = 8.1 Hz, 1H), 6.40 (d, *J* = 16.4 Hz, 1H), 6.07 (d, *J* = 1.0 Hz, 1H), 2.37 (s, 3H), 1.96 (s, 3H). **^{13}C{^{1}H} NMR** (101 MHz, $CDCl_3$) δ 199.5 (s), 164.7 (s), 160.6 (s), 153.4 (s), 147.4 (s), 144.4 (s), 139.7 (s), 138.0 (s), 133.9 (s), 132.3 (s), 130.5 (s), 128.7 (s), 125.0 (s), 119.6 (s), 118.4 (s), 117.1 (s), 116.4 (s), 112.1 (s), 69.6 (s), 27.6 (s), 26.9 (s). **HRMS** (ESI-TOF): m/z $[M+H]^+$ calcd for $C_{22}H_{19}N_2O_4$ 375.1300; found 375.1329.

***tert*-Butyl(*E*)-3-(2-(6-methoxy-2-oxo-2*H*-chromen-3-*yl*)-2-methyl-4-oxo-1,2,3,4-tetrahydroquinazolin-5-*yl*) acrylate (2.7ba).**

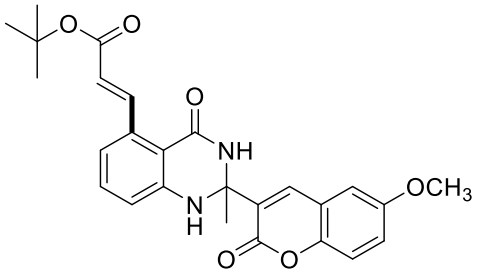

The compound **2.7ba** was synthesized using general procedure C and obtained as light-yellow solid compound, **2.7ba**, 80% (0.37 g); R_f = 0.5 (30% EtOAc + Hexane); **mp** 194-198 °C. **^{1}H NMR** (500 MHz, DMSO-d_6) δ 8.60 (d, *J* = 16.0 Hz, 1H), 8.57 (s, 1H), 7.85 (s, 1H), 7.32 (s, 1H), 7.27 (dd, *J* = 7.1, 2.1 Hz, 1H), 7.24 (s, 1H), 7.21 (d, *J* = 8.0 Hz, 1H), 6.93 (dd, *J* = 10.5, 8.0 Hz, 2H), 6.14 (d, *J* = 15.9 Hz, 1H), 3.87 (s, 3H), 1.80 (s, 3H), 1.46 (s, 9H). **^{13}C{^{1}H} NMR** (126 MHz, DMSO-d_6) δ 165.4 (s), 163.0 (s), 158.5 (s), 147.2 (s), 146.1 (s), 144.2 (s), 142.0 (s), 138.8 (s), 136.0 (s), 132.7 (s), 130.7 (s), 124.6 (s), 120.0 (s), 119.7 (s), 118.5 (s), 117.5 (s), 116.4 (s), 114.1 (s), 111.9 (s), 79.5 (s), 68.4 (s), 56.0 (s), 27.7 (s), 26.1 (s). **HRMS** (ESI-TOF): m/z $[M+H]^+$ calcd for $C_{26}H_{27}N_2O_6$ 463.1824; found 463.1854.

Methyl(*E*)-3-(2-(6-methoxy-2-oxo-2*H*-chromen-3-*yl*)-2-methyl-4-oxo-1,2,3,4-tetrahydroquinazolin-5-*yl*) acrylate (2.7bb).

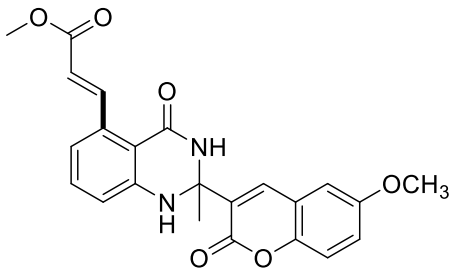

The compound **2.7bb** was synthesized using general procedure C and obtained as light-yellow solid compound, **2.7bb**, 82% (0.34 g); R_f = 0.5 (40% EtOAc + Hexane); **mp** 172-176 °C. **^{1}H NMR** (500 MHz, $CDCl_3$) δ 8.75 (d, *J* = 16.0 Hz, 1H), 7.96 (s, 1H), 7.92 (d, *J*

= 3.5 Hz, 1H), 7.22 (d, *J* = 7.9 Hz, 1H), 7.17 (d, *J* = 8.0 Hz, 1H), 7.08 – 7.06 (m, 1H), 7.05 (dd, *J* = 8.1, 1.2 Hz, 2H), 6.90 (d, *J* = 7.6 Hz, 1H), 6.75 (d, *J* = 8.0 Hz, 1H), 6.17 (d, *J* = 16.0 Hz, 1H), 3.94 (s, 3H), 3.75 (s, 3H), 2.01 (s, 3H). **^{13}C{^{1}H} NMR** (126 MHz, $CDCl_3$) δ 167.2 (s), 164.8 (s), 160.0 (s), 147.5 (s), 146.8 (s), 145.1 (s), 142.9 (s), 140.0 (s), 137.6 (s), 134.3 (s), 133.6 (s), 130.7 (s), 124.7 (s), 119.9 (s), 119.6 (s), 119.4 (s), 119.1 (s), 116.8 (s), 113.7 (s), 69.6 (s), 56.2 (s), 51.6 (s), 27.2 (s). **HRMS** (ESI-TOF): m/z $[M+H]^+$ calcd for $C_{23}H_{21}N_2O_6$ 421.1355; found 421.1369.

Ethyl(*E*)-3-(2-(6-methoxy-2-oxo-2*H*-chromen-3-*yl*)-2-methyl-4-oxo-1,2,3,4-tetrahydroquinazolin-5-*yl*) acrylate (**2.7bc**).

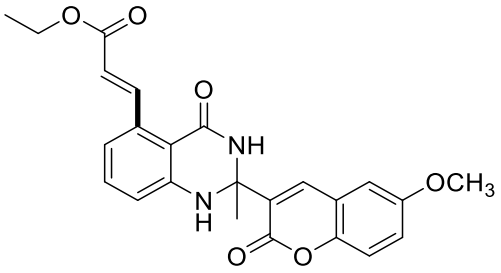

The compound **2.7bc** was synthesized using general procedure C and obtained as white solid compound, **2.7bc**, 86% (0.37 g); R_f = 0.5 (40% EtOAc + Hexane); **mp** 184-188 °C. **^{1}H NMR** (500 MHz, DMSO-d_6) δ 8.68 (d, *J* = 16.0 Hz, 1H), 8.59 (s, 1H), 7.86 (s, 1H), 7.34 (d, *J* = 0.8 Hz, 1H), 7.26 (dd, *J* = 6.9, 2.2 Hz, 1H), 7.23 (d, *J* = 7.6 Hz, 1H), 7.21 (t, *J* = 2.7 Hz, 2H), 6.97 (d, *J* = 8.1 Hz, 1H), 6.94 (d, *J* = 7.6 Hz, 1H), 6.24 (d, *J* = 16.0 Hz, 1H), 4.18 – 4.13 (q, 2H), 3.86 (s, 3H), 1.81 (s, 3H), 1.23 (t, *J* = 7.1 Hz, 3H). **^{13}C{^{1}H} NMR** (126 MHz, DMSO-d_6) δ 166.1 (s), 163.0 (s), 158.5 (s), 147.2 (s), 146.0 (s), 145.1 (s), 142.0 (s), 138.9 (s), 135.9 (s), 132.7 (s), 130.6 (s), 124.5 (s), 119.7 (s), 118.5 (s), 117.5 (s), 116.6 (s), 114.1 (s), 111.9 (s), 68.4 (s), 59.7 (s), 55.9 (s), 26.1 (s), 14.0 (s). **HRMS** (ESI-TOF): m/z $[M+H]^+$ calcd for $C_{24}H_{23}N_2O_6$ 435.1511; found 435.1531.

2-Ethylhexyl (*E*)-3-(2-(6-methoxy-2-oxo-2*H*-chromen-3-*yl*)-2-methyl-4-oxo-1,2,3,4-tetrahydroquinazolin-5-*yl*) acrylate (**2.7bf**).

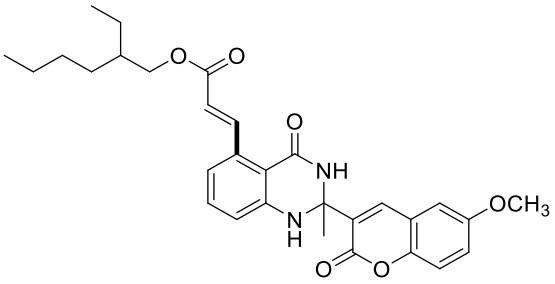

The compound **2.7bf** was synthesized using general procedure C and obtained as light-yellow solid compound, **2.7bf**, 78% (0.40 g); R_f = 0.6 (40% EtOAc + Hexane); **mp** 202-206 °C. **^{1}H NMR** (500 MHz, DMSO-d_6) δ 8.70 (d, *J* = 16.0 Hz, 1H), 8.61 (s, 1H), 7.85 (s, 1H), 7.35 (s, 1H), 7.24 (dd, *J* = 5.9, 3.6 Hz, 2H), 7.22 (d, *J* = 3.7 Hz, 2H), 6.96 (t, *J* = 7.3 Hz, 2H), 6.24 (d, *J* = 16.0 Hz, 1H), 4.03 (dt, *J* = 5.9, 2.9 Hz, 2H), 3.86 (s, 3H), 1.81 (s, 3H), 1.60 – 1.55 (m, 1H), 1.35 – 1.30 (m, 2H), 1.26 (dd, *J* = 12.0, 4.3 Hz, 6H), 0.86 (t, *J* = 6.8 Hz, 6H). **^{13}C{^{1}H} NMR** (126 MHz, DMSO-d_6) δ 166.1 (s), 163.0 (s), 158.5 (s), 147.2 (s), 146.1 (s), 145.1 (s), 142.0 (s), 138.8 (s), 135.9 (s), 132.7 (s), 130.7 (s), 124.5 (s), 119.6 (s), 118.4 (s), 117.5 (s), 116.6 (s), 114.1 (s), 111.9 (s), 68.4 (s), 65.8 (s), 55.9 (s), 38.1 (s), 29.6 (s), 28.2 (s), 26.1 (s), 23.1 (s), 22.2 (s), 13.7 (s), 10.6 (s). **HRMS** (ESI-TOF): m/z $[M+H]^+$ calcd for $C_{30}H_{35}N_2O_6$ 519.2450; found 519.2490.

(1*R*,2*R*,4*R*)-1,7,7-Trimethylbicyclo [2.2.1] heptan-2-*yl* (*E*)-3-(2-(6-methoxy-2-oxo-2*H*-chromen-3-*yl*)-2-methyl-4-oxo-1,2,3,4-tetrahydroquinazolin-5-*yl*) acrylate (**2.7bg**).

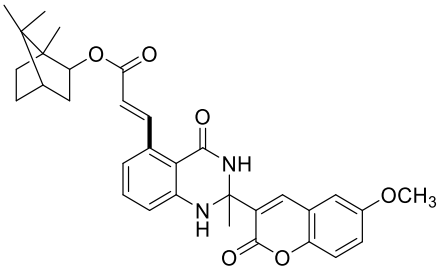

The compound **2.7bg** was synthesized using general procedure C and obtained as yellow solid compound, **2.7bg**, 76% (0.42 g); R_f = 0.5 (40% EtOAc + Hexane); **mp** 194-198 °C. **^{1}H NMR** (500 MHz, DMSO-d_6) δ 8.71 (dd, *J* = 16.0, 3.5 Hz, 1H), 8.62 (d, *J* = 13.4 Hz, 1H), 7.82 (d, *J* = 3.9 Hz, 1H), 7.35 (s, 1H), 7.25 – 7.22 (m, 1H), 7.20 (dd, *J* = 6.1, 2.7 Hz, 2H), 7.18 – 7.16 (m, 1H), 6.94 (dd, *J* = 13.6, 7.8 Hz, 2H), 6.17 (d, *J* = 16.0 Hz, 1H), 4.67 – 4.64 (m, 1H), 3.85 (s, 3H), 1.80 (s, 3H), 1.77 (d, *J* = 10.7 Hz, 2H), 1.71 (d, *J* = 2.8 Hz, 1H), 1.54 – 1.44 (m, 2H), 1.12 – 1.04 (m, 2H), 0.99 (s, 3H), 0.81 (dd, *J* = 10.2, 6.1 Hz, 6H). **^{13}C{^{1}H} NMR** (126 MHz, DMSO-d_6) δ 165.4 (s), 163.1 (s), 158.5 (s), 147.3 (s), 146.1 (s), 144.8 (s), 142.0 (s), 138.8 (s), 135.9 (s), 132.7 (s), 130.7 (s), 124.5 (s), 119.5 (s), 118.7 (s), 118.5 (s), 117.5 (s), 116.6 (s), 114.1 (s), 111.8 (s), 79.8 (s), 68.4 (s), 55.9 (s), 48.2 (s), 46.4 (s), 44.3 (s), 38.2 (s), 33.0 (s), 26.4 (s), 26.1 (s), 19.9 (s), 11.2 (s). **HRMS** (ESI-TOF): m/z $[M+H]^+$ calcd for $C_{32}H_{35}N_2O_6$ 543.2450; found 543.2485.

(*E*)-2-(6-Methoxy-2-oxo-2*H*-chromen-3-*yl*)-2-methyl-5-(3-oxobut-1-en-1-*yl*)-2,3-dihydroquinazolin-4(1*H*)-one (**2.7bh**).

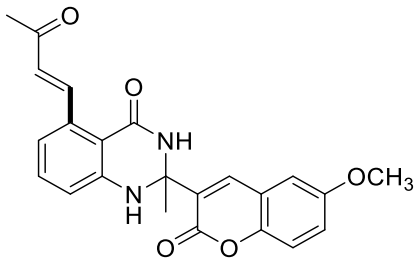

The compound **2.7bh** was synthesized using general procedure C and obtained as yellow solid compound, **2.7bh**, 74% (0.30 g); R_f = 0.5 (50% EtOAc + Hexane); **mp** 158-162 °C. **^{1}H NMR** (500 MHz, $CDCl_3$) δ 8.68 (d, *J* = 16.4 Hz, 1H), 7.93 (s, 1H), 7.66 (s, 1H), 7.23 (t, *J* = 7.9 Hz, 1H), 7.18 (d, *J* = 7.9 Hz, 1H), 7.09 (dd, *J* = 7.9, 1.1 Hz, 1H), 7.06 – 7.04 (m, 2H), 6.92 (d, *J* = 7.6 Hz, 1H), 6.75 (dd, *J* = 8.21, 2.3 Hz , 1H), 6.40 (d, *J* = 15.3 Hz, 1H), 3.93 (s, 3H), 2.37 (s, 3H), 1.98 (s, 3H). **^{13}C{^{1}H} NMR** (126 MHz, $CDCl_3$) δ 199.3 (s), 164.9 (s), 159.9 (s), 147.5 (s), 146.9 (s), 144.3 (s), 142.9 (s), 139.8 (s), 137.8 (s), 133.7 (s), 130.7 (s), 129.5 (s), 124.7 (s), 119.8 (s), 119.4 (s), 119.0 (s), 117.1 (s), 113.8 (s), 69.5 (s), 56.2 (s), 27.3 (s), 26.7 (s). **HRMS** (ESI-TOF): m/z $[M+H]^+$ calcd for $C_{23}H_{21}N_2O_5$ 405.1406; found 405.1425.

***tert*-Butyl(*E*)-3-(2-(6-chloro-2-oxo-2*H*-chromen-3-*yl*)-2-methyl-4-oxo-1,2,3,4-tetrahydroquinazolin-5-*yl*) acrylate (2.7ca).**

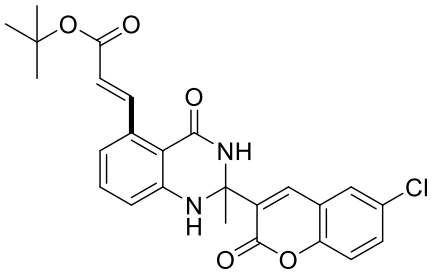

The compound **2.7ca** was synthesized using general procedure C and obtained as white solid compound, **2.7ca**, 78% (0.36 g); R_f = 0.5 (40% EtOAc + Hexane); **mp** 172-176 °C. **^{1}H NMR** (400 MHz, $CDCl_3$) δ 8.60 (d, *J* = 15.9 Hz, 1H), 7.96 (s, 1H), 7.90 (s, 1H), 7.51 (d, *J* = 2.4 Hz, 1H), 7.43 (dd, *J* = 8.8, 2.4 Hz, 1H), 7.22 (s, 1H), 7.20 (d, *J* = 1.8 Hz, 1H), 6.89 (d, *J* = 7.6 Hz, 1H), 6.70 (dd, *J* = 8.0, 0.6 Hz, 1H), 6.09 (d, *J* = 15.9 Hz, 1H), 6.00 (s, 1H), 1.97 (s, 3H), 1.46 (s, 9H). **^{13}C{^{1}H} NMR** (101 MHz, $CDCl_3$) δ 166.2 (s), 164.9 (s), 160.1 (s), 151.7 (s), 147.2 (s), 143.6 (s), 138.8 (s), 138.1 (s), 133.7 (s), 132.1 (s), 131.8 (s), 130.2 (s), 128.0 (s), 122.2 (s), 119.6 (s), 117.7 (s), 116.6 (s), 80.4 (s), 69.6 (s), 28.2 (s). **HRMS** (ESI-TOF): m/z $[M+H]^+$ calcd for $C_{25}H_{24}N_2O_5Cl$ 467.1295; found 467.1312.

Methyl (*E*)-3-(2-(6-chloro-2-oxo-2*H*-chromen-3-*yl*)-2-methyl-4-oxo-1,2,3,4-tetrahydroquinazolin-5-*yl*) acrylate (**2.7cb**).

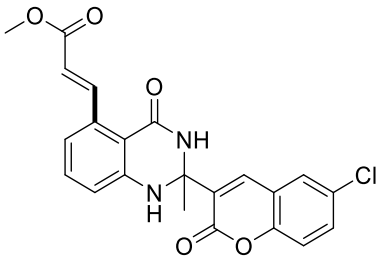

The compound **2.7cb** was synthesized using general procedure C and obtained as yellow solid compound, **2.7cb**, 79% (0.33 g); R_f = 0.5 (40% EtOAc + Hexane); **mp** 164-168 °C. **^{1}H NMR** (400 MHz, $CDCl_3$) δ 8.70 (d, *J* = 15.9 Hz, 1H), 7.89 (s, 1H), 7.64 (s, 1H), 7.52 (d, *J* = 2.3 Hz, 1H), 7.44 (dd, *J* = 8.8, 2.3 Hz, 1H), 7.25 (d, *J* = 0.5 Hz, 1H), 7.22 (d, *J* = 8.5 Hz, 1H), 6.90 (d, *J* = 7.6 Hz, 1H), 6.73 (d, *J* = 8.1 Hz, 1H), 6.17 (d, *J* = 15.9 Hz, 1H), 6.01 (s, 1H), 3.75 (s, 3H), 1.97 (s, 3H). **^{13}C{^{1}H} NMR** (101 MHz, $CDCl_3$) δ 167.3 (s), 160.1 (s), 151.7 (s), 147.2 (s), 145.0 (s), 138.8 (s), 137.8 (s), 133.8 (s), 132.2 (s), 131.7 (s), 130.3 (s), 127.9 (s), 120.0 (s), 117.8 (s), 116.9 (s), 69.6 (s), 51.8 (s), 27.3 (s). **HRMS** (ESI-TOF): m/z $[M+H]^+$ calcd for $C_{22}H_{18}N_2O_5Cl$ 425.0826; found 425.0867.

Ethtyl (*E*)-3-(2-(6-chloro-2-oxo-2*H*-chromen-3-*yl*)-2-methyl-4-oxo-1,2,3,4-tetrahydroquinazolin-5-*yl*) acrylate (**2.7cc**).

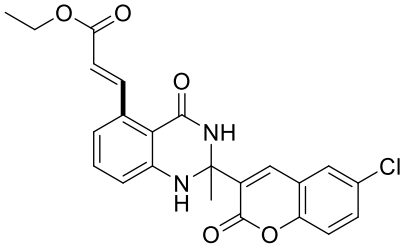

The compound **2.7cc** was synthesized using general procedure C and obtained as yellow solid compound, **2.7cc**, 80% (0.35 g); R_f = 0.5 (50% EtOAc + Hexane); **mp** 184-188 °C. **^{1}H NMR** (400 MHz, $CDCl_3$) δ 8.70 (d, *J* = 15.9 Hz, 1H), 7.90 (s, 1H), 7.86 (s, 1H), 7.52 (d, *J* = 2.4 Hz, 1H), 7.43 (dd, *J* = 8.8, 2.4 Hz, 1H), 7.22 (d, *J* = 2.1 Hz, 1H), 7.20 (s, 1H), 6.90 (d, *J* = 7.6 Hz, 1H), 6.72 (d, *J* = 7.8 Hz, 1H), 6.17 (d, *J* = 15.9 Hz, 1H), 6.01 (s, 1H), 4.20 (q, *J* = 7.1 Hz, 2H), 1.97 (s, 3H), 1.28 (t, *J* = 7.1 Hz, 3H). **^{13}C{^{1}H} NMR** (101 MHz, $CDCl_3$) δ 166.9 (s), 164.8 (s), 160.1 (s), 151.7 (s), 147.3 (s), 144.8 (s), 138.8 (s), 137.9 (s), 133.8 (s), 132.1 (s), 131.8 (s), 130.2 (s), 127.9 (s), 120.3 (s), 119.6 (s), 117.7 (s), 116.8 (s), 69.6 (s),

60.5 (s), 27.3 (s), 14.4 (s). **HRMS** (ESI-TOF): m/z $[M+H]^+$ calcd for $C_{23}H_{20}N_2O_5Cl$ 439.0982; found 439.0999.

2-Ethylhexyl (*E*)-3-(2-(6-chloro-2-oxo-2*H*-chromen-3-*yl*)-2-methyl-4-oxo-1,2,3,4-tetrahydroquinazolin-5-*yl*) acrylate (**2.7cf**).

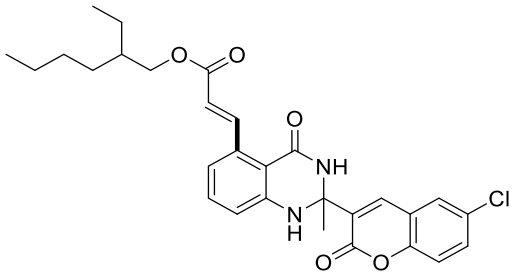

The compound **2.7cf** was synthesized using general procedure C and obtained as yellow solid compound, **2.7cf**, 76% (0.39 g); R_f = 0.6 (40% EtOAc + Hexane); **mp** 208-212 °C. **^{1}H NMR** (500 MHz, $CDCl_3$) δ 8.75 (d, *J* = 15.9 Hz, 1H), 8.21 (s, 1H), 7.91 (s, 1H), 7.65 (d, *J* = 2.2 Hz, 1H), 7.56 (dd, *J* = 8.8, 2.3 Hz, 1H), 7.23 (t, *J* = 7.9 Hz, 1H), 7.15 (d, *J* = 8.8 Hz, 1H), 6.93 (d, *J* = 7.6 Hz, 1H), 6.75 (d, *J* = 8.0 Hz, 1H), 6.19 (d, *J* = 15.9 Hz, 1H), 6.05 (s, 1H), 4.05 (td, *J* = 6.0, 3.5 Hz, 2H), 2.00 (s, 3H), 1.63 – 1.58 (m, 1H), 1.37 (dd, *J* = 13.7, 7.2 Hz, 2H), 1.31 – 1.25 (m, 6H), 0.88 (t, *J* = 7.3 Hz, 6H). **^{13}C{^{1}H} NMR** (126 MHz, $CDCl_3$) δ 167.0 (s), 164.9 (s), 159.9 (s), 152.1 (s), 147.2 (s), 138.6 (s), 137.8 (s), 134.7 (s), 133.6 (s), 130.9 (s), 120.2 (s), 120.0 (s), 119.6 (s), 117.9 (s), 117.4 (s), 116.7 (s), 112.3 (s), 69.6 (s), 66.9 (s), 38.7 (s), 30.3 (s), 28.9 (s), 27.2 (s), 23.7 (s), 22.9 (s), 14.0 (s), 10.9 (s). **HRMS** (ESI-TOF): m/z $[M+H]^+$calcd for $C_{29}H_{32}N_2O_5Cl$ 524.1892; found 524.1920.

(1*R*,2*R*,4*R*)-1,7,7-Trimethylbicyclo [2.2.1] heptan-2-*yl* (*E*)-3-(2-(6-chloro-2-oxo-2*H*-chromen-3-*yl*)-2-methyl-4-oxo-1,2,3,4-tetrahydroquinazolin-5-*yl*) acrylate (**2.7cg**).

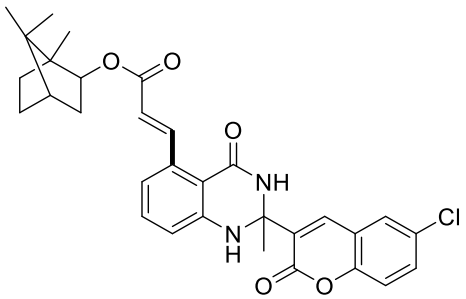

The compound **2.7cg** was synthesized using general procedure C and obtained as yellow solid compound, **2.7cg** 75% (0.41 g); R_f = 0.5 (40% EtOAc + Hexane); **mp** 212-216 °C. **^{1}H NMR** (500 MHz, DMSO-d_6) δ 8.63 (d, *J* = 16.0 Hz, 1H), 8.53 (d, *J* = 8.2 Hz, 1H), 7.86 (s, 1H), 7.78 (s, 1H), 7.57 (dd, *J* = 8.8, 1.9 Hz, 1H), 7.26 (s, 1H), 7.20 (d, *J* = 8.8 Hz,

1H), 7.16 (t, *J* = 7.8 Hz, 1H), 6.87 (dd, *J* = 12.5, 7.9 Hz, 2H), 6.09 (d, *J* = 16.0 Hz, 1H), 4.59 (d, *J* = 6.8 Hz, 1H), 1.73 (s, 3H), 1.68 (dd, *J* = 17.2, 9.2 Hz, 2H), 1.63 – 1.56 (m, 2H), 1.47 – 1.40 (m, 1H), 1.08 – 0.97 (m, 2H), 0.92 (s, 3H), 0.76 – 0.72 (m, 6H). **^{13}C{^{1}H} NMR** (126 MHz, DMSO-d_6) δ 165.5 (s), 163.0 (s), 158.4 (s), 151.7 (s), 147.1 (s), 145.0 (s), 137.5 (s), 136.0 (s), 134.2 (s), 132.7 (s), 131.8 (s), 130.6 (s), 119.9 (s), 118.7 (s), 117.5 (s), 116.6 (s), 111.9 (s), 79.8 (s), 79.0 (s), 78.8 (s), 78.5 (s), 68.4 (s), 48.3 (s), 46.4 (s), 44.3 (s), 38.3 (s), 33.1 (s), 26.5 (s), 26.1 (s), 19.8 (s), 11.2 (s). **HRMS** (ESI-TOF): m/z $[M+H]^+$ calcd for $C_{31}H_{32}N_2O_5Cl$ 547.1955; found 547.1990.

(*E*)-2-(6-Chloro-2-oxo-2*H*-chromen-3-*yl*)-2-methyl-5-(3-oxobut-1-en-1-*yl*)-2,3-dihydroquinazolin-4(1*H*)-one (**2.7ch**).

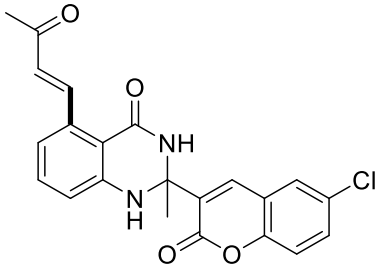

The compound **2.7ch** was synthesized using general procedure C and obtained as yellow solid compound, **2.7ch**, 72% (0.29 g); R_f = 0.4 (60% EtOAc + Hexane); **mp** 168-172 °C. **^{1}H NMR** (500 MHz, DMSO-d_6) δ 8.60 (d, *J* = 16.3 Hz, 1H), 8.55 (s, 1H), 8.06 (d, *J* = 2.3 Hz, 1H), 7.91 (s, 1H), 7.69 (dd, *J* = 8.8, 2.5 Hz, 1H), 7.34 – 7.30 (m, 2H), 7.25 (t, *J* = 7.9 Hz, 1H), 6.95 (d, *J* = 8.1 Hz, 1H), 6.91 (d, *J* = 7.6 Hz, 1H), 6.42 (d, *J* = 16.3 Hz, 1H), 2.29 (s, 3H), 1.81 (s, 3H). **^{13}C{^{1}H} NMR** (126 MHz, DMSO-d_6) δ 198.6 (s), 163.5 (s), 159.0 (s), 152.3 (s), 147.7 (s), 144.8 (s), 138.1 (s), 137.0 (s), 134.8 (s), 133.3 (s), 132.2 (s), 131.3 (s), 128.2 (s), 120.5 (s), 118.5 (s), 118.0 (s), 117.2 (s), 116.7 (s), 112.6 (s), 69.0 (s), 27.7 (s), 26.7 (s). **HRMS** (ESI-TOF): m/z $[M+H]^+$ calcd for $C_{22}H_{18}N_2O_4Cl$ 410.0847; found 410.0877.

***tert*-Butyl (*E*)-3-(2-(6-bromo-2-oxo-2*H*-chromen-3-*yl*)-2-methyl-4-oxo-1,2,3,4-tetrahydroquinazolin-5-*yl*) acrylate** (**2.7da**).

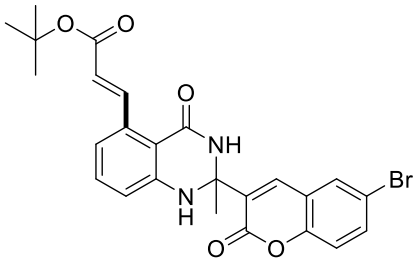

The compound **2.7da** was synthesized using general procedure C and obtained as white solid compound, **2.7da**, 76% (0.39 g); R_f = 0.5 (40% EtOAc + Hexane); **mp** 171-174 °C. **^{1}H NMR** (400 MHz, $CDCl_3$) δ 8.61 (d, *J* = 15.9 Hz, 1H), 8.49 (s, 1H), 7.90 (s, 1H), 7.61 (d, *J* = 1.6 Hz, 1H), 7.53 (dd, *J* = 8.7, 1.8 Hz, 1H), 7.20 (t, *J* = 7.9 Hz, 1H), 7.13 (d, *J* = 8.8 Hz, 1H), 6.88 (d, *J* = 7.6 Hz, 1H), 6.72 (d, *J* = 8.1 Hz, 1H), 6.10 (s, 1H), 6.05 (d, *J* = 5.4 Hz, 1H), 1.98 (s, 3H), 1.45 (s, 9H). **^{13}C{^{1}H} NMR** (101 MHz, $CDCl_3$) δ 166.2 (s), 165.2 (s), 160.0 (s), 152.1 (s), 147.3 (s), 143.7 (s), 138.8 (s), 138.1 (s), 134.8 (s), 133.7 (s), 131.8 (s), 131.0 (s), 122.1 (s), 120.1 (s), 119.6 (s), 118.0 (s), 117.4 (s), 116.6 (s), 112.3 (s), 80.4 (s), 69.6 (s), 31.6 (s), 28.2 (s). **HRMS** (ESI-TOF): m/z $[M+H]^+$ calcd for $C_{25}H_{24}N_2O_5{}^{79}Br$ 510.0790; found 510.0800, calcd for $C_{25}H_{24}N_2O_5{}^{81}Br$ 512.0770; found 512.0790.

Methyl (*E*)-3-(2-(6-bromo-2-oxo-2*H*-chromen-3-*yl*)-2-methyl-4-oxo-1,2,3,4-tetrahydroquinazolin-5-*yl*) acrylate (**2.7db**).

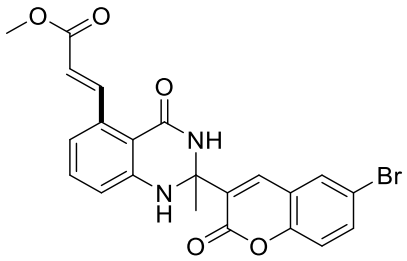

The compound **2.7db** was synthesized using general procedure C and obtained as white solid compound **2.7db** 75% (0.35 g); R_f = 0.5 (40% EtOAc + Hexane); **mp** 154-158 °C.**^{1}H NMR** (500 MHz, DMSO-d_6) δ 8.68 (d, *J* = 16.0 Hz, 1H), 8.61 (d, *J* = 1.0 Hz, 1H), 8.15 (d, *J* = 2.4 Hz, 1H), 7.93 (s, 1H), 7.73 (dd, *J* = 8.8, 2.4 Hz, 1H), 7.35 – 7.32 (m, 2H), 7.24 (t, *J* = 7.9 Hz, 1H), 6.94 (dd, *J* = 7.9, 3.0 Hz, 2H), 6.26 (d, *J* = 16.0 Hz, 1H), 3.70 (s, 3H), 2.52 (s, 3H). **^{13}C{^{1}H} NMR** (126 MHz, DMSO-d_6) δ 166.5 (s), 162.8 (s), 158.4 (s), 151.7 (s), 147.1 (s), 145.4 (s), 137.6 (s), 135.9 (s), 134.2 (s), 132.7 (s), 131.7 (s), 130.9 (s), 120.0 (s), 118.0 (s), 117.5 (s), 116.7 (s), 116.2 (s), 112.0 (s), 68.3 (s), 51.2 (s), 26.1 (s). **HRMS** (ESI-TOF): m/z $[M+H]^+$ calcd for $C_{22}H_{18}N_2O_5{}^{79}Br$ 468.0321; found 468.0332, calcd for $C_{22}H_{18}N_2O_5{}^{81}Br$ 470.0300; found 470.0316.

Ethyl (*E*)-3-(2-(6-bromo-2-oxo-2*H*-chromen-3-*yl*)-2-methyl-4-oxo-1,2,3,4-tetrahydroquinazolin-5-*yl*) acrylate (**2.7dc**).

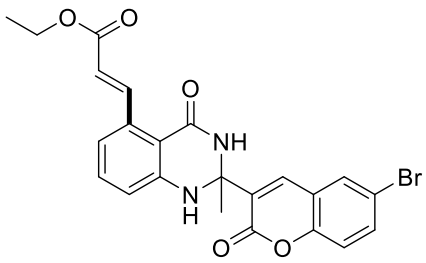

The compound **2.7dc** was synthesized using general procedure C and obtained as light-yellow solid compound, **2.7dc**, 78% (0.39 g); R_f = 0.5 (50% EtOAc + Hexane); **mp** 174-178 °C. **^{1}H NMR** (500 MHz, $CDCl_3$) δ 8.73 (d, *J* = 15.9 Hz, 1H), 8.34 (s, 1H), 7.91 (s, 1H), 7.65 (s, 1H), 7.56 (dd, *J* = 8.9, 1.8 Hz, 2H), 7.22 (d, *J* = 7.8 Hz, 1H), 7.15 (d, *J* = 8.8 Hz, 1H), 6.91 (d, *J* = 7.5 Hz, 1H), 6.17 (d, *J* = 15.9 Hz, 1H), 6.06 (s, 1H), 4.20 (q, *J* = 7.1 Hz, 2H), 1.99 (s, 3H), 1.28 (t, *J* = 7.1 Hz, 3H). **^{13}C{^{1}H} NMR** (126 MHz, $CDCl_3$) δ 166.8 (s), 165.0 (s), 159.9 (s), 152.1 (s), 147.3 (s), 144.7 (s), 138.6 (s), 137.8 (s), 134.7 (s), 133.7 (s), 131.8 (s), 130.9 (s), 120.1 (s), 119.5 (s), 117.9 (s), 117.4 (s), 116.7 (s), 112.2 (s), 69.6 (s), 60.4 (s), 29.7 (s), 27.1 (s), 14.3 (s). **HRMS** (ESI-TOF): m/z $[M+H]^+$ calcd for $C_{23}H_{20}N_2O_5{}^{79}Br$ 482.0477; found 482.0497, calcd for $C_{23}H_{20}N_2O_5{}^{81}Br$ 484.0457; found 484.0477.

2-Ethylhexyl (*E*)-3-(2-(6-bromo-2-oxo-2*H*-chromen-3-*yl*)-2-methyl-4-oxo-1,2,3,4-tetrahydroquinazolin-5-*yl*) acrylate (**2.7df**).

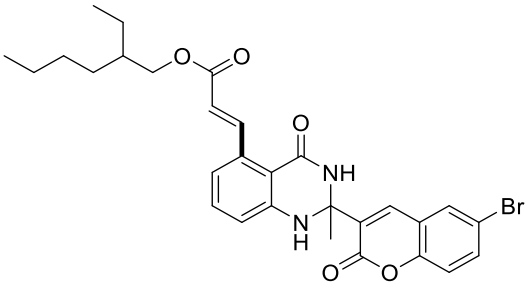

The compound **2.7df** was synthesized using general procedure C and obtained as light-yellow solid compound, **2.7df**, 74% (0.41 g); R_f = 0.6 (40% EtOAc + Hexane); **mp** 192-195 °C. **^{1}H NMR** (500 MHz, $CDCl_3$) δ 8.75 (d, *J* = 15.9 Hz, 1H), 8.21 (s, 1H), 7.91 (s, 1H), 7.65 (d, *J* = 2.2 Hz, 1H), 7.56 (dd, *J* = 8.8, 2.3 Hz, 1H), 7.23 (t, *J* = 7.9 Hz, 1H), 7.15 (d, *J* = 8.8 Hz, 1H), 6.93 (d, *J* = 7.6 Hz, 1H), 6.75 (d, *J* = 8.0 Hz, 1H), 6.19 (d, *J* = 15.9 Hz, 1H), 6.05 (s, 1H), 4.05 (td, *J* = 6.0, 3.5 Hz, 2H), 2.00 (s, 3H), 1.63 – 1.58 (m, 1H), 1.37 (dd, *J* = 13.7, 7.2 Hz, 2H), 1.31 – 1.25 (m, 6H), 0.88 (t, *J* = 7.3 Hz, 6H). **^{13}C{^{1}H} NMR** (126 MHz, $CDCl_3$) δ 167.0 (s), 164.9 (s), 159.9 (s), 152.1 (s), 147.2 (s), 138.6 (s), 137.8 (s), 134.7 (s), 133.6 (s), 130.9 (s), 120.2 (s), 120.0 (s), 119.6 (s), 117.9 (s), 117.4 (s), 116.7 (s), 112.3 (s), 69.6 (s), 66.9 (s), 38.7 (s), 30.3 (s), 28.9 (s), 27.2 (s), 23.7 (s), 22.9 (s), 14.0 (s), 10.9 (s).

HRMS (ESI-TOF): m/z $[M+H]^+$ calcd for $C_{29}H_{32}N_2O_5{}^{79}Br$ 566.1416; found 566.1426. calcd for $C_{29}H_{32}N_2O_5{}^{81}Br$ 568.1396; found 568.1386.

(1*R*,2*R*,4*R*)-1,7,7-Trimethylbicyclo [2.2.1] heptan-2-*yl* (*E*)-3-(2-(6-bromo-2-oxo-2*H*-chromen-3-*yl*)-2-methyl-4-oxo-1,2,3,4-tetrahydroquinazolin-5-*yl*) acrylate (**2.7dg**).

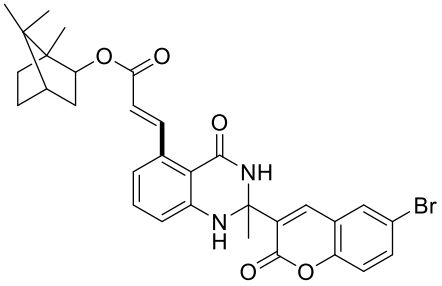

The compound **2.7dg** was synthesized using general procedure C and obtained as white solid compound, **2.7dg**, 73% (0.43 g); R_f = 0.5 (50% EtOAc + Hexane); **mp** 198-202 °C. **^{1}H NMR** (500 MHz, DMSO-d_6) δ 8.63 (d, J = 16.0 Hz, 1H), 8.53 (d, J = 8.2 Hz, 1H), 7.86 (s, 1H), 7.78 (s, 1H), 7.57 (dd, J = 8.8, 1.9 Hz, 1H), 7.26 (s, 1H), 7.20 (d, J = 8.8 Hz, 1H), 7.16 (t, J = 7.8 Hz, 1H), 6.87 (dd, J = 12.5, 7.9 Hz, 2H), 6.09 (d, J = 16.0 Hz, 1H), 4.59 (d, J = 6.8 Hz, 1H), 1.73 (s, 3H), 1.68 (dd, J = 17.2, 9.2 Hz, 2H), 1.63 – 1.56 (m, 2H), 1.47 – 1.40 (m, 1H), 1.08 – 0.97 (m, 2H), 0.92 (s, 3H), 0.76 – 0.72 (m, 6H). **^{13}C{^{1}H} NMR** (126 MHz, DMSO-d_6) δ 165.5 (s), 163.0 (s), 158.4 (s), 151.7 (s), 147.1 (s), 145.0 (s), 137.5 (s), 136.0 (s), 134.2 (s), 132.7 (s), 131.8 (s), 130.6 (s), 119.9 (s), 118.7 (s), 117.9 (s), 116.6 (s), 111.9 (s), 79.8 (s), 79.0 (s), 78.8 (s), 78.5 (s), 68.4 (s), 48.3 (s), 46.4 (s), 44.3 (s), 38.3 (s), 33.1 (s), 26.5 (s), 26.1 (s), 19.8 (s), 11.2 (s). **HRMS** (ESI-TOF): m/z $[M+H]^+$ calcd for $C_{31}H_{32}N_2O_5{}^{79}Br$ 590..1416; found 592.1436, calcd for $C_{31}H_{32}N_2O_5{}^{81}Br$ 592..1396; found 592.1406.

(*E*)-2-(6-Bromo-2-oxo-2*H*-chromen-3-*yl*)-2-methyl-5-(3-oxobut-1-en-1-*yl*)-2,3-dihydroquinazolin-4(1*H*)-one (**2.7dh**).

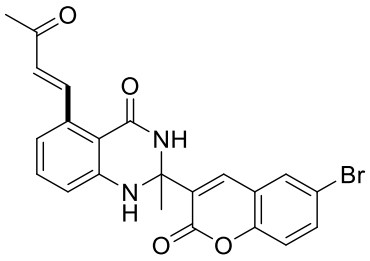

The compound **2.7dh** was synthesized using general procedure C and obtained as yellow solid compound, **2.7dh**, 70% (0.32 g); R_f = 0.5 (60% EtOAc + Hexane); **mp** 134-138

°C. **^{1}H NMR** (500 MHz, DMSO-d_6) δ 8.60 (d, J = 16.3 Hz, 1H), 8.55 (s, 1H), 8.06 (d, J = 2.3 Hz, 1H), 7.91 (s, 1H), 7.69 (dd, J = 8.8, 2.5 Hz, 1H), 7.34 – 7.30 (m, 2H), 7.25 (t, J = 7.9 Hz, 1H), 6.95 (d, J = 8.1 Hz, 1H), 6.91 (d, J = 7.6 Hz, 1H), 6.42 (d, J = 16.3 Hz, 1H), 2.29 (s, 3H), 1.82 (s, 3H). **^{13}C{^{1}H} NMR** (126 MHz, DMSO-d_6) δ 198.6 (s), 163.5 (s), 159.0 (s), 152.3 (s), 147.7 (s), 144.8 (s), 138.1 (s), 137.0 (s), 134.8 (s), 133.3 (s), 132.2 (s), 131.3 (s), 128.2 (s), 120.5 (s), 118.5 (s), 118.0 (s), 117.2 (s), 116.7 (s), 112.6 (s), 69.0 (s), 27.7 (s), 26.7 (s). **HRMS** (ESI-TOF): m/z $[M+H]^+$ calcd for $C_{22}H_{18}N_2O^{79}Br$ 453.0372; found 453.0395. calcd for $C_{22}H_{18}N_2O_4{}^{81}Br$ 455.0879; found 455.0895.

***tert*-Butyl (*E*)-3-(2-methyl-4-oxo-2-(2-oxo-2*H*-benzo[*f*]chromen-3-*yl*)-1,2,3,4-tetrahydroquinazolin-5-*yl*) acrylate (2.7ea).**

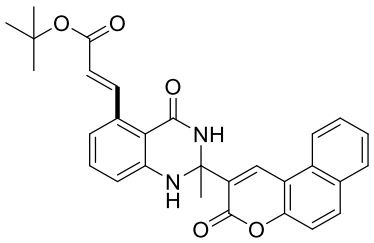

The compound **2.7ea** was synthesized using general procedure C and obtained as yellow solid compound, **2.7ea**, 70% (0.34 g); R_f = 0.5 (40% EtOAc + Hexane); **mp** 188-192 °C. **^{1}H NMR** (500 MHz, DMSO-d_6) δ 8.65 (d, J = 4.8 Hz, 1H), 8.60 (d, J = 8.4 Hz, 1H), 8.16 (d, J = 8.4 Hz, 1H), 8.09 (d, J = 9.1 Hz, 2H), 7.98 (d, J = 8.1 Hz, 1H), 7.77 (dd, J = 13.5, 6.4 Hz, 1H), 7.59 (t, J = 6.6 Hz, 1H), 7.55 (s, 1H), 7.49 (d, J = 9.0 Hz, 1H), 7.28 (t, J = 7.9 Hz, 1H), 7.09 (d, J = 8.1 Hz, 1H), 6.91 (d, J = 7.6 Hz, 1H), 6.10 (d, J = 15.9 Hz, 1H), 1.87 (s, 3H), 1.43 (s, 9H). **^{13}C{^{1}H} NMR** (126 MHz, DMSO-d_6) δ 165.3 (s), 163.1 (s), 158.7 (s), 152.5 (s), 147.5 (s), 144.1 (s), 136.1 (s), 134.1 (s), 133.1 (s), 132.8 (s), 129.6 (s), 128.9 (s), 128.4 (s), 125.9 (s), 120.7 (s), 120.1 (s), 117.6 (s), 116.4 (s), 116.1 (s), 112.0 (s), 111.6 (s), 79.5 (s), 68.8 (s), 27.6 (s), 26.3 (s). **HRMS** (ESI-TOF): m/z $[M+H]^+$ calcd for $C_{29}H_{27}N_2O_5$ 483.1875; found 483.1890.

Methyl (*E*)-3-(2-methyl-4-oxo-2-(2-oxo-2*H*-benzo[*f*]chromen-3-*yl*)-1,2,3,4-tetrahydroquinazolin-5-*yl*) acrylate (2.7eb).

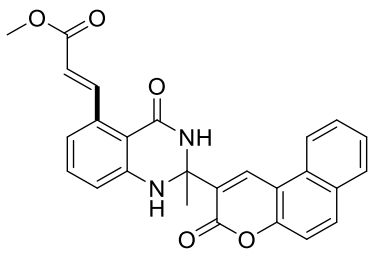

The compound **2.7eb** was synthesized using general procedure C and obtained as yellow solid compound, **2.7eb**, 72% (0.31 g); R_f = 0.5 (40% EtOAc + Hexane); **mp** 181-184 °C. **^{1}H NMR** (500 MHz, DMSO-d_6) δ 8.67 (s, 1H), 8.62 (d, *J* = 8.5 Hz, 1H), 8.20 (d, *J* = 8.5 Hz, 1H), 8.16 (d, *J* = 9.0 Hz, 1H), 8.04 (d, *J* = 8.0 Hz, 1H), 7.80 (d, *J* = 7.3 Hz, 1H), 7.62 (t, *J* = 7.5 Hz, 1H), 7.58 – 7.52 (m, 2H), 7.29 (t, *J* = 7.9 Hz, 1H), 7.10 (d, *J* = 8.1 Hz, 1H), 6.92 (d, *J* = 7.5 Hz, 1H), 6.22 (d, *J* = 16.0 Hz, 1H), 3.68 (s, 3H), 1.86 (s, 3H). **^{13}C{^{1}H} NMR** (126 MHz, DMSO-d_6) δ 166.4 (s), 163.0 (s), 158.7 (s), 152.5 (s), 147.5 (s), 145.1 (s), 136.0 (s), 134.2 (s), 133.2 (s), 132.9 (s), 129.7 (s), 129.0 (s), 128.4 (s), 126.0 (s), 120.8 (s), 118.2 (s), 117.7 (s), 116.6 (s), 116.2 (s), 112.0 (s), 111.7 (s), 68.8 (s), 51.2 (s), 26.4 (s). **HRMS** (ESI-TOF): m/z $[M+H]^+$ calcd for $C_{26}H_{21}N_2O_5$ 441.1406; found 441.1436.

Ethyl (*E*)-3-(2-methyl-4-oxo-2-(2-oxo-2*H*-benzo[*f*]chromen-3-*yl*)-1,2,3,4-tetrahydroquinazolin-5-*yl*) acrylate (**2.7ec**).

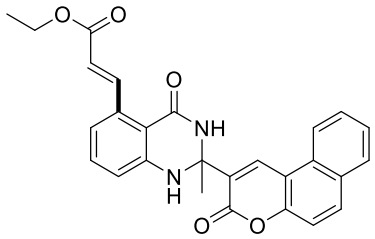

The compound **2.7ec** was synthesized using general procedure C and obtained as yellow solid compound, **2.7ec**, 72% (0.32 g); R_f = 0.5 (40% EtOAc + Hexane); **mp** 202-206 °C. **^{1}H NMR** (500 MHz, DMSO-d_6) δ 8.66 (d, *J* = 10.0 Hz, 1H), 8.61 (d, *J* = 6.7 Hz, 1H), 8.21 – 8.17 (m, 2H), 8.05 (d, *J* = 8.1 Hz, 1H), 7.81 (t, *J* = 7.8 Hz, 1H), 7.63 (d, *J* = 7.5 Hz, 1H), 7.56 (d, *J* = 4.7 Hz, 1H), 7.54 (s, 1H), 7.29 (t, *J* = 7.9 Hz, 1H), 7.09 (d, *J* = 8.1 Hz, 1H), 6.92 (d, *J* = 7.6 Hz, 1H), 6.20 (d, *J* = 16.0 Hz, 1H), 4.14 (q, *J* = 7.1 Hz, 2H), 1.86 (s, 3H), 1.22 (t, *J* = 7.1 Hz, 3H). **^{13}C{^{1}H} NMR** (126 MHz, DMSO-d_6) δ 166.0 (s), 163.0 (s), 158.7 (s), 152.6 (s), 147.5 (s), 145.0 (s), 136.0 (s), 134.2 (s), 133.2 (s), 132.9 (s), 129.7 (s), 129.0 (s), 128.4 (s), 126.0 (s), 120.8 (s), 118.5 (s), 117.7 (s), 116.5 (s), 116.2 (s), 112.0 (s), 111.7 (s), 68.8 (s), 59.7 (s), 26.3 (s), 14.0 (s). **HRMS** (ESI-TOF): m/z $[M+H]^+$ calcd for $C_{27}H_{23}N_2O_5$ 455.1562; found 455.1582.

2-Ethylhexyl (*E*)-3-(2-methyl-4-oxo-2-(2-oxo-2*H*-benzo[*f*]chromen-3-*yl*)-1,2,3,4-tetrahydroquinazolin-5-*yl*) acrylate (**2.7ef**).

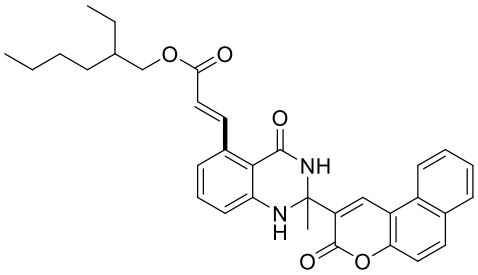

The compound **2.7ef** was synthesized using general procedure C and obtained as light-yellow solid compound, **2.7ef**, 68% (0.36 g); R_f = 0.6 (40% EtOAc + Hexane); **mp** 212-216 °C. **^{1}H NMR** (500 MHz, DMSO-d_6) δ 8.70 (s, 1H), 8.66 (d, *J* = 7.8 Hz, 2H), 8.16 (d, *J* = 8.5 Hz, 1H), 8.10 (d, *J* = 9.1 Hz, 1H), 7.99 (d, *J* = 8.1 Hz, 1H), 7.76 (t, *J* = 7.3 Hz, 1H), 7.59 (t, *J* = 7.5 Hz, 1H), 7.56 (s, 1H), 7.50 (d, *J* = 9.0 Hz,1H), 7.29 (t, *J* = 7.9 Hz, 1H), 7.09 (d, *J* = 8.1 Hz, 1H), 6.94 (d, *J* = 7.5 Hz, 1H), 6.20 (d, *J* = 16.0 Hz, 1H), 4.00 (q, *J* = 5.3 Hz, 2H), 1.86 (s, 3H), 1.56 – 1.51 (m, 1H), 1.30 (dd, *J* = 7.1, 3.9 Hz, 2H), 1.25 – 1.19 (m, 6H), 0.82 (td, *J* = 7.5, 5.5 Hz, 6H). **^{13}C{^{1}H} NMR** (126 MHz, DMSO-d_6) δ 166.1 (s), 163.1 (s), 158.7 (s), 152.5 (s), 147.5 (s), 145.0 (s), 136.0 (s), 134.1 (s), 133.1 (s), 132.8 (s), 129.7 (s), 128.9 (s), 128.3 (s), 125.9 (s), 120.7 (s), 118.5 (s), 117.6 (s), 116.6 (s), 116.1 (s), 111.9 (s), 111.7 (s), 68.8 (s), 65.7 (s), 38.0 (s), 29.6 (s), 28.1 (s), 26.3 (s), 23.1 (s), 22.2 (s), 13.7 (s), 10.6 (s). **HRMS** (ESI-TOF): m/z $[M+H]^+$ calcd for $C_{33}H_{35}N_2O_5$ 539.2501; found 539.2535.

(1*R*,2*R*,4*R*)-1,7,7-Trimethylbicyclo [2.2.1] heptan-2-*yl* (*E*)-3-(2-methyl-4-oxo-2-(3-oxo-3*H*-benzo[*f*]chromen-2-*yl*)-1,2,3,4-tetrahydroquinazolin-5-*yl*) acrylate (**2.7eg**).

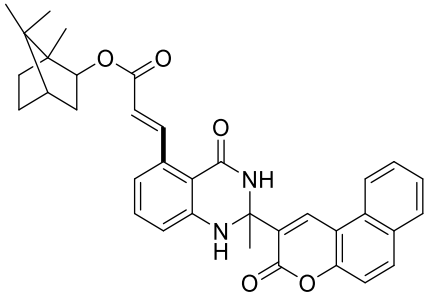

The compound **2.7eg** was synthesized using general procedure C and obtained as light-yellow solid compound, **2.7eg**, 68% (0.38 g); R_f = 0.5 (50% EtOAc + Hexane); **mp** 232-236 °C. **^{1}H NMR** (500 MHz, DMSO-d_6) δ 8.61 (s, 1H), 8.58 (s, 1H), 8.53 (s, 1H), 8.03 (dd, *J* = 11.3, 9.1 Hz, 2H), 7.91 (d, *J* = 8.1 Hz, 1H), 7.65 (t, *J* = 7.7 Hz, 1H), 7.50 (d, *J* = 7.1 Hz, 1H), 7.41 (d, *J* = 8.7 Hz, 2H), 7.15 (t, *J* = 7.9 Hz, 1H), 6.95 (dd, *J* = 8.2, 1.5 Hz, 1H), 6.81 (dd, *J* = 7.4, 3.8 Hz, 1H), 6.02 (d, *J* = 16.2 Hz, 1H), 4.53 (dd, *J* = 7.4, 2.9 Hz, 1H), 1.74 (s, 3H), 1.67 – 1.60 (m, 2H), 1.55-1.51 (m, 2H), 1.09 (s, 1H), 1.01 – 0.93 (m, 2H), 0.89 (d, *J* =

13.6 Hz, 3H), 0.74 – 0.69 (m, 6H). **^{13}C{^{1}H} NMR** (126 MHz, DMSO-d_6) δ 165.3 (s), 163.3 (s), 158.7 (s), 152.5 (s), 147.5 (s), 144.6 (s), 136.0 (s), 134.1 (s), 133.2 (s), 132.8 (s), 129.7 (s), 129.0 (s), 128.4 (s), 126.0 (s), 120.6 (s), 118.9 (s), 117.5 (s), 116.6 (s), 116.2 (s), 111.7 (s), 79.8 (s), 68.7 (s), 48.3 (s), 46.4 (s), 44.3 (s), 38.2 (s), 33.0 (s), 26.4 (s), 26.1 (s), 19.9 (s) 11.2 (s). **HRMS** (ESI-TOF): m/z $[M+H]^+$ calcd for $C_{35}H_{35}N_2O_5$ 563.2501; found 563.2536.

(*E*)-2-Methyl-2-(3-oxo-3*H*-benzo[*f*]chromen-2-*yl*)-5-(3-oxobut-1-en-1-*yl*)-2,3-dihydroquinazolin-4(1*H*)-one (**2.7eh**).

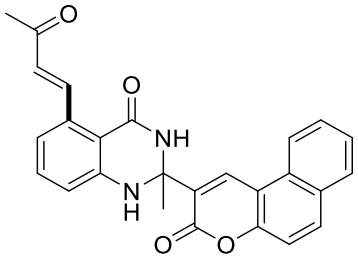

The compound **2.7eh** was synthesized using general procedure C and obtained as light yellow solid compound, **2.7eh**, 68 % (0.29 g); R_f = 0.5 (60% EtOAc + Hexane); **mp** = 170-175 °C. **^{1}H NMR** (500 MHz, $CDCl_3$) δ 8.80 (s, 1H), 8.68 (d, J = 16.3 Hz, 1H), 8.32 (s, 1H), 8.18 (dd, J = 6.5, 3.0 Hz, 1H), 7.92 (d, J = 9.0 Hz, 1H), 7.82 – 7.80 (m, 1H), 7.48 – 7.46 (m, 2H), 7.38 (d, J = 9.0 Hz, 1H), 7.25 (d, J = 8.0 Hz, 1H), 1H), 6.89 (d, J = 7.6 Hz, 1H), 6.83 (d, J = 8.1 Hz, 1H), 6.31 (d, J = 16.3 Hz, 2H), 2.26 (s, 3H), 2.07 (s, 3H). **^{13}C{^{1}H} NMR** (126 MHz, $CDCl_3$) δ 199.0 (s), 165.5 (s), 160.5 (s), 153.1 (s), 147.7 (s), 144.3 (s), 138.0 (s), 135.6 (s), 133.8 (s), 133.5 (s), 130.2 (s), 129.8 (s), 129.5 (s), 128.9 (s), 128.3 (s), 126.3 (s), 121.5 (s), 119.5 (s), 117.1 (s), 116.2 (s), 112.7 (s), 111.9 (s), 70.0 (s), 27.8 (s), 26.7 (s). **HRMS** (ESI-TOF): m/z $[M+H]^+$ calcd for $C_{26}H_{21}N_2O_4$ 425.1457; found 425.1480.

General procedure D for the saponification of ester:

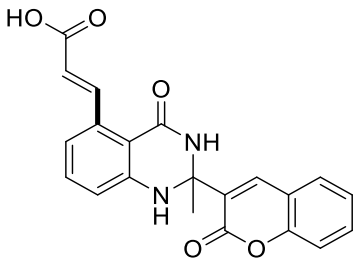

To a solution of **2.7aa** (0.43 g, 1.0 mmol, 1.0 eq) in H_2O (2 mL) and ethanol (2 mL) was added NaOH (0.04 g, 1 mmol, 1.0 eq) and the reaction mixture was stirred at 80 °C (in oil bath) for 2 h. The mixture was brought to *p*H 2 and then kept the reaction mixture at 5 °C

for 2 h, then a white crystalline solid **8a** was separated and filtered off, yield, **(*E*)-3-(2-Methyl-4-oxo-2-(2-oxo-2*H*-chromen-3-yl)-1,2,3,4-tetrahydroquinazolin-5-yl)acrylic acid (2.8a**) 60%, (0.23 g); mp = 212-216 °C. **^{1}H NMR** (500 MHz, **$CDCl_3$**) δ 9.73 (s, 1H), 9.04 (d, J = 15.9 Hz, 1H), 7.97 (s, 1H), 7.61 (d, J = 7.4 Hz, 1H), 7.52 (t, J = 7.2 Hz, 1H), 7.31 – 7.27 (m, 3H), 7.24 (s, 1H), 7.01 (d, J = 7.6 Hz, 1H), 6.74 (d, J = 8.1 Hz, 1H), 6.23 (d, J = 15.9 Hz, 1H), 6.14 (s, 1H), 1.98 (s, 3H). **^{13}C{^{1}H} NMR** (126 MHz, **$CDCl_3$**) δ 171.9 (s), 167.1 (s), 160.5 (s), 153.3 (s), 147.8 (s), 145.4 (s), 140.0 (s), 137.5 (s), 134.0 (s), 132.2 (s), 130.4 (s), 128.9 (s), 124.9 (s), 120.8 (s), 119.2 (s), 118.5 (s), 117.1 (s), 116.3 (s), 111.5 (s), 69.4 (s), 27.1 (s). **HRMS** (ESI-TOF): m/z $[M+H]^+$ calcd for $C_{21}H_{17}N_2O_5$ 433.1719; found 433.1739

CHAPTER 3

C(sp^2)-H Alkenylation of Chromeno[4,3-*c*]pyrazol-4-ones

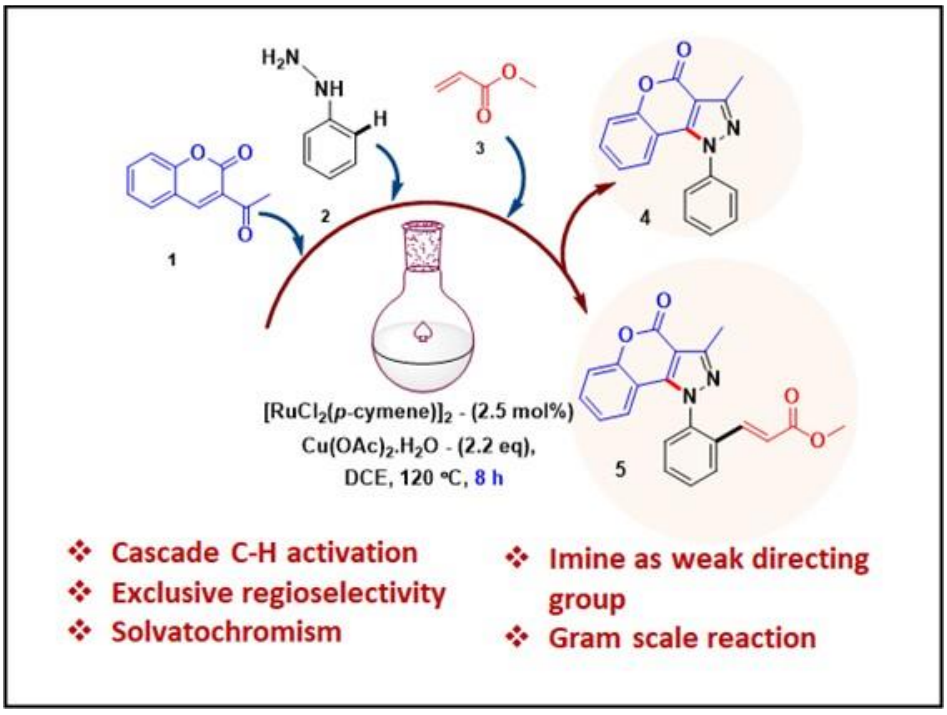

CHAPTER 3

3.1. Introduction

Fused π-conjugated heterocyclic compounds have significant importance in material science and pharmaceuticals.[76] The construction of new conjugates using different pharmacophores and their late-stage modification is an engrossing topic for the organic community.[77] Conjugates consisting of coumarin and pyrazole belong to enchant family of structurally distinct heterocycles having significant biological properties.[78] In addition, coumarin and pyrazole-based heterocyclic scaffolds could also be used as fluorescent materials, optical brighteners, and laser dyes.[79] Owing to their significant importance, incisive and effective synthesis of these heterocyclic moieties and their functionalization have claimed continual attention from organic chemists.[80] In 2008, Daugulis *et al.* carried out C5 arylation of unsubstituted *N*-phenylpyrazole (**Scheme 3.1a**).[81] After three years, in 2011, Gaulier *et al.*,

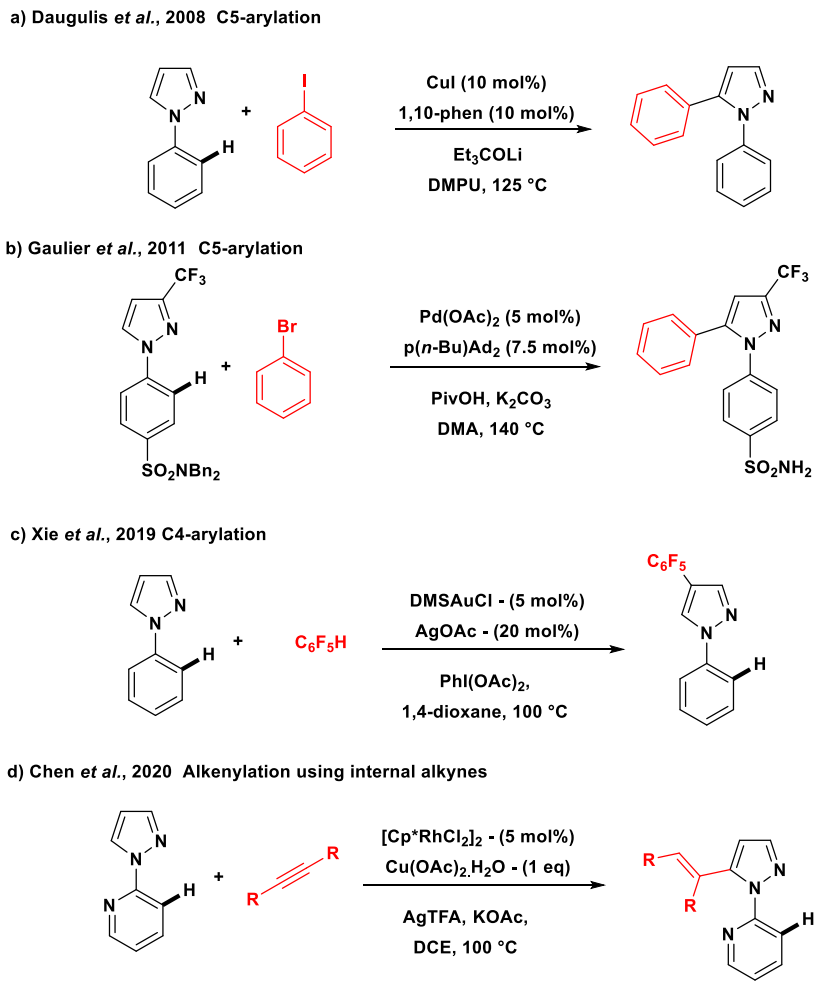

Scheme 3.1. Research background and present work

inspired from Daugulis's work demonstrated the synthesis of Celecoxib and achieved high regioselectivity (**Scheme 3.1b**).[82] In 2019, Xie group gave a unique approach to access C4-arylation of *N*-aryl pyrazoles with polyhalogenated aryl halide using electrophilic species such as Au(III) (**Scheme 3.1c**).[83] In 2020, Chen group performed alkenylation using internal alkynes under rhodium catalysis (**Scheme 3.1d**). Notably, all these methods of *N*-aryl pyrazole required either pre-functionalization of reacting material or silver additives for activating catalyst or multistep synthesis for starting material or difficulty installing other pharmacophores on pyrazole, due to which their synthetic applications are limited. Although literature has been reported for synthesis and functionalization of chromeno[4,3-*c*]pyrazol-4(1*H*)-ones, to the best of our knowledge, no approach has been known for one-pot synthesis and *in-situ* regioselective C–H functionalization of these compounds for late-stage modification. Hence, atom- and step-economical approaches are desirable. Recently, cascade one-pot[84] transition metal-catalyzed C–H functionalization[85] and late-stage functionalization are advantageous in step economy, as there is no need to install directing group or pre-functionalization of reacting species.

3.2. Objective

Herein, one-pot synthesis of 1-phenyl-1*H*-chromeno[4,3-*c*]pyrazol-4-one and *in situ* regioselective *ortho*-C–H alkenylation *via* ruthenium-catalyzed intermolecular dehydrogenative coupling of olefins in the absence of base and silver additive is reported. Later on, photophysical studies of final compounds are unveiled.

3.3. Results and Discussion

3.3.1. Optimization for Cascade Transformation

Primarily, our investigation commenced with validating the optimal conditions for cascade synthesis and C–H functionalization of 1-phenyl-1*H*-chromeno[4,3-*c*]pyrazol-4-one. I began with the reaction of 3-acetyl-2*H*-chromen-2-one **3.1a** (0.1 mmol, 1.0 eq.) with phenylhydrazine **3.2a** (0.1 mmol, 1.0 eq.), and methyl acrylate **3.3a** (0.3 mmol, 3.0 eq.). As acrylates exhibit more positive influence with ruthenium catalysis,[86] therefore, initially, solvents were investigated in the presence of $[RuCl_2(p\text{-cymene})]_2$ catalyst and $Cu(OAc)_2.H_2O$ (2.2 eq.) oxidant at 120 °C. Various polar and non-polar solvents were examined, where polar aprotic solvents such as NMP, 1,4-dioxane, THF, DMF, and DMSO demonstrated moderate compatibility (**Table 3.1**, entries 1-5).

Table 3.1. Optimization of Reaction Conditions[a]

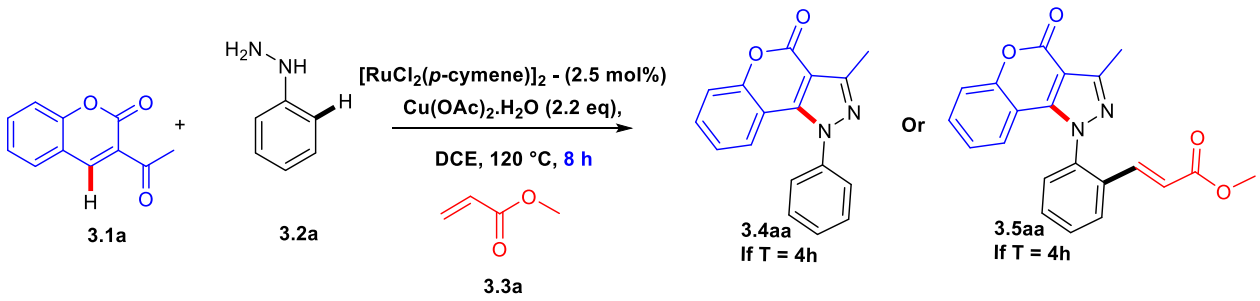

entry	solvent	additive	oxidant	yield **3.5aa**(%)[b]
1	NMP	…….	$Cu(OAc)_2.H_2O$	20
2	1,4-dioxane	$AgSbF_6$	$Cu(OAc)_2.H_2O$	25
3	THF	…….	$Cu(OAc)_2.H_2O$	30
4	DMF	K_2CO_3	$Cu(OAc)_2.H_2O$	40
5	DMSO	……	$Cu(OAc)_2.H_2O$	35
6	toluene	…….	$Cu(OAc)_2.H_2O$	traces
7	*o*-xylene	…….	$Cu(OAc)_2.H_2O$	traces
8	MeOH	…….	$Cu(OAc)_2.H_2O$	traces
9	AcOH	…….	$Cu(OAc)_2.H_2O$	traces
10	DCE	……	$Cu(OAc)_2.H_2O$	80
11[c]	DCE	…….	$Cu(OAc)_2.H_2O$	70
12	DCE	K_2CO_3	Ag_2CO_3	10
13	DCE	$AgNTf_2$	AgOAc	55
14	DCE	$AgSbF_6$	$Cu(OAc)_2.H_2O$	40
15	DCE	…….	AgOAc	65
16[d]	DCE	…….	$Cu(OAc)_2.H_2O$	…

[a]General reaction condition: **3.1a** (1 mmol), **3.2a** (1 mmol), **3.3a** (3 mmol), $[RuCl_2(p\text{-cymene})]_2$ (2.5 mol%), $Cu(OAc)_2.H_2O$ (2.2 equiv), solvent (2 mL), [b]Isolated yields after purification, [c]$Pd(OAc)_2$ is used as catalyst, [d]In absence of $[RuCl_2(p\text{-cymene})]_2$.

In contrast, non-polar (**Table 3.1**, entries 6-7) and polar protic (**Table 3.1**, entries 8-9) solvents were proved unsuccessful for this reaction. Furthermore, due to the specific

solubilizing and physicochemical characteristics of chlorinated and other halogenated solvents, they have found themselves in a unique position in the field of C−H bond activation chemistry. The key features that many of the solvents employed in C−H bond activation possess include a high polarity character in combination with both hydrophilic and hydrophobic moieties, I have tested chlorinated solvent DCE (**Table 3.1**, entry 10); gratifyingly, DCE gave 80% yield of the desired compound **3.5aa**. To increase the yield of **3.5aa** and to enhance the reaction rate, I used different catalysts such as CuI, $Cu(OTf)_2$, $Ni(OTf)_2$, $Pd\{P(C_6H_5)_4\}$ etc. Still, no yield and reaction rate improvement was observed, while $Pd(OAc)_2$ showed a comparable yield of 70% (**Table 3.1**, entry 11). Here, transition metals have significant role in C-H bond activation by forming five or six membered stable complexes. As oxidant plays a role in ruthenium-based functionalization, I also looked into different oxidants and additives (**Table 3.1**, entries 12-15). It is worth noting that no superior result was obtained in the case of alkali-based salts, while silver-based oxidants and additives improved the yield to 65% (**Table 3.1**, entry 15). In addition, no efficacy was maintained in the absence of $[RuCl_2(p\text{-cymene})]_2$ (**Table 3.1**, entry 16). At the same time, compound **3.4aa** obtained in excellent yield, and no C–H functionalization on **3.4aa** was observed in small traces. Notably, the reaction is highly regioselective for *ortho*-alkenylation throughout screening; neither dialkenylated product nor *meta*-or-*para* alkenylation was observed.[87]

Compound **3.4aa** was confirmed by ^1H and ^{13}C NMR spectra; compound showed characteristic signals of aromatic protons as a multiplet at δ 7.62-7.60 ppm of 3H, two multiplets at δ 7.56-7.53 and 7.47-7.43 ppm of 2H, two doublets of doublet at δ 7.10 ppm with J = 8.0, 1.1 Hz of 1H and at δ 7.03 ppm with J = 8.2, 6.7 Hz of 1H in aromatic region. Notably, a singlet at δ 1.95 Hz of 3H of CH_3 in the aliphatic region also confirmed the formation of **3.4aa**. Furthermore, characteristic signals in ^{13}C NMR, such as at δ 13.0 ppm of methyl group confirmed the structure. Similarly, compound **3.5aa** was confirmed by ^1H and ^{13}C NMR spectra; compound showed characteristic signals of aromatic protons as doublet of doublet at δ 7.88 ppm with J = 8.0, 1.6 Hz of 1H, doublet of 1H at δ 7.68 ppm with J = 7.7, 1.6 Hz, two doublets of doublet at δ 7.62 ppm with J = 7.7, 1.6 Hz of 1H and at δ 7.47 ppm with J = 7.9, 1.5 Hz of 1H, multiplet at δ 7.44-7.42 ppm of 2H, doublet at δ 7.24 ppm with J = 16.2 Hz of 1H due to vinylic hydrogen of alkene, multiplet at δ 7.00-6.96 ppm of 1H, doublet of doublet at δ 6.72 ppm with J = 8.6, 1.4 Hz of 1H, and doublet at δ 6.33 ppm with J = 16.0 Hz of 1H due to vinylic hydrogen. Notably, two vinylic protons have almost same J value (c. 16.0 Hz), confirming no cyclization. In addition, signals of two singlets at δ 3.68

and 2.72 ppm of 3H of methoxy and methyl groups confirmed the incorporation of acrylate to the starting substrate. Furthermore, characteristic signals in ^{13}C NMR at δ 166.4 ppm for carbonyl carbon of acrylate, δ 51.9 ppm showed methoxy, and δ 13.1 ppm of methyl group confirmed the structure.

3.3.2. Substrate Scope for Cascade Transformation

Next, I examined the electronic effects and substrate scope of this cascade transformation. Firstly, unsubstituted and substituted phenylhydrazines **3.2a-l** were tested with **3.1a** and **3.3a** under optimized conditions. Substrates, substituting at *para*-position of aryl ring with bromo **3.2b**, chloro **3.2c**, methyl **3.2d**, fluoro **3.2e**, nitro **3.2f**, and cyano **3.2g** underwent cascade transformation smoothly to give respective scaffolds **3.5ab-3.5ag** in 63-86% yields. Phenylhydrazines with electron-donating groups are more compatible than those with electron-withdrawing groups. Similarly, substrates having *meta*-substituted aryl ring with bromo **3.2h**, chloro **3.2i**, and nitro **3.2j** were also subjected to general reaction conditions and gave corresponding compounds **3.5ah-3.5aj** in 62-67% yields. Notably, *ortho*-substituted phenylhydrazine with chloro **3.2k** and *o*,*p*-dichloro **3.2l** gave desired compounds **3.5ak-3.5al** in 50-55% yields, while no alkenylated product was obtained on substituting methyl **3.2m** and ethyl **3.2n** groups at *ortho*-position of phenylhydrazine. It might be due to the bulky group at *ortho*-position, which may restrict the rotation of the aryl ring. Further, substituted coumarins **3.1a-d** were investigated with phenylhydrazine **3.2a** and methyl acrylate **3.3a**. Those having electron-rich groups such as chloro **3.1b**, bromo **3.1c**, and methoxy **3.1d** were more compatible for the designed transformation and yielded **3.5ba-3.5da** up to 85% yield. Various electron-donating groups such as *N,N*-diethylamine and hydroxy groups were also tested, but unfortunately, the reaction did not proceed as they may hinder the nucleophilic attack of phenylhydrazine on 3-acetyl-2*H*-chromen-2-one by increasing the electron density. After coumarin, I explored different alkenes **3.3a-I** with **3.1a** and **3.2a**; interestingly, acrylates showed significant tolerance for this transformation, whereas *α,β*-unsaturated ketones, *iso*-boronylacrylate, and electron-deficient alkenes such as acrylic acid, acrylonitrile, and vinyl phenyl sulphone all were found unsuccessful. In addition, vinyl phenyl sulfone **3f** also gave the desired compound **3.5aq** in 45% yield (**Scheme 3.2**). In addition, I have also successfully isolated intermediates **3.4aa-3.4al** and **3.4ba-3.4da** in excellent yields after 1 h, i.e., before alkene insertion to decipher their photophysical behaviour and compared them with alkenylated

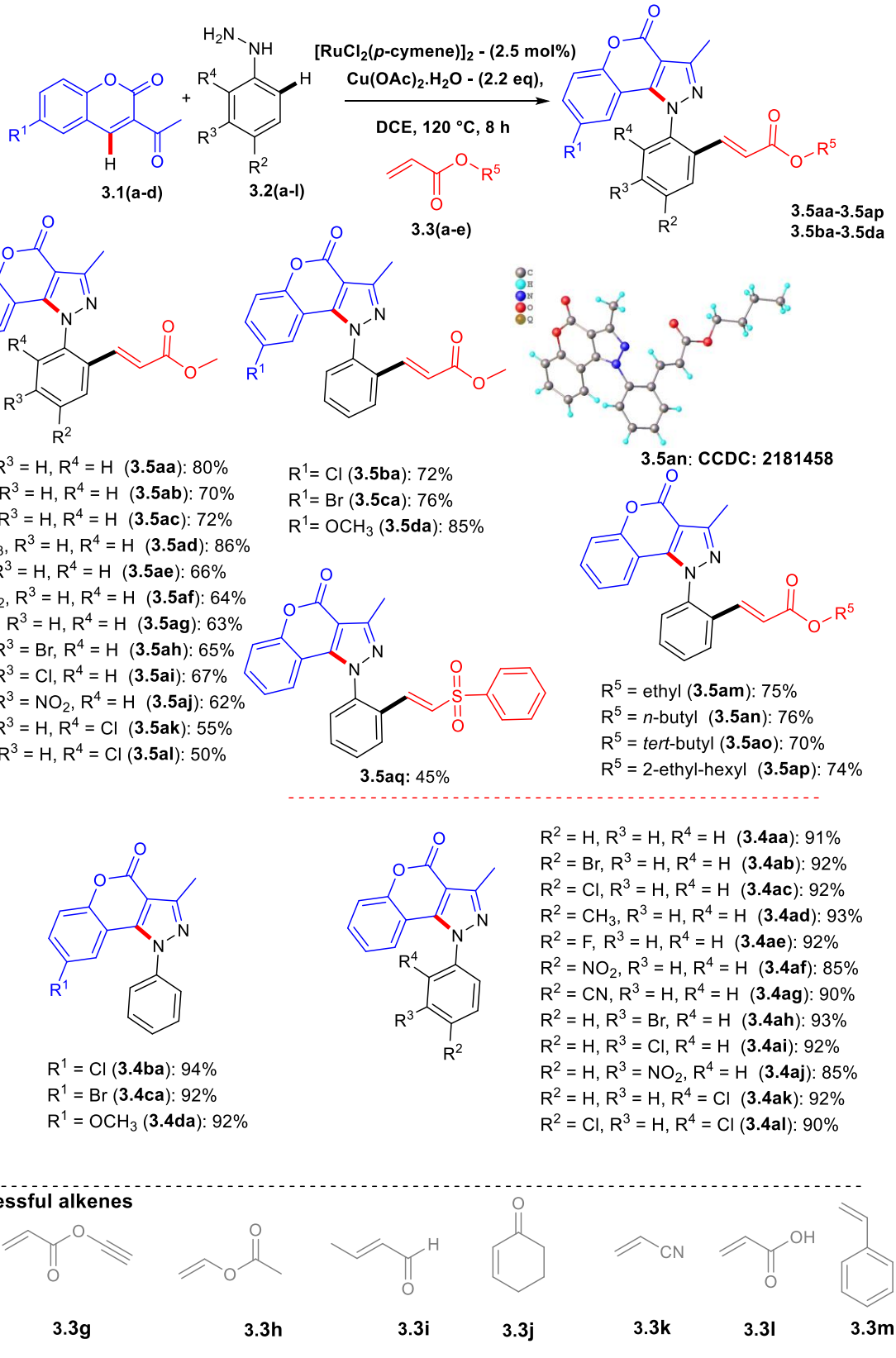

Scheme 3.2. Substrate scope for one-pot reaction

compounds **3.5aa-3.5ap** and **3.5ba-3.5da**. Compound **3.5an** was further characterized by single-crystal X-ray crystallography (**CCDC no.** 2181458) to provide more insights into regioselectivity and cascade alkenylation. Compound **3.5an** comprises three planar fragments, coumarin, *N*-phenylpyrazole, and butyl acrylate, which are in conjugation with each other. Compound **3.5an**, has Z = 2 and exhibits triclinic structure in the space group P-1 (**Table 3.2**). These data revealed that the electronic factors dominate this hybrid system for regioselective C–H functionalization.

Table 3.2. X-ray analysis of compound **3.5an**

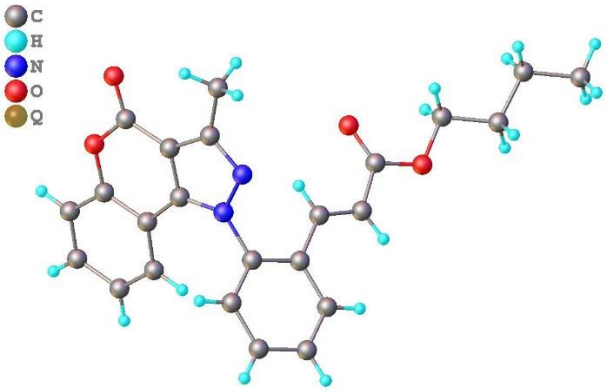

Identification code	**Ex-Ptla-CPB-1-4**
Empirical formula	$C_{24}H_{22}N_2O_4$
Formula weight	402.43
Temperature/K	293(2)
Crystal system	triclinic
Space group	P-1
a/Å	8.7664(4)
b/Å	12.9985(6)
c/Å	19.6277(10)
α/°	93.836(4)
β/°	95.077(4)
γ/°	109.248(4)
Volume/Å3	2092.26(19)
Z	2
ρcalcg/cm3	1.278
μ/mm-1	0.088

F(000)	848.0
Crystal size/mm3	0.04 × 0.03 × 0.025
Radiation	MoKα (λ = 0.71073)
2Θ range for data collection/° 6.528 to 54.786	
Index ranges	-10 ≤ h ≤ 11, -14 ≤ k ≤ 16, -25 ≤ l ≤ 25
Reflections collected	28247
Independent reflections	8820
Data/restraints/parameters	1.075
Goodness-of-fit on F2	R1 = 0.1189, wR2 = 0.2014
Final R indexes [all data]	

3.3.3. Gram Scale Reactions

A scale-up experiment was set up to examine the efficacy of the present methodology and industrial utility, giving 88% yield of the alkenylated product (**Scheme 3.3a**) and reducing the catalyst and co-catalyst loads gave **3.5aa** in 70% yield along with the recovery of 25% of starting material (**Scheme 3.3b**).

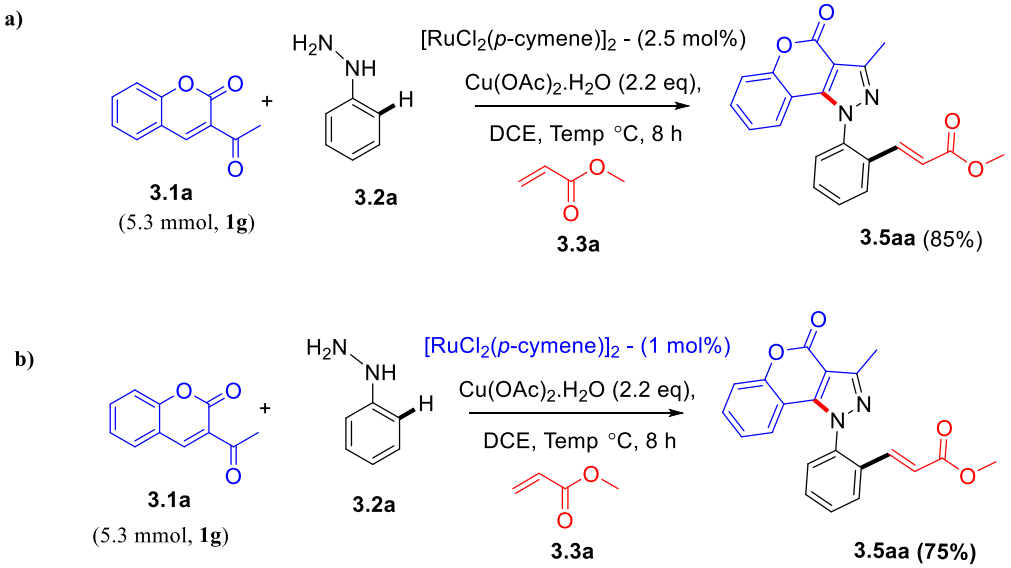

Scheme 3.3. Gram scale reactions

3.3.4. Deuterium Labelled and Control Experiments

After the myriad screening, I then turned around to descry the mechanistic pathway of the reaction, for which, various control experiments were performed. In **Scheme 3.4a**, the reaction was monitored periodically; after 10 min, **Int-A** was obtained in 95% yield, which was readily formed by the nucleophilic attack of phenyl-hydrazine on carbonyl carbon of acetyl group of coumarin.

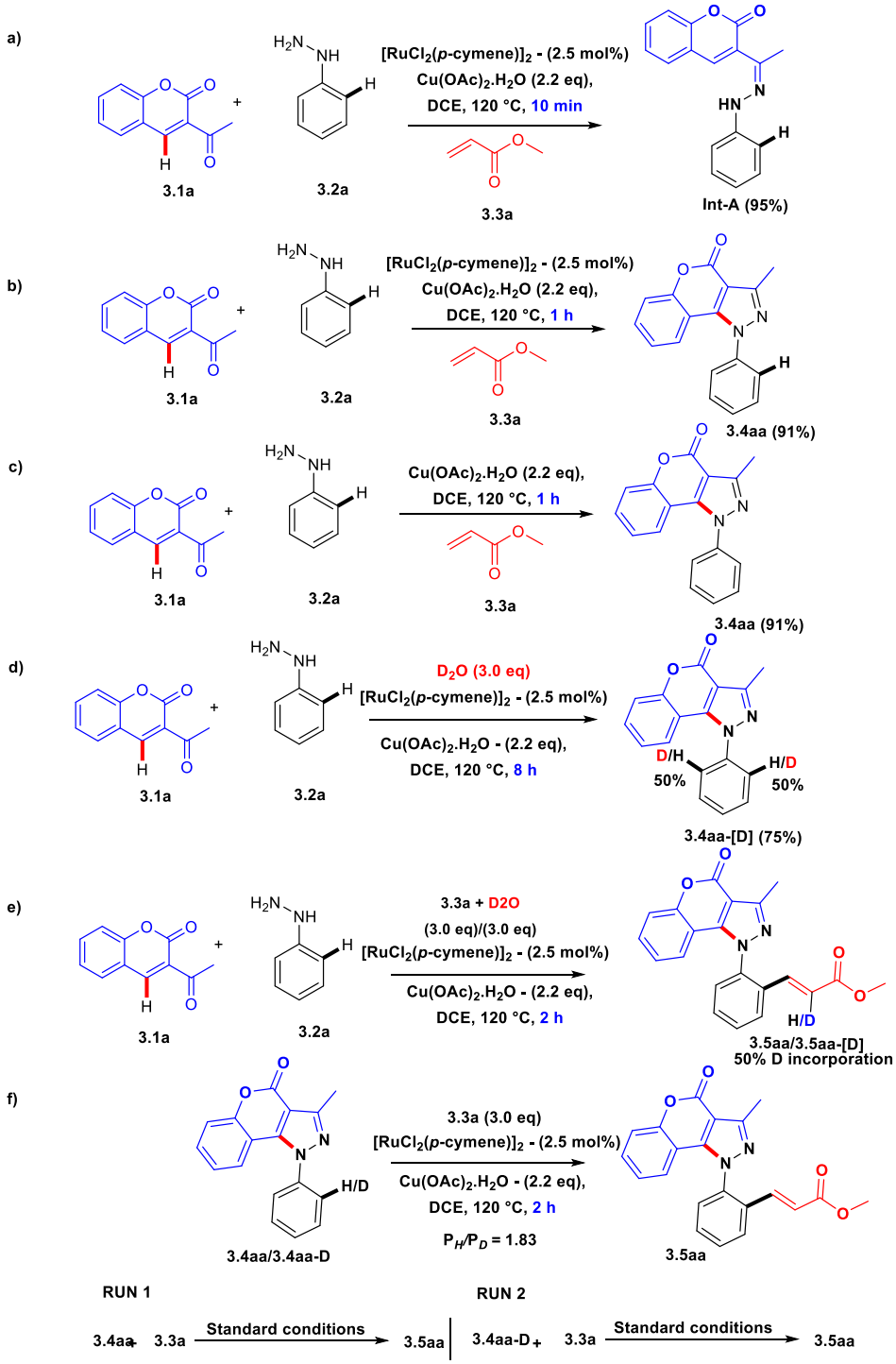

Scheme 3.4. Control experiments

It is noteworthy that when the reaction was monitored *via* TLC, **Int-A** was entirely consumed after 1 h. On isolation, compound **3.4aa** was obtained in 91% yield (**Scheme 3.4b**). Here, neither alkene insertion nor ruthenium complex formation was obtained. To check the participation of ruthenium complex in the formation of compound **3.4aa**, reaction without ruthenium catalyst was performed, and again, compound **3.4aa** was obtained in excellent yield (**Scheme 3.4c**). To get more mechanistic insights, substrates **3.1a** and **3.2a** were subjected to optimal reaction conditions in the presence of D_2O (3.0 eq.), wherein 50% H-D exchange was seen in isotopically labelled structure **3.4aa-[D]** (**Scheme 3.4d**), which indicates that the C–H activation phase may be reversible.[88] Furthermore, when substrates **3.1a** and **3.2a** were concomitantly exposed to acrylate and deuterium source in one pot, 50% deuterium incorporation in **3.5aa/3.5aa-[D]** was perceived at one of vinylic hydrogen (**Scheme 3.4e**), confirming the presence of protodemetalation phase. In addition, to find the kinetic isotopic effect (*KIE*), I have carried out parallel reactions between **3.4aa/3.4aa-[D]** using optimized conditions and obtained a relevant *KIE* as P_H/P_D = 1.83, which demonstrated C–H activation step, might be rate-determining step (**Scheme 3.4f**).[89,90]

3.4. Proposed Mechanism

I proposed a three-step domino reaction mechanism based on experimental observations and literature precedent (**Scheme 3.5**). Initially, intermediate **Int-A** was formed through a nucleophilic attack of phenylhydrazine on 3-acetyl-2*H*-chromen-2-one, which was further

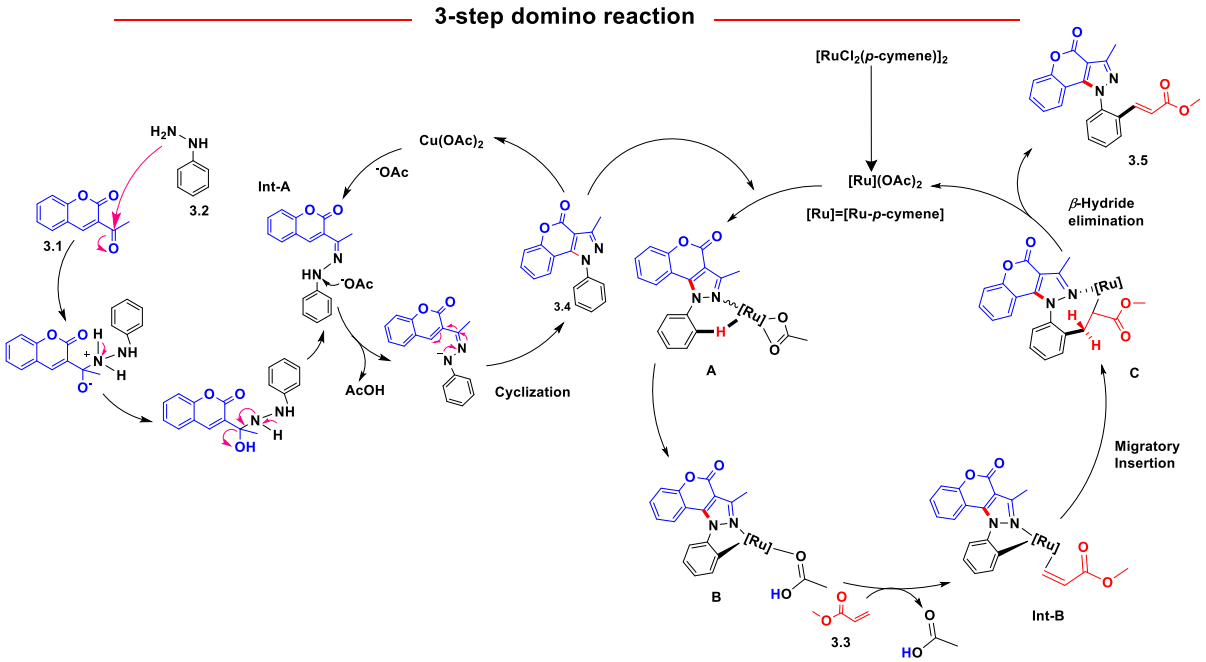

Scheme 3.5. Plausible Mechanism of One-Pot Cascade Transformation

processed by acetate ion followed by cyclization to give compound **3.4**. Afterward, **3.4** underwent C–H functionalization using pyrazole's imine as a weak directing group. Imine formed a coordination bond with an active ruthenium catalyst to give complex **A**, which underwent sp^2 C–H insertion and produced a five-membered complex **B**. After coordination with an alkene, it gave **Int-B**, followed by migratory insertion to complex **C**. Finally, *β*-hydride elimination followed by the protodemetalation step, the desired compound **3.5** was obtained.

3.5. Photophysical Studies

Several donor and acceptor groups on these scaffolds were examined to investigate the push-pull effect on chromeno[4,3-c]pyrazol-4-ones.[91] On substitution, absorption maxima have no significant impact and lie in the range of 264 nm to 298 nm, while emission maxima exist in 327 nm to 420 nm. Parent compound **3.4aa** has an emission maximum at 372 nm with Stokes shift 9500 cm^{-1}, while substitution of different acrylates to **3.4aa** *via* C–H functionalization shifted the emission maxima to 393 nm - 400 nm for compounds **3.5aa**, **3.5am**-**3.5ap**, and six-fold enhancement in fluorescence intensity with respect to the fluorescence intensity of compound **3.4aa** was observed (**Figure 3.1a**). In addition, I have deciphered the unknown preliminary photophysical properties of all the synthesized scaffolds. It has been observed that quantum yield and Stokes Shift of compounds **3.5aa**, **3.5am**-**3.5ap** differ significantly from the parental chromenopyrazolone **3.4aa**. The quantum yield of alkenylated products (**3.5aa**, **3.5am**-**3.5ap**) ranges from 0.20 to 0.45, whereas the quantum yield of **3.4aa** is 0.03; these values indicate a 15 times quantum yield enhancement. Similarly, Stokes Shift of alkenylated products (**3.5aa**, **3.5am**-**3.5ap**) is in the range of 11500 cm^{-1}-1200 cm^{-1} whereas compound **3.4aa** has 9500 cm^{-1}. Notably, compounds **3.5ab** and **3.5ad** have quantum yields of 0.66 and 0.62, respectively. Moreover, substitution with Cl and Br on coumarin nucleus, compounds **3.5ba** and **3.5ca** have emission maxima at 368 nm (10700 cm^{-1}) and 361 nm (10100 cm^{-1}) with quantum yields of 0.25 and 0.15, respectively. In comparison, OCH_3 group (**3.5de**) has a bathochromic shift at 420 nm (13000 cm^{-1}), having a quantum yield of 0.35. Notably, acceptors on the *N*-aryl ring at different positions have emission maxima in the range of 327 nm to 451 nm. In contrast, the weak donor group (-CH_3) on *N*-aryl ring such as **3.4ad** and **3.5ad** have emission maxima at 405 nm (9000 cm^{-1}) and 391 nm (11300 cm^{-1}), respectively. Notably, the quantum yield of parental compound **3.4ab** is 0.04, whereas the corresponding alkenylated product **3.5ab** has 0.66, nearly 16.5 times enhancement in

quantum yield. Similarly, the quantum yield of parental compound **3.4ad** is 0.30, whereas the corresponding alkenylated product **3.5ad** has 0.62. Hence the insertion of *α,β*-unsaturated

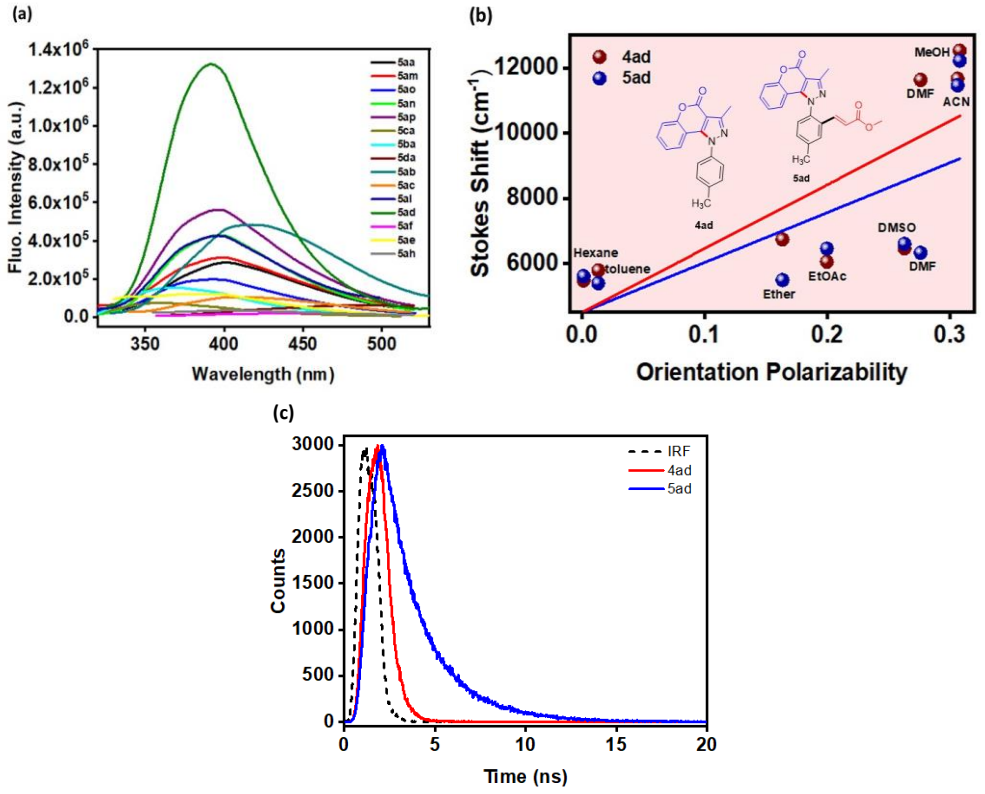

Figure 3.1. (**a**) Emission spectra of C–H functionalized compounds, (**b**) Lippert plot of 4ad and **3.5ad**, (**c**) Time-resolved spectra of **3.4ad** and **3.5ad**

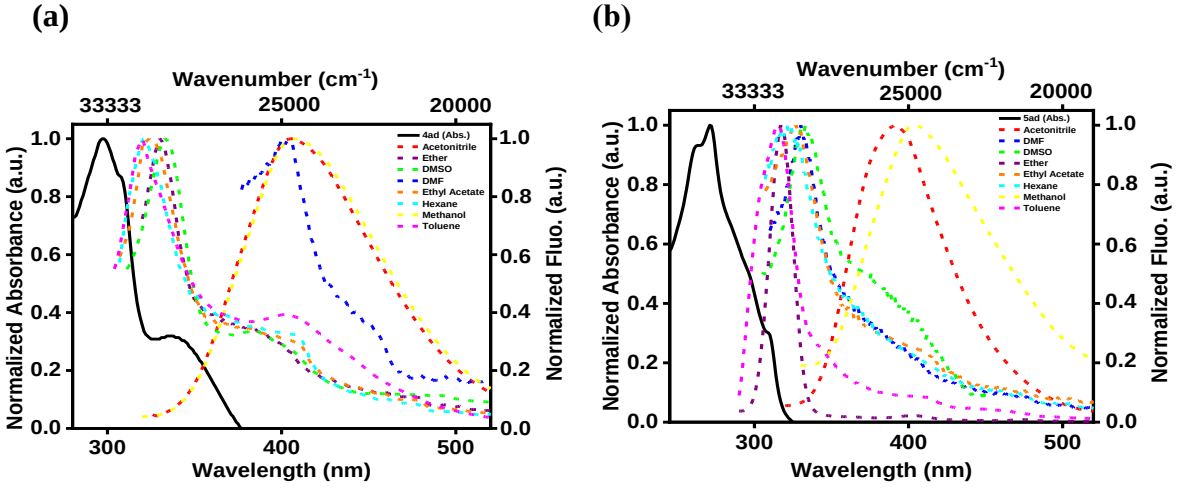

Figure 3.2: Absorption maxima (solid line) in acetonitrile and emission maxima (dashed lines) of **(a)** 3.**4ad** (**b**) **3.5ad** in different solvents

carbonyl compounds has the potential to improve the quantum yield of parental chromenopyrazolones. Furthermore, with the combined effect of positive inductive effect and

the bulkiness of alkenes for compounds 3.5aa, 3.5am-3.5ap, I observed a gradual increase in the quantum yield from 0.20 to 0.45.[92] Fascinated by quantum yield improvement, I performed solvatochromic studies on compounds 3.4ad and 3.5ad. Both compounds show positive solvatochromism, and the emission maxima range from 316 nm to 408 nm in different solvents. Figure 3.1b shows the Lippert plot of both the compounds (3.4ad and 3.5ad) and gives a satisfactory linear correlation. In addition, Figure 3.1c shows the lifetime fluorescence of both compounds.

Table 3.3. Photophysical properties of **3.4ad** and **3.5ad** in different solvents

	3.4ad			**3.5ad**		
solvent	$\lambda_{max,Abs}$ (nm)	$\lambda_{max,Em}$ (nm)	Stokes Shift (cm^{-1})	$\lambda_{max,Abs}$ (nm)	$\lambda_{max,Em}$ (nm)	Stokes Shift (cm^{-1})
ACN	275	405	11700	270	391	11500
Ether	270	330	6700	270	317	5500
DMSO	274	333	6500	273	333	6600
DMF	273	400	11600	273	330	6300
Methanol	270	408	12500	270	403	12200
Hexane	273	321	5500	272	321	5600
EtOAc	273	327	6000	270	327	6500
Toluene	270	320	5800	270	316	5400

Remarkably, compound **3.4ad** has 0.971 ns decay time while compound **3.5ad** has a significant decay time of 2 ns, which indicates that lifetime can be improved after C–H functionalization to these scaffolds. Although, absorption solvatochromism was not observed, as absorption maxima lie in the range of 270-275 nm (**Table 3.3**). However, both compounds exhibit emission solvatochromism; compound **3.4ad** has emission maxima, ranging from 320 nm in toluene to 408 nm in methanol, and **Figure 3.2** shows the emission solvatochromism of compound **3.4ad.** Similarly, compound **3.5ad** has emission maxima ranging from 316 nm in toluene to 403 nm in methanol, and **Figure 3.3** shows the emission solvatochromism of compound **3.5ad.**

3.6. Conclusion

Significant progress has been made in developing a step- and atom-economy one-pot cascade transformation to synthesize substituted 3-methyl-1-phenylchromeno[4,3-*c*]pyrazol-

4(1*H*)-ones and their *in-situ* late-stage modification *via ortho* C–H alkenylation using imine as a weak directing group. Various electron-donating and -withdrawing groups have shown great compatibility towards developed reaction conditions and gave 20 examples of C-H functionalized compounds in good to excellent yields. The efficacy of reaction was also examined on a gram scale. Further, several time-dependent studies and deuterium-labeled experiments shed more mechanistic insights, and I proposed a 3-step domino reaction mechanism. Due to their unique fused π conjugation, I performed photophysical analyses, and various electron donor and acceptor combinations were developed. Selected compounds demonstrated positive solvatochromism. Hence, these molecules may have valuable properties in material sciences.

3.7. Experimental Section

General procedure A: Synthesis of 3-acetyl-2*H*-chromen-2-one is same as mentioned in Chapter 2

.**General procedure C:** For the synthesis of alkenylated products:

In an oven-dried 50 ml round bottom flask, a solution was made of coumarin (188 mg, 1 mmol, 1.0 eq), phenylhydrazine (108 mg, 1 mmol, 1.0 eq), and acrylate (258 mg, 0.27 ml, 3 mmol, 3.0 eq) in DCE (5 ml) followed by the addition of $Cu(OAc)_2.H_2O$ (2.2 mmol, 2.2 eq), and then loaded with $[RuCl_2(p\text{-cymene})]_2$ (2.5 mol%). The resulting reaction mixture was refluxed at 120 °C (using an oil bath) for **8 h**. The reaction was quenched with DCM (20 ml) and passed through the celite pad, followed by the extraction with DCM (3 × 50 ml); the combined organic layers were washed with brine solution and dried over sodium sulfate, and the solvent was concentrated under reduced pressure. The crude product was purified using column chromatography (EtOAc: Hexane 5: 95 to 15:85) to yield the desired compound.

Synthesis of **3.4aa**

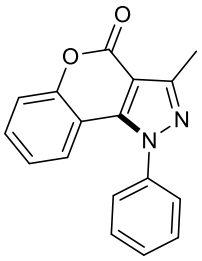

3-Methyl-1-phenylchromeno[4,3-*c*]pyrazol-4(1*H*)-one (**3.4aa**). The compound **3.4aa** was synthesized using general procedure B and obtained as white solid compound, 91% (251 mg); R_f = 0.5 (EtOAc + Hexane 3:97); **mp** 224-226 °C. **^{1}H NMR** (400 MHz, $CDCl_3$) δ 7.62 – 7.60

(m, 3H), 7.56 – 7.53 (m, 2H), 7.47 – 7.43 (m, 2H), 7.10 (dd, *J* = 8.0, 1.1 Hz, 1H), 7.03 (dd, *J* = 8.2, 6.7 Hz, 1H), 2.69 (s, 3H). **^{13}C{^{1}H} NMR** (101 MHz, $CDCl_3$) δ 157.4, 152.2, 151.0, 140.4, 138.9, 133.9, 130.2, 126.8, 125.2, 119.8, 116.7, 113.5, 106.6, 13.0. HRMS (ESI-TOF): m/z $[M+H]^+$ calcd for $C_{17}H_{13}N_2O_2$ 277.0932; found 277.0942.

Synthesis of **3.4ab**

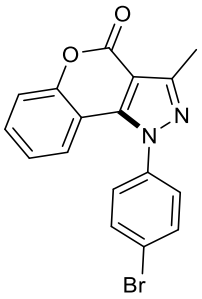

1-(4-Bromophenyl)-3-methylchromeno[4,3-*c*]pyrazol-4(1*H*)-one (**3.4ab).** The compound **3.4ab** was synthesized using general procedure B and obtained as white solid compound, 92% (327 mg); R_f = 0.5 (EtOAc + Hexane 5:95)**; mp** 254-258 °C. **^{1}H NMR** (400 MHz, $CDCl_3$) δ 7.56 (dd, *J* = 8.6, 1.4 Hz, 2H), 7.50 (s, 1H), 7.43 (ddd, *J* = 6.9, 3.5, 1.8 Hz, 1H), 7.40 – 7.35 (m, 1H), 7.31 (d, *J* = 1.2 Hz, 1H), 7.11 (dt, *J* = 8.2, 1.7 Hz, 1H), 7.07 – 7.03 (m, 1H), 2.68 (s, 3H). **^{13}C{^{1}H} NMR** (101 MHz, $CDCl_3$) δ 155.4, 153.3, 151.2, 147.6, 134.5, 130.4, 130.2, 128.3, 125.1, 124.1, 122.4, 118.3, 116.7, 111.7, 106.7, 12.9. **HRMS** (ESI-TOF): m/z $[M+H]^+$ calcd for $C_{17}H_{12}N_2O_2{}^{79}Br$ 355.9983; found 355.9993, calcd for $C_{17}H_{12}N_2O_2{}^{81}Br$ 357.0185; found 357.0195.

Synthesis of **3.4ac**

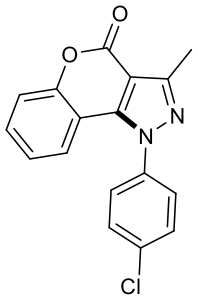

1-(4-Chlorophenyl)-3-methylchromeno[4,3-*c*]pyrazol-4(1*H*)-one (**3.4ac).** The compound **3.4ac** was synthesized using general procedure B and obtained as white solid compound, 92% (211 mg); R_f = 0.5 (EtOAc + Hexane 5:95)**; mp** 202-206 °C. **^{1}H NMR** (400 MHz, $CDCl_3$) δ 7.73 (d, *J* = 8.5 Hz, 2H), 7.49 – 7.45 (m, 1H), 7.44 (t, *J* = 1.6 Hz, 1H), 7.42 (dd, *J* = 3.5, 1.3 Hz, 2H), 7.14 (dd, *J* = 8.0, 1.5 Hz, 1H), 7.07 (ddd, *J* = 8.2, 6.9, 1.5 Hz, 1H), 2.66 (s, 3H). **^{13}C{^{1}H} NMR** (101 MHz, $CDCl_3$) δ 157.9, 153.4, 151.3, 147.6, 141.9, 138.5, 133.2,

131.4, 128.5, 124.3, 124.2, 122.4, 118.3, 116.8, 111.7, 106.8, 12.9. **HRMS** (ESI-TOF): m/z $[M+H]^+$ calcd for $C_{17}H_{12}N_2O_2Cl$ 312.0480; found 312.0490.

Synthesis of **3.4ad**

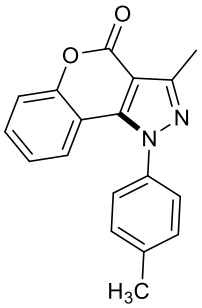

3-Methyl-1-(*p*-tolyl)chromeno[4,3-*c*]pyrazol-4(1*H*)-one (**3.4ad).** The compound **3.4ad** was synthesized using general procedure B and obtained as white solid compound 93% (260 mg); R_f = 0.6 (EtOAc + Hexane 5:95)**; mp** 188-192 °C. **^{1}H NMR** (400 MHz, $CDCl_3$) δ 7.46 – 7.40 (m, 2H), 7.39 (s, 1H), 7.38 (d, *J* = 2.8 Hz, 2H), 7.35 – 7.31 (m, 1H), 7.13 – 7.09 (m, 1H), 7.02 (ddd, *J* = 8.2, 6.5, 1.9 Hz, 1H), 2.67 (s, 3H), 2.49 (s, 3H). **^{13}C{^{1}H} NMR** (101 MHz, $CDCl_3$) δ 158.2, 153.4, 150.8, 147.6, 140.5, 134.5, 131.1, 130.5, 126.7, 125.1, 123.9, 122.6, 118.1, 116.8, 112.0, 106.3, 21.5, 13.0. **HRMS** (ESI-TOF): m/z $[M+H]^+$ calcd for $C_{18}H_{15}N_2O_2$ 290.1089; found 290.1097.

Synthesis of **3.4ae**

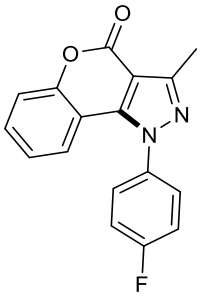

1-(4-Fluorophenyl)-3-methylchromeno[4,3-*c*]pyrazol-4(1*H*)-one (**3.4ae).** The compound **3.4ae** was synthesized using general procedure B and obtained as white solid compound, 92% (268 mg); R_f = 0.4 (EtOAc + Hexane 5:95)**; mp** 194-198 °C. **^{1}H NMR** (400 MHz, $CDCl_3$) δ 7.55 – 7.52 (m, 2H), 7.46 – 7.43 (m, 1H), 7.41 (t, *J* = 1.0 Hz, 1H), 7.31 – 7.27 (m, 2H), 7.06 (d, *J* = 1.1 Hz, 1H), 7.05 (d, *J* = 2.5 Hz, 1H), 2.65 (s, 3H). **^{13}C{^{1}H} NMR** (101 MHz, $CDCl_3$) δ 164.6, 162.1, 157.9, 153.4, 151.0, 142.0, 131.3, 129.0, 124.1, 122.3, 118.3, 117.2 116.9, 111.8, 106.5, 12.9. **HRMS** (ESI-TOF): m/z $[M+H]^+$ calcd for $C_{17}H_{12}N_2O_2F$ 295.0838; found 295.0855.

Synthesis of **3.4af**

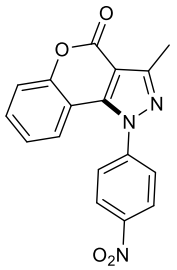

3-Methyl-1-(4-nitrophenyl)chromeno[4,3-*c*]pyrazol-4(1*H*)-one (**3.4af).** The compound **3.4af** was synthesized using general procedure B and obtained as white solid compound, 85% (282 mg); R_f = 0.4 (EtOAc + Hexane 6:94)**; mp** 222-226 °C. **^{1}H NMR** (400 MHz, $CDCl_3$) δ 7.69 – 7.66 (m, 2H), 7.52 (dt, *J* = 3.6, 1.6 Hz, 1H), 7.49-7.45 (m, 3H), 7.20 (dt, *J* = 3.8, 1.8 Hz, 1H), 7.07 – 7.02 (m, 1H), 2.67 (s, 3H). **^{13}C{^{1}H} NMR** (101 MHz, $CDCl_3$) δ 157.3, 151.8, 151.6, 141.7, 137.7, 137.6, 132.8, 131.5, 129.5, 128.8, 128.2, 122.2, 121.6, 119.6, 112.6, 106.6, 13.1. **HRMS** (ESI-TOF): m/z $[M+H]^+$ calcd for $C_{17}H_{12}N_3O_4$ 322.0783; found 322.0798.

Synthesis of **3.4ag**

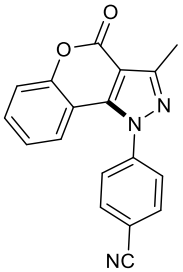

4-(3-Methyl-4-oxochromeno[4,3-*c*]pyrazol-1(4*H*)-yl)benzonitrile (**3.4ag).** The compound **3.4ag** was synthesized using general procedure B and obtained as a white solid compound, 90% (270 mg); R_f = 0.4 (EtOAc + Hexane 6:94)**; mp** 198-202 °C. **^{1}H NMR** (400 MHz, $CDCl_3$) δ 7.91 (d, *J* = 8.5 Hz, 2H), 7.73 (d, *J* = 8.5 Hz, 2H), 7.51 – 7.47 (m, 1H), 7.42 (dd, *J* = 8.3, 0.9 Hz, 1H), 7.17 (dd, *J* = 8.1, 1.4 Hz, 1H), 7.12 – 7.07 (m, 1H), 2.64 (s, 3H). **^{13}C{^{1}H} NMR** (101 MHz, $CDCl_3$) δ 157.6, 153.4, 151.9, 143.0, 141.9, 133.8, 131.8, 127.6, 124.2, 122.2, 118.5, 117.6, 113.9, 111.4, 107.5, 12.9. **HRMS** (ESI-TOF): m/z $[M+H]^+$ calcd for $C_{18}H_{12}N_3O_2$ 302.0885; found 302.0896.

Synthesis of **3.4ah**

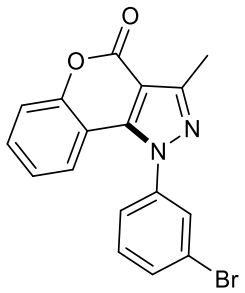

1-(3-Bromophenyl)-3-methylchromeno[4,3-*c*]pyrazol-4(1*H*)-one (**3.4ah).** The compound **3.4ah** was synthesized using general procedure B and obtained as white solid compound, 93% (330 mg); R_f = 0.4 (EtOAc + Hexane 4:96)**; mp** 252-256 °C. **^{1}H NMR** (400 MHz, $CDCl_3$) δ 7.74 – 7.71 (m, 2H), 7.50 – 7.48 (m, 1H), 7.48 – 7.43 (m, 2H), 7.39 (dd, *J* = 8.4, 1.1 Hz, 1H), 7.14 (dd, *J* = 8.1, 1.5 Hz, 1H), 7.07 (ddd, *J* = 8.2, 7.1, 1.3 Hz, 1H), 2.63 (s, 3H). **^{13}C{^{1}H} NMR** (101 MHz, $CDCl_3$) δ 157.8, 153.4, 151.3, 141.9, 140.5, 133.4, 131.4, 131.1, 130.2, 125.6, 124.2, 123.3, 122.4, 118.3, 111.6, 106.7, 12.9. **HRMS** (ESI-TOF): m/z $[M+H]^+$ calcd for $C_{17}H_{12}N_2O_2{}^{79}Br$ 355.9983; found 355.9997, calcd for $C_{17}H_{12}N_2O_2{}^{81}Br$ 357.0185; found 357.0199.

Synthesis of **3.4ai**

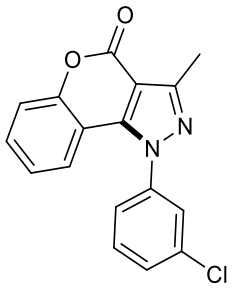

1-(3-Chlorophenyl)-3-methylchromeno[4,3-*c*]pyrazol-4(1*H*)-one (**3.4ai).** The compound **3.4ai** was synthesized using general procedure B and obtained as white solid compound, 92% (285 mg); R_f = 0.4 (EtOAc + Hexane 7:93)**; mp** 212-216 °C. **^{1}H NMR** (400 MHz, $CDCl_3$) δ 7.61-7.57 (m, 3H), 7.55 – 7.52 (m, 2H), 7.42 – 7.40 (m, 1H), 7.09 (dd, *J* = 8.3, 1.2 Hz, 1H), 7.04 – 6.99 (m, 1H), 2.66 (s, 3H). **^{13}C{^{1}H} NMR** (101 MHz, $CDCl_3$) δ 157.6, 153.4, 151.9, 143.0, 141.9, 133.8, 131.7, 127.6, 124.2, 122.2, 118.5, 114.0, 111.4, 107.4, 13.0. **HRMS** (ESI-TOF): m/z $[M+H]^+$ calcd for $C_{17}H_{12}N_2O_2Cl$ 312.0480; found 312.0495.

Synthesis of **3.4aj**

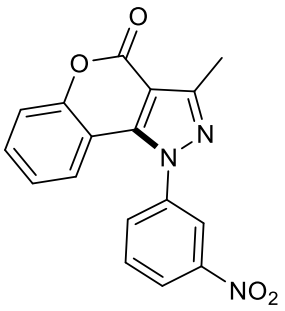

3-Methyl-1-(3-nitrophenyl)chromeno[4,3-*c*]pyrazol-4(1*H*)-one (**3.4aj).** The compound **3.4aj** was synthesized using general procedure B and obtained as white solid compound, 85% (272 mg); R_f = 0.4 (EtOAc + Hexane 8:92)**; mp** 224-228 °C. **^{1}H NMR** (400 MHz, $CDCl_3$) δ 7.70 – 7.66 (m, 2H), 7.51 (d, *J* = 1.8 Hz, 1H), 7.50 – 7.45 (m, 3H), 7.20 (dt, *J* = 3.8, 1.8 Hz, 1H), 7.13 – 7.07 (m, 1H), 2.70 (s, 3H). **^{13}C{^{1}H} NMR** (101 MHz, $CDCl_3$) δ 157.3, 151.8, 151.6, 141.7, 137.7, 137.6, 132.8, 131.3, 129.5, 128.8, 128.2, 122.3, 121.6, 119.6, 112.6, 106.6, 13.0. **HRMS** (ESI-TOF): m/z $[M+H]^+$ calcd for $C_{17}H_{12}N_3O_4$ 322.0780; found 322.0798.

Synthesis of **3.4ak**

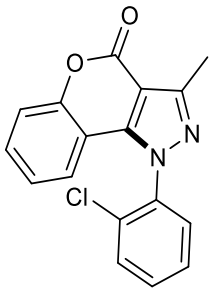

1-(2-Chlorophenyl)-3-methylchromeno[4,3-*c*]pyrazol-4(1*H*)-one (**3.4ak).** The compound **3.4ak** was synthesized using general procedure B and obtained as white solid compound, 92% (286 mg); R_f = 0.4 (EtOAc + Hexane 6:94)**; mp** 210-214 °C. **^{1}H NMR** (400 MHz, $CDCl_3$) δ 7.59-7.56 (m, 2H), 7.55 – 7.50 (m, 1H), 7.48 – 7.38 (m, 3H), 7.14 (dd, *J* = 8.0, 1.5 Hz, 1H), 7.07 (ddd, *J* = 8.2, 7.0, 1.6 Hz, 1H), 2.64 (s, 3H). **^{13}C{^{1}H} NMR** (101 MHz, $CDCl_3$) δ 157.4, 152.1, 151.0, 140.4, 138.9, 133.9, 130.6, 130.1, 126.8, 125.2, 119.8, 116.6, 113.5, 106.7, 13.0. **HRMS** (ESI-TOF): m/z $[M+H]^+$ calcd for $C_{17}H_{12}N_2O_2Cl$ 312.0480; found 312.0495.

Synthesis of **4al**

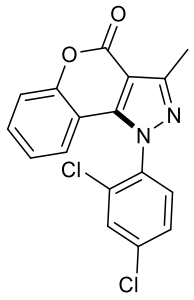

1-(2,4-Dichlorophenyl)-3-methylchromeno[4,3-*c*]pyrazol-4(1*H*)-one (**3.4al).** The compound **3.4al** was synthesized using general procedure B and obtained as white solid compound, 90% (310 mg); R_f = 0.4 (EtOAc + Hexane 6:94)**; mp** 236-240 °C. **^{1}H NMR** (400 MHz, $CDCl_3$) δ 7.62 – 7.58 (m, 3H), 7.55 – 7.54 (m, 1H), 7.41 (dd, *J* = 2.7, 1.5 Hz, 1H), 7.09 (dd, *J* = 8.0, 1.6 Hz, 1H), 7.03 – 7.00 (m, 1H), 2.67 (s, 3H). **^{13}C NMR** (101 MHz, $CDCl_3$) δ 158.0, 153.3, 150.9, 141.8, 139.5, 131.1, 123.0, 127.0, 124.0, 122.5, 118.1, 111.9, 106.4, 13.0. **HRMS** (ESI-TOF): m/z $[M+H]^+$ calcd for $C_{17}H_{11}N_2O_2Cl_2$ 346.0080; found 346.0099.

Synthesis of **3.4ba**

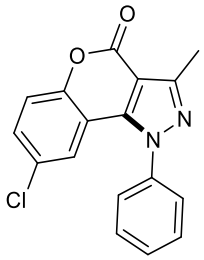

8-Chloro-3-methyl-1-phenylchromeno[4,3-*c*]pyrazol-4(1*H*)-one (**3.4ba).** The compound **3.4ba** was synthesized using general procedure B and obtained as white solid compound, 94% (284 mg); R_f = 0.5 (EtOAc + Hexane 5:95)**; mp** 282-286 °C. **^{1}H NMR** (400 MHz, $CDCl_3$) δ 7.63 (dd, *J* = 5.0, 2.1 Hz, 3H), 7.53 – 7.51 (m, 1H), 7.36 (dt, *J* = 15.3, 5.6 Hz, 3H), 7.01 (d, *J* = 2.3 Hz, 1H), 2.66 (s, 3H). **^{13}C{^{1}H} NMR** (101 MHz, $CDCl_3$) δ 157.6, 151.7, 151.1, 140.6, 138.9, 131.1, 130.6, 130.1, 129.3, 126.8, 122.2, 119.5, 113.0, 106.6, 12.9. **HRMS** (ESI-TOF): m/z $[M+H]^+$ calcd for $C_{17}H_{12}N_2O_2Cl$ 312.0480; found 312.0494.

Synthesis of **3.4ca**

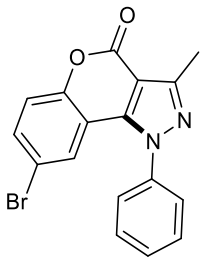

8-Bromo-3-methyl-1-phenylchromeno[4,3-*c*]pyrazol-4(1*H*)-one (**3.4ca).** The compound **3.4ca** was synthesized using general procedure B and obtained as white solid compound, 92% (328 mg); R_f = 0.5 (EtOAc + Hexane 5:95)**; mp** 202-206 °C. **^{1}H NMR** (400 MHz, $CDCl_3$) δ 7.64 (d, *J* = 2.3 Hz, 2H), 7.63 – 7.61 (m, 1H), 7.55 – 7.52 (m, 2H), 7.51 – 7.50 (m, 1H), 7.29 (d, *J* = 9.0 Hz, 1H), 7.17 (d, *J* = 2.4 Hz, 1H), 2.67 (s, 3H). **^{13}C{^{1}H} NMR** (101 MHz, $CDCl_3$) δ 157.5, 152.2, 151.1, 140.4, 139.0, 138.8, 133.9, 130.6, 130.1, 126.8, 125.2, 119.8, 116.7, 113.5, 106.6, 12.9. **HRMS** (ESI-TOF): m/z $[M+H]^+$ calcd for $C_{17}H_{12}N_2O_2{}^{79}Br$ 355.9983; found 355.9993, calcd for $C_{17}H_{12}N_2O_2{}^{81}Br$ 357.0185; found 357.0193.

Synthesis of **3.4da**

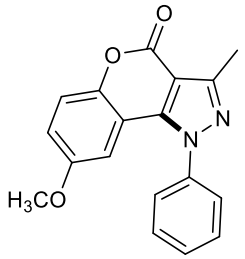

8-Methoxy-3-methyl-1-phenylchromeno[4,3-*c*]pyrazol-4(1*H*)-one (**3.4da).** The compound **3.4da** was synthesized using general procedure B and obtained as white solid compound, 92% (282 mg); R_f = 0.4 (EtOAc + Hexane 6:94)**; mp** 228-232 °C. **^{1}H NMR** (400 MHz, $CDCl_3$) δ 7.61 – 7.56 (m, 3H), 7.53 (dd, *J* = 4.4, 1.8 Hz, 2H), 7.00 – 6.93 (m, 2H), 6.64 (dd, *J* = 7.9, 1.7 Hz, 1H), 3.94 (s, 3H), 2.67 (s, 3H). **^{13}C NMR** (101 MHz, $CDCl_3$) δ 157.4, 150.9, 148.2, 143.1, 139.5, 130.2, 129.9, 127.1, 123.8, 113.9, 112.8, 112.6, 100.0, 56.3, 13.0. **HRMS** (ESI-TOF): m/z $[M+H]^+$ calcd for $C_{18}H_{15}N_2O_3$ 307.1038; found 307.1049.

Synthesis of **3.5aa**

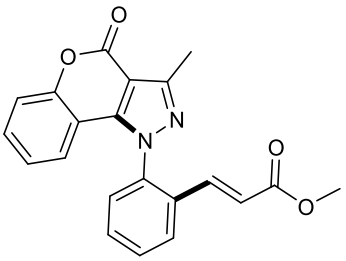

Methyl (*E*)-3-(2-(3-methyl-4-oxochromeno[4,3-*c*]pyrazol-1(4*H*)-yl)phenyl) acrylate (**3.5aa).** The compound **3.5aa** was synthesized using general procedure C and obtained as white solid compound, 80% (288 mg); R_f = 0.5 (EtOAc + Hexane 7:93)**; mp** 230-234 °C. **^{1}H NMR** (400 MHz, $CDCl_3$) δ 7.88 (dd, *J* = 8.0, 1.6 Hz, 1H), 7.68 (td, *J* = 7.7, 1.6 Hz, 1H), 7.62 (td, *J* = 7.7, 1.6 Hz, 1H), 7.47 (dd, *J* = 7.9, 1.5 Hz, 1H), 7.44 – 7.42 (m, 2H), 7.24 (d, *J* = 16.2 Hz, 1H),

7.00 – 6.96 (m, 1H), 6.72 (dd, *J* = 8.6, 1.4 Hz, 1H), 6.33 (d, *J* = 16.0 Hz, 1H), 3.68 (s, 3H), 2.72 (s, 3H). **^{13}C{^{1}H} NMR** (101 MHz, $CDCl_3$) δ 166.4, 157.3, 151.4, 148.2, 143.2, 138.3, 137.8, 132.9, 131.4, 131.1, 129.1, 128.1, 124.2, 122.0, 113.3, 113.1, 112.2, 106.4, 51.9, 13.1. **HRMS** (ESI-TOF): m/z $[M+H]^+$ calcd for $C_{21}H_{17}N_2O_4$ 361.1144; found 361.1154.

Synthesis of **3.5ab**

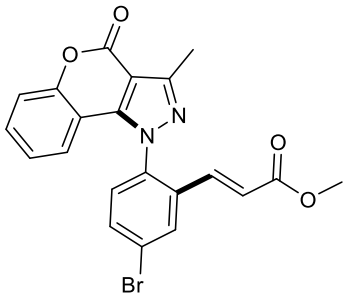

Methyl (*E*)-3-(5-bromo-2-(3-methyl-4-oxochromeno[4,3-*c*]pyrazol-1(4*H*)-yl)phenyl) acrylate (**3.5ab).** The compound **3.5ab** was synthesized using general procedure C and obtained as light-yellow solid compound, 70% (308 mg); R_f = 0.4 (EtOAc + Hexane 8:92)**; mp** 258-262 °C. **^{1}H NMR** (400 MHz**,** $CDCl_3$**)** δ 7.83 (d, *J* = 2.5 Hz, 1H), 7.57 (dd, *J* = 8.5, 2.3 Hz, 1H), 7.45 (dd, *J* = 6.8, 1.5 Hz, 1H), 7.43 (d, *J* = 1.6 Hz, 1H), 7.42 (d, *J* = 3.0 Hz, 1H), 7.15 (d, *J* = 16.0 Hz, 1H), 7.02 (ddd, *J* = 8.5, 5.7, 1.8 Hz, 1H), 6.76 (dd, *J* = 8.0, 1.6 Hz, 1H), 6.34 (d, *J* = 16.0 Hz, 1H), 3.67 (s, 3H), 2.69 (s, 3H). **^{13}C{^{1}H} NMR** (101 MHz, $CDCl_3$) δ 166.0, 157.7, 153.5, 151.8, 143.1, 137.2, 136.6, 136.5, 134.6, 131.6, 131.3, 130.3, 128.0, 124.4, 123.3, 121.8, 118.4, 111.4, 106.6, 52.1, 13.1. **HRMS** (ESI-TOF): m/z $[M+H]^+$ calcd for $C_{21}H_{16}N_2O_4{}^{79}Br$ 438.0215; found 438.0230, calcd for $C_{21}H_{16}N_2O_4{}^{81}Br$ 440.0185; found 440.0195.

Synthesis of **3.5ac**

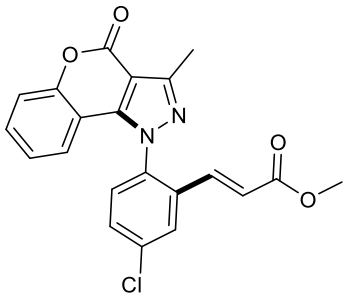

Methyl (*E*)-3-(5-chloro-2-(3-methyl-4-oxochromeno[4,3-*c*]pyrazol-1(4*H*)-yl)phenyl) acrylate (**3.5ac).** The compound **3.5ac** was synthesized using general procedure C and obtained as light-yellow solid compound, 72% (283 mg); R_f = 0.5 (EtOAc + Hexane 7:93)**; mp** 212-216

°C. **^{1}H NMR** (400 MHz, $CDCl_3$) δ 7.99 (d, *J* = 2.3 Hz, 1H), 7.72 (dd, *J* = 8.4, 2.2 Hz, 1H), 7.48 – 7.44 (m, 1H), 7.44 – 7.42 (m, 1H), 7.34 (d, *J* = 8.5 Hz, 1H), 7.14 (d, *J* = 16.0 Hz, 1H), 7.05 – 7.01 (m, 1H), 6.77 (dd, *J* = 8.1, 1.4 Hz, 1H), 6.33 (d, *J* = 16.0 Hz, 1H), 3.67 (s, 3H), 2.69 (s, 3H). **^{13}C{^{1}H} NMR** (101 MHz, $CDCl_3$) δ 166.0, 157.7, 153.5, 151.8, 143.1, 137.2, 136.5, 134.8, 134.3, 131.6, 131.0, 130.5, 125.3, 124.4, 123.3, 121.8, 118.4, 111.4, 106.6, 52.1, 13.1. **HRMS** (ESI-TOF): m/z $[M+H]^+$ calcd for $C_{21}H_{16}ClN_2O_4$ 395.0720; found 395.0730.

Synthesis of **3.5ad**

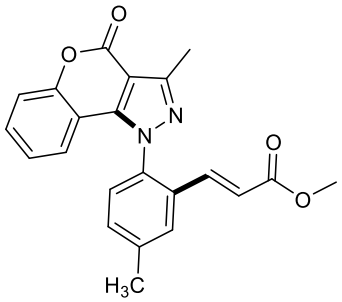

Methyl (*E*)-3-(5-methyl-2-(3-methyl-4-oxochromeno[4,3-*c*]pyrazol-1(4*H*)-yl)phenyl) acrylate (**3.5ad).** The compound **3.5ad** was synthesized using general procedure C and obtained as light-yellow solid compound, 86% (321 mg); R_f = 0.5 (EtOAc + Hexane 8:92)**; mp** 196-200 °C. **^{1}H NMR** (400 MHz, $CDCl_3$) δ 7.65 (d, *J* = 2.0 Hz, 1H), 7.43 – 7.41 (m, 2H), 7.40 – 7.38 (m, 1H), 7.33 (d, *J* = 8.0 Hz, 1H), 7.18 (d, *J* = 16.0 Hz, 1H), 6.98 (ddd, *J* = 5.8, 4.3, 2.1 Hz, 1H), 6.77 – 6.71 (m, 1H), 6.29 (d, *J* = 16.0 Hz, 1H), 3.66 (s, 3H), 2.69 (s, 3H), 2.53 (s, 3H). **^{13}C{^{1}H} NMR** (101 MHz, $CDCl_3$) δ 166.5, 157.9, 153.4, 151.4, 143.0, 141.5, 138.0, 135.8, 132.5, 132.2, 131.3, 128.6, 124.2, 122.0, 121.7, 118.2, 111.7, 106.3, 51.9, 21.6, 13.1. **HRMS** (ESI-TOF): m/z $[M+H]^+$ calcd for $C_{22}H_{19}N_2O_4$ 375.1300; found 375.1314.

Synthesis of **3.5ae**

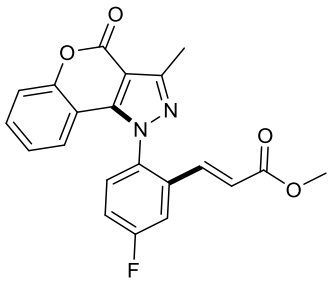

Methyl (*E*)-3-(5-fluoro-2-(3-methyl-4-oxochromeno[4,3-*c*]pyrazol-1(4*H*)-yl)phenyl) acrylate (**3.5ae).** The compound **3.5ae** was synthesized using general procedure C and obtained as

light-yellow solid compound, 66% (250 mg); R_f = 0.4 (EtOAc + Hexane 7:93)**; mp** 210-214 °C. **^{1}H NMR** (400 MHz, $CDCl_3$) δ 7.54 (dd, *J* = 9.0, 2.8 Hz, 1H), 7.48 – 7.46 (m, 1H), 7.45 (d, *J* = 2.0 Hz, 1H), 7.42 (dd, *J* = 8.0, 1.8 Hz, 1H), 7.30 (dd, *J* = 8.7, 7.5 Hz, 1H), 7.17 – 7.11 (m, 1H), 7.03 – 6.99 (d, *J* = 16.0 Hz, 1H), 6.72 (dd, *J* = 7.8, 1.2 Hz, 1H), 6.33 (d, *J* = 16.0 Hz, 1H), 3.68 (s, 3H), 2.69 (s, 3H). **^{13}C{^{1}H} NMR** (101 MHz, $CDCl_3$) δ 166.0, 162.3, 157.7, 153.5, 151.6, 143.2, 136.7, 135.3, 131.5, 131.1, 124.3, 123.3, 121.7, 118.6, 118.4, 114.8, 114.5, 111.5, 106.6, 52.1, 13.1. **^{19}F{^{1}H} NMR** (376 MHz, $CDCl_3$) δ -107.5. **HRMS** (ESI-TOF): m/z $[M+H]^+$ calcd for $C_{21}H_{16}FN_2O_4$ 379.1049; found 379.1064

Synthesis of **3.5af**

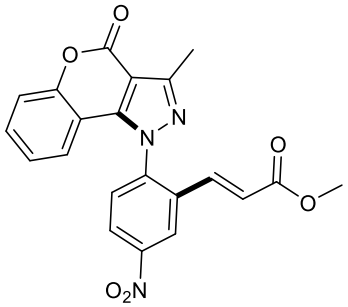

Methyl (*E*)-3-(2-(3-methyl-4-oxochromeno[4,3-*c*]pyrazol-1(4*H*)-yl)-5-nitrophenyl) acrylate (**3.5af)**. The compound **3.5af** was synthesized using general procedure C and obtained as light-yellow solid compound. 64% (260 mg); R_f = 0.4 (EtOAc + Hexane 10:90)**; mp** 230-234 °C. **^{1}H NMR** (400 MHz, $CDCl_3$) δ 8.42 (d, *J* = 2.5 Hz, 1H), 7.81 (d, *J* = 2.0 Hz, 1H), 7.79 (t, *J* = 2.5 Hz, 1H), 7.49 (dd, *J* = 3.6, 1.8 Hz, 1H), 7.27 (d, *J* = 16.0 Hz, 1H), 7.21 (dd, *J* = 8.0, 1.8 Hz, 1H), 7.13 – 7.08 (m, 1H), 6.69 (d, *J* = 12.4 Hz, 1H), 6.53 (d, *J* = 16.0 Hz, 1H), 3.71 (s, 3H), 2.70 (s, 3H). **^{13}C{^{1}H} NMR** (101 MHz, $CDCl_3$) δ 166.5, 158.0, 153.4, 151.4, 143.0, 141.4, 138.0, 135.9, 132.5, 132.2, 131.3, 128.6, 124.2, 122.0, 121.7, 118.9, 111.7, 106.3, 52.0, 13.1. **HRMS** (ESI-TOF): m/z $[M+H]^+$ calcd for $C_{21}H_{16}N_3O_6$ 406.0994; found 406.0107.

Synthesis of **3.5ag**

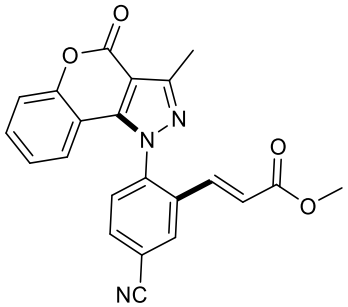

Methyl (*E*)-3-(5-cyano-2-(3-methyl-4-oxochromeno[4,3-*c*]pyrazol-1(4*H*)-yl)phenyl) acrylate (**3.5ag).** The compound **3.5ag** was synthesized using general procedure C and obtained as light-yellow solid compound, 63% (242 mg); R_f = 0.4 (EtOAc + Hexane 8:92)**; mp** 210-214 °C. **^{1}H NMR** (400 MHz, $CDCl_3$) δ 7.80 (d, *J* = 8.0 Hz, 1H), 7.68 (dd, *J* = 8.6, 4.5 Hz, 2H), 7.52 – 7.49 (m, 1H), 7.28 (d, *J* = 16.1 Hz, 1H), 7.21 (dd, *J* = 8.1, 1.6 Hz, 1H), 7.03 (dd, *J* = 2.8, 1.4 Hz, 1H), 6.69 (d, *J* = 12.1 Hz, 1H), 6.52 (d, *J* = 16.0 Hz, 1H), 3.71 (s, 3H), 2.70 (s, 3H). **^{13}C{^{1}H} NMR** (101 MHz, $CDCl_3$) δ 166.4, 157.2, 151.4, 148.2, 143.1, 138.3, 137.8, 132.9, 131.3, 131.1, 129.0, 128.0, 124.2, 121.9, 113.3, 113.0, 112.2, 106.3, 52.0, 13.1. **HRMS** (ESI-TOF): m/z $[M+H]^+$ calcd for $C_{22}H_{16}N_3O_4$ 386.1096; found 386.1086.

Synthesis of **3.5ah**

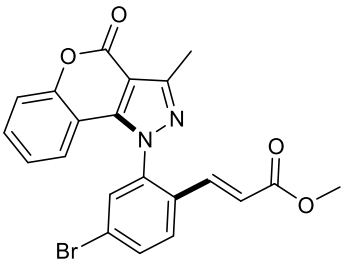

Methyl (*E*)-3-(2-bromo-6-(3-methyl-4-oxochromeno[4,3-*c*]pyrazol-1(4*H*)-yl)phenyl) acrylate (**3.5ah).** The compound **3.5ah** was synthesized using general procedure C and obtained as light-yellow solid compound, 65% (285 mg); R_f = 0.5 (EtOAc + Hexane 7:93)**; mp** 270-274 °C. **^{1}H NMR** (400 MHz, $CDCl_3$) δ 7.80 (dd, *J* = 8.5, 1.9 Hz, 1H), 7.73 (d, *J* = 8.5 Hz, 1H), 7.64 (d, *J* = 2.0 Hz, 1H), 7.50 – 7.45 (m, 1H), 7.44 (dd, *J* = 3.4, 1.5 Hz, 1H), 7.15 (d, *J* = 16.0 Hz, 1H), 7.03 (dd, *J* = 8.3, 6.9, Hz, 1H), 6.76 (dd, *J* = 8.0, 1.2 Hz, 1H), 6.32 (d, *J* = 16.0 Hz, 1H), 3.66 (s, 3H), 2.69 (s, 3H). **^{13}C{^{1}H} NMR** (101 MHz, $CDCl_3$) δ 166.2, 157.6, 153.5, 151.8, 143.1, 139.1, 136.7, 134.4, 132.2, 131.9, 131.6, 129.1, 124.7, 124.4, 122.5, 121.8, 118.4, 111.3, 106.6, 52.1, 13.1. **HRMS** (ESI-TOF): m/z $[M+H]^+$ calcd for $C_{21}H_{16}{}^{79}BrN_2O_4$ 438.0215; found 438.0227. calcd for $C_{21}H_{16}{}^{81}BrN_2O_4$ 440.0185; found 440.0199.

Synthesis of **3.5ai**

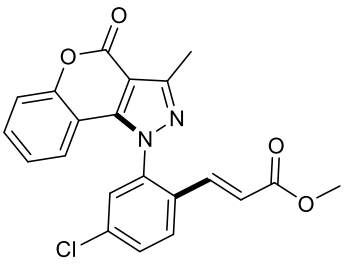

Methyl (*E*)-3-(2-chloro-6-(3-methyl-4-oxochromeno[4,3-*c*]pyrazol-1(4*H*)-yl)phenyl) acrylate (**3.5ai).** The compound **3.5ai** was synthesized using general procedure C and obtained as light-yellow solid compound, 67% (263 mg); R_f = 0.5 (EtOAc + Hexane 6:94)**; mp** 240-244 °C. **^{1}H NMR** (400 MHz, $CDCl_3$) δ 7.80 (dd, *J* = 8.6, 1.9 Hz, 1H), 7.73 (d, *J* = 8.5 Hz, 1H), 7.65 (t, *J* = 2.5 Hz, 1H), 7.49 – 7.43 (m, 2H), 7.15 (d, *J* = 16.0 Hz, 1H), 7.07 – 7.00 (m, 1H), 6.76 (dd, *J* = 8.0, 1.5 Hz, 1H), 6.32 (d, *J* = 16.0 Hz, 1H), 3.66 (s, 3H), 2.69 (s, 3H). **^{13}C{^{1}H} NMR** (101 MHz, $CDCl_3$) δ 166.4, 157.3, 151.4, 148.3, 143.2, 138.3, 137.8, 133.0, 131.3, 131.1, 129.0, 124.1, 122.0, 113.3, 113.1, 112.2, 106.4, 52.0, 13.1. **HRMS** (ESI-TOF): m/z $[M+H]^+$ calcd for $C_{21}H_{16}ClN_2O_4$ 395.0720; found 395.0735.

Synthesis of **3.5aj**

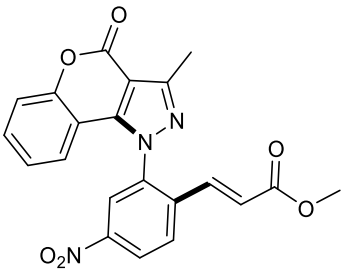

Methyl (*E*)-3-(2-(3-methyl-4-oxochromeno[4,3-*c*]pyrazol-1(4*H*)-yl)-6-nitrophenyl) acrylate (**3.5aj).** The compound **3.5aj** was synthesized using general procedure C and obtained as light-yellow solid compound, 62% (251 mg); R_f = 0.5 (EtOAc + Hexane 8:92)**; mp** 234-238 °C. **^{1}H NMR** (400 MHz, $CDCl_3$) δ 8.42 (d, *J* = 2.5 Hz, 1H), 7.80 (d, *J* = 8.0 Hz, 1H), 7.68 (d, *J* = 4.1 Hz, 1H), 7.50 – 7.46 (m, 1H), 7.28 (d, *J* = 16.0 Hz, 1H), 7.21 (dd, *J* = 8.1, 1.6 Hz, 1H), 7.14 – 7.08 (m, 1H), 6.69 (d, *J* = 12.1 Hz, 1H), 6.52 (d, *J* = 16.0 Hz, 1H), 3.71 (s, 3H), 2.70 (s, 3H). **^{13}C{^{1}H} NMR** (101 MHz, $CDCl_3$) δ 166.5, 158.0, 153.4, 151.4, 143.0, 141.4, 138.0, 135.9, 132.5, 132.2, 131.3, 128.6, 124.2, 122.0, 121.7, 118.9, 111.7, 106.3, 52.0, 13.1. **HRMS** (ESI-TOF): m/z $[M+H]^+$ calcd for $C_{21}H_{16}N_3O_6$ 406.0994; found 406.0110.

Synthesis of **3.5ak**

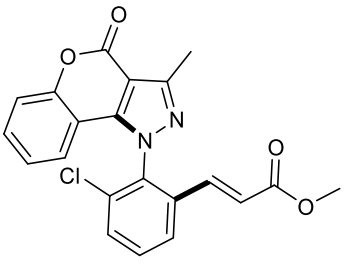

Methyl (*E*)-3-(3-chloro-2-(3-methyl-4-oxochromeno[4,3-*c*]pyrazol-1(4*H*)-yl)phenyl) acrylate (**3.5ak).** The compound **3.5ak** was synthesized using general procedure C and obtained as light-yellow solid compound, 55% (216 mg); R_f = 0.5 (EtOAc + Hexane 10:90)**; mp** 222-226 °C. **^{1}H NMR** (400 MHz, $CDCl_3$) δ 7.80 (d, *J* = 8.0 Hz, 1H), 7.70 – 7.65 (m, 2H), 7.50 (d, *J* = 6.9 Hz, 1H), 7.24 (d, *J* = 16.1 Hz, 1H), 7.21 (dd, *J* = 8.3, 1.8 Hz, 1H), 7.13 – 7.07 (m, 1H), 6.74 (d, *J* = 6.2 Hz, 1H), 6.52 (d, *J* = 16.0 Hz, 1H), 3.71 (s, 3H), 2.70 (s, 3H). **^{13}C{^{1}H} NMR** (101 MHz, $CDCl_3$) δ 166.4, 157.3, 151.7, 141.7, 137.6, 132.8, 131.5, 131.3, 129.5, 128.8, 128.2, 122.3, 121.6, 119.6, 112.6, 106.6, 52.0, 13.1. **HRMS** (ESI-TOF): m/z $[M+H]^+$ calcd for $C_{21}H_{16}ClN_2O_4$ 395.0720; found 395.0737.

Synthesis of **3.5al**

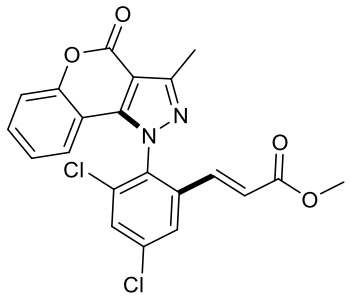

Methyl (*E*)-3-(3,5-dichloro-2-(3-methyl-4-oxochromeno[4,3-*c*]pyrazol-1(4*H*)-yl)phenyl) acrylate (**3.5al).** The compound **3.5al** was synthesized using general procedure C and obtained as light-yellow solid compound, 50% (214 mg); R_f = 0.5 (EtOAc + Hexane 7:93)**; mp** 256-260 °C. **^{1}H NMR** (400 MHz, $CDCl_3$) δ 7.89 (dd, *J* = 7.8, 1.7 Hz, 1H), 7.67 (td, *J* = 7.7, 1.4 Hz, 1H), 7.61 (td, *J* = 7.5, 1.6 Hz, 1H), 7.44 – 7.41 (m, 1H), 7.41 – 7.39 (m, 1H), 7.16 (d, *J* = 16.0 Hz, 1H), 6.72 (d, *J* = 8.0 Hz, 1H), 6.35 (d, *J* = 16.0 Hz, 1H), 3.67 (s, 3H), 2.70 (s, 3H). **^{13}C{^{1}H} NMR** (101 MHz, $CDCl_3$) δ 166.5, 157.9, 153.4, 151.4, 142.9, 141.5, 138.0, 135.8, 132.5, 132.2, 131.3, 128.7, 128.5, 124.2, 122.0, 121.7, 118.2, 111.7, 106.3, 51.9, 13.1. **HRMS** (ESI-TOF): m/z $[M+H]^+$ calcd for $C_{21}H_{15}Cl_2N_2O_4$ 430.0301; found 430.0320.

Synthesis of **3.5am**

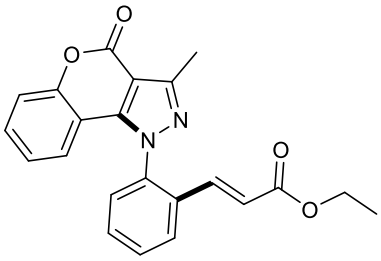

Ethyl (*E*)-3-(2-(3-methyl-4-oxochromeno[4,3-*c*]pyrazol-1(4*H*)-yl)phenyl) acrylate (**3.5am)** The compound **3.5am** was synthesized using general procedure C and obtained as light-yellow solid compound, 75% (280 mg); R_f = 0.5 (EtOAc + Hexane 6:94)**; mp** 230-234 °C. **^{1}H NMR** (400 MHz, $CDCl_3$) δ 7.87 (dd, *J* = 7.8, 1.3 Hz, 1H), 7.69 – 7.65 (m, 1H), 7.62 – 7.58 (m, 1H), 7.46 (dd, *J* = 7.8, 1.3 Hz, 1H), 7.43 – 7.42 (m, 1H), 7.41 (d, *J* = 0.5 Hz, 1H), 7.21 (d, *J* = 16.0 Hz, 1H), 6.99 – 6.95 (m, 1H), 6.73 – 6.70 (m, 1H), 6.34 (d, *J* = 16.0 Hz, 1H), 4.14 (q, *J* = 8.0 Hz, 2H), 2.70 (s, 3H), 1.21 (t, *J* = 7.1 Hz, 3H). **^{13}C{^{1}H} NMR** (101 MHz, $CDCl_3$) δ 165.9, 157.9, 153.4, 151.5, 143.1, 138.3, 137.6, 133.0, 131.4, 131.2, 128.9, 128.0, 124.2, 122.5, 121.9, 118.2, 111.6, 106.4, 60.8, 14.2, 13.1. **HRMS** (ESI-TOF): m/z $[M+H]^+$ calcd for $C_{22}H_{19}N_2O_4$ 375.1300; found 375.1316.

Synthesis of **3.5an**

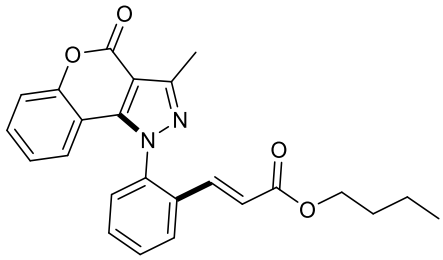

Butyl (*E*)-3-(2-(3-methyl-4-oxochromeno[4,3-*c*]pyrazol-1(4*H*)-yl)phenyl) acrylate (**3.5an).** The compound **3.5an** was synthesized using general procedure C and obtained as light-yellow solid compound, 76% (300 mg); R_f = 0.5 (EtOAc + Hexane 10:90)**; mp** 220-224 °C. **^{1}H NMR** (400 MHz, $CDCl_3$) δ 7.87 (dd, *J* = 8.0, 1.9 Hz, 1H), 7.67 (td, *J* = 7.8, 1.6 Hz, 1H), 7.60 (td, *J* = 7.7, 1.7 Hz, 1H), 7.47 (dd, *J* = 7.8, 1.6 Hz, 1H), 7.43 – 7.41 (m, 1H), 7.41 (s, 1H), 7.18 (d, *J* = 16.1 Hz, 1H), 6.97 (ddd, *J* = 8.6, 6.2, 2.6 Hz, 1H), 6.75 – 6.70 (m, 1H), 6.36 (s, 1H), 4.05 (t, *J* = 8.0 Hz, 2H), 2.69 (s, 3H), 1.60 – 1.44 (m, 2H), 1.27 (dt, *J* = 14.8, 7.6 Hz, 2H), 0.86 (t, *J* = 8.0 Hz, 3H**). ^{13}C{^{1}H} NMR** (101 MHz, $CDCl_3$) δ 165.9, 157.8, 153.5, 151.4, 143.0, 138.3, 137.5, 133.0, 131.3, 131.1, 128.8, 127.9, 124.2, 122.5, 121.9, 118.2, 111.6, 106.4, 64.7, 30.6, 19.2, 13.7, 13.1. **HRMS** (ESI-TOF): m/z $[M+H]^+$ calcd for $C_{24}H_{23}N_2O_4$ 403.1613; found 403.1623.

Synthesis of **3.5ao**

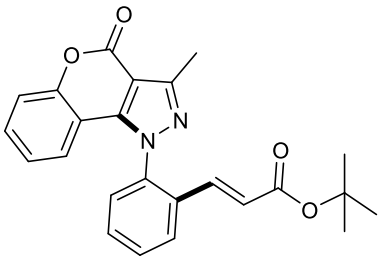

tert-Butyl (*E*)-3-(2-(3-methyl-4-oxochromeno[4,3-*c*]pyrazol-1(4*H*)-yl)phenyl)acrylate (**3.5ao).** The compound **3.5ao** was synthesized using general procedure C and obtained as light-yellow solid compound, 70% (273 mg); R_f = 0.6 (EtOAc + Hexane 5:95)**; mp** 196-200 °C. **^{1}H NMR** (400 MHz, $CDCl_3$) δ 7.87 (dd, *J* = 7.9, 1.4 Hz, 1H), 7.67 – 7.63 (m, 1H), 7.59 (td, *J* = 7.6, 1.5 Hz, 1H), 7.46 (dd, *J* = 7.7, 1.3 Hz, 1H), 7.43 – 7.42 (m, 1H), 7.41 (d, *J* = 0.9 Hz, 1H), 7.10 (d, *J* = 16.0 Hz, 1H), 6.97 (ddd, *J* = 8.4, 5.7, 2.8 Hz, 1H), 6.74 – 6.71 (m, 1H), 6.30 (d, *J* = 16.0 Hz, 1H), 2.70 (s, 3H), 1.38 (s, 9H). **^{13}C{^{1}H} NMR** (101 MHz, $CDCl_3$) δ 165.2, 157.9, 153.5, 151.4, 143.1, 138.2, 136.4, 133.2, 131.3, 131.2, 131.1, 128.8, 127.7, 124.2, 122.1, 118.9, 111.7, 106.3, 81.1, 28.1, 13.1. **HRMS** (ESI-TOF): m/z $[M+H]^+$ calcd for $C_{24}H_{23}N_2O_4$ 403.1613; found 403.1630.

Synthesis of **3.5ap**

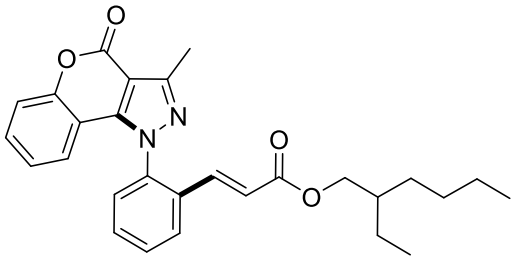

2-Ethylhexyl (*E*)-3-(2-(3-methyl-4-oxochromeno[4,3-*c*]pyrazol-1(4*H*)-yl)phenyl) acrylate (**3.5ap).** The compound **3.5ap** was synthesized using general procedure C and obtained as light-yellow solid compound, 74% (338 mg); R_f = 0.5 (EtOAc + Hexane 5:95)**; mp** 198-202 °C. **^{1}H NMR** (400 MHz, $CDCl_3$) δ 7.88 (d, *J* = 6.3 Hz, 1H), 7.67 (d, *J* = 1.5 Hz, 1H), 7.61 (d, *J* = 1.5 Hz, 1H), 7.49 (d, *J* = 6.3 Hz, 1H), 7.41 (s, 1H), 7.41 (s, 1H), 7.14 (s, 1H), 6.97 (m, 1H), 6.73 (d, *J* = 8.0 Hz, 1H), 6.33 (d, *J* = 16.0 Hz, 1H), 4.00-3.91 (m, 2H), 2.69 (s, 3H), 1.51 – 1.42 (m, 1H), 1.35-1.26 (m, 2H), 1.23 – 1.08 (m, 6H), 0.79 (dd, *J* = 6.1, 2.3 Hz, 6H). **^{13}C{^{1}H} NMR** (101 MHz, $CDCl_3$) δ 166.0, 157.8, 153.5, 151.4, 143.0, 138.3, 137.3, 133.0, 131.4, 131.1, 128.9, 127.8, 124.2, 122.5, 121.9, 118.2, 111.6, 106.3, 66.9, 38.7, 30.4, 28.9, 23.9, 22.9, 14.1, 13.0, 11.0. **HRMS** (ESI-TOF): m/z $[M+H]^+$ calcd for $C_{28}H_{31}N_2O_4$ 459.2239; found 459.2255.

Synthesis of **3.5ba**

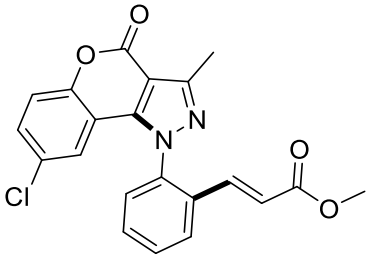

Methyl (*E*)-3-(2-(8-chloro-3-methyl-4-oxochromeno[4,3-*c*]pyrazol-1(4*H*)-yl)phenyl) acrylate (**3.5ba).** The compound **3.5ba** was synthesized using general procedure C and obtained as light-yellow solid compound, 72% (285 mg); R_f = 0.5 (EtOAc + Hexane 12:88)**; mp** 244-248 °C. **^{1}H NMR** (400 MHz, $CDCl_3$) δ 7.89 (dd, *J* = 7.9, 1.7 Hz, 1H), 7.70 (td, *J* = 7.7, 1.5 Hz, 1H), 7.64 (td, *J* = 7.6, 1.5 Hz, 1H), 7.45 (dd, *J* = 7.7, 1.5 Hz, 1H), 7.36 (d, *J* = 2.1 Hz, 1H), 7.35 (d, *J* = 8.1 Hz, 1H), 7.19 (d, *J* = 16.0 Hz, 1H), 6.61 – 6.60 (m, 1H), 6.35 (d, *J* = 16.0 Hz, 1H), 3.68 (s, 3H), 2.70 (s, 3H). **^{13}C{^{1}H} NMR** (101 MHz, $CDCl_3$) δ 166.4, 157.3, 151.7, 151.6, 141.8, 137.6, 132.8, 131.5, 131.4, 131.3, 129.5, 128.8, 128.3, 122.3, 121.6, 119.6, 112.6, 106.6, 52.0, 13.1. **HRMS** (ESI-TOF): m/z $[M+H]^+$ calcd for $C_{21}H_{16}ClN_2O_4$ 395.0720; found 395.0735.

Synthesis of **3.5ca**

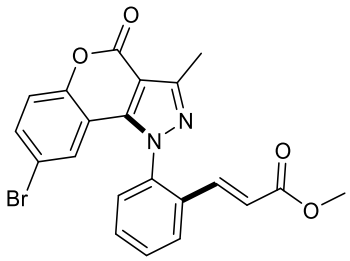

Methyl (*E*)-3-(2-(8-bromo-3-methyl-4-oxochromeno[4,3-*c*]pyrazol-1(4*H*)-yl)phenyl) acrylate (**3.5ca).** The compound **3.5ca** was synthesized using general procedure C and obtained as light-yellow solid compound, 76% (325 mg); R_f = 0.5 (EtOAc + Hexane 10:90)**; mp** 236-240 °C. **^{1}H NMR** (400 MHz, $CDCl_3$) δ 7.89 (dd, *J* = 7.9, 1.7 Hz, 1H), 7.71 (td, *J* = 7.7, 1.6 Hz, 1H), 7.66 – 7.62 (m, 1H), 7.51 (dd, *J* = 8.9, 2.3 Hz, 1H), 7.45 (dd, *J* = 7.8, 1.6 Hz, 1H), 7.29 (d, *J* = 8.9 Hz, 1H), 7.19 (d, *J* = 16.0 Hz, 1H), 6.76 (d, *J* = 2.3 Hz, 1H), 6.35 (d, *J* = 16.0 Hz, 1H), 3.68 (s, 3H), 2.70 (s, 3H). **^{13}C{^{1}H} NMR** (101 MHz, $CDCl_3$) δ 166.4, 157.3, 152.3, 151.6, 141.7, 137.6, 134.2, 132.9, 131.5, 128.8, 128.3, 124.7, 122.3, 119.8, 116.9, 113.2, 106.6, 52.1, 13.1. **HRMS** (ESI-TOF): m/z $[M+H]^+$ calcd for $C_{21}H_{16}{}^{79}BrN_2O_4$ 438.0215; found 438.0235. calcd for $C_{21}H_{16}{}^{81}BrN_2O_4$ 440.0185; found 440.0195.

Synthesis of **3.5da**

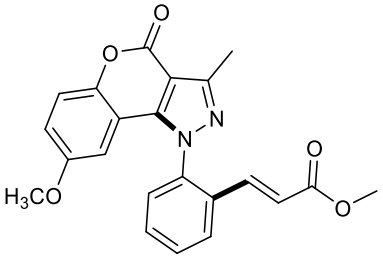

Methyl (*E*)-3-(2-(8-methoxy-3-methyl-4-oxochromeno[4,3-*c*]pyrazol-1(4*H*)-yl)phenyl) acrylate (**3.5da).** The compound **3.5da** was synthesized using general procedure C and obtained as light-yellow solid compound, 85% (331 mg); R_f = 0.5 (EtOAc + Hexane 12:88)**; mp** 248-252 °C. **^{1}H NMR** (400 MHz, $CDCl_3$) δ 7.85 (dd, *J* = 7.8, 1.4 Hz, 1H), 7.68 – 7.64 (m, 1H), 7.60 (td, *J* = 7.6, 1.5 Hz, 1H), 7.45 (dd, *J* = 7.8, 1.3 Hz, 1H), 7.19 (d, *J* = 16.1 Hz, 1H), 6.98 (dd, *J* = 8.2, 1.3 Hz, 1H), 6.89 (t, *J* = 8.1 Hz, 1H), 6.29 (d, *J* = 13.8 Hz, 1H), 6.26 (d, *J* = 7.2 Hz, 1H), 3.93 (s, 3H), 3.66 (s, 3H), 2.70 (s, 3H). **^{13}C{^{1}H} NMR** (101 MHz, $CDCl_3$) δ 166.4, 157.3, 151.4, 148.3, 143.2, 138.3, 137.8, 132.9, 131.4, 131.1, 129.1, 128.1, 124.2, 122.0, 121.9, 113.3, 113.1, 112.2, 106.4, 56.3, 51.9, 13.1. **HRMS** (ESI-TOF): m/z $[M+H]^+$ calcd for $C_{22}H_{19}N_2O_5$ 391.1249; found 391.1259.

Synthesis of **3.5aq**

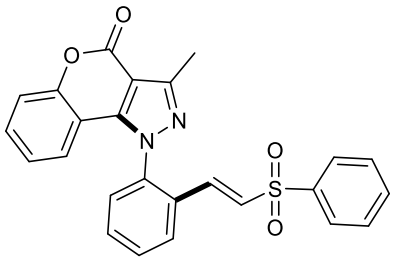

(*E*)-3-methyl-1-(2-(2-(phenylsulfonyl)vinyl)phenyl)chromeno[4,3-*c*]pyrazol-4(1*H*)-one (**3.5aq**). The compound **3.5aq** was synthesized using general procedure C and obtained as yellow solid compound, 45% (198 mg); R_f = 0.6 (EtOAc + Hexane 7:93); **mp** 288-292 °C. **^{1}H NMR** (400 MHz, $CDCl_3$) δ 8.76 (d, *J* = 15.3 Hz, 1H), 7.97 (d, *J* = 4.3 Hz, 1H), 7.94 – 7.92 (m, 2H), 7.58 (dd, *J* = 7.9, 1.6 Hz, 1H), 7.53 – 7.49 (m, 2H), 7.45 (d, *J* = 1.5 Hz, 2H), 7.29 (d, *J* = 1.0 Hz, 2H), 7.19 (d, *J* = 8.0 Hz, 1H), 6.77 (d, *J* = 3.9 Hz, 2H), 6.58 (d, *J* = 15.1 Hz, 1H), 2.00 (s, 3H). **^{13}C{^{1}H} NMR** (101 MHz, $CDCl_3$) δ 165.0, 160.6, 153.4, 147.6, 144.1, 140.9, 140.1, 135.5, 133.9, 133.3, 132.3, 130.5, 129.2, 128.3, 128.2, 127.7, 125.0, 119.6, 118.5, 117.7, 116.4, 69.7. **HRMS** (ESI-TOF): m/z $[M+H]^+$ calcd for $C_{25}H_{19}N_2O_4S$ 443.1021; found 443.1029.

CHAPTER 4

Benzimidazole Assisted [4+2] Oxidative Annulation of 3-(1*H*-benzo[*d*]imidazol-2-yl)-2*H*-chromen-2-one

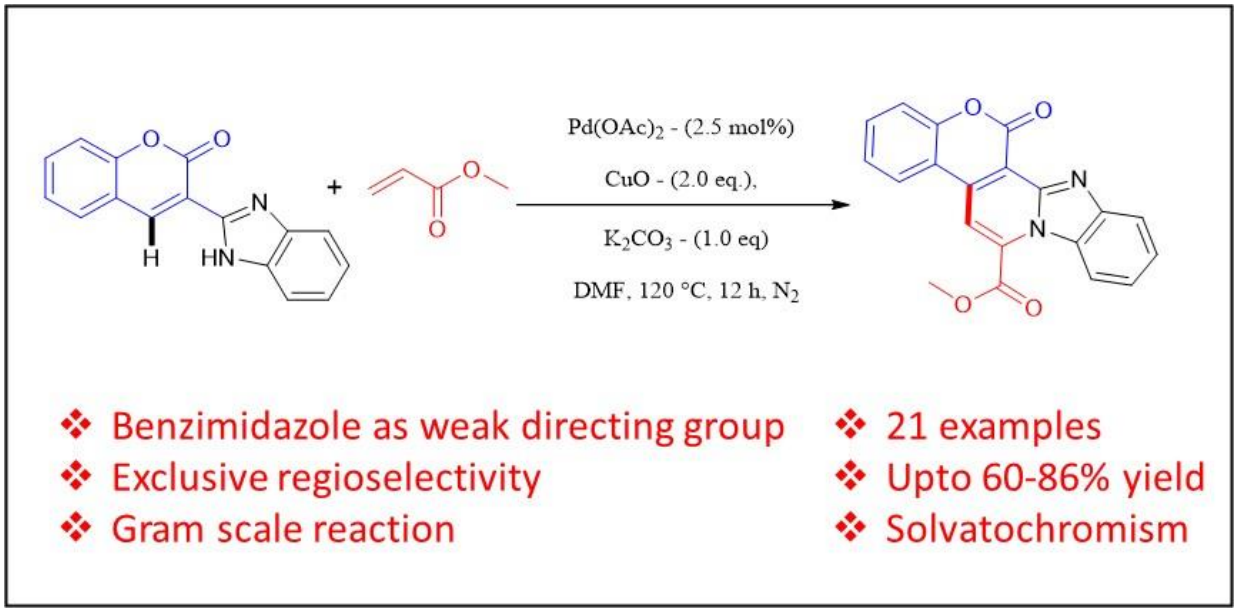

CHAPTER 4

4.1. Introduction

Polycyclic aromatic hydrocarbons (PAHs) are recognized as privileged structural motifs in many pharmaceuticals and natural products.[93] In this context, polycyclic aromatic imidazo[1,2-*a*]pyridines and coumarins, as one of the typical scaffolds, have claimed considerable attention from organic chemists for their significant applications and pharmacological properties, such as anti-oxidants, a bronchodilator, anti-inflammatory, inotropic agent, antihypertensive, and anti-cancer.[94] Furthermore, these PAHs have the potential as fluorescent materials, laser dyes, and optical brighteners.[95-97] Subsequently, the efficient synthesis of polycyclic aromatic scaffolds of these heterocyclic moieties is a fascinating topic for the synthetic community.[98,99] In 2013, Wang group demonstrated oxidative annulation of cyclic *trans*-enamines to access substituted pyrroles (**Scheme 4.1a**).[100] In 2014, Gryko and co-workers showed oxidative annulation of methyl 2-oxo-2*H*-chromene-3-carboxylate with resorcinol to synthesize bis-coumarin (**Scheme 4.1b**).[101] In 2016 and 2019, Gogoi group performed C3 functionalization of 4-hydroxycoumarin under palladium catalysis for direct synthesis of coumestans and bis-coumarins, respectively (**Scheme 4.1c**).[47,48] Notably, all these approaches are effective for oxidative annulation to synthesize coumarin-based derivatives. Although the literature has been reported for C3/C4 functionalization of coumarin, however, there is no literature precedent for [4+2] oxidative annulation to access imidazo[1,2-*a*]chromeno[3,4-*c*]pyridine.[102-104] Hence, effective and incisive approaches are desirable. Despite the myriad development in regioselective C-H functionalization of coumarin to extend π conjugation, this scaffold has never been used for C4 functionalization using benzimidazole as directing the group to access the oxidative annulation.[105-111]

4.2. Objective

Herein, benzimidazole-assisted C-H activation for [4+2] oxidative annulation at C4 of coumarin using palladium-catalysis, which is the first example to build up coumarin-imidazo[1,2-*a*]pyridine ring system is reported (**Scheme 4.1d**). It is proposed that this transformation is carried out *via* the cyclometallation activation route, and benzimidazole serves as the weak directing group. In addition, solvatochromic studies of synthesized scaffolds are also discussed.

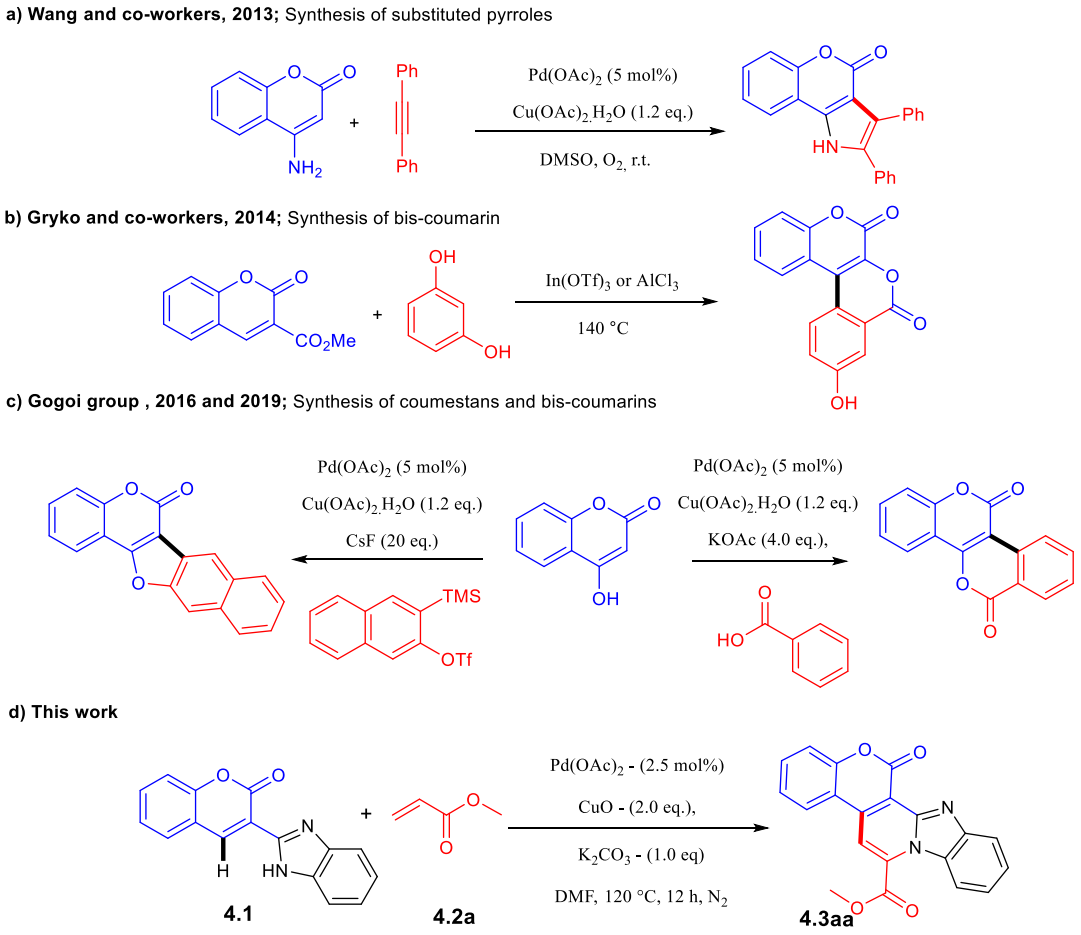

Scheme 4.1. Research background and present work

4.3. Results and Discussion

4.3.1. Synthesis of Coumarin-Benzimidazole Hybrid

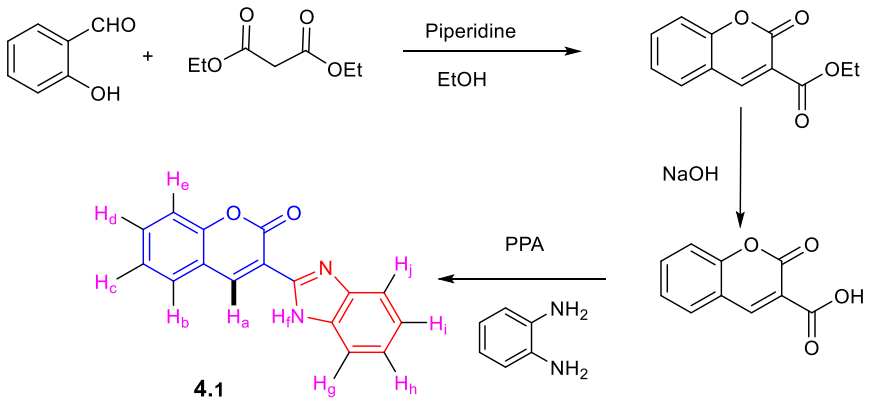

Scheme 4.2. Synthesis of coumarin-benzimidazole conjugates

To evaluate the envisioned reaction hypothesis, I have first synthesized coumarin-benzimidazole hybrid as starting substrate, according to **Scheme 4.2**. Initially, Knoevenagel condensation was performed by reacting salicylaldehyde with diethyl malonate using piperidine as a weak base in ethanol and gave ethyl 2-oxo-2*H*-chromene-3-carboxylate which was hydrolyzed to 2-oxo-2*H*-chromene-3-carboxylic acid and further reacted with *o*-phenyldiamine to give 3-(1*H*-benzo[*d*]imidazol-2-yl)-2*H*-chromen-2-one (**4.1**). Compound **4.1** was confirmed by ^{1}H NMR spectrum, as the compound showed two 1H (H_a and H_f respectively) singlets at δ 8.42 and 7.77 ppm, 2H (H_c and H_h respectively) doublet of doublet at δ 7.55 ppm with J = 6.1, 4.0 Hz, 1H_b doublet of double at δ 7.46 ppm with J = 7.8, 2.2 Hz, 2H (H_d and H_i respectively) multiplet at δ 7.26- 7.21 ppm, 1H_e doublet at δ 7.14 ppm with J = 1.8 Hz, 1H_j doublet at δ 6.81 ppm with J = 8.0 Hz and multiplet of 1H_g at δ 6.63-6.58 ppm of aromatic protons.

4.3.2. Optimization

Primarily, the investigation was initiated by confirming the optimal reaction conditions for [4+2] oxidative annulation. I began with 3-(1*H*-benzo[*d*]imidazol-2-yl)-2*H*-chromen-2-one **4.1a** (0.1 mmol, 1.0 eq.) and methyl acrylate **4.2a** (0.3 mmol, 3.0 eq.) in the presence of palladium catalysis. As acrylates for oxidative annulation exhibit greater tunning with palladium catalysis, therefore, initially, several solvents were screened in the presence of $Pd(OAc)_2$ as the catalyst, K_2CO_3 (1.0 eq.) as an additive/base, and CuO (2.0 eq.) as an oxidant at 120 °C. Number of polar, non-polar, and chlorinated solvents were investigated, wherein aprotic polar solvents such as NMP, 1,4-dioxane, DMSO, THF, and chlorinated solvent DCE displayed low to moderate conversion of **4.1a** (**Table 4.1**, entries 1-5). However, non-polar solvents such as toluene, *o*-xylene (**Table 1**, entries 6-7), and polar protic solvents as MeOH and AcOH (**Table 4.1**, entries 8-9) showed very low conversion and proved ineffective for this reaction. In contrast, polar aprotic solvent such as DMF (**Table 4.1**, entry 10) gave 80% yield of the final compound **4.3aa**. In addition, $[RuCl_2(p\text{-cymene})]_2$ was also employed (**Table 4.1**, entries 11), but no improvement in yield was observed. After initial screening, I looked into various oxidants and additives (**Table 4.1**, entries 12-15) to increase the yield of **4.3aa**. Noteworthy, silver-based oxidants also could not improve the yield and gave only 65% of the desired compound (**Table 4.1**, entry 15). Furthermore, no efficacy was attained in the absence of $Pd(OAc)_2$ (**Table 4.1**, entry 16).[112]

Table 4.1. Optimization of reaction conditions[a]

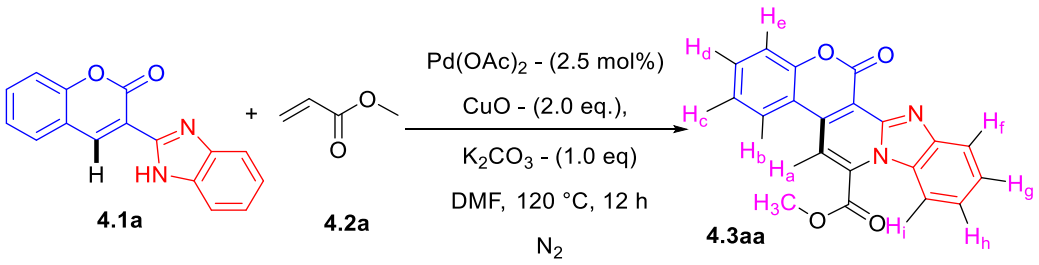

entry	solvent	additive/base	oxidant	yield **4.3aa** (%)[b]
1	NMP	…….	CuO	traces
2	1,4-dioxane	$AgSbF_6$	CuO	25
3	THF	…….	CuO	30
4	DMSO	K_2CO_3	CuO	45
5	DCE	K_2CO_3	CuO	35
6	Toluene	K_2CO_3	CuO	Traces
7	*o*-xylene	K_2CO_3	CuO	Traces
8	MeOH	K_2CO_3	CuO	Traces
9	AcOH	K_2CO_3	CuO	Traces
10	DMF	K_2CO_3	CuO	80
11[c]	DMF	K_2CO_3	CuO	70
12	DMF	K_2CO_3	Ag_2CO_3	10
13	DMF	$AgNTf_2$	AgOAc	55
14	DMF	$AgSbF_6$	$Cu(OAc)_2.H_2O$	40
15	DMF	K_2CO_3	AgOAc	65
16[d]	DMF	K_2CO_3	CuO	…

[a]General reaction condition: **4.1a** (1 mmol), **4.2a** (3 mmol), $Pd(OAc)_2$ (2.5 mol%), CuO (2.0 eq.), K_2CO_3 (1.0 eq.) solvent (2 mL), [b]Isolated yields after purification, [c] $[Ru(p\text{-cymene})Cl_2]_2$ used as a catalyst, [d]In the absence of $Pd(OAc)_2$.

Compound **4.3aa** was confirmed by ^1H and ^{13}C NMR spectra; compound showed characteristic signals of aromatic protons as doublet at δ 8.20 ppm with J = 8.2 Hz of $1H_b$, doublet at δ 8.04 ppm with J = 8.0 Hz of $1H_i$, doublet at δ 7.86 ppm with J = 8.5 Hz of $1H_e$, singlet of $1H_a$ at δ 7.84 ppm, doublet of triplet at δ 7.60 ppm with J = 20.4, 7.7 Hz of 2H (H_d and H_h), multiplet at δ 7.48-7.37 ppm of 3H (H_c, H_f, and H_g) in aromatic region. Noteworthy, singlet of compound **4.1a** at δ 8.42 is missing and a new singlet of 1H in aromatic region at δ

7.84 is observed. In addition, in aliphatic region, signals as singlet at δ 4.21 Hz of 3H of OCH_3 confirmed the formation of cyclized product. Furthermore, characteristic signal at δ 54.1 ppm for methoxy group of methyl acrylate in ^{13}C NMR, also confirmed the structure.

4.3.3. Substrate Scope

After the intensive investigation, I explored the electronic effects and substrate scope of this [4+2] oxidative annulation. Firstly, different alkenes **4.2a-l** were tested with **4.1a** under optimized reaction conditions. Olefins, **4.2a-e** having ester group linkage transformed smoothly to afford corresponding scaffolds **4.3aa-4.3ae** in 70-82% yields. In addition, to check the catalytic activity of various cyclic, electron-deficient, and substituted alkenes like methyl vinyl ketone, propargyl acrylate, crotonaldehyde, cyclohexenone, acrylonitrile, and acrylic acid, **4.2f-l** having low reactivity and varying terminal functional groups were also employed under optimized conditions, and surprisingly, only methyl vinyl ketone **4.2f** underwent oxidative annulation to give annulated product **4.3af** in 60% yield (**Scheme 4.3**).

Further, different electron-donating and -withdrawing groups on coumarin and benzimidazole nuclei were examined, which showed great compatibility with present oxidative annulation. Substitution of methyl group (electron-donating) on benzimidazole aryl ring with **4.1b** gave **4.3ba** in 84% yield (**Scheme 4.4**). In contrast, substitution with an electron-withdrawing group such as nitro in the case of **4.1c** gave **4.3ca** in 60% yield, and bromo **4.1d** gave **4.3da** in 74% yield, which indicated electron donating groups have better compatibility than electron-withdrawing groups for this annulation. Similarly, various substitutions on coumarin nuclei were also subjected to general reaction conditions with the same alkenes and gave corresponding compounds in 60% to 80% yields . Substitution on aryl ring of coumarin with bromo **4.1e** reacted with three different alkenes **4.2a-c** and gave corresponding compounds **4.3ea-4.3ec** in 70-77% yields; here again, similar behavior of alkenes was observed, alkenes having branching chain (such as *tert*-butyl acrylate **4.2c**) gave lesser yields compared to other alkenes. When the bromo was replaced with chloro, substrate **4.1f** gave respective compounds **4.3fa-4.3fc** with alkenes **4.2a-c** in 60-64% yields. However, when the electron-donating methoxy group was substituted, substrate **4.1g** was screened with same alkenes and gave a higher yield of corresponding annulated products **4.3ga-4.3gc** in 75-86% yields. Furthermore, conjugation extended with aryl ring substrate **4.1h** was

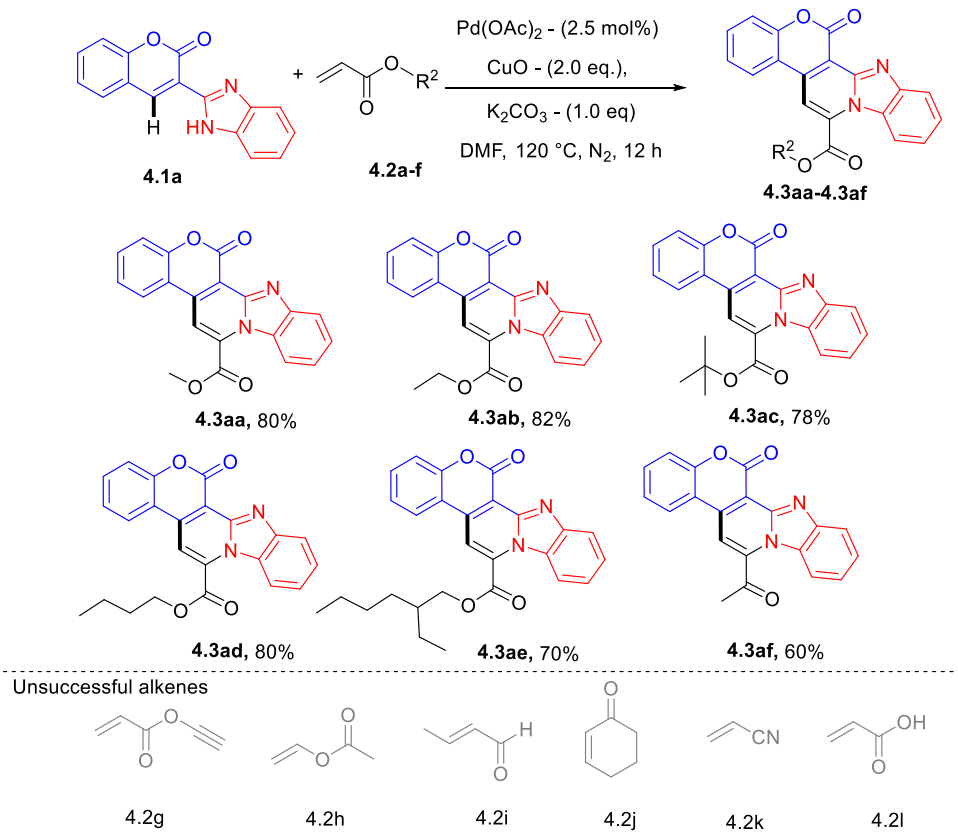

Scheme 4.3. Alkene scope for [4+2] oxidative annulation

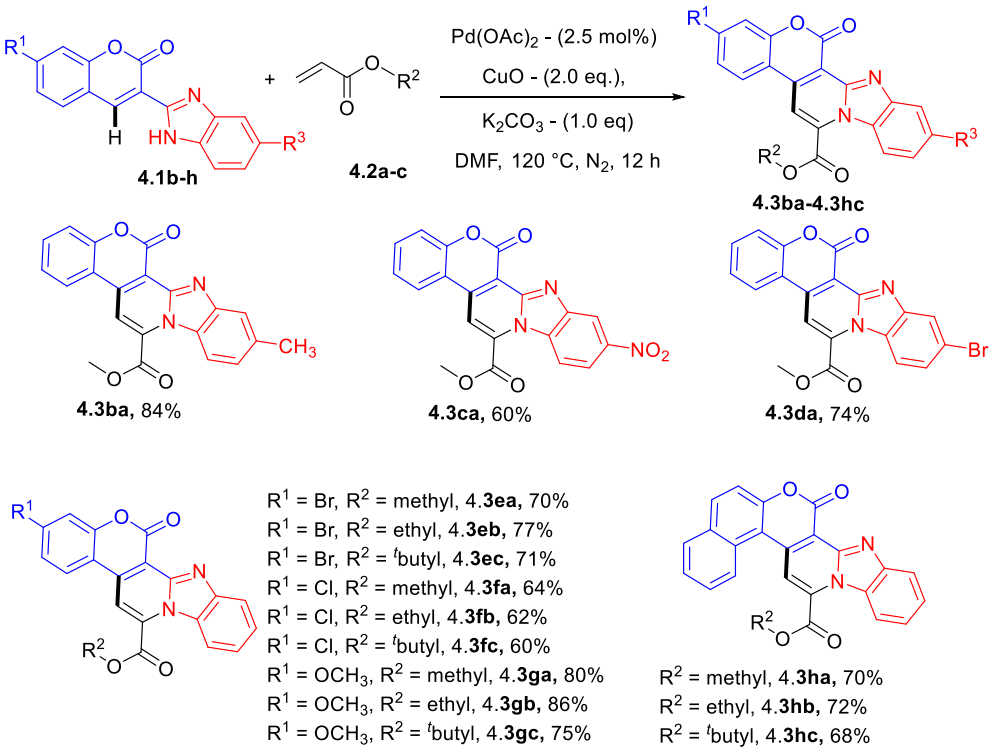

Scheme 4.4. Substrate scope for [4+2] oxidative annulation

also subjected to the same conditions with alkenes, which reacted well and gave compounds **4.3ha-4.3hc** in 68-72% yields (**Scheme 4.4**).

4.3.4. Gram Scale Reactions

A scale-up experiment was set up to examine the efficacy of the present methodology and industrial utility, giving 85% yield of the annulated product (**Scheme 4.5a**). On the other hand, reducing the catalyst load, gave **4.7aa** in 75% yield along with recovery of 25% of starting material (**Scheme 4.5b**).

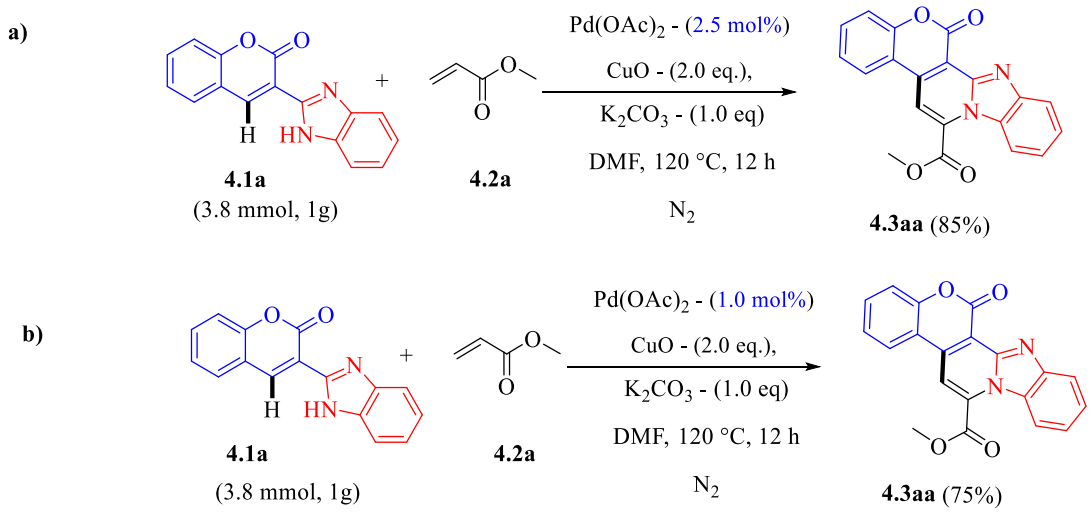

Scheme 4.5. Gram scale reaction

4.3.5. Deuterium Labeled and Control Experiments

After myriad investigations, to explore the reaction's mechanistic pathway, several control experiments were performed. To examine the role of benzimidazole as directing group and [4+2] oxidative annulation**,** I have performed the reaction with **4.1i** having *N*-methyl benzimidazole under the same optimized conditions with different alkenes **4.2a-4.2b**, where instead of annulation, alkenylated products **4.3ia-4.3ib** were obtained in 55-60% yields (**Scheme 4.6a)** that suggested one nitrogen atom of benzimidazole nuclei must be unsubstituted for oxidative annulation. To shed more-light on mechanistic insights, substrate **4.1a** was subjected to the same reaction conditions using **D_2O** (5.0 eq.) in **Scheme 4.6b**, wherein isotopically labeled compound **4.1a-[D]** showed 100% H-D exchange analyzed by NMR which indicates the C-H bond activation step may be reversible.[113]

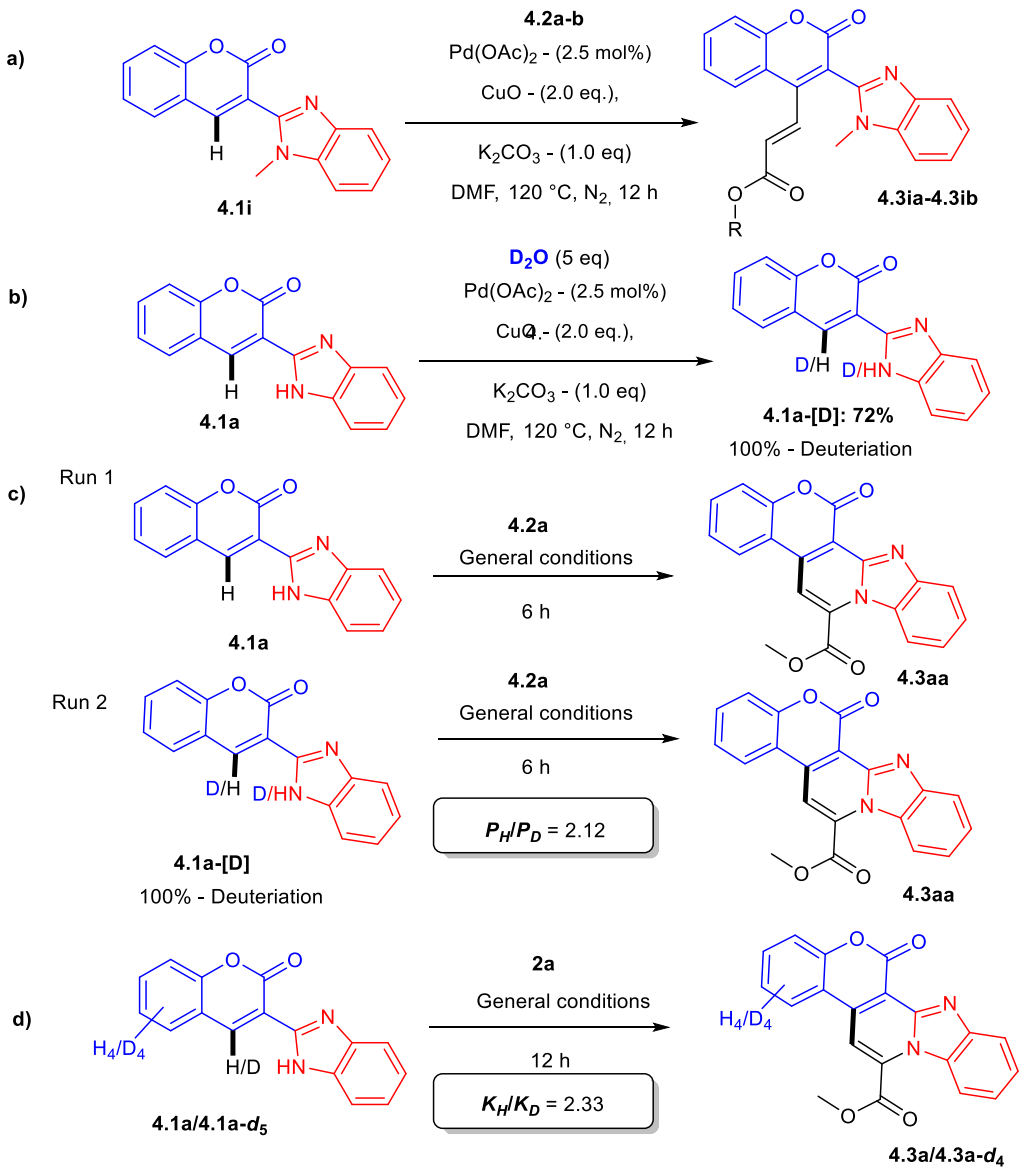

Scheme 4.6. Control experiments

In addition, to determine the kinetic isotopic effect (*KIE*), I have performed a parallel reaction experiment between **4.1a/4.1a-[D]** using the same conditions reacting with **4.2a** for 6 h and obtained a relevant *KIE* as P_H/P_D = 2.12, which showed C-H activation phase might be a rate-determining step (**Scheme 4.6c**).[114] To throw more light on the rate-determining step, I performed an intermolecular competition experiment in **Scheme 4.6d** using **4.1a** and **4.1a-D_4** under the same conditions, in an oven-dried 50 ml round bottom flask, a solution was made of **4.1a** (130 mg, 0.5 mmol, 0.5 eq), **4.1a-[D5]** (130 mg, 0.5 mmol, 0.5 eq), methyl acrylate **4.2a** (3 mmol, 3.0 eq) in DMF (2 ml) in an inert atmosphere of nitrogen followed by the addition of CuO (160 mg, 2.0 mmol, 2.0 eq), then loaded the catalyst $Pd(OAc)_2$ (2.5 mol%). The resulting reaction mixture was refluxed under nitrogen at 120 °C (using an oil bath) for 3 h.

NMR analysis was carried out on a crude sample. where *KIE* as K_H/K_D = **2.33** was obtained, which is relevant to **2.63** as P_H/P_D = **2.12.**

4.4. Proposed Mechanism

Based on control experiments and literature precedent,[115] I proposed a plausible catalytic cycle for [4+2] oxidative annulation as shown in **Scheme 4.7**. Initially, substrate **4.1a** reacts with $Pd(OAc)_2$ and gives intermediate **A,** followed by intramolecular C-H activation of resulting intermediate **A** and forms a five-membered palladacycle to give complex **B**. Subsequently; alkene insertion gives complex **C,** which readily converts into seven-membered cyclic palladium complex **D**, that undergoes reductive elimination and dehydrogenation annulated compound **4.3aa** was obtained.

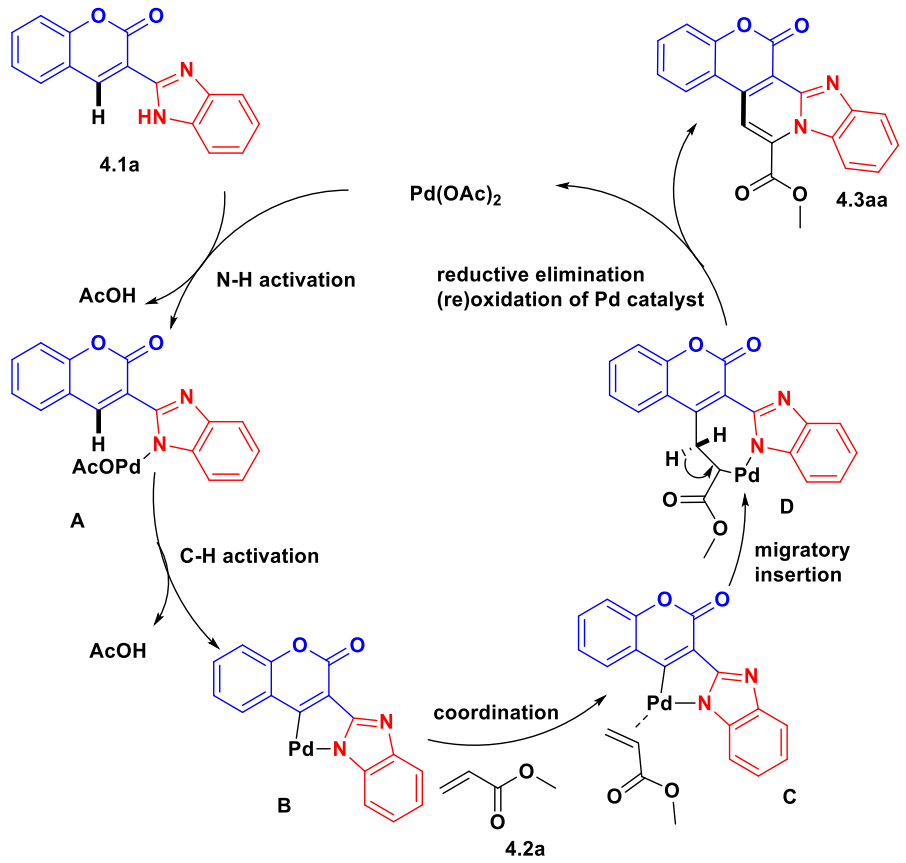

Scheme 4.7. Proposed mechanism

4.5. Photophysical Studies

With these versatile annulated molecules in hand, I then turned around to decipher the photophysical properties of **4.3aa-4.3hc** by recording their UV-vis and emission spectra in MeCN (20 μM). Absorption maxima on substitution have no significant effect and lie in the range of 315 nm to 340 nm. In contrast, emission maxima showed a broad range between 440 nm and 492 nm. Parent compound **4.3aa** showed an emission maximum at 460 nm with Stoke's shift 8500 cm^{-1}, having a quantum yield of 0.40, while substitution of different alkenes on **4.3aa** displayed a bathochromic shift in emission maxima from 450 nm to 470 nm for compounds **4.3aa-4.3af.**

Table 4.2. Photophysical properties of **4.3gb** in different solvents

solvent	$\lambda_{max, Abs}$ (nm)	$\lambda_{max, Em}$ (nm)	Stoke's Shift (cm^{-1})
Toluene	315	410	7400
Diethyl ether	325	415	6700
Ethyl acetate	340	480	8600
Acetonitrile	335	492	9600
Dimethylformamide	340	510	9800
Dimethylsulphoxide	340	515	10000
Methanol	345	550	10800

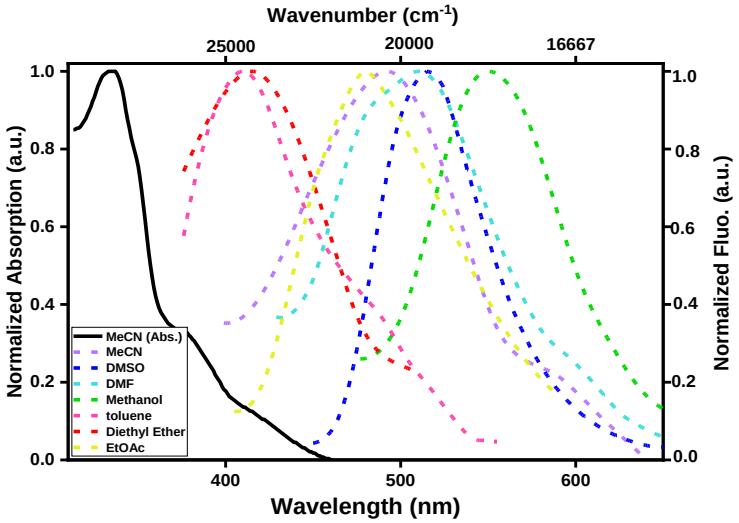

Figure 4.1. Absorption maxima (solid line) in acetonitrile and emission maxima (dashed lines) of **4.3gb** in different solvents

Compounds **4.3ba-4.3da** having substitution on the aryl ring of benzimidazole showed emission maxima in the range of 440 nm to 460 nm with low quantum yield. In contrast, photophysical properties are significantly related to π-conjugation and substitution on the peripheral coumarin ring. Compounds **4.3ea-4.3hc** offered an emission range from 440 nm to 492 nm. The electron-donating groups **(4.3ga-4.3gc)** and extended π-conjugation (**4.3ha-4.3hc**) showed better emission maxima range than bromo and chloro-substituted scaffolds. Compound **4.3gb** showed emission maxima at 492 nm with a higher quantum yield (0.70) than other derivatives. Relative quantum yields were determined with reference to hymecromone ($\Phi_F = 0.74$). Fascinated by bathochromic shift, I investigated the solvent effect of compound **4.3gb** by recording their emission maxima in different polar and non-polar solvents (**Table 4.2**). Interestingly, compound **4.3gb** showed positive emission solvatochromism in the range from 410 nm in toluene to 550 nm in methanol (**Figure 4.1).** Lippert plot of **4.3gb** gave a satisfactory linear correlation that indicated compounds have solvatochromism.

4.6. Conclusion

A protocol to access polycyclic aromatic hydrocarbons of imidazo[1,2-*a*]chromeno[3,4-*c*]pyridine by palladium-catalyzed oxidative annulation of 3-(1*H*-benzo[*d*]imidazol-2-yl)-2*H*-chromen-2-one with alkenes using benzimidazole as a directing group has been developed. This transformation involves C4-H, N-H functionalization, and cyclization of the coumarin-benzimidazole hybrids. Various electron donating and withdrawing groups have shown great compatibility towards developed reaction conditions and gave 22 annulated compounds in upto 80% yield. The efficacy of reaction was also examined on a gram scale. Further, several deuterium-labeled experiments shed more mechanistic insights, and based on these observations; I have proposed the mechanism. Owing to the unique significance of polycyclic aromatic hydrocarbons, their photophysical properties have been well elucidated with improved quantum yields. I have performed photophysical studies where various electron donor and acceptor combinations were developed. Selected compounds demonstrated positive solvatochromism. Hence, these molecules may have valuable properties in material sciences.

4.7. Experimental Section

General procedure A involved synthesizing 3-(1*H*-benzo[*d*]imidazol-2-yl)-2*H*-chromen-2-one. Initially, in an oven-dried 50 ml round bottom flask, salicylaldehyde (610 mg, 0.5 mL, 5 mmol, 1.0 eq) was taken in ethanol (5 mL), and the solution was stirred at room temperature for 15 min, followed by the addition of a catalytic amount of piperidine (10 mol%) followed by diethyl malonate (1.20 g, 1.1 mL, 7.5 mmol, 1.5 eq) and the resulting solution was stirred at 80 °C for 2 h (using oil bath). The reaction mixture was diluted using water and stirred further for 15 min; the white solid was separated and filtered off. The resulting crude was subjected to basic hydrolysis for 2 h followed by adding acidic water to adjust *p*H at 2. The solid was separated out and filtered off to yield 2-oxo-2*H*-chromene-3-carboxylic acid. Subsequently, the resulting acid was reacted with *ortho*-phenylenediamine in the presence of polyphosphoric acid (PPA) for 12 h at 100 °C (using an oil bath). After completion of the reaction, monitored by TLC, ice-cold water was poured in the reaction mixture, followed by the dropwise addition of ammonium hydroxide solution to neutralize the excess of PPA; a yellow solid was obtained which was filtered off and was purified using column chromatography (DCM: Hexane 80:20) to yield 3-(1*H*-benzo[*d*]imidazol-2-yl)-2*H*-chromen-2-one **(4.1)**.

Synthesis of **4.1a**

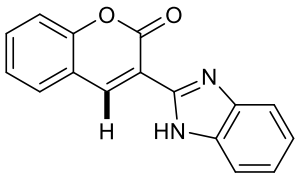

3-(1*H*-Benzo[*d*]imidazol-2-yl)-2*H*-chromen-2-one (**4.1a**). The compound **4.1a** was synthesized using general procedure A and obtained as a yellow solid, 80% (209 mg); R_f = 0.5 (80% DCM + Hexane); **mp** 294-296 °C. **^{1}H NMR** (400 MHz, $CDCl_3$) δ 8.42 (s, 1H), 7.77 (s, 1H), 7.55 (dd, *J* = 6.1, 4.0 Hz, 2H), 7.46 (dd, *J* = 7.8, 2.2 Hz, 1H), 7.26 – 7.21 (m, 2H), 7.14 (d, *J* = 1.8 Hz, 1H), 6.81 (d, *J* = 8.0 Hz, 1H), 6.63 – 6.58 (m, 1H).

Synthesis of **4.1b**

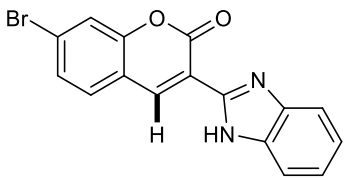

3-(1*H*-Benzo[*d*]imidazol-2-yl)-7-bromo-2*H*-chromen-2-one (**4.1b**). The compound **4.1b** was synthesized using general procedure A and obtained as yellow solid, 78% (264 mg); R_f =

0.5 (70% DCM + Hexane); **mp** 244-246 °C. **^{1}H NMR** (400 MHz, $CDCl_3$) δ 8.20 (s, 1H), 7.94 (s, 1H), 7.49 (d, *J* = 2.1 Hz, 1H), 7.42 (dd, *J* = 6.8, 2.1 Hz, 2H), 7.21 (d, *J* = 1.9 Hz, 1H), 7.19 (d, *J* = 2.1 Hz, 1H), 7.07 (d, *J* = 6.5 Hz, 1H), 7.03 – 7.01 (m, 1H).

Synthesis of **4.1c**

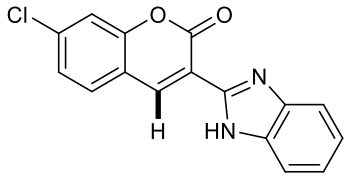

3-(1*H*-Benzo[*d*]imidazol-2-yl)-7-chloro-2*H*-chromen-2-one (**4.1c**). The compound **4.1c** was synthesized using general procedure A and obtained as yellow solid, 63% (186 mg); R_f = 0.5 (90% DCM + Hexane); **mp** 254-256 °C. **^{1}H NMR** (400 MHz, $CDCl_3$) δ 7.87 (s, 1H), 7.81 – 7.74 (m, 2H), 7.46 (d, *J* = 2.4 Hz, 1H), 7.43 – 7.40 (m, 2H), 7.20 (d, *J* = 8.1 Hz, 1H), 6.76 (t, *J* = 7.9 Hz, 1H), 6.66 (d, *J* = 8.2 Hz, 1H).

Synthesis of **4.1d**

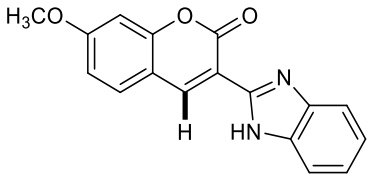

3-(1*H*-Benzo[*d*]imidazol-2-yl)-7-methoxy-2*H*-chromen-2-one (**4.1d**). The compound **4.1d** was synthesized using general procedure A and obtained as yellow solid, 70% (204 mg); R_f = 0.3 (80% DCM + Hexane); **mp** 194-196 °C. **^{1}H NMR** (400 MHz, DMSO-d_6) δ 7.88 (s, 1H), 7.78 (dd, *J* = 7.8, 1.4 Hz, 1H), 7.66 (s, 1H), 7.24 – 7.21 (m, 1H), 7.11 (t, *J* = 7.9 Hz, 1H), 6.98 (dt, *J* = 8.2, 3.3 Hz, 2H), 6.72 (t, *J* = 7.6 Hz, 1H), 6.67 (d, *J* = 8.0 Hz, 1H), 3.89 (s, 3H).

Synthesis of **4.1e**

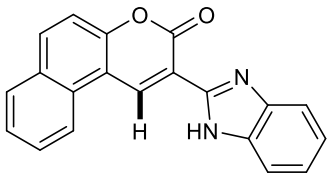

2-(1*H*-Benzo[*d*]imidazol-2-yl)-3*H*-benzo[*f*]chromen-3-one (**4.1e**). The compound **4.1e** was synthesized using general procedure A and obtained as yellow solid, 82% (255 mg); R_f = 0.6 (70% DCM + Hexane); **mp** 254-256 °C. **^{1}H NMR** (400 MHz, $CDCl_3$) δ 7.88 (s, 1H), 7.79 – 7.77 (m, 1H), 7.66 (s, 1H), 7.25 – 7.22 (m, 2H), 7.20 (d, *J* = 1.5 Hz, 1H), 7.10 (d, *J* = 7.8 Hz,

1H), 6.99 (dd, *J* = 6.8, 1.6 Hz, 2H), 6.72 (t, *J* = 7.6 Hz, 1H), 6.67 (d, *J* = 8.0 Hz, 1H), 6.04 (d, *J* =1.7 Hz, 1H).

Synthesis of **4.1f**

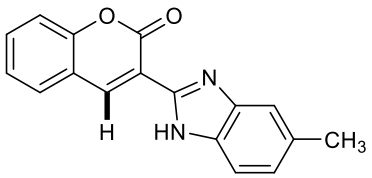

3-(5-Methyl-1*H*-benzo[*d*]imidazol-2-yl)-2*H*-chromen-2-one (**4.1f**). The compound **4.1f** was synthesized using general procedure A and obtained as yellow solid, 75% (207 mg); R_f = 0.5 (60% DCM + Hexane); **mp** 200-202 °C. **^{1}H NMR** (400 MHz, $CDCl_3$) δ 7.88 (s, 1H), 7.65 (s, 1H), 7.22 (t, *J* = 1.4 Hz, 1H), 7.20 (d, *J* = 1.5 Hz, 1H), 7.11 (s, 1H), 7.00 (d, *J* = 1.5 Hz, 2H), 6.98 – 6.97 (m, 1H), 6.67 (d, *J* = 8.0 Hz, 1H), 1.98 (s, 3H).

Synthesis of **4.1g**

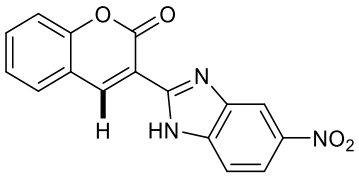

3-(5-Nitro-1*H*-benzo[*d*]imidazol-2-yl)-2*H*-chromen-2-one (**4.1g**). The compound **4.1g** was synthesized using general procedure A and obtained as yellow solid, 60% (184 mg); R_f = 0.4 (90% DCM + Hexane); **mp** 294-296 °C. **^{1}H NMR** (400 MHz, $CDCl_3$) δ 8.75 (s, 1H), 8.29 (d, *J* = 8.9 Hz, 1H), 8.20 (s, 1H), 7.97 (d, *J* = 8.4 Hz, 1H), 7.87 (d, *J* = 8.2 Hz, 1H), 7.75 (dd, *J* = 9.7, 1.6 Hz, 1H), 7.66 (dt, *J* = 8.7, 4.4 Hz, 1H), 7.56 (s, 1H), 7.39 (d, *J* = 9.1 Hz, 1H).

Synthesis of **4.1h**

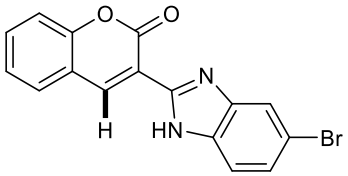

3-(5-Bromo-1*H*-benzo[*d*]imidazol-2-yl)-2*H*-chromen-2-one (**4.1h**). The compound **4.1h** was synthesized using general procedure A and obtained as yellow solid, 70% (239 mg); R_f = 0.5 (70% DCM + Hexane); **mp** 244-246 °C. **^{1}H NMR** (400 MHz, $CDCl_3$) δ 8.20 (s, 1H), 7.90 (s, 1H), 7.49 (s, 1H), 7.42 (dd, *J* = 9.7, 1.6 Hz, 1H), 7.21 (d, *J* = 2.0 Hz, 2H), 7.19 (d, *J* = 1.9 Hz, 1H), 7.07 (d, *J* = 6.2 Hz, 1H), 6.88 (t, *J* = 8.1 Hz, 1H).

General procedure B: Palladium-catalyzed oxidative annulation

In an oven-dried 50 mL round bottom flask, a solution was made with 3-(1*H*-benzo[*d*]imidazol-2-yl)-2*H*-chromen-2-one (1.0 mmol, 1.0 eq), acrylate (3 mmol, 3.0 eq) in 2 mL DMF in an inert atmosphere of nitrogen followed by the addition of CuO (2.0 mmol, 2.0 eq) as oxidant and K_2CO_3 (1.0 eq) as an additive, then loaded the catalytic system: $Pd(OAc)_2$ (2.5 mol%). The reaction mixture was refluxed under nitrogen at 120 °C (using an oil bath) for 12 h. The reaction was quenched with EtOAc (10 mL) and then passed through the celite pad, followed by the extraction with EtOAc (3 × 50 mL); the combined organic layers were washed with brine solution and dried over sodium sulfate and then concentrated under reduced pressure. To yield the desired compound, the crude product was purified using column chromatography (DCM: Hexane 60:40 to 100:00).

Synthesis of **4.3aa**

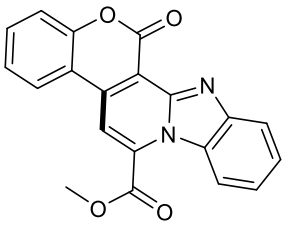

Methyl 1-oxo-1*H*-benzo[4,5]imidazo[1,2-*a*]chromeno[3,4-*c*]pyridine-8-carboxylate (**4.3aa**). The compound **4.3aa** was synthesized using general procedure B and obtained as yellow solid, 80% (275 mg); R_f = 0.5 (60% DCM + Hexane); **mp** 252-256 °C. **^{1}H NMR** (400 MHz, $CDCl_3$) δ 8.20 (d, *J* = 8.2 Hz, 1H), 8.04 (d, *J* = 8.0 Hz, 1H), 7.86 (d, *J* = 8.5 Hz, 1H), 7.84 (s, 1H), 7.60 (dt, *J* = 20.4, 7.7 Hz, 2H), 7.48 – 7.37 (m, 3H), 4.21 (s, 3H). **^{13}C{^{1}H} NMR** (101 MHz, $CDCl_3$) δ 162.1, 156.2, 153.2, 145.9, 145.0, 138.6, 135.4, 133.3, 128.3, 126.7, 125.0, 123.9, 123.3, 121.7, 118.1, 115.8, 114.3, 110.0, 107.3, 54.1. **HRMS** (ESI-TOF): m/z $[M+H]^+$ calcd for $C_{20}H_{13}N_2O_4$ 345.0831; found 345.0842.

Synthesis of **4.3ab**

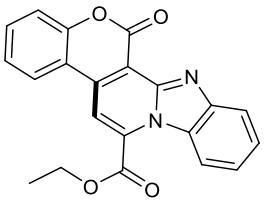

Ethyl 1-oxo-1*H*-benzo[4,5]imidazo[1,2-*a*]chromeno[3,4-*c*]pyridine-8-carboxylate (**4.3ab**). The compound **4.3ab** was synthesized using general procedure B and obtained as yellow

solid, 82% (290 mg); R_f = 0.5 (60% DCM + Hexane); **mp** 260-262 °C. **^{1}H NMR** (400 MHz, $CDCl_3$) δ 8.22 (d, *J* = 8.3 Hz, 1H), 8.06 (dd, *J* = 8.1, 1.5 Hz, 1H), 7.90 (d, *J* = 8.5 Hz, 1H), 7.82 (s, 1H), 7.66 – 7.57 (m, 2H), 7.47 (dd, *J* = 8.3, 1.2 Hz, 1H), 7.45 – 7.40 (m, 2H), 4.71 (q, *J* = 7.2 Hz, 2H), 1.58 (t, *J* = 7.2 Hz, 3H). **^{13}C{^{1}H} NMR** (101 MHz, $CDCl_3$) δ 161.6, 156.0, 153.1, 144.9, 138.6, 135.8, 133.1, 128.3, 126.6, 124.9, 123.6, 123.1, 121.6, 117.9, 115.7, 114.2, 106.7, 63.7, 14.2. **HRMS** (ESI-TOF): m/z $[M+H]^+$ calcd for $C_{21}H_{15}N_2O_4$ 359.0977; found 359.0985.

Synthesis of **4.3ac**

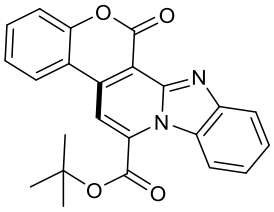

tert-Butyl 1-oxo-1*H*-benzo[4,5]imidazo[1,2-*a*]chromeno[3,4-*c*]pyridine-8-carboxylate (**4.3af**). The compound **4.3ac** was synthesized using general procedure B and obtained as light-yellow solid, 78% (300 mg); R_f = 0.7 (60% DCM + Hexane); **mp** 240-242 °C. **^{1}H NMR** (400 MHz, $CDCl_3$) δ 8.63 (d, *J* = 4.5 Hz, 1H), 7.95 (s, 1H), 7.55 – 7.47 (m, 2H), 7.28 (d, *J* = 7.5 Hz, 1H), 7.20 (dd, *J* = 4.6, 3.4 Hz, 2H), 6.89 (d, *J* = 7.3 Hz, 1H), 6.69 (d, *J* = 8.0 Hz, 1H), 1.48 (s, 9H). **^{13}C{^{1}H} NMR** (101 MHz, $CDCl_3$) δ 166.2, 165.0, 160.7, 153.3, 147.5, 143.8, 140.0, 138.1, 133.6, 132.2, 130.6, 128.8, 124.9, 122.1, 119.6, 118.6, 116.6, 116.3, 112.4, 80.3, 28.2. **HRMS** (ESI-TOF): m/z $[M+H]^+$ calcd for $C_{21}H_{19}N_2O_4$ 387.1300; found 387.1307.

Synthesis of **4.3ad**

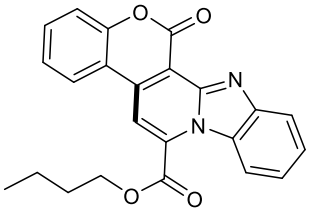

Butyl 1-oxo-1*H*-benzo[4,5]imidazo[1,2-*a*]chromeno[3,4-*c*]pyridine-8-carboxylate (**4.3ad**). The compound **4.3ad** was synthesized using general procedure B and obtained as light-yellow solid, 80% (300 mg); R_f = 0.5 (70% DCM + Hexane); **mp** 266-270 °C. **^{1}H NMR** (400 MHz, $CDCl_3$) δ 8.75 (d, *J* = 8.7 Hz, 1H), 8.00 (s, 1H), 7.54 – 7.48 (m, 2H), 7.28 (d, *J* = 8.8 Hz, 2H), 7.22 (d, *J* = 7.9 Hz, 1H), 6.90 (d, *J* = 7.4 Hz, 1H), 6.74 (d, *J* = 8.1 Hz, 1H), 4.12 (t, *J* = 6.8 Hz, 2H), 1.70 – 1.55 (m, 2H), 1.38 (dd, *J* = 9.4, 4.7 Hz, 2H), 0.92 (t, *J* = 7.4 Hz, 3H).

$^{13}C\{^{1}H\}$ NMR (101 MHz, $CDCl_3$) δ 166.9, 165.0, 160.6, 153.3, 147.5, 144.8, 139.9, 137.8, 133.6, 132.1, 130.6, 128.7, 124.8, 120.2, 119.5, 118.5, 116.7, 116.2, 64.3, 30.7, 19.1, 13.7. **HRMS** (ESI-TOF): m/z $[M+H]^+$ calcd for $C_{21}H_{19}N_2O_4$ 387.1300; found 387.1304.

Synthesis of **4.3ae**

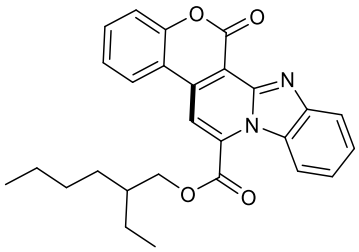

2-Ethylhexyl 1-oxo-1*H*-benzo[4,5]imidazo[1,2-*a*]chromeno[3,4-*c*]pyridine-8-carboxylate (**4.3ae**). The compound **4.3ae** was synthesized using general procedure B and obtained as yellow solid, 70% (309 mg); R_f = 0.4 (50% DCM + Hexane); **mp** 290-292 °C. **^{1}H NMR** (400 MHz, $CDCl_3$) δ 8.78 (d, *J* = 4.2 Hz, 1H), 8.00 (s, 1H), 7.53 – 7.51 (m, 1H), 7.48 (ddd, *J* = 8.9, 7.2, 1.8 Hz, 1H), 7.25 (t, *J* = 2.0 Hz, 2H), 7.22 (dd, *J* = 4.7, 2.9 Hz, 1H), 6.88 (s, 1H), 6.73 (d, *J* = 8.5 Hz, 1H), 4.03-3.99 (m, 2H), 1.40 – 1.28 (m, 2H), 1.27 (d, *J* = 2.4 Hz, 1H), 1.25 (d, *J* = 3.7 Hz, 6H), 0.84 (t, *J* = 7.1, 6H). **$^{13}C\{^{1}H\}$ NMR** (101 MHz, $CDCl_3$) δ 167.2, 165.4, 160.7, 153.4, 147.6, 145.0, 140.1, 137.8, 133.6, 132.1, 130.7, 128.8, 124.9, 120.1, 119.5, 118.6, 116.9, 116.3, 112.5, 69.7, 38.8, 30.4, 28.3, 27.3, 23.8, 23.0, 14.2, 11.0. **HRMS** (ESI-TOF): m/z $[M+H]^+$ calcd for $C_{27}H_{27}N_2O_4$ 443.1926; found 443.1934.

Synthesis of **4.3af**

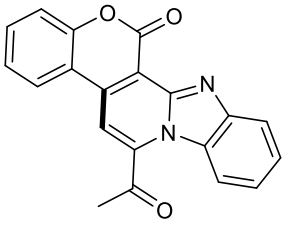

8-Acetyl-1*H*-benzo[4,5]imidazo[1,2-*a*]chromeno[3,4-*c*]pyridin-1-one (**4.3af**). The compound **4.3af** was synthesized using general procedure B and obtained as light-yellow solid, 75% (246 mg); R_f = 0.5 (60% DCM + Hexane); **mp** 230-232 °C. **^{1}H NMR** (400 MHz, $CDCl_3$) δ 8.65 (d, *J* = 6.6 Hz, 1H), 7.94 (s, 1H), 7.54 (d, *J* = 7.8 Hz,, 1H), 7.51 (d, *J* = 8.5 Hz,, 1H), 7.30 (d, *J* = 8.5 Hz,, 1H), 7.29 – 7.27 (m, 1H), 7.23 (d, *J* = 8.0 Hz, 1H), 6.92 (d, *J* = 7.6 Hz, 1H), 6.74 (d, *J* = 8.1 Hz, 1H), 2.37 (s, 3H). **$^{13}C\{^{1}H\}$ NMR** (101 MHz, $CDCl_3$) δ 199.5, 164.7, 160.6, 153.4, 147.5, 144.4, 139.7, 138.0, 133.9, 132.4, 130.5, 129.7, 128.7, 125.0, 119.6,

118.5, 117.1, 116.5, 26.9. **HRMS** (ESI-TOF): m/z $[M+H]^+$ calcd for $C_{20}H_{13}N_2O_3$ 329.0881; found 329.0875.

Synthesis of **4.3ba**

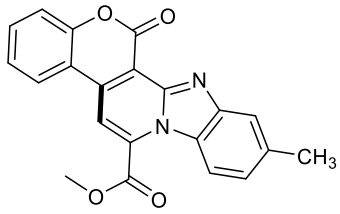

Methyl-12-methyl-1-oxo-1*H*-benzo[4,5]imidazo[1,2-*a*]chromeno[3,4-*c*]pyridine-8-carboxylate (**4.3ba**). The compound **4.3ba** was synthesized using general procedure B and obtained as light-yellow solid, 84% (300 mg); R_f = 0.5 (70% DCM + Hexane); **mp** 252-254 °C. **^{1}H NMR** (400 MHz, $CDCl_3$) δ 7.96 (s, 1H), 7.92 (d, *J* = 3.6 Hz, 1H), 7.23 (dd, *J* = 12.9, 5.0 Hz, 1H), 7.18 (d, *J* = 3.3 Hz, 1H), 7.08 – 7.06 (m, 1H), 7.05 (d, *J* = 6.6 Hz, 1H), 6.90 (d, *J* = 7.4 Hz, 1H), 6.75 (d, *J* = 7.6 Hz, 1H), 3.94 (s, 3H), 2.01 (s, 3H). **^{13}C{^{1}H} NMR** (101 MHz, $CDCl_3$) δ 167.2, 164.9, 160.1, 147.5, 146.9, 145.1, 142.9, 139.9, 137.7, 134.4, 133.6, 130.8, 124.7, 119.6, 119.2, 119.1, 116.8, 113.8, 56.2, 51.6. **HRMS** (ESI-TOF): m/z $[M+H]^+$ calcd for $C_{21}H_{15}N_2O_4$ 359.0987; found 359.0995.

Synthesis of **4.3ca**

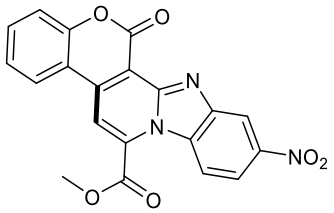

Methyl-12-nitro-1-oxo-1*H*-benzo[4,5]imidazo[1,2-*a*]chromeno[3,4-*c*]pyridine-8-carboxylate (**4.3ca**). The compound **4.3ca** was synthesized using general procedure B and obtained as light-yellow solid, 60% (233 mg); R_f = 0.5 (80% DCM + Hexane); **mp** 282-286 °C. **^{1}H NMR** (400 MHz, DMSO-d_6) δ 8.67 (s, 1H), 8.62 (d, *J* = 8.7 Hz, 1H), 8.18 (d, *J* = 11.9 Hz, 1H), 8.04 (d, *J* = 8.3 Hz, 1H), 7.81 (t, *J* = 7.7 Hz, 1H), 7.55 (dd, *J* = 10.8, 6.5 Hz, 2H), 7.29 (t, *J* = 8.0 Hz, 1H), 3.68 (s, 3H). **^{13}C{^{1}H} NMR** (101 MHz, DMSO-d_6) δ 166.5, 163.1, 158.7, 152.6, 147.5, 145.2, 136.0, 134.2, 132.9, 129.7, 129.0, 128.5, 126.1, 120.8, 118.2, 117.7, 116.7, 116.4, 112.0, 51.2. **HRMS** (ESI-TOF): m/z $[M+H]^+$ calcd for $C_{20}H_{12}N_3O_6$ 390.0681; found 390.0692.

Synthesis of **4.3da**

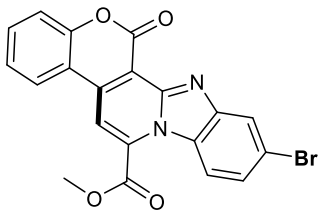

Methyl-12-bromo-1-oxo-1*H*-benzo[4,5]imidazo[1,2-*a*]chromeno[3,4-*c*]pyridine-8-carboxylate (**4.3da**). The compound **4.3da** was synthesized using general procedure B and obtained as light-yellow solid, 75% (315 mg); R_f = 0.6 (50% DCM + Hexane); **mp** 295-297 °C. **^{1}H NMR** (400 MHz, DMSO-d_6) δ 8.68 (d, *J* = 9.2 Hz, 1H), 8.15 (d, *J* = 2.4 Hz, 1H), 7.93 (s, 1H), 7.74 – 7.72 (m, 1H), 7.33 (d, *J* = 3.1 Hz, 1H), 7.24 (t, *J* = 7.9 Hz, 1H), 6.96 – 6.93 (m, 2H), 3.72 (s, 3H). **^{13}C{^{1}H} NMR** (101 MHz, DMSO-d_6) δ 166.6, 162.8, 158.4, 151.7, 147.1, 145.4, 137.6, 135.9, 134.2, 132.7, 131.3, 120.0, 118.1, 117.6, 116.7, 116.2, 112.0, 51.2. **HRMS** (ESI-TOF): m/z $[M+H]^+$ calcd for $C_{20}H_{12}N_2O_4{}^{79}Br$ 421.9902; found 421.9912 calcd for $C_{20}H_{12}N_2O_4{}^{81}Br$ 423.9882; found 423.9890.

Synthesis of **4.3ea**

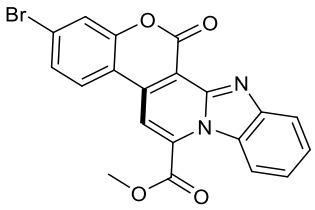

Methyl-4-bromo-1-oxo-1*H*-benzo[4,5]imidazo[1,2-*a*]chromeno[3,4-*c*]pyridine-8-carboxylate (**4.3ea**). The compound **4.3ea** was synthesized using general procedure B and obtained as light-yellow solid, 70% (295 mg); R_f = 0.6 (80% DCM + Hexane); **mp** 282-286 °C. **^{1}H NMR** (400 MHz, DMSO-d_6) δ 8.61 (d, *J* = 1.7 Hz, 1H), 8.15 (d, *J* = 2.4 Hz, 1H), 7.93 (s, 1H), 7.74 – 7.71 (m, 1H), 7.33 (d, *J* = 3.1 Hz, 1H), 7.24 (t, *J* = 7.9 Hz, 1H), 6.95 (d, *J* = 3.1 Hz, 1H), 6.94 (d, *J* = 2.4 Hz, 1H), 3.70 (s, 3H). **^{13}C{^{1}H} NMR** (101 MHz, DMSO-d_6) δ 162.7, 159.0, 154.5, 147.9, 143.2, 141.6, 133.7, 132.0, 130.4, 128.9, 127.8, 127.0, 116.1, 113.9, 113.6, 113.3, 112.9, 112.3, 108.2, 64.5. **HRMS** (ESI-TOF): m/z $[M+H]^+$ calcd for $C_{20}H_{12}N_2O_4{}^{79}Br$ 421.9902; found 421.9896 calcd for $C_{20}H_{12}N_2O_4{}^{81}Br$ 423.9882; found 423.9875.

Synthesis of **4.3eb**

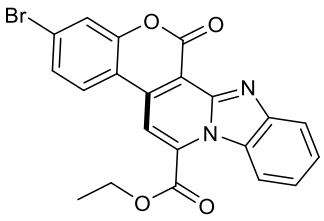

Ethyl-4-bromo-1-oxo-1*H*-benzo[4,5]imidazo[1,2-*a*]chromeno[3,4-*c*]pyridine-8-carboxylate (**4.3eb)**. The compound **4.3eb** was synthesized using general procedure B and obtained as light-yellow solid, 77% (316 mg); R_f = 0.5 (70% DCM + Hexane); **mp** 278-280 °C. **^{1}H NMR** (400 MHz, $CDCl_3$) δ 8.78 (d, *J* = 8.1 Hz, 1H), 8.34 (s, 1H), 7.65 (s, 1H), 7.55 (d, *J* = 8.7 Hz, 1H), 7.23 (t, *J* = 8.0 Hz, 2H), 7.15 (dd, *J* = 8.6 Hz, 1H), 6.91 (d, *J* = 8.1 Hz, 1H), 4.22-4.18 (q, 2H), 1.26 (t, *J* = 7.1 Hz, 3H). **^{13}C{^{1}H} NMR** (101 MHz, $CDCl_3$) δ 166.8, 165.1, 159.9, 152.1, 147.3, 144.8, 138.7, 134.8, 133.7, 131.8, 130.9, 120.2, 119.6, 117.9, 116.7, 60.4, 14.3. **HRMS** (ESI-TOF): m/z $[M+H]^+$ calcd for $C_{21}H_{14}N_2O_4{}^{79}Br$ 436.0059; found 436.0054 calcd for $C_{21}H_{14}N_2O_4{}^{81}Br$ 438.0038; found 438.0048.

Synthesis of **4.3ec**

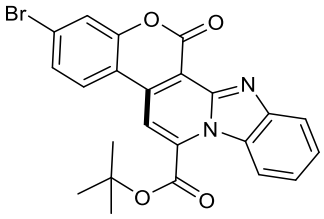

tert-Butyl 4-bromo-1-oxo-1*H*-benzo[4,5]imidazo[1,2-*a*]chromeno[3,4-*c*]pyridine-8-carboxylate (**4.3ec**). The compound **4.3ec** was synthesized using general procedure B and obtained as light-yellow solid, 71% (320 mg); R_f = 0.3 (60% DCM + Hexane); **mp** 296-298 °C. **^{1}H NMR** (400 MHz, $CDCl_3$) δ 8.61 (d, *J* = 16.0 Hz, 1H), 7.90 (s, 1H), 7.61 (d, *J* = 2.4 Hz, 1H), 7.55 – 7.52 (m, 1H), 7.20 (t, *J* = 7.9 Hz, 1H), 7.13 (d, *J* = 8.9 Hz, 1H), 6.88 (d, *J* = 7.6 Hz, 1H), 6.73 – 6.69 (m, 1H), 1.45 (s, 9H). **^{13}C{^{1}H} NMR** (101 MHz, $CDCl_3$) δ 166.2, 165.3, 160.1, 152.2, 147.4, 143.7, 138.8, 138.1, 134.8, 133.7, 131.9, 131.0, 122.2, 120.1, 119.7, 118.0, 117.5, 116.6, 112.3, 80.4, 28.2. **HRMS** (ESI-TOF): m/z $[M+H]^+$ calcd for $C_{23}H_{18}N_2O_4{}^{79}Br$ 464.0372; found 464.0383 calcd for $C_{23}H_{18}N_2O_4{}^{81}Br$ 466.0351; found 466.0359.

Synthesis of **4.3fa**

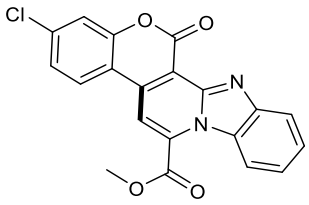

Methyl 4-chloro-1-oxo-1*H*-benzo[4,5]imidazo[1,2-*a*]chromeno[3,4-*c*]pyridine-8-carboxylate (**4.3fa**). The compound **4.3fa** was synthesized using general procedure B and obtained as light-yellow solid, 64% (240 mg); R_f = 0.5 (50% DCM + Hexane); **mp** 268-272 °C. **^{1}H NMR** (400 MHz, $CDCl_3$) δ 8.66 (d, *J* = 5.6 Hz, 1H), 7.93 (s, 1H), 7.23 (t, *J* = 8.0 Hz, 1H), 7.19 (t, *J* = 8.0 Hz, 1H), 7.09 (dd, *J* = 7.9, 1.5 Hz, 1H), 7.06 – 7.04 (m, 1H), 6.92 (d, *J* = 7.2 Hz, 1H), 6.75 (dd, *J* = 7.9, 1.5 Hz, 1H), 3.93 (s, 3H). **^{13}C{^{1}H} NMR** (101 MHz, $CDCl_3$) δ 164.9, 160.0, 147.5, 146.9, 144.3, 143.0, 139.8, 137.9, 133.7, 130.8, 129.6, 124.8, 119.9, 119.5, 119.2, 117.1, 113.8, 56.3. **HRMS** (ESI-TOF): m/z $[M+H]^+$ calcd for $C_{20}H_{12}N_2O_4Cl$ 380.0378; found 380.0385.

Synthesis of **4.3fb**

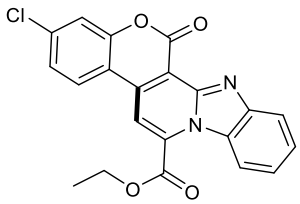

Ethyl 4-chloro-1-oxo-1*H*-benzo[4,5]imidazo[1,2-*a*]chromeno[3,4-*c*]pyridine-8-carboxylate (**4.3fb**). The compound **4.3fb** was synthesized using general procedure B and obtained as light-yellow solid, 62% (240 mg); R_f = 0.4 (60% DCM + Hexane); **mp** 272-274 °C. **^{1}H NMR** (400 MHz, $CDCl_3$) δ 8.77 (d, *J* = 7.9 Hz, 1H), 7.90 (s, 1H), 7.52 (d, *J* = 2.2 Hz, 1H), 7.43 (d, *J* = 6.5 Hz, 1H), 7.21 (dd, *J* = 8.5, 1.8 Hz, 2H), 6.90 (d, *J* = 7.3 Hz, 1H), 6.72 (d, *J* = 7.4 Hz, 1H), 4.22-4.17 (q, 2H), 1.28 (t, *J* = 7.1 Hz, 3H). **^{13}C{^{1}H} NMR** (101 MHz, $CDCl_3$) δ 166.9, 160.1, 151.7, 147.3, 144.8, 138.8, 137.9, 133.8, 132.1, 131.8, 130.3, 127.9, 120.3, 119.6, 117.8, 116.8, 60.5, 14.4. **HRMS** (ESI-TOF): m/z $[M+H]^+$ calcd for $C_{21}H_{14}N_2O_4Cl$ 394.0534; found 394.0545.

Synthesis of **4.3fc**

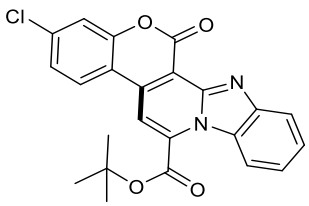

tert-Butyl 4-chloro-1-oxo-1*H*-benzo[4,5]imidazo[1,2-*a*]chromeno[3,4-*c*]pyridine-8-carboxylate (**4.3fc**). The compound **4.3fc** was synthesized using general procedure B and obtained as light-yellow solid, 60% (252 mg); R_f = 0.7 (90% DCM + Hexane); **mp** 292-296 °C. **^{1}H NMR** (400 MHz, $CDCl_3$) δ 8.64 (d, *J* = 8.2 Hz, 1H), 7.90 (s, 1H), 7.51 (d, *J* = 2.3 Hz, 1H), 7.43 (dd, *J* = 8.8, 2.4 Hz, 1H), 7.20 (dd, *J* = 8.3, 6.6 Hz, 2H), 6.90 (d, *J* = 13.0 Hz, 1H), 6.70 (dd, *J* = 8.0, 1.0 Hz, 1H), 1.46 (s, 9H). **^{13}C{^{1}H} NMR** (101 MHz, $CDCl_3$) δ 166.2, 164.9, 160.1, 151.7, 147.3, 143.7, 138.8, 138.1, 133.7, 132.1, 131.9, 130.2, 128.0, 122.2, 119.7, 117.7, 116.6, 80.5, 28.2. **HRMS** (ESI-TOF): m/z $[M+H]^+$ calcd for $C_{23}H_{18}N_2O_4Cl$ 422.0848; found 422.0859.

Synthesis of **4.3ga**

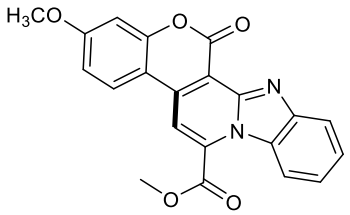

Methyl 4-methoxy-1-oxo-1*H*-benzo[4,5]imidazo[1,2-*a*]chromeno[3,4-*c*]pyridine-8-carboxylate (**4.3ga**). The compound **4.3ga** was synthesized using general procedure B and obtained as light-yellow solid, 80% (300 mg); R_f = 0.5 (60% DCM + Hexane); **mp** 252-254 °C. **^{1}H NMR** (400 MHz, $CDCl_3$) δ 7.96 (s, 1H), 7.92 (d, *J* = 3.6 Hz, 1H), 7.23 (t, *J* = 7.9 Hz, 1H), 7.19 – 7.16 (m, 1H), 7.08 (dd, *J* = 4.5, 3.1 Hz, 1H, 1H), 7.05 (dd, *J* = 4.9, 3.4 Hz, 1H), 6.90 (d, *J* = 7.4 Hz, 1H), 6.75 (d, *J* = 7.6 Hz, 1H), 3.94 (s, 3H), 3.75 (s, 3H). **^{13}C{^{1}H} NMR** (101 MHz, $CDCl_3$) δ 167.2, 164.9, 160.1, 147.5, 146.9, 145.1, 142.9, 140.0, 137.6, 134.4, 133.6, 130.8, 124.7, 119.9, 119.5, 119.4, 119.3, 116.9, 113.8, 56.2, 51.6. **HRMS** (ESI-TOF): m/z $[M+H]^+$ calcd for $C_{21}H_{15}N_2O_5$ 375.0936; found 375.0947.

Synthesis of **4.3gb**

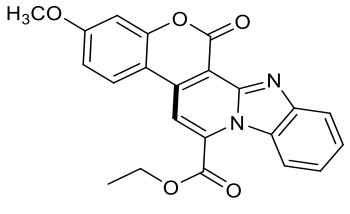

Ethyl 4-methoxy-1-oxo-1*H*-benzo[4,5]imidazo[1,2-*a*]chromeno[3,4-*c*]pyridine-8-carboxylate (**4.3gb**). The compound **4.3gb** was synthesized using general procedure B and obtained as light-yellow solid, 86% (330 mg); R_f = 0.5 (60% DCM + Hexane); **mp** 262-266 °C. **^{1}H NMR** (400 MHz, DMSO-d_6) δ 8.65 (d, *J* = 8.2 Hz, 1H), 7.86 (s, 1H), 7.34 (d, *J* = 1.7 Hz, 1H), 7.27

– 7.23 (m, 1H), 7.21 (dd, *J* = 6.7, 4.3 Hz, 2H), 6.97 (d, *J* = 8.5, 1H), 6.93 (d, *J* = 4.1 Hz, 1H), 4.17-4.15 (q, 2H), 3.86 (s, 3H), 1.23 (t, *J* = 7.1 Hz, 3H). **^{13}C{^{1}H} NMR** (101 MHz, DMSO-d_6) δ 166.1, 163.0, 158.5, 147.3, 146.1, 145.1, 142.2, 138.9, 136.0, 132.8, 130.7, 124.6, 119.7, 118.5, 117.6, 116.6, 114.1, 112.0, 59.7, 56.0, 14.1. **HRMS** (ESI-TOF): m/z $[M+H]^+$ calcd for $C_{22}H_{17}N_2O_5$ 389.1093; found 389.1098.

Synthesis of **4.3gc**

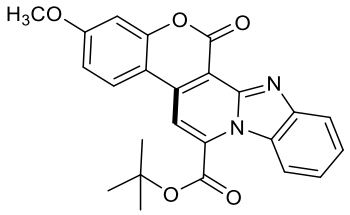

tert-Butyl-methoxy-1-oxo-1*H*-benzo[4,5]imidazo[1,2-*a*]chromeno[3,4-*c*]pyridine-8-carboxylate (**4.3gc**). The compound **4.3gc** was synthesized using general procedure B and obtained as light-yellow solid, 75% (310 mg); R_f = 0.5 (70% DCM + Hexane); **mp** 278-280 °C. **^{1}H NMR** (400 MHz, DMSO-d_6) δ 8.57 (d, *J* = 1.2 Hz, 1H), 7.85 (s, 1H), 7.32 (d, *J* = 1.4 Hz, 1H), 7.27 (dd, *J* = 7.2, 2.2 Hz, 1H), 7.24 (d, *J* = 4.0 Hz, 1H), 7.21 (d, *J* = 8.1 Hz, 1H), 6.95 (d, *J* = 8.1 Hz, 1H), 6.92 (d, *J* = 7.6 Hz, 1H), 3.87 (s, 3H), 1.46 (s, 9H). **^{13}C{^{1}H} NMR** (101 MHz, DMSO-d_6) δ 171.0, 168.5, 164.1, 152.8, 151.6, 149.7, 147.5, 144.4, 141.5, 138.2, 136.2, 130.1, 125.7, 125.4, 124.1, 123.0, 122.0, 119.7, 117.4, 85.1, 61.5, 33.2. **HRMS** (ESI-TOF): m/z $[M+H]^+$ calcd for $C_{24}H_{21}N_2O_5$ 417.1406; found 417.1412.

Synthesis of **4.3ha**

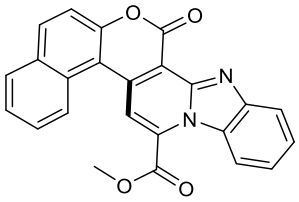

Methyl 1-oxo-1*H*-benzo[4,5]imidazo[1,2-*a*]benzo[5,6]chromeno[3,4-*c*]pyridine-10-carboxylate (**4.3ha**). The compound **4.3ha** was synthesized using general procedure B and obtained as light-yellow solid, 70% (275 mg); R_f = 0.5 (80% DCM + Hexane); **mp** 298-300 °C. **^{1}H NMR** (400 MHz, DMSO-d_6) δ 8.67 (s, 1H), 8.62 (d, *J* = 8.7 Hz, 1H), 8.20 (d, *J* = 8.5 Hz, 1H), 8.04 (d, *J* = 8.3 Hz, 1H), 7.84 – 7.78 (m, 1H), 7.63 (dd, *J* = 13.1, 5.7 Hz, 1H), 7.57 – 7.52 (m, 2H), 7.29 (t, *J* = 8.0 Hz, 1H), 7.10 (d, *J* = 8.1 Hz, 1H), 6.92 (d, *J* = 7.6 Hz, 1H), 3.68 (s, 3H). **^{13}C{^{1}H} NMR** (101 MHz, DMSO-d_6) δ 166.5, 163.1, 158.7, 152.6, 147.5, 145.2, 136.0, 134.2, 133.1, 132.7, 132.4, 129.7, 129.0, 128.5, 126.1, 120.8, 118.2, 117.7, 116.7,

116.4, 111.9, 111.5, 111.3, 51.2. **HRMS** (ESI-TOF): m/z $[M+H]^+$ calcd for $C_{24}H_{15}N_2O_4$ 395.0987; found 395.0999.

Synthesis of **4.3hb**

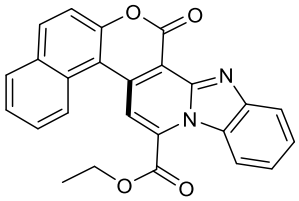

Ethyl 1-oxo-1*H*-benzo[4,5]imidazo[1,2-*a*]benzo[5,6]chromeno[3,4-*c*]pyridine-10-carboxylate (**4.3hb**). The compound **4.3hb** was synthesized using general procedure B and obtained as light-yellow solid, 68% (296 mg); R_f = 0.6 (70% DCM + Hexane); **mp** 302-304 °C. **^{1}H NMR** (400 MHz, DMSO-d_6) δ 8.68 (s, 1H), 8.61 (d, *J* = 6.7 Hz, 1H), 8.20 (d, *J* = 8.5 Hz, 1H), 8.16 (d, *J* = 9.0 Hz, 1H), 8.05 (d, *J* = 8.1 Hz, 1H), 7.83 – 7.79 (m, 1H), 7.65 – 7.62 (m, 1H), 7.56 (d, *J* = 4.7 Hz, 1H), 7.31 – 7.27 (m, 1H), 7.09 (d, *J* = 8.3 Hz, 1H), 6.92 (d, *J* = 7.6 Hz, 1H), 4.16-4.13 (q, 2H), 1.21 (t, *J* = 7.2 Hz, 3H). **^{13}C{^{1}H} NMR** (101 MHz, DMSO-d_6) δ 166.0, 163.1, 158.7, 152.6, 147.5, 145.0, 136.1, 134.2, 133.1, 132.7, 129.8, 129.1, 128.5, 128.4, 126.1, 120.8, 118.5, 117.7, 116.6, 116.2, 112.0, 111.7, 59.7, 14.0. **HRMS** (ESI-TOF): m/z $[M+H]^+$ calcd for $C_{25}H_{17}N_2O_4$ 409.1144; found 409.1152.

Synthesis of **4.3hc**

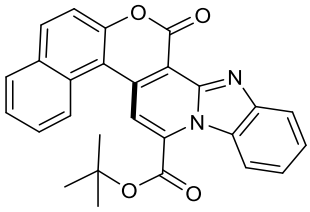

tert-Butyl 1-oxo-1*H*-benzo[4,5]imidazo[1,2-*a*]benzo[5,6]chromeno[3,4-*c*]pyridine-10-carboxylate (**4.3hc**). The compound **4.3hc** was synthesized using general procedure B and obtained as light-yellow solid, 68% (296 mg); R_f = 0.6 (70% DCM + Hexane); **mp** 286-288 °C. **^{1}H NMR** (400 MHz, DMSO-d_6) δ 8.65 (s, 1H), 8.60 (d, *J* = 2.1 Hz, 1H), 8.16 (dd, *J* = 8.5, 3.3 Hz, 1H), 8.09 (d, *J* = 9.0 Hz, 1H), 7.98 (d, *J* = 8.1 Hz, 1H), 7.77 (dd, *J* = 8.3, 6.3 Hz, 1H), 7.61 – 7.57 (m, 1H), 7.50 – 7.48 (m, 1H), 7.28 (dd, *J* = 8.0, 3.0 Hz, 1H), 7.08 (d, *J* = 8.3 Hz, 1H), 6.91 (d, *J* = 7.6 Hz, 1H), 1.43 (s, 9H). **^{13}C{^{1}H} NMR** (101 MHz, DMSO-d_6) δ 165.4, 163.1, 158.7, 152.5, 147.5, 144.1, 136.2, 134.2, 133.2, 133.0, 129.7, 128.7, 126.0, 120.7, 120.2, 117.0, 116.4, 116.3, 111.8, 79.5, 27.7. **HRMS** (ESI-TOF): m/z $[M+H]^+$ calcd for $C_{27}H_{21}N_2O_4$ 437.1457; found 437.1465.

General procedure C: Synthesis of 3-(1-methyl-1*H*-benzo[*d*]imidazol-2-yl)-2*H*-chromen-2-one[3]

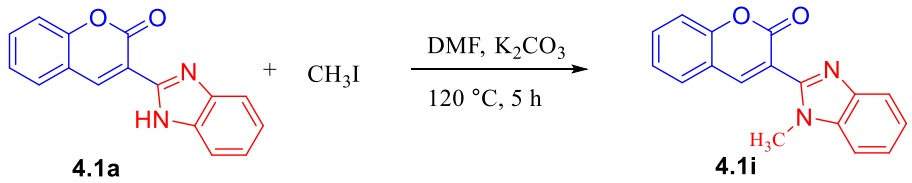

General procedure C, Initially, in an oven-dried 50 ml round bottom flask, 3-(1*H*-benzo[*d*]imidazol-2-yl)-2*H*-chromen-2-one **4.1a** (262 mg, 1 mmol, 1.0 eq) and CH_3I (141 mg, 1 mmol, 1.0 eq) were taken in DMF (5 mL) followed by addition of K_2CO_3 (134 mg, 1 mmol, 1.0 eq.) and the resulting solution was refluxed at 120 °C for 5 h (using oil bath). The reaction mixture was diluted using water and stirred further for 15 min; the white solid was separated which was filtered off and was purified using column chromatography (DCM: Hexane 80:20) to yield 3-(1-methyl-1*H*-benzo[*d*]imidazol-2-yl)-2*H*-chromen-2-one **(4.1i)**, **mp** 298-300 °C. **^{1}H NMR** (400 MHz, $CDCl_3$) δ 7.96 (s, 1H), 7.92 (d, *J* = 3.6 Hz, 1H), 7.22 (d, *J* = 7.9 Hz, 1H), 7.18 – 7.16 (m, 1H), 7.09 – 7.07 (m, 1H), 7.04 (dt, *J* = 9.7, 2.4 Hz, 2H), 6.90 (d, *J* = 7.4 Hz, 1H), 6.75 (d, *J* = 7.6 Hz, 1H), 3.75 (s, 3H). **^{13}C{^{1}H} NMR** (101 MHz, $CDCl_3$) δ 167.2, 164.8, 160.0, 147.5, 146.8, 145.1, 142.9, 140.0, 137.6, 134.4, 133.6, 130.8, 124.7, 119.8, 119.5, 116.9, 113.7, 27.2. **HRMS** (ESI-TOF): m/z $[M+H]^+$ calcd for $C_{17}H_{13}N_2O_2$ 277.0942; found 277.0949.

Synthesis of **4.3ia**

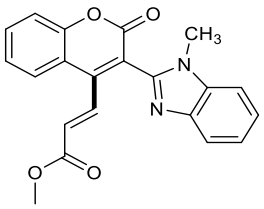

Methyl (*E*)-3-(3-(1-methyl-1*H*-benzo[*d*]imidazol-2-yl)-2-oxo-2*H*-chromen-4-yl)acrylate (**4.3ia**). The compound **4.3ia** was synthesized using general procedure B and obtained as light-yellow solid, 60% (224 mg); R_f = 0.6 (70% DCM + Hexane); **mp** 276-278 °C. **^{1}H NMR** (400 MHz, $CDCl_3$) δ 8.75 (d, *J* = 15.9 Hz, 1H), 7.92 (d, *J* = 3.6 Hz, 1H), 7.23 (t, *J* = 7.9 Hz, 1H), 7.18 (s, 1H), 7.08 (d, *J* = 1.5 Hz, 1H), 7.07 – 7.04 (m, 2H), 6.90 (d, *J* = 7.4 Hz, 1H), 6.76 (s, 1H), 6.19 (d, *J* = 15.2 Hz, 1H), 3.94 (s, 3H), 3.75 (s, 3H). **^{13}C{^{1}H} NMR** (101 MHz, $CDCl_3$) δ 167.2, 164.8, 160.1, 147.5, 146.8, 145.1, 142.9, 140.0, 137.6, 133.6, 130.8, 124.7, 119.8, 119.4, 119.2, 116.9, 113.7, 51.6, 27.2. **HRMS** (ESI-TOF): m/z $[M+H]^+$ calcd for $C_{21}H_{17}N_2O_4$ 361.1144; found 361.1154.

Synthesis of **4.3ib**

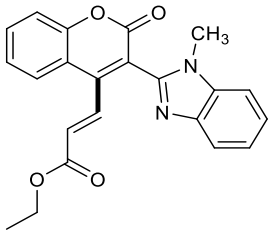

Ethyl (*E*)-3-(3-(1-methyl-1*H*-benzo[*d*]imidazol-2-yl)-2-oxo-2*H*-chromen-4-yl)acrylate (**4.3ib**). The compound **4.3ib** was synthesized using general procedure B and obtained as light-yellow solid, 55% (204 mg); R_f = 0.8 (70% DCM + Hexane); **mp** 288-290 °C. **^{1}H NMR** (400 MHz, DMSO-d_6) δ 8.68 (d, *J* = 15.9 Hz, 1H), 8.59 (d, *J* = 1.9 Hz, 1H), 7.34 (d, *J* = 2.2 Hz, 1H), 7.26 (d, *J* = 4.5 Hz, 1H), 7.23 (d, *J* = 7.6 Hz, 1H), 7.22 – 7.20 (m, 2H), 6.97 (d, *J* = 8.1 Hz, 1H), 6.94 (d, *J* = 7.6 Hz, 1H), 6.24 (d, *J* = 15.9 Hz, 1H), 4.18-4.15 (q, 2H), 3.86 (s, 3H), 1.24 (t, *J* = 6.2 Hz, 3H). **^{13}C{^{1}H} NMR** (101 MHz, DMSO-d_6) δ 166.1, 163.0, 158.5, 147.2, 146.1, 145.1, 142.0, 138.9, 135.9, 132.7, 130.7, 124.5, 119.7, 118.5, 117.1, 114.1, 112.0, 59.7, 26.1, 14.1. **HRMS** (ESI-TOF): m/z $[M+H]^+$ calcd for $C_{22}H_{19}N_2O_4$ 375.1300; found 375.1307

CHAPTER 5

In-vitro Evaluation of C-H Functionalized Compounds

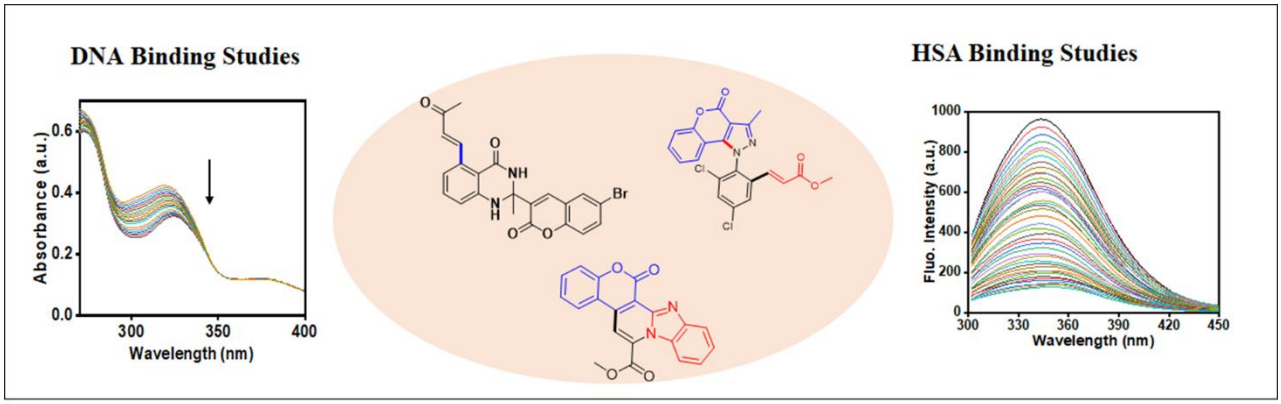

CHAPTER 5

5.1. Introduction

Chemotherapy[116] is the most effective way to cure metastatic cancer. Subsequently, the discovery of high-potential and low-toxicity anticancer drugs has claimed significant attention from organic and medicinal chemists.[117-120] In this context, various heterocyclic moieties, such as coumarin, quinazolinone, benzimidazole, pyrazole, etc., have been recognized as potent nuclei for anticancer activity. The efficacy of conventional prescribed antineoplastic drugs is often limited due to their high toxicity,[121-124] difficulty in delivering existing drugs to target sites, and development of drug resistance. Therefore, developing new anticancer drugs is of utmost importance to improve drug perfusion, oral bioavailability, and their antitumor potential.[125-130]

Several subsets of structurally related compounds have been prepared as in previous chapters and further evaluated extensively for their cytotoxic effect. The potency of chemotherapeutic agents has been improved by synthesizing the compounds through systematic

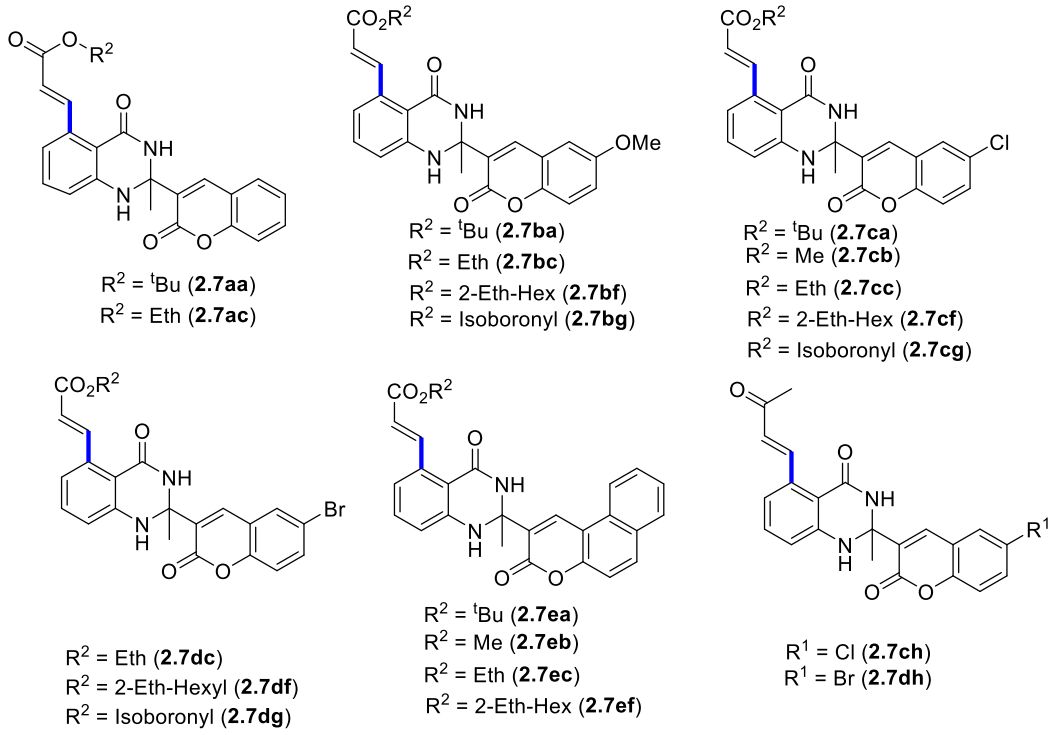

Scheme 5.1. First subset of C-H functionalized compounds (To avoid confusion with compound numbers, I have given the same numbering as in chapter 2)

strategies[131-134] and molecular hybridization techniques.[135] Nevertheless, most of these molecules are designed to exert cytotoxicity by interacting with DNA and subsequently causing DNA damage leading to the induction of cell death. These subsets of compounds comprising coumarin and quinazolinone (from chapter 2), are shown in **Scheme 5.1**, coumarin-pyrazole hybrid (from chapter 3) in **Scheme 5.2**. and coumarin-imidazopyridine (from chapter 4) in **Scheme 5.3**.

5.2. Cytotoxicity Studies

5.2.1. Coumarin-quinazolinone Conjugates (From Chapter 2)

5.2.1.1. Cytotoxicity Against Human Cancer Cell Lines

As a prelude, I elucidated the cytotoxic effects of the library of C-H functionalized coumarin and quinazolinone conjugates against a panel of National Cancer Institute (NCI)-60 human cancer cell lines at a single dose concentration (10^{-5} M).[136] Diverse and strong cytotoxic effects were observed on the evaluated panel of cancer cell lines. Notably, several compounds expressed more than 50% inhibition for tumor growth at micromolar concentration. From the results of the first 20 tested compounds (C5-alkenylated quinazolinone-coumarin conjugates), I found nine compounds showed a wide range of growth inhibitory activity in the range from -66 to 99.17 at 10 μM (**Table 5.1**).

Table 5.1. Overview of the preliminary cytotoxic assay at a single dose concentration of 10 μM

compd	mean growth percent	[a]range of growth inhibition	most sensitive cell lines	[b]positive cytostatic effect	[c]positive cytotoxic effect	no. of sensitive cell lines/Total cell lines
2.7ab	61.27	-2.01 to 79.28	SK-MEL-2	15/60	1/60	16/60
2.7ac	59.54	4.26 to 80.82	RXF 393	16/58	0/58	16/58
2.7ba	38.43	-59.79 to 96.31	SK-MEL-5	42/60	2/60	44/60
2.7bc	58.30	11.70 to 74.48	SW-620	15/60	0/60	15/60
2.7bf	62.97	7.93 to 83.33	HL-60(TB)	13/60	0/60	13/60
2.7bg	61.05	15.95 to 76.13	HL-60(TB)	15/60	0/60	15/60
2.7ca	38.37	-14.62 to 98.01	MOLT-4	33/58	3/58	36/58
2.7cb	59.54	4.26 to 80.82	RXF 393	16/58	0/58	16/58
2.7cc	28.36	-1.21 to 98.12	RXF 393	51/58	2/58	53/58

2.7cf	98.27	0.12 to 25.96	MDA-MB-468	0/58	0/58	0/58
2.7cg	58.70	-6.79 to 78.81	MDA-MB-468	17/59	1/59	18/59
2.7ch	77.66	22.61 to 82.88	MDA-MB-468	2/58	0/58	2/58
2.7dc	41.65	-66.32 to 81.81	BT-549	43/60	1/60	44/60
2.7df	59.36	4.34 to 78.43	RPMI-8226	18/58	0/58	18/58
2.7dg	76.55	0.83 to 86.61	MDA-MB-468	7/58	0/58	7/58
2.7dh	26.63	-29.33 to 99.17	HL-60(TB)	4/58	7/58	11/58
2.7ea	83.46	1.12 to 41.52	LOX IMVI	1/60	0/60	1/60
2.7eb	50.65	-0.79 to 94.22	RXF-3930	29/60	1/60	30/60
2.7ec	74.13	11.97 to 66.32	SF-539	3/60	0/60	3/60
2.7ef	92.87	0.64 to 39.65	SR	0/60	0/60	0/60

Compounds **7ca-7cg, 7ch** and **7dh** substituted with halogen such as Cl, Br on coumarin nucleus showed better activity than other derivatives with cytotoxic effects to most of the cell lines. In addition, most of the compounds showed broad spectrum cytotoxicity over various subpanels of cancer cell lines. Compounds **7cc**, **7dc** and **7dh** were found to be highly effective against renal cancer cell lines (RXF-393), breast cancer cell line (BT-549) and leukemia cell lines (HL-60(TB)), respectively. **Tables 5.2** and **5.3** demonstrate the detail overview of anti-tumor growth inhibition of all tested compounds against NCI-60 human cancer cell lines at the concentration of 10 μM.

Table 5.2. Percent growth inhibition of coumarin-quinazolinone conjugates (**7ab-7cf**) at 10 μM

Panel/Cell Line	**2.7ab**	**2.7ac**	**2.7ba**	**2.7bc**	**2.7bf**	**2.7bg**	**2.7ca**	**2.7cb**	**2.7cc**	**2.7cf**
Leukemia										
CCRF-CEM	16.26	15.32	67.93	45.62	37.67	41.29	75.83	15.32	62.55	13.95
HL-60(TB)	59.99	49.48	-----	47.94	83.33	76.13	-6.16	49.48	97.64	3.99
K-562	43.35	50.48	74.48	41.94	54.50	55.56	82.93	50.48	81.01	23.47
MOLT-4	39.97	49.35	81.88	63.85	51.60	51.16	-14.62	49.35	95.25	11.31
RPMI-8226	17.39	47.67	71.49	46.94	55.65	61.25	98.01	47.67	82.33	6.01

SR	41.26	63.94	73.8	46.46	50.36	42.11	91.14	63.94	98.12	14.75
Non-Small Cell Lung Cancer										
A549/ATCC	32.13	25.52	72.71	53.02	50.08	51.88	72.58	25.52	52.80	12.24
EXVX	21.82	41.09	62.93	47.25	49.71	46.83	63.76	41.09	68.15	-----
HOP-62	27.61	18.93	38.99	26.64	15.86	17.90	35.99	18.93	44.33	1.58
HOP-92	49.25	-----	67.71	43.84	46.21	42.22	-----	-----	-----	-----
NCI-H226	36.94	28.87	55.25	47.66	38.06	38.20	49.44	28.87	53.86	3.54
NCI-H23	23.34	20.45	71.47	51.00	52.88	63.65	47.03	20.45	49.09	-----
NCI-H322M	6.29	21.63	33.06	30.84	20.63	25.76	39.11	21.63	43.60	9.2
NCI-H460	55.53	21.81	52.81	32.14	23.78	29.03	56.13	21.81	52.58	-----
NCI-522	38.01	37.32	72.2	41.45	54.51	58.48	65.13	37.32	66.20	0.12
Colon Cancer										
COLO 205	36.92	24.71	55.10	24.25	31.12	49.08	80.56	24.71	68.35	-----
HCC-2998	25.56	26.73	37.92	17.64	15.69	15.95	47.09	26.73	61.28	-----
HCT-116	55.35	60.85	70.05	46.04	45.4	48.16	68.50	60.85	82.35	7.79
HCT-15	63.70	58.35	67.36	45.59	43.64	56.35	59.73	58.35	79.15	8.91
HT29	30.17	22.46	60.85	37.99	36.47	50.27	55.67	22.46	67.47	-----
KM12	31.23	37.05	52.96	27.61	25.73	33.40	80.07	37.05	74.02	1.89
SW-620	27.79	29.67	36.22	11.74	3.91	16.11	44.29	29.67	59.11	-----
CNS Cancer										
SF-268	17.66	18.96	41.94	41.90	23.68	26.65	48.64	18.96	54.50	4.31
SF-295	15.06	40.23	60.71	25.12	34.36	36.55	75.11	40.23	80.67	-----
SF-539	26.75	27.21	37.42	30.17	13.49	18.59	33.33	27.21	61.45	-----
SNB-19	18.47	35.33	49.25	44.19	29.55	33.71	47.92	35.33	66.25	6.53
SNB-75	58.45	-----	43.68	53.79	31.73	33.72	-----	-----	-----	-----
U251	42.07	47.35	51.60	37.88	36.73	36.28	57.57	47.35	66.14	-----
Melanoma										
LOX IMVI	61.14	53.23	50.87	69.99	21.91	26.51	58.86	53.23	77.8	0.97
MALME-3M	41.31	33.84	59.49	20.28	7.93	17.98	47.82	33.84	67.33	-----
M14	58.33	62.50	51.35	36.11	28.69	37.47	50.74	62.50	77.69	-----
SK-MEL-2	-2.01	59.33	92.40	53.24	58.40	31.91	46.43	59.33	92.90	-----
SK-MEL-28	24.62	21.70	59.40	33.28	25.11	29.61	46.26	21.70	46.15	-----
SK-MEL-5	21.54	67.96	-59.79	46.93	39.67	32.24	71.58	67.96	89.77	-----

UACC-257	22.31	31.14	67.41	27.70	22.60	27.17	58.26	31.14	55.74	-----
UACC-62	57.23	62.90	79.57	67.74	47.80	43.04	64.01	62.90	86.55	12.57
Ovarian Cancer										
IGROV1	68.02	62.27	58.35	52.24	35.67	29.79	55.31	62.27	86.95	0.23
OVCAR-3	25.90	28.71	44.57	26.86	16.32	29.89	56.25	26.71	65.60	-----
OVCAR-4	29.97	33.12	58.57	49.88	30.91	24.68	56.11	33.12	63.32	5.02
OVCAR-5	22.42	4.26	39.13	12.54	21.10	33.72	32.85	4.26	49.65	-----
OVCAR-8	33.12	35.31	62.06	39.74	41.00	40.10	60.88	35.31	60.88	-----
NCI/ADR-RES	19.95	33.86	63.42	41.81	43.36	43.65	74.62	33.86	77.31	-----
SK-OV-3	58.32	69.41	48.77	18.11	29.07	31.94	52.37	69.41	-0.63	-----
Renal Cancer										
786-0	41.07	43.87	33.34	35.29	34.30	26.58	45.51	43.87	68.62	-----
A498	50.30	30.37	42.16	33.35	20.21	13.15	-----	30.37	69.67	1.74
ACHN	69.20	72.98	71.43	47.74	32.48	32.10	80.35	72.98	89.98	8.28
CAKI-1	79.28	71.13	60.08	65.32	50.44	51.20	57.58	71.13	89.53	-----
RXF 393	41.07	80.82	59.67	52.98	44.13	51.36	89.75	80.82	-1.21	-----
SN12C	26.25	28.27	59.40	34.46	46.41	47.17	49.98	28.27	68.49	12.37
TK-10	51.03	17.90	43.32	41.65	33.10	35.63	33.77	17.90	53.82	7.86
UO-31	68.68	66.85	74.98	87.06	55.93	54.85	79.22	66.85	88.29	11.9
Prostate Cancer										
PC-3	41.14	51.90	86.38	59.17	80.30	79.79	87.54	51.90	82.57	-----
DU-145	37.31	38.29	30.51	31.29	14.25	19.50	38.87	38.29	62.27	20.50
Breast Cancer										
MCF7	17.77	47.92	75.57	56.92	65.77	73.49	82.47	47.92	73.51	13.77
MDA-MB-231/ATCC	23.70	15.71	50.88	38.36	28.95	21.86	32.86	15.71	67.86	-----
HS 578T	27.98	18.38	40.04	38.86	13.98	20.83	34.86	18.38	59.01	-----
BT-549	41.84	47.73	96.31	67.74	40.04	40.47	84.76	47.73	75.30	-----
T-47D	48.63	42.08	93.42	74.48	71.95	52.05	-3.39	42.08	83.74	13.88
MDA-MB	35.25	46.76	68.33	53.63	42.03	47.50	88.40	46.76	96.12	25.96

-- indicates GI < 10%; 30-40% growth inhibition; 40-50% growth inhibition; 50-70% growth inhibition; 70-90% growth inhibition; 90-100% growth inhibition; lethal to cancer cells

Table 5.3. Percent growth inhibition of coumarin-quinazolinone conjugates (**2.7cg-2.7ef**) at 10 μM

Panel/Cell Line	**2.7cg**	**2.7ch**	**2.7dc**	**2.7df**	**2.7dg**	**2.7dh**	**2.7ea**	**2.7eb**	**2.7ec**	**2.7ef**
Leukemia										
CCRF-CEM	40.60	28.36	63.23	31.10	17.78	99.17	30.40	47.04	14.94	18.87
HL-60(TB)	71.01	38.19	72.71	59.25	51.05	-29.33	23.15	45.34	11.97	13.74
K-562	78.39	47.68	75.92	71.36	71.62	99.09	38.24	53.32	49.99	22.50
MOLT-4	78.81	34.51	69.56	75.05	53.05	-6.34	20.21	41.32	20.59	10.18
RPMI-8226	78.00	46.61	68.02	78.43	64.21	97.29	20.37	59.83	28.24	10.96
SR	57.80	31.61	72.25	50.94	33.21	-0.63	53.02	72.02	25.75	39.65
Non-Small Cell Lung Cancer										
A549/ATCC	58.35	20.50	59.86	49.37	45.35	44.94	19.75	73.12	28.99	12.77
EXVX	50.59	25.10	56.25	51.28	37.87	65.66	17.01	32.48	14.06	9.81
HOP-62	28.50	12.87	34.41	19.63	7.54	50.01	12.64	66.27	20.76	-----
HOP-92	59.21	-----	59.84	-----	-----	-----	36.08	52.92	62.30	-----
NCI-H226	33.05	22.91	56.74	34.63	24.09	65.73	26.23	69.49	45.19	16.71
NCI-H23	36.57	29.78	60.24	30.90	20.94	82.14	34.98	48.76	28.71	24.01
NCI-H322M	29.52	10.84	11.96	27.62	18.84	47.48	7.25	32.04	12.12	11.63
NCI-H460	32.82	11.08	53.87	30.21	26.42	48.11	16.54	76.89	24.37	-----
NCI-522	63.17	23.79	70.92	51.70	31.72	73.23	22.37	47.05	28.37	14.37
Colon Cancer										
COLO 205	51.24	17.06	53.53	26.93	11.34	20.38	-----	47.03	20.58	-----
HCC-2998	57.37	15.24	31.23	24.68	4.12	76.65	-----	31.51	20.65	-----
HCT-116	59.61	24.26	67.85	54.81	46.24	84.93	17.24	55.53	22.60	17.6
HCT-15	33.59	7.85	73.57	40.38	17.13	85.40	25.05	45.38	18.55	15.8
HT29	39.08	10.61	56.47	38.24	11.26	72.37	9.95	67.06	29.00	-----
KM12	35.22	20.09	58.93	45.52	27.17	74.66	3.98	46.31	12.78	-----
SW-620	26.97	7.57	38.77	24.17	10.85	67.72	22.71	45.75	13.90	18.99
CNS Cancer										
SF-268	21.50	9.28	50.23	37.54	17.23	43.89	4.81	57.15	20.63	0.64
SF-295	53.94	24.70	63.3	50.14	35.95	60.95	1.12	24.74	41.46	-----

SF-539	12.80	15.83	26.09	19.06	3.18	80.83	13.76	55.25	66.32	1.82
SNB-19	47.06	23.96	51.27	45.07	28.04	48.18	15.68	50.30	16.09	11.29
SNB-75	-----	-----	61.73	-----	-----	-----	24.72	38.18	-----	11.67
U251	47.49	6.55	52.85	42.23	30.15	81.36	20.41	56.18	24.09	39.06
Melanoma										
LOX IMVI	21.13	17.94	55.74	40.11	15.53	85.17	41.52	93.68	46.49	13.53
MALME-3M	15.35	82.88	29.01	13.67	-----	68.65	4.24	80.38	34.29	-----
M14	30.44	19.09	57.60	38.61	13.97	68.62	6.53	44.14	22.52	-----
MDA-MB-435	18.99	9.15	45.30	13.06	0.83	57.67	5.06	23.90	25.10	0.72
SK-MEL-2	46.30	17.23	94.28	31.05	7.30	-0.79	14.44	20.57	27.39	11.27
SK-MEL-28	24.60	8.16	41.93	23.92	13.46	41.17	6.68	41.96	24.01	7.73
SK-MEL-5	38.75	47.39	51.78	41.01	25.46	86.93	4.45	20.54	4.96	0.07
UACC-257	42.82	36.33	35.43	33.68	23.04	72.81	2.13	22.15	13.47	2.35
UACC-62	37.36	43.92	68.58	51.64	20.24	87.00	36.53	50.83	45.44	16.38
Ovarian Cancer										
IGROV1	23.88	23.93	81.77	49.52	7.40	74.70	31.68	34.80	15.00	0.93
OVCAR-3	31.02	15.20	51.56	34.58	16.87	71.93	-----	68.04	-----	-----
OVCAR-4	45.58	27.04	59.81	37.57	24.61	72.78	10.6	94.22	38.64	1.76
OVCAR-5	19.41	1.65	23.56	14.22	7.44	69.15	6.45	36.66	24.06	4.98
OVCAR-8	29.62	11.89	62.22	32.19	11.03	75.09	16.23	45.68	17.06	10.57
NCI/ADR-RES	35.98	21.60	57.77	40.64	26.02	67.11	20.48	64.78	26.90	11.2
SK-OV-3	33.94	31.63	61.37	42.6	13.57	47.42	23.92	4.43	48.71	0.93
Renal Cancer										
786-0	30.13	13.08	40.61	30.60	8.54	66.84	9.61	16.10	6.03	8.2
A498	-----	-----	40.24	4.34	-----	-----	-----	9.36	17.41	-----
ACHN	38.30	28.90	71.93	51.89	23.44	77.3	15.17	59.91	43.13	1.33
CAKI-1	40.36	27.17	79.77	51.44	21.82	78.67	31.16	38.13	38.56	20.17
RXF 393	48.04	22.61	64.44	62.4	24.75	-12.92	1.19	-0.79	51.42	-----
SN12C	41.53	11.42	46.74	37.88	24.49	87.25	28.77	64.94	24.92	31.64
TK-10	20.75	-----	41.62	8.67	-----	41.42	-----	0.3	-----	-----
UO-31	57.18	45.58	80.2	67.85	40.22	77.96	39.74	34.61	14.9	22.35

Prostate Cancer										
PC-3	74.31	34.57	74.6	69.71	63.46	78.37	27.88	61.09	45.12	24.13
DU-145	28.75	8.30	50.42	38.13	15.65	80.92	10.68	53.91	21.76	3.52
Breast Cancer										
MCF7	62.58	36.85	64.68	55.56	49.42	86.63	37.28	52.79	23.12	23.54
MDA-MB-231/ATCC	24.90	12.05	44.05	25.52	1.75	82.04	22.76	71.47	19.10	7.15
HS 578T	27.24	14.69	36.84	18.60	4.21	53.41	9.54	70.55	43.05	-----
BT-549	40.65	32.98	-66.32	36.10	16.13	-8.15	6.44	54.77	34.44	-----
T-47D	75.60	46.48	81.81	69.71	53.83	67.97	34.91	28.20	34.27	13.16
MDA-MB-468	-6.79	60.97	67.79	78.26	86.61	-6.53	20.17	59.00	37.05	13.85

-- indicates GI < 10%; 30-40% growth inhibition; 40-50% growth inhibition; 50-70% growth inhibition; 70-90% growth inhibition; 90-100% growth inhibition; lethal to cancer cells

It is noteworthy that compound **2.7dh** has shown significant growth inhibition in the preliminary investigation at single-dose screening. Subsequently, it was evaluated further for 5-dose assay at different concentrations (10^{-4} M to 10^{-8} M) against NCI-60 cancer cell lines. The mean GI_{50} graph of **2.7dh** showed potent activity against the central nervous system (CNS), non-small cell lung, colon, renal and leukemia cancer subpanels (**Table 5.4**).

Table 5.4. Median growth inhibitory (GI_{50}, μM), total growth inhibitory (TGI, μM) and median lethal concentrations (LC_{50}, μM) of *in vitro* evaluation of compound **2.7dh** against subpanels of human tumor cancer cell lines

Panel of Cancer Cell lines	**GI_{50}**	**TGI**	**LC_{50}**
Leukemia	4.04	33.80	*b*
Non-Small cell Lung cancer	2.19	26.40	58.70
Colon cancer	7.13	40.90	54.10
CNS cancer	1.30	19.30	50.70
Melanoma	7.01	21.61	48.10
Ovarian cancer	7.56	32.90	67.30

Renal cancer	3.87	10.70	39.20
Prostate cancer	5.95	22.30	51.50
Breast cancer	4.28	18.90	47.30
MIG-MID[a]	4.82	25.20	52.12

[a]Full panel mean-graph midpoint (MIG-MID) (μM). [b]Compounds showed values > 100 μM.

5.2.2. Coumarin-pyrazole conjugates (From Chapter 3)

As I have synthesized several compounds in chapter 3 and also isolated various intermediates during time-dependent studies, so, for systematic studies, I have selected only C-H functionalized compounds (**Scheme 5.2**) as a second subset for the evaluation of their cytotoxicity. These compounds comprise coumarin, N-phenyl pyrazole, and acrylates (having different aliphatic side chains).

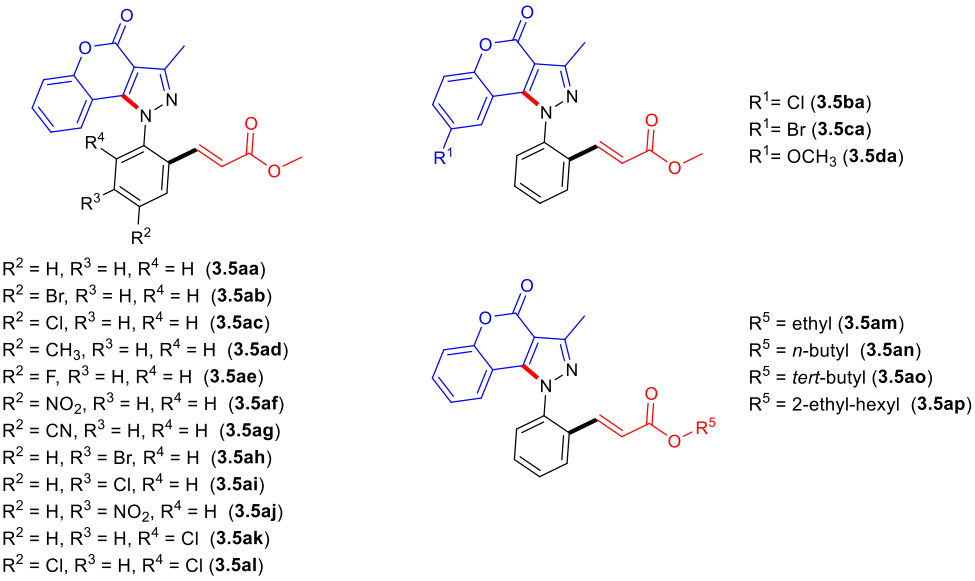

Scheme 5.2. Second subset of C-H functionalized compounds (To avoid confusion with compound numbers, I have given the same numbering as in chapter 3)

Tables 5.5 and **5.6** represent growth inhibition at 10 μM against NCI-60 cancer cell lines. Compounds substituted with halogen such as Cl, Br, and F on phenyl ring showed better activity than other derivatives with cytotoxic effects towards most of the cell lines. In addition, most of

the compounds showed broad spectrum cytotoxicity over various subpanels of cancer cell lines. Compounds **3.5ab**, **3.5ae, 3.5al** and **3.5am** were found to be highly effective and selected for five doses.

Table 5.5. Percent growth inhibition of coumarin-pyrazole conjugates (**5aa-5aj**) at 10 μM

Panel/Cell Line	**3.5aa**	**3.5ab**	**3.5ac**	**3.5ad**	**3.5ae**	**3.5af**	**3.5ag**	**3.5ah**	**3.5ai**	**3.5aj**
Leukemia										
CCRF-CEM	5.36	84.75	13.77	47.30	-----	96.01	88.39	48.69	79.69	19.60
HL-60(TB)	0.07	-17.71	41.53	76.90	20.11	-45.72	-14.08	71.32	-36.93	4.31
K-562	-----	77.71	14.51	76.77	18.01	84.36	89.21	68.65	82.98	14.89
MOLT-4	-----	69.92	13.96	25.18	-----	86.01	78.91	30.13	49.38	23.21
RPMI-8226	7.69	76.69	45.61	37.21	-----	77.63	70.95	24.33	48.47	25.71
SR	9.24	79.54	52.93	81.45	14.97	88.46	73.9	87.52	96.31	12.53
Non-Small Cell Lung Cancer										
A549/ATCC	1.33	44.24	9.72	25.54	-----	52.34	46.69	40.33	55.59	6.54
EXVX	9.70	61.99	4.34	45.41	2.04	64.52	74.79	10.44	29.31	11.44
HOP-62	14.58	62.16	13.84	41.53	8.41	66.39	65.13	67.24	78.03	15.68
HOP-92	27.12	55.44	53.07	59.98	-----	68.39	36.6	5.55	17.01	-----
NCI-H226	8.98	31.77	10.11	18.76	-----	36.49	25.99	-----	20.73	11.89
NCI-H23	0.22	53.90		43.49	4.01	71.04	70.06	12.45	27.44	14.55
NCI-H322M	6.23	8.21	6.62	8.86	3.29	36.69	12.75	10.25	15.98	6.85
NCI-H460	-----	62.89	3.62	25.89	-----	87.77	62.67	51.21	79.44	3.89
NCI-522	-----	92.28	9.65	95.41	-----	80.79	96.96	82.82	99.28	9.04
Colon Cancer										
COLO 205	-----	85.26	-----	54.58	-----	92.24	96.33	75.41	95.39	-----
HCC-2998	-----	41.04	3.92	47.68	-----	-25.33	76.3	21.10	40.8	3.73
HCT-116	5.66	77.52	22.8	71.95	-----	76.43	81.16	60.90	72.34	-----
HCT-15	1.22	81.69	7.33	71.79	4.87	89.24	80.31	51.21	67.88	7.73
HT29	-----	80.81	-----	60.16	-----	93.66	90.05	55.43	89.51	-----
KM12	-----	80.91	20.86	76.69	-----	72.04	80.18	63.32	68.24	1.23
SW-620	-----	86.423	2.07	69.84	-----	85.32	57.97	65.59	83.8	0.99

CNS Cancer										
SF-268	12.71	44.38	19.22	38.41	-----	42.10	37.38	12.65	36.28	16.35
SF-295	-----	-21.78	-----	99.43	0.99	78.66	-----	33.25	57.11	6.58
SF-539	14.05	87.90	20.75	74.33	4.32	86.79	-----	38.71	64.50	9.55
SNB-19	3.91	61.43	9.04	43.59	1.10	64.41	72.42	26.43	33.69	7.02
SNB-75	26.64	92.10	48.12	72.14	11.06	-9.23	-----	78.8	-----	41.11
U251	-----	63.25	8.42	37.50	-----	65.84	77.12	18.66	65.12	10.60
Melanoma										
LOX IMVI	2.32	60.16	2.95	62.67	10.68	63.79	61.71	45.34	59.6	13.09
MALME-3M	-----	77.21	-----	66.75	-----	64.91	63.88	48.16	64.99	6.38
M14	-----	84.53	-----	69.08	2.63	81.37	-----	45.7	58.71	0.90
MDA-MB-435	0.8	-----	-----	71.96	-----	51.43	-----	-----	-----	4.19
SK-MEL-2	-----	69.68	-----	80.05	-----	-----	90.40	36.72	68.54	-----
SK-MEL-28	-----	47.86	-----	50.12	0.77	48.28	46.65	39.71	42.60	0.27
SK-MEL-5	6.62	96.12	13.83	80.65	-----	83.76	80.83	39.75	50.86	12.95
UACC-257	-----	50.28	-----	47.56	-----	37.40	29.23	27.27	34.84	9.88
UACC-62	15.83	77.92	27.58	82.72	12.85	80.84	75.36	57.23	67.97	34.18
Ovarian Cancer										
IGROV1	8.15	51.42	3.25	53.36	2.13	57.83	60.16	16.78	41.36	16.4
OVCAR-3	-----	-2.05	-----	92.77	-----	98.61	-3.46	47.91	67.89	4.87
OVCAR-4	1.37	34.42	9.48	31.41	0.49	37.02	32.3	19.89	21.88	31.76
OVCAR-5	11.01	49.11	14.74	31.13	3.61	65.49	78.18	10.96	27.52	0.55
OVCAR-8	4.63	64.47	11.23	40.02	-0.52	67.95	74.33	48.62	54.27	15.63
NCI/ADR-RES	-----	39.94	-----	23.53	-----	44.61	43.30	35.37	43.12	3.99
SK-OV-3	8.15	51.42	3.25	42.60	13.57	47.42	23.92	4.43	48.71	0.93
Renal Cancer										
786-0	-----	27.54	18.75	36.24	-----	40.62	56.74	8.61	16.27	5.85
A498	-----	-----	0.58	0.77	-----	8.62	-----	-----	1.95	0.64
ACHN	9.63	57.97	13.38	58.53	7.26	54.58	47.51	30.34	50.69	23.51
CAKI-1	22.07	68.27	43.2	70.9	16.55	68.02	68.85	61.63	65.56	37.99
RXF 393	3.89	42.61	19.81	58.12	-----	-10.53	-6.71	21.76	35.41	14.73

SN12C	7.77	41.83	12.74	21.64	5.12	60.08	48.62	9.68	17.03	20.92
TK-10	-----	26.67	15.63	19.34	-----	42.45	22.43	2.53	12.36	3.57
UO-31	39.25	55.95	35.66	56.68	34.55	65.04	61.21	31.75	48.97	51.84
Prostate Cancer										
PC-3	11.00	67.10	34.19	50.74	-----	69.48	71.56	19.14	47.62	15.89
DU-145	-----	65.23	2.09	19.42	-----	67.13	75.12	8.18	45.84	8.43
Breast Cancer										
MCF7	3.92	85.38	-----	82.68	4.20	81.04	82.49	52.51	75.80	11.96
MDA-MB-231/ATCC	15.33	47.65	26.78	25.02	10.93	58.06	82.35	24.15	30.62	20.66
HS 578T	18.09	-6.08	27.07	88.89	-----	-7.34	75.02	52.54	82.29	26.12
BT-549	10.52	57.12	30.03	35.77	19.41	49.29	55.38	33.50	86.29	15.53
T-47D	4.44	53.19	15.50	41.07	0.44	58.56	51.86	23.61	59.41	38.93
MDA-MB-468	10.68	96.80	16.45	84.03	-----	-30.50	-30.27	32.63	52.64	16.82

-- indicates GI < 10%; 30-40% growth inhibition; 40-50% growth inhibition; 50-70% growth inhibition; 70-90% growth inhibition; 90-100% growth inhibition; lethal to cancer cells

Table 5.6. Percent growth inhibition of coumarin-pyrazole conjugates (**5ak-5da**) at 10 μM

Panel/Cell Line	**3.5ak**	**3.5al**	**3.5am**	**3.5an**	**3.5ao**	**3.5ap**	**3.5ba**	**3.5ca**	**3.5da**
Leukemia									
CCRF-CEM	21.62	4.06	70.79	-----	-----	11.72	0.44	97.9	19.98
HL-60(TB)	32.21	-----	88.32	8.58	-----	-----	27.37	-----	-----
K-562	30.24	-----	76.02	7.18	-----	-----	-----	91.58	51.42
MOLT-4	33.12	-----	91.1	0.15	-----	10.83	12.06	96.88	-----
RPMI-8226	52.07	1.41	75.17	1.45	-----	21.08	6.96	83.04	10.12
SR	38.69	-----	90.58	5.93	-----	13.06	13.13	88.57	53.91
Non-Small Cell Lung Cancer									
A549/ATCC	21.20	-----	57.16	3.98	-5.06	0.60	1.18	63.87	1.91
EXVX	18.91	-----	40.33	3.16	-----	23.91	9.95	69.37	4.59
HOP-62	6.26	7.43	21.49	14.62	-----	16.49	6.78	67.4	17.08

HOP-92	67.28	-----	61.34	-----	-----	9.46	26.85	63.71	4.32
NCI-H226	9.63	-----	38.27	3.39	-----	8.42	12.13	-----	-----
NCI-H23	22.44	2.10	37.09	-----	-----	10.06	1.62	75.06	9.19
NCI-H322M	6.26	3.25	21.45	-----	-----	1.25	8.04	36.23	4.77
NCI-H460	8.73	-----	56.27	-----	-----	-----	-----	86.51	-----
NCI-522	22.28	4.32	46.77	11.94	0.97	8.97	5.43	-23.42	64.96
Colon Cancer									
COLO 205	-----	-----	50.47	-----	-----	-----	-----	-----	-----
HCC-2998	12.58	-----	27.45	9.43	-----	-----	-----	-31.95	7.93
HCT-116	44.47	-----	58.03	5.93	-----	7.10	-----	87.74	8.45
HCT-15	16.65	-----	55.18	9.96	-----	3.75	8.17	96.73	36.69
HT29	5.01	-----	42.58	-5.88	-----	-----	0.92	-6.09	-----
KM12	27.14	-----	60.76	5.72	-----	12.01	4.62	86.40	23.35
SW-620	14.13	-----	43.20	4.90	-----	-----	0.85	77.40	30.42
CNS Cancer									
SF-268	24.38	-----	41.95	6.56	-----	11.34	7.57	40.37	-----
SF-295	26.5	-----	53.05	9.44	-----	1.06	-----	-24.23	11.11
SF-539	13.10	5.14	13.28	-----	-----	10.22	7.25	-32.89	21.27
SNB-19	9.53	-----	36.12	9.01	-----	9.20	12.05	66.13	5.87
SNB-75	24.24	-----	38.57	24.60	8.98	23.84	24.05	98.72	32.13
U251	12.19	-----	25.82	-----	-----	1.74	-----	78.57	1.48
Melanoma									
LOX IMVI	20.22	7.8	33.91	6.97	-----	5.82	13.68	66.22	26.92
MALME-3M	11.55	-----	41.36	4.44	-----	-----	-----	58.26	32.9
M14	21.61	-----	32.35	-----	-----	-----	-----	91.67	18.21
MDA-MB-435	7.79	-----	39.65	2.23	-----	-----	-----	-52.94	90.89
SK-MEL-2	7.21	-----	16.27	-----	-----	-----	-----	-11.16	-----
SK-MEL-28		-----	31.62	-----	-----	-----	-----	54.82	37.6
SK-MEL-5	8.88	-----	45.27	-----	-----	7.47	2.16	82.61	20.67
UACC-257	15.11	-----	31.7	2.27	-----	-----	-----	30.86	15.61
UACC-62	45.76	9.81	46.32	23.3	-----	16.64	28.71	81.73	51.22
Ovarian Cancer									

IGROV1	32.27	-----	50.84	4.80	-----	27.97	5.33	66.13	9.32
OVCAR-3	12.63	-----	42.86	-----	-----	2.40	-----	-17.47	4.82
OVCAR-4	22.96	2.23	57.90	16.45	-----	12.26	6.88	36.32	10.33
OVCAR-5	4.97	-----	14.23	-----	-----	1.87	-----	77.09	5.59
OVCAR-8	11.55	-----	47.3	5.03	-----	4.68	1.17	82.2	-----
NCI/ADR-RES	-----	2.67	26.60	1.48	-----	3.13	-----	44.74	11.77
SK-OV-3	33.94	31.63	50.84	4.80	-----	27.97	23.92	4.43	48.71
Renal Cancer									
786-0	19.59	-----	24.2	14.35	-----	-----	-----	54.69	5.44
A498			18.15	7.08	0.64			4.55	0.46
ACHN	32.82	5.62	51.73	12.68	-----	10.23	8.70	54.61	15.70
CAKI-1	64.15	15.04	55.85	46.73	4.62	21.91	30.73	71.65	46.91
RXF 393	19.27	-----	37.00	15.92	-----	-----	-----	-9.64	22.78
SN12C	14.56	3.12	39.71	4.51	-----	7.97	5.85	60.44	8.36
TK-10	6.02	-----	8.76	5.97	-----	-----	-----	40.04	-----
UO-31	32.32	32.35	73.81	18.45	7.02	36.89	31.78	67.67	43.31
Prostate Cancer									
PC-3	66.76		78.34	5.39	-----	13.10	24.77	76.32	7.64
DU-145	8.21		33.84	-----	-----	-----	-----	73.75	-----
Breast Cancer									
MCF7	16.32	6.56	67.01	6.31	2.01	21.48	12.95	86.98	33.58
MDA-MB-231/ATCC	25.68	10.88	29.65	16.31	-----	20.76	21.77	81.54	14.80
HS 578T	23.42	-----	40.84	16.66	-----	6.24	5.27	-10.24	36.44
BT-549	-----	-----	91.96	-----	-----	5.25	-----	68.26	29.32
T-47D	50.15	-----	94.01	17.66	0.31	8.94	11.97	51.98	4.85
MDA-MB-468	18.39		45.25	2.06		3.01	12.15	-28.72	15.7

-- indicates GI < 10%; 30-40% growth inhibition; 40-50% growth inhibition; 50-70% growth inhibition; 70-90% growth inhibition; 90-100% growth inhibition; lethal to cancer cells

5.2.3. Coumarin-imidazopyridine conjugates (From Chapter 4)

As I have synthesized several compounds in chapter 4, I have selected some compounds (**Scheme 5.3**) as a third subset to evaluate anticancer activity. Compounds are comprised of coumarin and imidazopyridine. **Table 5.7** represents percent growth inhibition at the concentration of 10 μM against NCI-60 cancer cell lines. Compounds substituted with halogen such as Cl and Br on coumarin nucleus showed better activity than other derivatives with cytotoxic effects towards 30 to 45 cell lines. In addition, most of the compounds showed broad spectrum cytotoxicity over various subpanels of cancer cell lines. Compound **4.3aa** was found to be highly effective against breast cancer cell line (MDA-MB).

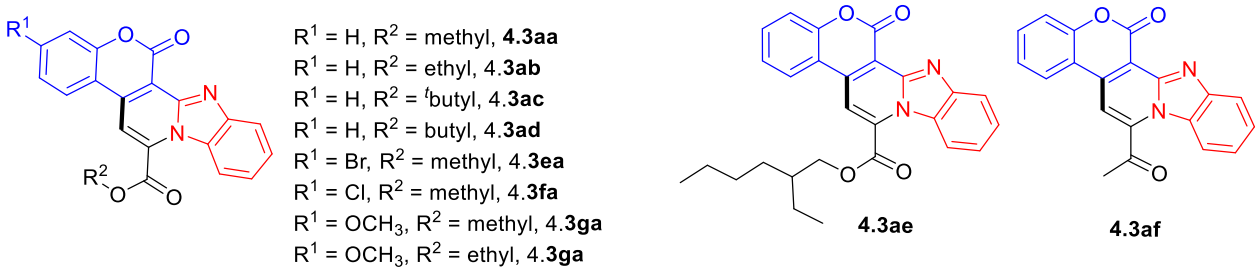

Scheme 5.3. The third subset of C-H functionalized compounds (To avoid confusion with compound numbers, I have given the same numbering as in chapter 4)

Table 5.7. Percent growth inhibition of oxidative annulated compounds (**3aa-3gb**) at 10 μM

Panel/Cell Line	4.3aa	4.3ab	4.3ac	4.3ad	4.3ae	4.3af	4.3ea	4.3fa	4.3ga	4.3gb
Leukemia										
CCRF-CEM	41.60	22.36	68.28	32.10	17.78	91.17	30.40	47.04	14.94	18.87
HL-60(TB)	72.01	32.19	78.72	59.13	55.05	-30.33	21.10	45.34	11.97	13.74
K-562	75.39	45.65	74.92	72.21	76.62	95.07	39.25	53.32	49.99	22.50
MOLT-4	79.81	35.10	68.55	73.07	55.05	-3.34	20.21	41.32	20.59	10.18
RPMI-8226	73.00	44.77	67.20	79.51	66.23	92.29	12.31	59.83	28.24	10.96
SR	57.80	35.68	73.30	52.95	38.22	-0.63	55.01	72.02	25.75	39.65
Non-Small Cell Lung Cancer										
A549/ATC	53.38	22.51	51.81	48.37	44.35	45.94	17.75	74.12	20.99	13.77

EXVX	59.10	22.12	52.26	55.18	34.87	66.66	12.01	31.48	12.06	19.81
HOP-62	28.50	14.77	33.41	18.13	1.54	52.01	14.64	65.27	25.76	-----
HOP-92	51.11	-----	54.44	-----	-----	-----	35.08	53.92	64.30	-----
NCI-H226	32.15	21.11	51.44	31.63	14.09	61.73	28.23	61.49	48.19	14.71
NCI-H23	33.47	27.18	62.34	33.90	0.94	83.14	36.98	44.76	28.71	28.01
NCI-H322M	20.62	11.64	11.76	28.62	15.84	48.48	7.05	33.14	10.12	10.63
NCI-H460	31.92	13.18	51.87	38.21	21.42	41.11	26.54	70.19	20.37	-----
NCI-522	65.27	24.69	74.92	51.70	32.72	71.23	23.37	40.05	27.37	25.37
Colon Cancer										
COLO 205	19.27	-----	37.00	15.92	-----	-----	-----	34.01	20.78	20.27
HCC-2998	50.37	11.24	315.23	21.68	4.12	70.65	-----	30.11	22.65	-----
HCT-116	58.61	25.26	62.85	51.81	46.24	80.93	17.24	50.53	28.60	18.60
HCT-15	32.59	7.85	73.57	40.38	17.13	84.40	25.05	45.38	18.55	15.80
HT29	31.08	10.61	56.47	38.24	11.26	71.37	9.95	67.06	-----	29.00
KM12	34.22	20.09	58.93	45.52	27.17	78.66	3.98	46.31	-----	12.78
SW-620	27.97	7.57	38.77	24.17	10.85	68.72	22.71	45.75	13.90	12.88
CNS Cancer										
SF-268	-----	9.28	50.23	37.54	17.23	43.89	4.81	57.15	20.63	0.64
SF-295	53.94	24.70	63.3	50.14	35.95	60.95	1.12	24.74	41.46	-----
SF-539	-----	15.83	-----	-----	-----	80.83	13.76	55.25	66.32	1.82
SNB-19	45.06	23.96	51.27	45.07	28.04	48.18	15.68	50.30	16.09	-----
SNB-75	-----	-----	61.73	-----	-----	-----	24.72	38.18	-----	11.67
U251	41.49	6.55	52.85	42.23	30.15	81.36	20.41	56.18	24.09	-----
Melanoma										
LOX IMVI	-----	17.94	55.74	40.11	15.53	85.17	41.52	93.68	46.49	13.53
MALME-3M	-----	82.88	29.01	13.67	-----	68.65	4.24	80.38	34.29	-----
M14	30.44	19.09	57.60	38.61	13.97	68.62	6.53	44.14	22.52	-----
MDA-MB-435	18.99	9.15	45.30	13.06	0.83	57.67	5.06	23.90	25.10	0.72
SK-MEL-2	46.30	17.23	-----	-----	7.30	-0.79	14.44	20.57	27.39	-----
SK-MEL-28	24.60	-----	41.93	23.92	-----	41.17	6.68	41.96	24.01	7.73
UACC-257	-----	36.33	35.43	-----	-----	72.81	2.13	-----	13.47	2.35
UACC-62	-----	43.92	68.58	51.64	20.24	87.00	36.53	50.83	45.44	16.38

Ovarian Cancer										
IGROV1	23.93	23.88	81.77	49.52	7.40	74.70	31.68	34.80	15.00	0.93
OVCAR-3	15.20	31.02	51.56	34.58	16.87	71.93	-----	68.04	-----	-----
OVCAR-4	27.04	45.58	59.81	37.57	24.61	72.78	10.60	94.22	38.64	1.76
OVCAR-5	1.65	19.41	23.56	14.22	7.44	69.15	6.45	36.66	24.06	4.98
OVCAR-8	11.89	29.62	62.22	32.19	11.03	75.09	16.23	45.68	17.06	10.57
NCI/ADR	21.60	35.98	57.77	40.64	26.02	67.11	20.48	64.78	26.90	11.20
SK-OV-3	33.94	31.63	61.37	42.60	13.57	47.42	23.92	4.43	48.71	0.93
Renal Cancer										
786-0	13.08	30.13	40.61	30.60	8.54	66.84	9.61	16.10	8.20	6.03
A498	-----	-----	40.24	4.34	-----	-----	-----	9.36	-----	17.41
ACHN	28.90	38.30	71.93	51.89	23.44	77.3	15.17	59.91	1.33	43.13
CAKI-1	27.17	40.36	79.77	51.44	21.82	78.67	31.16	38.13	20.17	38.56
RXF 393	22.61	48.04	64.44	62.40	24.75	-12.92	1.19	-0.79	-----	51.42
SN12C	11.42	41.53	46.74	37.88	24.49	87.25	28.77	64.94	31.64	24.92
TK-10	-----	20.75	41.62	8.67	-----	41.42	-----	0.30	-----	-----
UO-31	45.58	57.18	80.2	67.85	40.22	77.96	39.74	34.61	22.35	14.9
Prostate Cancer										
PC-3	62.58	36.85	64.68	55.56	49.42	86.63	37.28	52.79	23.12	23.54
DU-145	24.90	12.05	44.05	25.52	1.75	82.04	22.76	71.47	19.10	7.15
Breast Cancer										
MCF7	74.31	34.57	74.60	69.71	63.46	78.37	27.88	61.09	45.12	24.13
MDA-MB-231/ATCC	28.75	8.30	50.42	38.13	15.65	80.92	10.68	53.91	21.76	3.52
HS 578T	27.24	14.69	36.84	18.60	4.21	53.41	9.54	70.55	43.05	-----
BT-549	62.58	32.98	-66.32	-----	53.83	-----	6.44	54.77	34.44	-----
T-47D	24.90	46.48	81.81	69.71	-----	67.97	-----	-----	34.27	13.16
MDA-MB	-6.79	60.97	67.79	78.26	86.61	-6.53	20.17	59.00	37.05	13.85

-- indicates GI < 10%; 30-40% growth inhibition; 40-50% growth inhibition; 50-70% growth inhibition; 70-90% growth inhibition; 90-100% growth inhibition; lethal to cancer cells

5.3. Cytotoxicity against human normal cell line

In order to measure the safety of compounds, toxicity effects of potent compound **2.7dh** was evaluated against normal cell line Hek293 (human kidney) using MTT assay at different concentrations from 10^{-4} to 10^{-8} M. Notably, compound **2.7dh** showed only 14.4%, 13.2%, 12.8%, 12.5% and 12.2% cytotoxicity to Hek293 cells at above-mentioned concentrations (**Figure 5.1**). As only 12.8% toxicity to HeK293 of compound **2.7dh** was observed, that indicated compound has the potential to kill cancer cells selectively

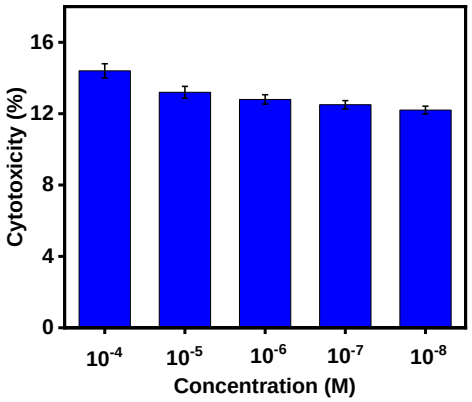

Figure 5.1. MTT assay on normal human cell lines HeK293 with compound **2.7dh**

5.4. DNA interaction studies

In order to understand the mode of action of anticancer activity by coumarin-quinazolinone conjugates, I initially investigated whether the observed cytotoxic effect is governed due to interactions between DNA and compound. In this context, I selected the most potent compound **2.7dh,** which exhibited the cytotoxic effect at both single-dose and five-dose concentration levels. Characterization with X-ray crystal data revealed that the compound is planar; earlier studies have also shown that planar compounds act as an effective intercalating agent. Therefore, I studied the binding capacity of the C-H functionalized compound (**2.7dh**) with ct-DNA using various spectroscopic techniques, such as UV-vis and fluorescence spectroscopy as well as circular dichroism.

5.4.1 UV-visible spectroscopy

Compound **2.7dh** (20 μM) has shown absorption maximum at 325 nm. On incremental addition of ct-DNA (0-15 μM), quenching of absorption band (hypochromic shift) was observed in phosphate buffer at *p*H 7.4. On titration with ct-DNA, decrease in absorbance by 21.95% of compound **2.7dh** was observed (**Figure 5.2a**); an isosbestic point at 380 nm was also seen that indicated a single mode of binding. Moreover, the presence of ct-DNA, hypochromic effect in absorption spectra also throws some light on intercalative binding.[137] Affinity of compound **2.7dh** to bind with ct-DNA was calculated by determining binding constant (K_b) for compound-DNA complex using Benesi-Hildebrand equation[138] which was found to be 5.51×10^4 M^{-1} for **2.7dh (Figure 5.2b**).

(a) **(b)**

Figure 5.2. **(a)** Effect of incremental addition of ct-DNA on absorption spectrum of compound **2.7dh** in phosphate buffer (*p*H 7.4) at 298 K and **(b)** Benesi-Hildebrand plot for compound **2.7dh**

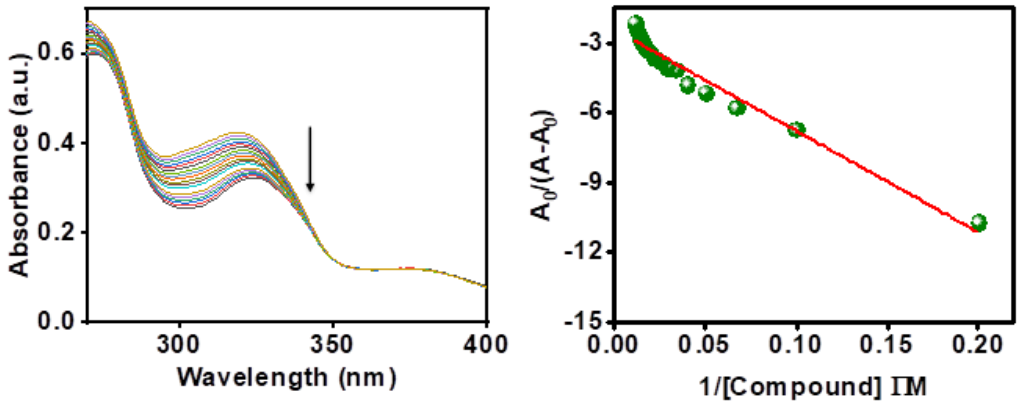

5.4.2. Fluorescence spectroscopy

Emission studies further confirmed interactions between compound and DNA. The binding of compound **2.7dh** with DNA was examined by incremental addition of DNA (from 0 to110 μM) to 5 μM of compound in phosphate buffer (*p*H 7.4) at 298 K. Compound **2.7dh** has emission maxima at 428 nm. On incremental addition of ct-DNA to compound, fluorescence quenching by 78.26% was observed without any significant change in emission maximum (**Figure 5.3a**). I have applied the Stern-Volmer equation (K_{SV}) to shed more-light on fluorescence quenching.[139]

Value of K_{SV} was determined from the ratio of slope to intercept of Stern-Volmer plot as 0.56 $\times 10^4$ M^{-1} at 298 K (**Figure 5.3b**) (**Table 5.8**). The value of K_{SV} indicates that compound **2.7dh** is bound firmly to ct-DNA either by static or dynamic interaction. Modified Stern-Volmer equation[140] is generally used to calculate the binding constant (K_b) and the number of binding sites (n). In the present study, K_b and n were found to be 31.4 × 10^4 M^{-1} and 1.71, respectively, at 298 K (**Table 5.8**, **Figure 5.3c**). The analysis confirms that compound **2.7dh** bound strongly to ct-DNA with binding constant was comparable to the earlier reports.[141]

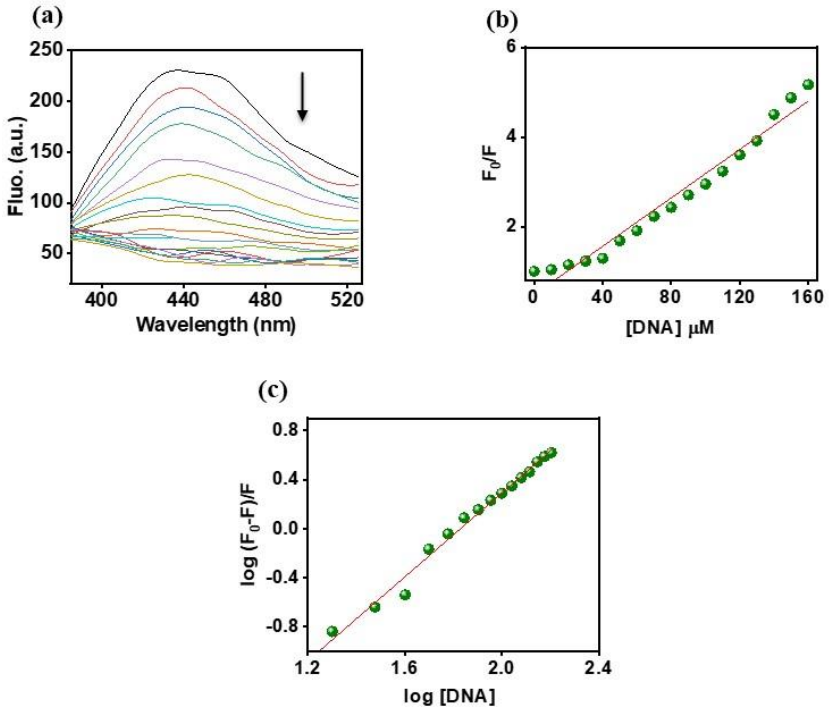

Figure 5.3. (a) Effect of incremental addition of ct-DNA on emission spectra of compound **2.7dh** in phosphate buffer (*p*H 7.4) at 298 K**, (b)** Stern-Volmer plot and **(c)** Modified Stern-Volmer plot for the interaction of compound **2.7dh** with ct-DNA at 298K

Table 5.8. Quenching and binding parameters of compound **2.7dh** upon interaction with ct-DNA

Compd	**K_{SV} ($\times 10^5$)(M^{-1})**	**R^2**	**K_b ($\times 10^5$ M^{-1})**	**n**	**R^2**
2.7dh	5.6	0.97	3.14	1.71	0.99

R^2 is the correlation coefficient

5.4.3. Ethidium Bromide (EB) displacement

To examine the intercalation properties, I have performed Ethidium Bromide (EB) displacement assay of compound **2.7dh** with DNA. EB, a fluorescent moiety, has the potential to bind with DNA through intercalation due to its planar structure.[142] The emission spectra of EB-ct DNA complex (3 μM : 30 μM) showed an intense band at 620 nm. However, after the incremental addition of compound (0-100 μM), the fluorescence intensity of the EB-DNA complex decreased. This revealed that some of the ethidium bromides, having intercalation with DNA base pairs, have been replaced by compound and released into the aqueous medium (**Figure 5.4a**).

5.4.4. Circular Dichroism (CD)

To get insight into the conformation of ct-DNA upon interaction with compounds, the circular dichroism technique was used, since the study reveals about the secondary structure of a biomolecule (i.e. DNA in this case). CD spectrum obtained helps to determine the effect of

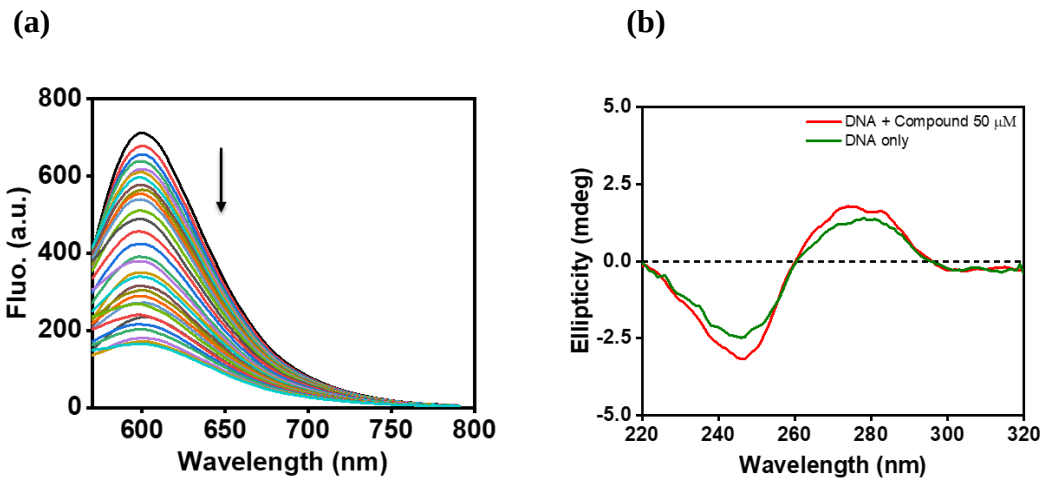

Figure 5.4. (a) Effect of incremental addition of compound **2.7dh** on emission spectra of complex of EB (3 μM) with ct-DNA (30 μM) and **(b)** CD spectra of free ct-DNA (40 μM) (green line), **2.7dh**/ct-DNA complex (red line) at ratio r[compound/ct-DNA] = 0.050

binding of a compound on the conformation of DNA since the mutual orientation of the molecule and the DNA could be derived, consequently, giving useful information about modes of interaction. As expected, I obtained a CD signal of DNA in the UV region i.e., one negative band at 246 nm indicative of the right-handed helicity and one positive band at 278 nm due to the base stacking, showing a characteristic spectrum of β-form of DNA.[143] Addition of compound **2.7dh** resulted in an increase in ellipticity at both 246 nm as well as 278 nm with no measurable

shifts in the peak (**Figure 5.4b**), which clearly shows that the compound **2.7dh** inserts partially into the DNA base pairs *via* its planar aromatic groups, ultimately stabilizing the base stacking.[144] The results confirm that the compound intercalates with ct-DNA without affecting its helical conformation.[145,146] As compound contains double bond adjacent to electron withdrawing group so it could be Michael acceptor also and act as good electrophile. The potential of the Michael acceptor moiety to interact with functionally relevant cysteines of proteins potentially renders them effective and sustained enzyme activity modulator.

5.5. Protein albumin (HSA) interaction studies

Albumins belong to the class of fully folded structural proteins known as globular proteins. These are commonly found in blood plasma at a concentration of 35-50 mg/mL with an average half-life of approximately 90 days. Various studies reported using HSA as a model protein to determine the binding potential of various bioactive molecules, such as amino acids, peptides, hormones, nutrients, fatty acids, metal ions, and drugs. The reason is the presence of the protein in both intravascular and extravascular systems; therefore, it is readily available for the molecules to bind. Taking this into account, I have studied the binding tendency of compound **2.7dh** to Human Serum Albumin (HSA) using various spectroscopic techniques, like absorption and emission spectroscopy to highlight the binding constant, nature of the binding, number of binding sites, etc.

5.5.1. UV-visible spectroscopy

To investigate structural changes in protein and to study protein-ligand complex formation, I used UV-visible spectrophotometer. Absorption spectra of HSA (10 μM) have been studied in phosphate buffer (*p*H 7.4) with incremental addition of compound **2.7dh** at the concentration of 0-130 μM. HSA has several aromatic amino acids such as Trp, Tyr, and Phe, due to which a characteristic sharp absorption band at 280 nm was obtained. Interaction of this protein with ligand can be easily examined by a change in an absorption band.[147] Gradual increase in the absorption by incremental addition of compound with a slight blue shift has been observed (**Figure 5.5**). These changes in the absorption band are entirely due to environmental changes around a protein that bring conformational changes. These conformational changes result from a compound's binding to the protein. The binding constant (K_b) was calculated using the Benesi-

Hildebrand equation, that to be found as 2.26 $\times 10^5$ M^{-1} for **2.7dh**. These data confirmed a strong binding with the protein as reported in the literature.[148]

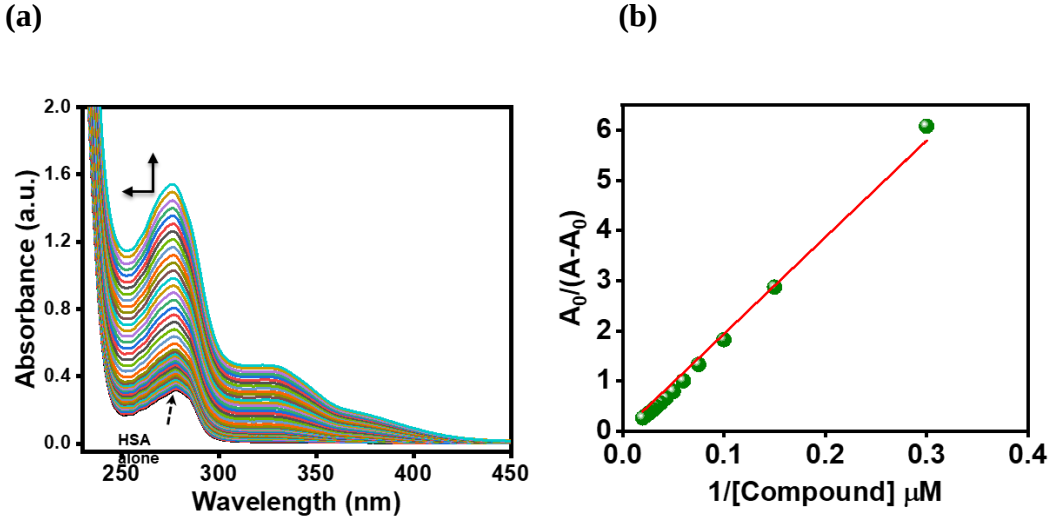

Figure 5.5. **(a)** Effect of incremental addition of compound **2.7dh** on absorption spectrum of HSA **2.7dh** in phosphate buffer (*p*H 7.4) at 298 K and **(b)** Benesi-Hildebrand plots for compound **2.7dh**

5.5.2. Fluorescence spectroscopy

Tryptophan, tyrosine, and phenylalanine are the three different amino acids responsible for the emission. Tryptophan is an intrinsic fluorophore that is very sensitive to the microenvironment around it, giving brief information about structural changes in the protein upon binding to a molecule. Steady-state emission spectra clearly showed a decrease in fluorescence emission intensity at 350 nm (87% at 50 μM of a compound) in a concentration-dependent manner, indicating a strong complex formation between compound and protein (**Figure 5.6a**). It has been reported earlier that the quenching in tryptophan fluorescence is observed when other amino acids, e.g., histidine, phenylalanine, etc., or disulfide bonds come in close proximity to tryptophan, therefore, indicating a structural change in the protein. I also observed a slight red shift of 10 nm (from 347 nm in the absence of compound to 357 nm) in the tryptophan fluorescence upon increasing the compound concentration, indicating tryptophan exposure to more polar environment influenced by strong interaction between compound and protein.

To examine the detailed changes in the microenvironment around the specific amino acid residues (typically tryptophan) in HSA, I performed **synchronous fluorescence spectroscopy,**

which gives emission wavelength shift due to changes in polarity around tryptophan. The difference between the emission and excitation wavelength reveals the different nature or microenvironment around tryptophan. Notably, $\Delta\lambda = 60$ nm gives characteristic information about tryptophan. I observed a drastic decrease in emission intensity (**Figure 5.6b**) upon adding compound **2.7dh,** indicating the conformational changes in protein around tryptophan. Further, the binding affinity was determined using the Stern-Volmer equation. The Stern-Volmer constant (K_{sv}) was calculated to determine the extent of quenching due to the interaction of compound with protein. A linear Stern-Volmer plot was obtained which is indicative of single mode of binding that could be either static or dynamic. The value of K_{sv} obtained was 0.38×10^4 M^{-1} at 298 K (**Figure 5.6c**). Moreover, the binding constant (K_b) and the average number of binding sites (n) were calculated using modified Stern-Volmer equation from the plot of log $(F_o\text{-}F)/F$ versus log [compound] (**Figure 5.6d**) and were found to 0.31×10^5 M^{-1} and 1.32, respectively (**Table 5.9.**). These binding parameters for the interaction suggested that serum albumin might act as an effective protein carrier for these compounds and their metabolites in delivering them to target tissues.

5.6. Structure-Activity Relationship (SAR) studies

Structure-activity relationship was studied for the correlation between the substituent effect on biological activity. Based on number of cancer cell lines that were inhibited by various compounds from chapter 2 revealed that nature of substituents at the coumarin nucleus, as well as various alkenes at C5 position of quinazolinone, affected the biological activity. It was found that halogen substitution at coumarin nuclei or halogen-substituted moieties showed better activity than other compounds. Compounds **2.7ca, 2.7cc, 7ch, 2.7dc,** and **2.7dh** showed higher activity, out of which **2.7dh** having bromo on the coumarin nucleus, were selected for five dose assays. Compounds with hydrogen, methoxy, or phenyl groups on coumarin showed moderate activity. Anticancer activity of these moieties has been slightly increased by change in alkenes on C-5 position of quinazolinone. Cyclic and long carbon chain alkenes have no significant effect, whereas bioactivity has shown significant improvement if methyl vinyl ketone is used instead of acrylate. Hence, compound **2.7dh** having bromo on coumarin nucleus and methyl vinyl ketone at C5 position of quinazolinone, was found to be the most active compound and was observed to be most potent against leukemia cancer.

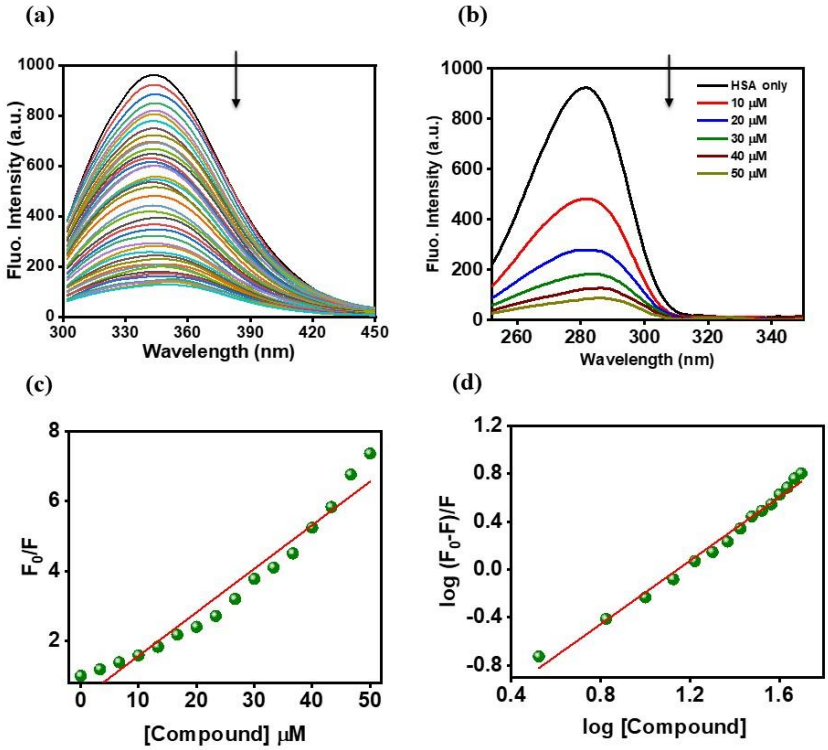

Figure 5.6. (a) Effect of incremental addition of HSA on emission spectra of compound **2.7dh** in phosphate buffer (*p*H 7.4) at 298 K**, (b)** Synchronous, **(c)** Stern-Volmer plot and **(d)** Modified Stern-Volmer plot for interaction of compound **2.7dh** with HSA at 298K

Table 5.9. Quenching and binding parameters of compound **7dh** upon interaction with HSA

Compd	**K_{SV} ($\times10^5$)(M^{-1})**	**R^2**	**K_b ($\times10^5$ M^{-1})**	**n**	**R^2**
2.7dh	3.8	0.96	0.31	1.32	0.99

R^2 is the correlation coefficients

Similarly, in the series of coumarin-pyrazole conjugates (from Chapter 3) revealed that nature of substituents at the coumarin nucleus, at phenyl ring as well as various alkenes at phenyl ring, affected the biological activity. Compounds substituted with halogen such as Cl, Br, and F on phenyl ring showed better activity than other derivatives. Compound **3.5ab** having bromo, and methyl acrylate at phenyl ring, **3.5ae** having fluoro**,** and methyl acrylate at phenyl ring, and **3.5al**

having two chloro, and methyl acrylate at phenyl ring were found to be most potent molecules and selected for five doses assay.

Similarly, in the series of coumarin and imidazopyridine (from Chapter 4) revealed that nature of substituents at the coumarin nucleus, as well as various alkenes at C4 position of coumarin, affected the biological activity. It was found that halogen substitution at coumarin nuclei or halogen-substituted moieties showed better activity than other compounds. Compounds **4.3ea** and **4.3ef** showed higher activity. Compounds with hydrogen, methoxy, or phenyl groups on coumarin showed moderate activity. While compound **4.3aa** having hydrogen on coumarin nucleus and ethyl acrylate at C4 position of coumarin found to be more effective against breast cancer cell lines (**MDA-MB**).

5.7. Conclusion

Evaluation of anticancer activity of C-H functionalized compounds against NCI-60 cancer cell lines has been examined. Halogen-substituted scaffolds were found to be more potent against number of cancer cell lines. Compounds **2.7dh** (from coumarin quinazolinone conjugates series), **3.5ab**, **3.5ae**, **3.5al**, and **3.5am** (from coumarin-pyrozole series), and **4.3aa** (from coumarin benzimidazole series) were found to be excellent potency against leukemia cancer and selected for five doses assay. Further, structure-activity relationship has also been developed to understand the effect of substitution on bioactivity. Moreover, to decipher mode of action of compound, DNA and HSA binding studies of compound **2.7dh** were performed where compound **2.7dh** has shown significant interaction with ct-DNA and albumin protein (HSA).

References

1. Ferro, A., Peleteiro, B., Malvezzi, M., Bosetti, C., Bertuccio, P., Levi, F., Negri, E., La Vecchia, C., and Lunet, N. *Eur. J. Cancer.*, **2014**, *50*, 1330-1344.
2. Lilja, H., Vickers, A. J., Sjoberg, D., Johansson, R., Granfors, T., Johansson, M., Pettersson, K., Scardino, P. T., Hallmans, G., and Stattin, P. *J. Clin. Oncol*., **2014**, *32*, 5081-5082.
3. Collins, I., and Workman, P. *Nat. Chem. Biol.,* **2006**, *2,* 689-700.
4. Siegel, R. L., Miller, K. D., and Jemal. *CA Cancer. J. Clin*., **2016**, *66*, 7-30.
5. DeVita, V. T., and Chu, E., *Cancer Res.*, **2008**, *68*, 8643-8653.
6. Miller, K. D., Nogueira, L., Mariotto, A. B., Rowland, J. H., Yabroff, K. R., Alfano, C. M., and Siegel, R. L. *CA Cancer. J. Clin.*, **2019**, *69*, 363-385.
7. Singh, P., Raj, R., Kumar, V., Mahajan, M. P., Bedi, P., Kaur, T., and Saxena, A. *Eur. J. Med. Chem.*, **2012**, *47*, 594-600.
8. Reed, J. C. *Cancer cell***.**, **2003**, *3*, 17-22.
9. Hopkins, A. L. *Nat. Chemi. Biol.,* **2008**, *4*, 682-690.
10. Guillemard, L., Kaplaneris, N., Ackermann, L., and Johansson, M. J. *Nat. Rev. Chem.* **2021**, *5*, 522-545 and references therein.
11. Gediya, L. K., and Njar, V. C. *Expert Opin. Drug Discov*., **2009**, *4*, 1099-1111.
12. Viegas-Junior, C., Danuello, A., da Silva, B. V., Barreiro, E. J., and Fraga, C. A. *Curr. Med. Chem.,* **2007,** *14*, 1829-1852.
13. Singla, P., Luxami, V., and Paul, K. *Eur. J. Med. Chem*., **2015**, *117*, 59-69.
14. Kraljevic, T.G., Harej, A., Sedic, M., Pavelic, S. K., Stepanic, V., Drenjancevic, D., Talapko, J., and Malic, S. R. *Eur. J. Med. Chem.*, **2016,** *124*, 794-808
15. Galayev, O., Garazd, Y., Garazd, M., and Lesyk, R., *Eur. J. Med. Chem.,* **2015**, *105*, 171-181.
16. McGlacken, G. P., and Bateman, L. M. *Chem. Soc. Rev.* **2009**, *38*, 2447-2464.
17. Zhang, L., and Ritter, T. *J. Am. Chem. Soc.* **2022**, *144*, 2399-2414.
18. "The Nobel Prize in Chemistry 2010-Press Release". Noble prize org. Nobel Media AB 2013. Web. 25 Feb 2014. http://www.nobelprize.org/nobel_prizes/chemistry/laureates/2010/press.html.
19. Zhu, W., and Gunnoe, T. B. *J. Am. Chem. Soc*., **2021**, *143*, 6746-6766.

20. Sambiagio, C., Schönbauer, D., Blieck, R., Dao-Huy, T., Pototschnig, G., Schaaf, P., and Schnürch, M.. *Chem. Soc. Rev.*, **2018**, *47*, 6603-6743.

21. Wang, Q., Han, J., Wang, C., Zhang, J., Huang, Z., Shi, D., and Zhao, Y. *Chem. Sci.*, **2014**, *5*, 4962-4967.

22. Jaiswal, Y., Kumar, Y., and Kumar, A. *J. Org. Chem.*, **2018**, *83*, 1223-1231.

23. Chen, X. Y., Ozturk, S., and Sorensen, E. J. *Org. Lett.*, **2017**, *19*, 1140–1143.

24. Li, Y., Wang, Z., Xu, S., and Cheng, J. *Tetrahedron Letters*, **2020**, *61*, 152387-152390.

25. Bettadapur, K. R., Lanke, V., and Prabhu, K. R. *Org. Lett.*, **2015**, *17*, 4658-4661.

26. Liu, X., Li, X., Liu, H., Guo, Q., Lan, J., Wang, R., and You, J. *Org. Lett.*, **2015**, *17*, 2936-2939.

27. Chen, S., Feng, B., Zheng, X., Yin, J., Yang, S., and You, J. *Org. Lett.*, **2017**, *19*, 2502-2505.

28. Pipaliya, B. V., and Chakraborti, A. K. *J. Org. Chem.*, **2017**, *82*, 3767-3780.

29. Wang, Y. Y., Liu, M., and Dong, L. *Org. Chem. Front.*, **2021**, *8*, 2487-2493.

30. Khan, I., Ibrar, A., Abbas, N., and Saeed, A. *Eur. J. Med. Chem.* **2014**, *76*, 193-244 and references therein.

31. Rawat, A., and Reddy, A. V. B. *Eur. J. Med. Chem.*, **2022**, 100038-100057.

32. Akhtar, J., Khan, A. A., Ali, Z., Haider, R., and Yar, M. S. *Eur. J. Med. Chem.*, **2017**, *125*, 143-189.

33. Sayeed, I. B., Nayak, V. L., Shareef, M. A., Chouhan, N. K. and Kamal, A. *MedChemComm*, **2017**, *8*, 1000-1006.

34. Zheng, Y., Song, W. B., Zhang, S. W., and Xuan, L. J. *Org. Biomol. Chem.*, **2015**, *13*, 6474-6478.

35. Das, D., Biswas, A., Karmakar, U., Chand, S. and Samanta, R. *J. Org. Chem.*, **2016**, *81*, 842-848.

36. Viveki, A. B. and Mhaske, S. B., *J. Org. Chem.*, **2018**, *83*, 8906-8913.

37. Lou, M., Deng, Z., Mao, X., Fu, Y., Yang, Q. and Peng, Y., *Org. Biomol. Chem.* **2018**, *16*, 1851-1859.

38. Bairy, G., Das, S., Begam, H. M. and Jana, R., *Org. Lett.* **2018**, *20*, 7107-7112.

39. Hashimoto, Y., Ueyama, T., Fukutani, T., Hirano, K., Satoh, T., and Miura, M. *Chem. Lett.*, **2011**, *40*, 1165-1166.

40. Wang, X., Fang, X., Xiao, H., Gong, D., Yang, X., and Wu, F. *Tetrahedron*, **2013**, *69*, 6993-7000.

41. Wu, S., Wang, Z., Ma, D., Chen, C., and Zhu, B. *Org. Chem. Front.*, **2020**, *7*, 1158-1163.

42. Nguyen, T. T., Le, L. V., Pham, H. H.; Nguyen, D. H.; Phan, N. T.; Le, H. V. and Phan, A. N. *RSC Adv.*, **2021**, *11*, 9349-9352.

43. Khoobi, M., Alipour, M., Zarei, S., Jafarpour, F., and Shafiee, A. *Chem. Comm.*, **2012**, *48*, 2985-2987.

44. Min, M., Kim, Y., and Hong, S. *Chem. Comm.*, **2013**, *49*, 196-198.

45. Wang, Y. J., Wang, T. T., Yao, L., Wang, Q. L., and Zhao, L. M. *J. Org. Chem.*, **2020**, *85*, 9514-9524.

46. Han, F., Xun, S., Jia, L., Zhang, Y., Zou, L., and Hu, X. *Org. Lett.*, **2019**, *21*, 5907-5911.

47. Neog, K., Borah, A., and Gogoi, P. *J. Org. Chem.*, **2016**, *81*, 11971-11977.

48. Sharma, K., Neog, K., and Gogoi, P. *Org. Lett.*, **2019**, *22*, 73-77.

49. Dick, A. R., and Sanford, M. S. *Tetrahedron*, **2006**, *11*, 2439-2463.

50. Jazzar, R., Hitce, J., Renaudat, A., Sofack- Kreutzer, J., and Baudoin, O. *Chem. Eur. J.*, **2010**, *16*, 2654-2672.

51. Labinger, J. A., and Bercaw, J. E. *Nature*, **2002**, *417*, 507-514.

52. Hameed, A., Al-Rashida, M., Uroos, M., Ali, S. A., Arshia, Ishtiaq, M., and Khan, K. M. *Expert Opin. Ther. Pat.* **2018**, *28*, 281-297.

53. Galvani, G., Vardhan Reddy, K. H.; Beauvineau, C., Ghermani, N., Mahuteau-Betzer, F., Alami, M., and Messaoudi, S. *Org. Lett.* **2017**, *19*, 910-913.

54. Liu, H. L., Li, T. X., Tian, H. Z., and Sun, X. W. *Org. Lett.* **2021**, *23*, 4579-4583.

55. Ghosh, P., Ganguly, B., and Das, S. *Org. Biomol. Chem.* **2020**, *18*, 4497-4518.

56. Choi, S. Y., Kim, H. D., Park, J. U., Park, S. A., and Kim, J. H. *Org. Lett.*, **2019**, *21*, 10038-10042.

57. Bhakta, S., and Ghosh, T. *Org. Chem. Front.*, **2022**, *9*, 5074-5103.

58. Wu, X., Wang, B., Zhou, S., Zhou, Y., and Liu, H. *ACS Catal.* **2017**, *7*, 2494-2499.

59. Choi, J. H., Kim, K., Oh, H., Han, S., Mishra, N. K., and Kim, I. S. *Org. Biomol. Chem.* **2020**, *18*, 9611-9622.

60. Reddy, B. S., Narasimhulu, G., Umadevi, N., and Yadav, J. S. *Synlett*, **2012**, *23*, 1364-1370.

61. Garad, D. N., Viveki, A. B., and Mhaske, S. B. *J. Org. Chem.*, **2017**, *82*, 6366-6372.

62. Sinha, S. K., Guin, S., Maiti, S., Biswas, J. P., Porey, S., Maiti, D. *Chem. Rev.* **2022**, *122*, 5682-5841.

63. Valadbeigi, E., and Ghodsi, S. *Med. Chem.* **2017**, *7*, 178-185.

64. Pereira, T. M., Vitório, F., Amaral, R. C., Zanoni, K. P. S., Iha, N. Y. M., and Kümmerle, A. E. *New J. Chem.* **2016**, *40*, 8846-8854.

65. Jayashree, B. S., Arora, S., and Venugopala, K. N. *Asian J. Org. Chem.* **2008**, *20*, 1-7.

66. Sugino, T., and Tanaka, K. *Chem. Lett.* **2001**, *30*, 110-111.

67. Ilango, K., Valentina, P., Sathish, D., and Murugan, *J. Pharm. Sci. Res.* **2016**, *8*, 1030-1033.

68. Zhao, P., Yu, X. X., Zhou, Y., Geng, X., Wang, C., Huang, C., Wu, Y. D., Zhu, Y. P., and Wu, A. X. *Org. Lett.* **2020**, *22*, 7103-7107.

69. Kim, H., Thombal, R. S., Khanal, H. D., and Lee, Y. R. *Chem. Comm.* **2019**, *55*, 13402-13405.

70. Patel, H. H., and Sigman, M. S. *J. Am. Chem. Soc.* **2016**, *138*, 14226-14229.

71. Paul, K., Sharma, A., and Luxami, V. *Bioorg. Med. Chem.* **2014**, *24*, 624-629.

72. Zhang, G. F., Li, Y., Xie, X. Q., and Ding, C. R., *Org. Lett.* **2017**, *19*, 1216-1219.

73. Chen, S. Q., Li, X. R., Li, C. J., Fan, J., Liu, Z. W., and Shi, X. Y. *Org. Lett.* **2020**, *22*, 1259-1264.

74. Götzinger, A. C., Theßeling, F. A., Hoppe, C., Müller, T. J. *J. Org. Chem.* **2016**, *81*, 10328-10338.

75. Zhi, H., Wang, J., Wang, S., and Wei, Y. *J. Spectrosc.* **2013**, 147128-147130.

76. Sahoo, S., and Pal, S. *J. Org. Chem.* **2021**, *86*, 4081-4097.

77. Fershtat, L. L., and Makhova, N. N. *ChemMedChem*., **2017**, *12*, 622-638.

78. Patel, B., Zunk, M., Grant, G., and Rudrawar, S. *Bioorg. Med. Chem. Lett.*, **2021**, *39*, 127853-127866.

79. He, H. Z., Li, K., Yu, K. K., Lu, P. L., Feng, M. L., Chen, S. Y., and Yu, X. Q. *Chem. Comm.*, **2020**, *56*, 6870-6873.

80. Liu, H., Ren, Z. L., Wang, W., Gong, J. X., Chu, M. J., Ma, Q. W., Wang, J. C., and Lv, X. H. *Eur. J. Med. Chem.*, **2018**, *157*, 81-87.

81. Zhu, M., Ma, L., Wen, J., Dong, B., Wang, Y., Wang, Z., Zhou, J., Zhang, G., Wang, J., and Guo, Y. *Eur. J. Med. Chem.*, **2020**, *186*, 111900-111914.

82. Jeong, S., and Joo, J. M. *Acc. Chem. Res.*, **2021**, *54*, 4518-4529.

83. Zheng, Q., Liu, C. F., Chen, J., and Rao, G. W. *Adv. Synth. Catal.* **2020**, *362*, 1406-1446.

84. Mishra, R., Jana, A., Panday, A. K., and Choudhury, L. H. *New J. Chem.,* **2019**, *43*, 2920-2932.

85. Chowdhury, D., Koner, M., Ghosh, S. and Baidya, M. *Org. Lett*., **2022**, *24*, 3606-3608.

86. Ali, W., Prakash, G., and Maiti, D. *Chem. Sci.*, **2021**, *12*, 2735-2759.

87. Chen, J., Liu, W., Ma, J., Xu, H., Wu, J., Tang, X., Fan, Z., and Wang, P. *J. Org. Chem.,* **2012**, *77*, 3475-3482.

88. Korvorapun, K., Kaplaneris, N., Rogge, T., Warratz, S., Stückl, A. C., and Ackermann, L. *ACS. Catal.*, **2018**, *8*, 886-892.

89. Chen, W., Liu, F. X., Bian, M., Li, L., Zhou, Z., and Yi, W. *J. Org. Chem.,* **2019**, *84*, 15557-15566.

90. Dong, Y., Yang, J., Zhang, H., Zhan, X. Y., He, S., Shi, Z. C., Zhang, X. M., and Wang, J. Y. *Org. Lett.* **2020**, *22*, 5151-5156.

91. Yoshida, T., Furuyama, T., Asai, M., and Kobayashi, N. *Chem Lett.*, **2015**, 44, 1056-1058.

92. Prusty, N., Banjare, S. K., Mohanty, S. R., Nanda, T., Yadav, K., and Ravikumar, P. C. *Org. Lett.*, **2021**, *23*, 9041-9046.

93. (a) Kitano, H., Matsuoka, W., and Ito, H., and Itami, K. *Chem. Sci.,* **2018**, *9*, 7556-7561. (b) Anthony, J. E. *Angew. Chem. Int. Ed.*, **2008**, *47*, 452-483. (c) Dyan, O. T., Borodkin, G. I., and Zaikin, P. A. *Eur. J. Org. Chem.*, **2019**, *44*, 7271-7306.

94. (a) Almirante, L., Polo, L., Mugnaini, A., Provinciali, E., Rugarli, P., Biancotti, A., and Murmann, W. *J. Med. Chem.*, **1965**, *8*, 305-312. (b) Dymińska, L. *Bioorg. Med. Chem.,* **2015**, *23***,** 6087-6099.

95. Wang, Y., Cheng, F. X., Yuan, X. L., Tang, W. J., Shi, J. B., Liao, C. Z. and Liu, X. H. *Eur. J. Med. Chem.,* **2016**, *112*, 231-251.

96. Tran, C., and Hamze, A. *Molecules*, **2022**, *27*, 3461-3504.

97. Li, P., Sun, Y., Zhang, X., Wu, X., Li, R., Cao, D. and Ma, L. *J. Photochem. Photobiol. A: Chem.*, **2021**, *411*, 113197-1131202.

98. Wang, K.; Zhang, J.; Hu, R.; Liu, C.; Bartholome, T. A.; Ge, H.; Li, B. *ACS. Catal*., **2022**, *12*, 2796-2820.

99. Wang, P., Verma, P., Xia, G., Shi, J., Qiao, J. X., Tao, S., Cheng, P. T. W., Poss, M. A., Farmer, M. E., Yeung, K., and Yu, J. Q. *Nature* **2017**, *551*, 489–493.

100. Peng, S., Wang, L., Huang, J., Sun, S., Guo, H., and Wang, J. *Adv. Syn. Catal.*, **2013**, *355*, 2550-2557.

101. Tasior, M., Poronik, Y. M., Vakuliuk, O., Sadowski, B., Karczewski, M., and Gryko, D. T. *J. Org. Chem.*, **2014**, *79*, 8723-8732.

102. Min, M., and Hong, S. *Chem. Comm.*, **2012**, *48*, 9613-9615.

103. Dhole, S., and Sun, C. M. *Adv. Synth. Catal.*, **2019**, *361*, 535-541.

104. Zhao, Q., Xie, R., Zeng, Y., Li, W., Xiao, G., Li, Y., and Chen, G. *RSC Adv.*, **2022**, *12*, 24930-24934.

105. Li, S., Liu, L., Wang, R., Yang, Y., Li, J. and Wei, J. *Org. Lett.*, **2020**, *22*, 7470-7474.

106. Rui, X., Wang, C., Si, D., Hui, X., Li, K., Wen, H., Li, W. and Liu, J. *J. Org. Chem.,* **2021**, *86*, 6622-6632.

107. Zhong, X., Lin, S., Gao, H., Liu, F. X., Zhou, Z., and Yi, W. *Org. Lett.*, **2021**, *23*, 2285-2291.

108. Cui, H. L., Liu, S. W., and Xiao, X. *Eur. J. Org. Chem.*, **2020**, *35*, 5729-5734.

109. Yang, J., Ji, D. W., Hu, Y. C., Min, X. T., Zhou, X., and Chen, Q. A. *Chem. Sci.*, **2019**, *10*, 9560-9564.

110. Jayakumar, J., Vedarethinam, G., Hsiao, H. C., Sun, S. Y., and Chuang, S. C. *Angew. Chem.*, **2020**, *132*, 699-704.

111. Dhawa, U., Kaplaneris, N., and Ackermann, L. *Org. Chem. Front.*, **2021,** *8*, 4886-4913.

112. Tanaka III, K., Morita, N., and Tamura, O*rg. Lett.*, **2021**, *23*, 1659-1663.

113. Wu, L., Meng, Y., Ferguson, J., Wang, L., and Zeng, F. *J. Org. Chem.,* **2017**, *82*, 4121-4128.

114. Neog, K., Dutta, D., Das, B., and Gogoi, P. *Org. Lett.,* **2017**, *19*, 730-733.

115. Wang, Y., Gu, J. Y., and Shi, Z. J. *Org. Lett.*, **2017**, *19*, 1326-1329.

116. Prinz, H., Ridder, A. K., Vogel, K., Böhm, K. J., Ivanov, I., Ghasemi, J. B., Aghaee, E., and Müller, K. J. *Med. Chem.,* **2017**, *60*, 749-755.

117. Morphy, R., Kay, C., and Rankovic, Z. *Drug Discov. Today*, **2004**, *9*, 641-651.

118. Walsh, J., and Bell, A. *Curr. Pharm. Des*., **2009**, *15*, 2970- 2985.

119. Nepali, K., Sharma, S., Sharma, M., Bedi, P. M. S., and Dhar, K. L. *Eur. J. Med. Chem.*, **2014**, *77*, 422-487.

120. Zhuang, C., Zhang, W., Sheng, C., Zhang, W., Xing, C., and Miao, Z. *Chem. Rev.*, **2017**, *117*, 7762-7810.

121. Gong, H. H., Addla, D., Lv, J. S., and Zhou, C. H. *Curr. Top. Med. Chem.*, **2016**, *16*, 3303-3364.

122. Banerjee, S., Veale, E. B., Phelan, C. M., Murphy, S. A., Tocci, G. M., Gillespie, L. J., Frimannsson, D. O., Kelly, J. M., and Gunnlaugsson, T. *Chem. Soc. Rev.,* **2013**, *42*, 1601-1618.

123. Lv, J. S., Peng, X. M., Kishore, B., and Zhou, C. H. *Bioorg. Med. Chem. Lett.,* **2014**, *24*, 308-313.

124. Dai, F. J., Li, Q., Wang, Y. X., Ge, C. C., Feng, C. Y., Xie, S. Q., He, H. Y., Xu, X. J., and Wang, C. J. *J. Med. Chem.,* **2017**, *60*, 2071-2083.

125. Xu, K., Schwarz, P. M., and Ludueña, R. F. *Drug Dev. Res.,* **2002**, *55*, 91-96.

126. Morphy, R. and Rankovic, Z. *J. Med. Chem.,* **2005**, *48*, 6523-6543.

127. Rask-Andersen, M., Almén, M. S., and Schiöth, H. B. *Nat. Rev. Drug Discov.,* **2011,** *10*, 579-590.

128. Fortin, S., and Bérubé, G. *Expert Opin. Drug Discov.,* **2013**, *8*, 1029-1047.

129. Pantziarka, P., Bouche, G., Meheus, L., Sukhatme, V., and Sukhatme, V. P. *ecancermedicalscience,* **2014**, *8*, 443-459.

130. Hegde, M., Kumar, K. S. S., Thomas, E., Ananda, E., Raghavan, S. C., and Rangappa, K. S. *RSC Adv.,* **2015,** *5*, 93194-93208.

131. Espinoza, P. Q., Acosta, P. M., Amesty, A., Rodríguez, P. M., Castrillejo, I. L., Pérez, L. F., Machín, F., and Braun, A. E., *Bioorg. Med. Chem.,* **2017**, *25*, 1976-1983.

132. Keri, R. S., Patil, M. R., Patil, S. A, and Budagumpi, S. *Eur. J. Med. Chem.,* **2015**, *89*, 207-251.

133. Patil, S. A., Patil, R., and Miller, D. D. *Future Med. Chem.,* **2012**, *4*, 2085-2115.

134. Lin, X., Kang, D., Li, X., Zhan, P., Liu, X., and Zhang, Q. *Eur. J. Med. Chem.,* **2014**, *82*, 293-307.

135. Osmaniye, D. S., Levent, A. B., Karaduman, S., Ilgın, Y., Özkay, Z. A., and Kaplancıklı, *Molecules*, **2018**, *23*, 1054-1068.

136. Grever, M. R., Sehepartz, S. A., and Chabners, B. A. *Semin. Oncol.* **1992**, *19*, 622-638;

137. Arjmand, F. and Aziz, M. *Eur. J. Med. Chem.,* **2009**, *44*, 834-844.

138. Benesi, H. A., and Hildebrand, J. H. *J. Am. Chem. Soc.,* **1949**, *71*, 2703-2707.

139. Palchaudhuri, R., and Hergenrother, P. J. *Curr. Opin. Biotechnol.,* **2007**, *18*, 497-503.

140. Parveen, I., Khan, P., Ali, S., Hassan, I. Md., and Ahmed, N. *Eur. J. Med. Chem.,* **2018**, *159*, 166-177.

141. Singh, I., Luxami, V., Choudhury, D., and Paul, K. *RSC Adv.,* **2022**, *12*, 483-497.

142. Lepecq, J. B., and Paoletti, C. *J. Mol. Biol.,* **1967**, *27*, 87-106.

143. Eriksson, M., and Nordén, B. *Methods Enzymol.,* **2001**, *340*, 68-98.

144. Yusof, E. N. M., Azam, M., Sirat, S. S., Ravoof, T. B., Page, A. J., Veerakumarasivam, A., and Razali, M. R. *Bioinorg. Chem.,* **2022**, 641

145. Lipinski, C. A., Lombardo, F., Dominy, B. W., and Feeney, P. J. *Adv. Drug Deliv. Rev.*, **1997**, *23*, 3-25.

146. Lipinski, C. A., Lombardo, F., Dominy, B. W., and Feeney, P. J. *Adv. Drug Deliv. Rev.*, **1997**, *23*, 3-25.

147. Ertl, P., Rodhe, B., and Selzer, P. *J. Med. Chem.*, **2000**, *43*, 3714-3717.

148. Bhat, A. A., Singh, I., Tandon, N., Tandon, R. *Eur. J. Med. Chem.*, **2022**, 114954-114980.

SUMMARY

1. Introduction

During the last decades, cancer has been a major worldwide health problem.[1] Cancer is a lethal disease,[2] second leading cause of mortality exceeding cardiovascular disease. Despite many therapeutic successes, cancer remains one of the most promising challenges of the 21st century. The American Cancer Society (ACS) statistics estimated that in 2022, over 19,18,030 cases were diagnosed in the United States alone, and over 6,90,360 people died from this disease.[3] Cancer is characterized by aberrations in cellular growth and proliferation pathways, resulting in an uncontrolled division of abnormal cells to form lumps or masses of tissue called a tumor.[4] It releases a hormone that can alter the body's function and affects the digestive, nervous, circulatory, and many other systems. Cancer can be found in any organ, such as the lung, pancreas, brain, colon, breast, skin, bones, ovarian, blood, or nervous tissue.[5]

Currently, chemotherapy is the most effective way to cure metastatic cancer. A chemotherapeutic agent targets particular cellular DNA and inhibits DNA replication and transcription by intercalation or blocking various enzymes used in DNA synthesis, such as Topoisomerase, which causes cell cycle arrest and leads to programmed cell death The discovery and development of high-potential and low-toxic anticancer drugs continue to be a tremendous challenge for medicinal chemistry.[6] The potency of chemotherapeutic agents has also improved by late-stage modification through C-H functionalization. It is noteworthy that anticancer drugs may have various fluorophores having interesting photophysical properties and thus have wide applications in the pharmaceutical industry and material sciences. Hence, synthesis and late-stage modification of heterocyclic organic compounds using different

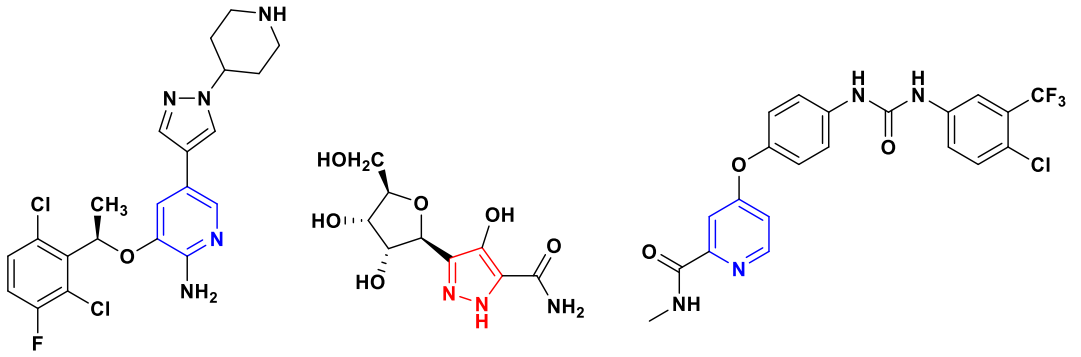

33
Crizotinib (anti-cancer)

34
Pyrazofurin (anti-cancer)

35
Sorafenib (anti-cancer)

Figure 1.1. Heterocycles based anti-cancer drugs

pharmacophores and fluorophores through various methodologies such as C-H functionalization[7], one-pot synthesis, etc., are fascinating topics and claimed constant attention from an organic community from the last decade (**Figure 1.1**).

In 2018, Jana *et al.* reported the first distinctive and easy redox-neutral methodology to synthesize dihydroisoquinoline-fused quinazolinone moiety (**3**) *via* Ru(II)-catalyzed regioselective C-H bond functionalization and subsequently intermolecular cascade hydroamination of 2-arylquinazolinone (**1**).[8] The reaction was carried out with [Ru(*p*-cymene)$_2$Cl$_2$]$_2$ in the presence of silver-based co-catalyst $AgSbF_6$ using AdCOOH as an additive in DCE. Substitution with various groups on the aryl ring of quinazolinone at different positions gave compounds in upto 90% yield **(Scheme 1.1)**. However, *para*-substituted substrates showed low compatibility compared to *ortho*- and *meta*-substituted

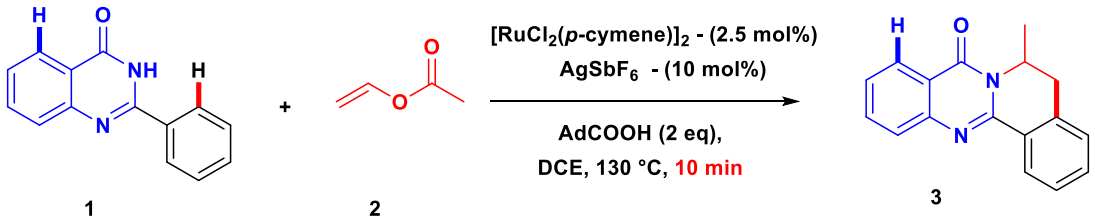

1 2 3

Scheme 1.1. Synthesize dihydroisoquinoline-fused quinazolinone

quinazolinone. In addition, several heterocyclic congeners at C-2 position also showed good compatibility to afford respective compounds in good yield. Again, the reaction was assisted using amide as a weak directing group through a nitrogen atom that formed a five-membered ruthenacycle.

Zhu and co-workers, in 2020, reported rhodium-catalyzed switchable C-H functionalization of 2-(1*H*-pyrazole-1-yl)pyridine (**4**) using internal alkynes (**5**).[9] The reaction used *N*,*N*-bidentate chelating substrates with alkynes, which gave rapid access to diverse alkenylation.

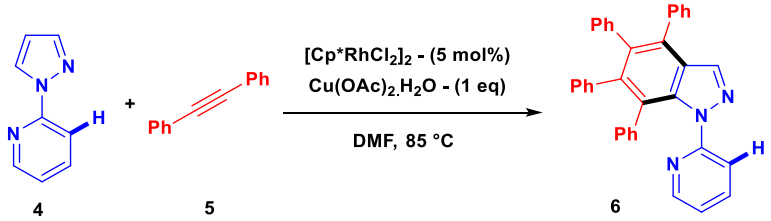

4 5 6

Scheme 1.2. Switchable C-H functionalization of 2-(1*H*-pyrazole-1-yl)pyridine

Various control experiments suggested the engrossment of a rollover mechanism. The reaction was performed using $[Cp^*RhCl_2]_2$ and $Cu(OAc)_2.H_2O$ in DMF at 85 °C for 24 h (**Scheme 1.2**). Several diarylalkynes and dialkylalkynes were employed to afford the corresponding compound (**6**) in good yield. In addition, substitutions with electron-donating and -withdrawing groups at different positions of the aromatic ring also showed satisfactory results.

In 2016 Gogoi group performed a cascade reaction of 4-hydroxycoumarins (**7**) with *in-situ* arynes using palladium catalyst for the synthesis of coumestans (**8**) in 65% to 88% yields. This approach involved C-H activation and further forming C-C and C-O bonds (**Scheme 1.3a**). After three years, they again functionalized 4-hydroxycoumarin (**7**) at the C_3 position with aryl carboxylic acids and demonstrated oxidative annulation *via* palladium catalyst for the synthesis of bis-coumarins (**9**). Various substituted bis-coumarins with broad functional group tolerance were synthesized in upto 85% yields(**Scheme 1.3b**).[10]

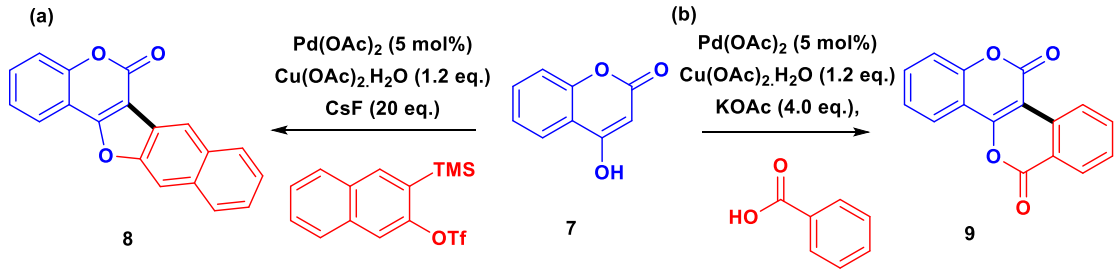

Scheme 1.3. Synthesis of coumestans and bis-coumarins

The literature was reviewed in details to find the gaps in the present study. It has been found that the following areas have not been much explored till now:

- C-H bond activation or C-H functionalization using transition metal catalysts on coumarin-based heterocyclic moieties are rare.
- The evaluation of C-H functionalized heterocyclic compounds for anti-tumor activities is rare.
- C-H activation on molecular hybrids of various heterocyclic compounds, such as coumarin, pyrazole, benzimidazole/benzothiazole, etc., has not been explored much.
- Anti-tumor activity on C-H functionalized hybrid molecules is not explained.

Keeping in view the above points, the following objectives have been designed

1. To functionalize on biological active heterocyclic moieties with C-H activation by using transition metals catalyst.
2. To synthesize and characterize hybrids of biologically active moieties, *viz.*, coumarin, pyrazole, benzimidazole, naphthalimide, indole, etc.
3. To functionalize hybrids of two pharmacophores with C-H activation using a transition metal catalyst.
4. *In vitro* evaluation of C-H functionalized compounds for anticancer activity and to develop their structure-activity relationship

Here, I have used various heterocyclic moieties such as coumarin, quinazoline, benzimidazole, pyrazole, etc., as pharmacophores and fluorophores and performed regioselective C-H functionalization using transition metal catalysts. After that, these synthesized compounds were evaluated for their anticancer activity against 60 human cancer cell lines. In addition, these compounds were also evaluated for their photophysical behavior.

2. Chapter 2: C5-H Alkenylation of Quinazolinone-Coumarin Conjugates

2.1.1. Synthesis

Various reaction parameters such as solvents, catalyst, and oxidants and their quantities were screened to establish a suitable reaction condition. Followed by intensive screening, the optimized reaction condition was $[RuCl_2(p\text{-cymene})]_2$ (2.5 mol %), $AgSbF_6$ (10 mol %), $Cu(OAc)_2.H_2O$ (1.5 equiv), and solvent (2 mL). After optimization of the feasible reaction condition, I then turned to examine the scope of this catalytic conversion by reacting 2-methyl-2-(2-oxo-2*H*-chromen-3-yl)-2,3- dihydroquinazolin-4(1*H*)-one (**1**) with various acrylates. Methyl, ethyl, and *n*-butyl acrylates (**2b-d**) reacted well with 1 to give corresponding alkenylated products up to 90% yields. On the other hand, as coumarin has significant photophysical properties, I have primarily substituted the coumarin nucleus with electron-withdrawing and -donating groups to check the reaction scope and photophysical behaviour. Initially, the electron-donating effect was investigated using a methoxy group on coumarin nucleus (**1b**) with various alkenes; the corresponding compounds were obtained in excellent yields. Similarly, electron-withdrawing groups on coumarin nuclei, such as Br, Cl, and aryl (**1c-1e**), were also investigated with same alkenes and gave the desired products (**3ca-3eg**) in 68% to 80%, shown in **Scheme 2.**

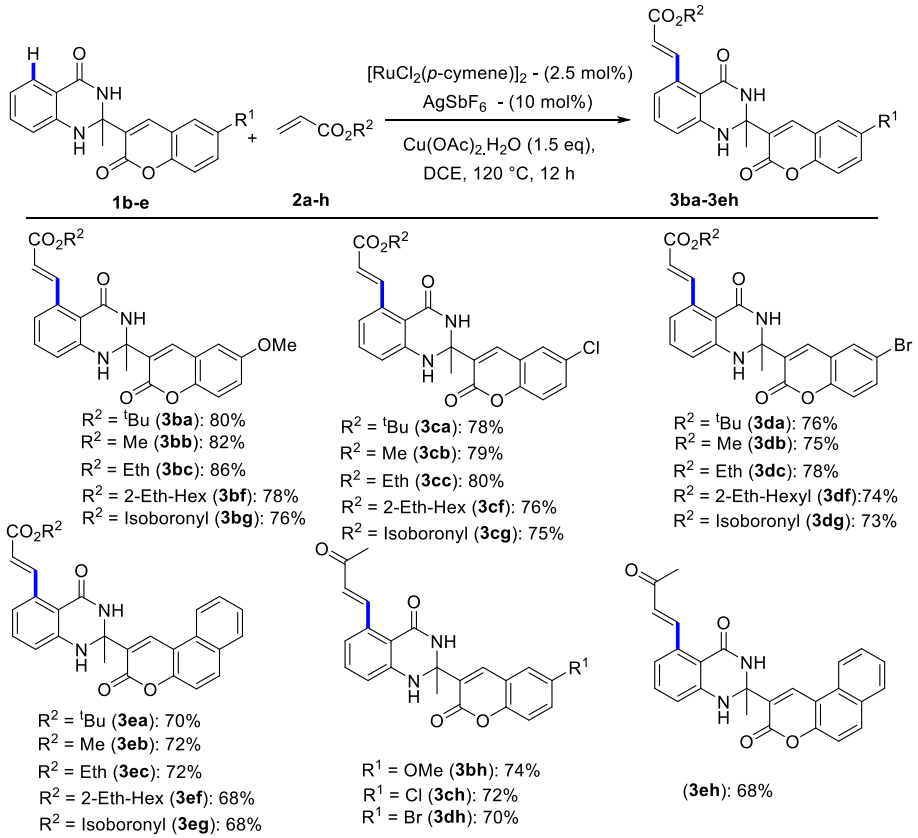

Scheme 2.1. C5-H alkenylation of quinazolinone

2.1.2. Plausible Reaction Mechanism

Based on the control experiments and literature precedent, I proposed a plausible mechanism for Ru(II) catalyzed C–5 alkenylations of **1a** based on experimental analysis, computational studies, and literature precedent

2.2. Characterization

All ^{1}H and ^{13}C NMR characterization were performed on Jeol ECS 400 NMR spectrometer, operated at 400 MHz for ^{1}H nuclei and 100 MHz for ^{13}C nuclei, taking $CDCl_3$ as the solvent and further characterized by Electrospray ionization high resolution mass spectrometry was performed on a Bruker micrOTOF spectrometer.

2.3. Photophysical Studies

Further, photophysical studies of synthesized compounds have been performed to investigate the substitution effect on the coumarin nucleus. The parent has absorption maxima at 345 nm. Compounds substituted with chloro and bromo have absorption maxima at 326 nm, while increasing π conjugation on the coumarin nucleus, compound **3eh** has an absorption band at 316 nm. These compounds have shown hypsochromic shift with electron-withdrawing groups

in the absorption band. Relative quantum yields[11] were calculated with hymecromone as standard (Φ_F = 0.74).[12] Fascinated by increased absorption and emission efficiency, I performed solvatochromic studies using **3bh** to investigate the solvent effect by recording its absorption and emission spectra in different solvents of different polarities. Notably, no solvatochromic is observed in absorption maxima, as it remains almost the same between 338 to 350 nm. However, solvent polarity significantly impacts emission maxima, ranging from 404 nm in toluene to 541 nm in methanol.

2.4. Conclusion

In summary, I have developed the first ruthenium-catalyzed regioselective C–5 alkenylation of quinazolinone-coumarin conjugates. This was accomplished using the concept of cyclometallation. This methodology has led to the synthesis of 32 novel alkenylated quinazolinone conjugates with absolute regioselectivity and up to 90% yield that allowed access to late-stage functionalization. Moreover, photophysical properties indicate that the emission is solvatochromic.

3. Chapter 3: C(sp2)-H Alkenylation of Chromeno[4,3-c]pyrazol-4-ones

3.1.1. Synthesis

Primarily, our investigation commenced with validating the optimal conditions for cascade synthesis and C–H functionalization of 1-phenyl-1*H*-chromeno[4,3-*c*]pyrazol-4-one. Next, I examined this cascade transformation's electronic effects and substrate scope. Firstly, unsubstituted and substituted phenylhydrazines **2a-l** were tested with **1a** and **3a** under optimized conditions. Substrates, substituting at *para*-position of aryl ring with bromo **2b**, chloro **2c**, methyl **2d**, fluoro **2e**, nitro **2f**, and cyano **2g** underwent cascade transformation to give respective scaffolds **5ab-5ag** in 63-86% yields (**Scheme 3.1**). Phenylhydrazines with electron-donating groups are more compatible than those with electron-withdrawing groups. Similarly, substrates having *meta*-substituted aryl ring with bromo **2h**, chloro **2i**, and nitro **2j** were also subjected to general reaction conditions and gave corresponding compounds **5ah-5aj** in 62-67% yields. Notably, *ortho*-substituted phenylhydrazine with chloro **2k** and *o,p*-dichloro **2l** gave desired compounds **5ak-5al** in 50-55% yields. At the same time, no alkenylated product was obtained on substituting methyl **2m** and ethyl **2n** groups at the *ortho*-position of phenylhydrazine. Further, substituted coumarins **1a-d** and acrylates were investigated with phenylhydrazine **2a.** Electron-rich groups such as chloro **1b**, bromo **1c**, and methoxy **1d** were more compatible for the designed transformation and yielded corresponding compounds up to 85%.

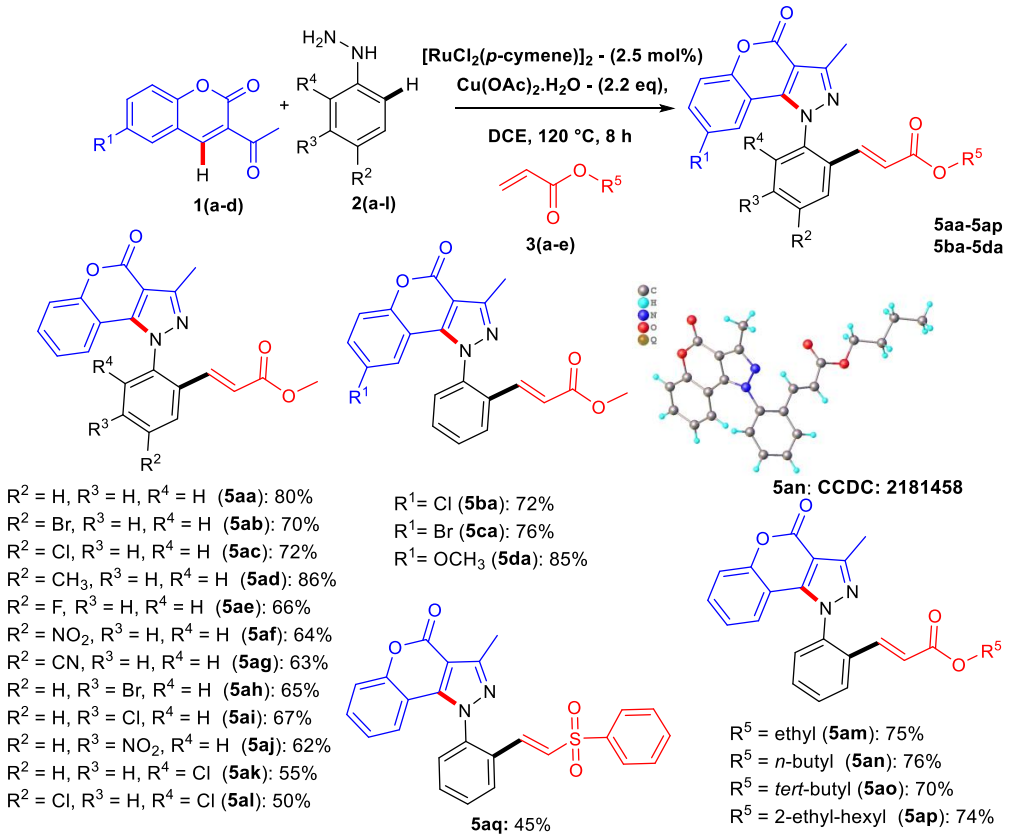

Scheme 3.1. One-pot C-H functionalization of chromeno[4,3-*c*]pyrazol-4-ones

---

3.1.2. Plausible Reaction Mechanism

I proposed a three-step domino reaction mechanism based on experimental observations and literature precedent.

3.2. Characterization

All ^{1}H and ^{13}C NMR characterization were performed on Jeol ECS 400 NMR spectrometer, operated at 400 MHz for ^{1}H nuclei and 100 MHz for ^{13}C nuclei, taking $CDCl_3$ as the solvent and further characterized by Electrospray ionization high resolution mass spectrometry was performed on a Bruker micrOTOF spectrometer.

3.3. Photophysical Studies

Several donor and acceptor groups on these scaffolds were examined to investigate the push-pull effect on chromeno[4,3-*c*]pyrazol-4-ones. On substitution, absorption maxima have no significant impact and lie in the range of 264 nm to 298 nm, while emission maxima exist in the range of 327 nm to 420 nm. In addition, I have deciphered the unknown preliminary photophysical properties of all the synthesized scaffolds and observed that quantum yield and

Stokes Shift of compounds **5aa**, **5am-5ap** differ significantly from the parental chromenopyrazolone. Fascinated by quantum yield improvement, I performed solvatochromic studies on compound **5ad**. The compound showed positive solvatochromism, and the emission maxima range from 316 nm to 408 nm in different solvents.

3.4. Conclusion

I have made significant progress in developing a step and atom economy one-pot cascade transformation to synthesize substituted 3-methyl-1-phenylchromeno[4,3-*c*]pyrazol-4(1*H*)-ones and their *in-situ* late-stage modification *via ortho* C–H alkenylation using imine as a weak directing group. I have performed photophysical studies to their unique fused π conjugation, demonstrating positive solvatochromism.

4. Chapter 4: Benzimidazole Assisted [4+2] Oxidative Annulation of 3-(1*H*-benzo[*d*]imidazol-2-yl)-2*H*-chromen-2-one

4.1. Synthesis

After optimized the reaction conditions, I explored the electronic effects and substrate scope of this [4+2] oxidative annulation. Firstly, different alkenes **2a-l** were tested with **1a** under optimized reaction conditions. Olefins, **2a-e** having ester group linkage transformed smoothly to afford corresponding scaffolds **3aa-3ae** in 70-82% yields (**Scheme 4.1**).

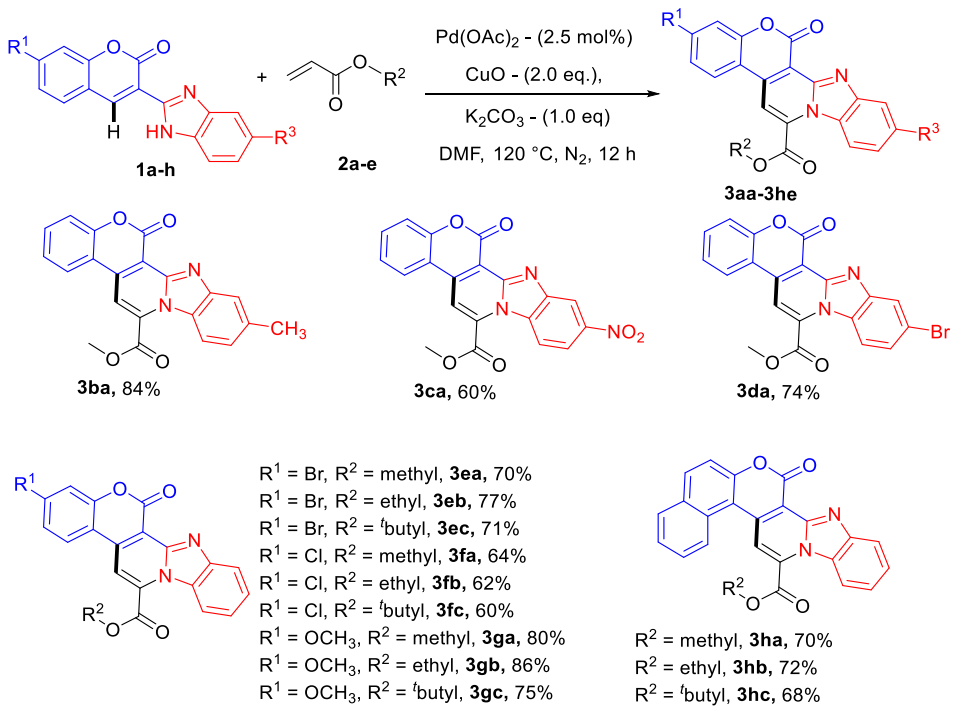

Scheme 4.1. Pd(II)-catalyzed [4+2] oxidative annulation

Further, different electron-donating and -withdrawing groups on coumarin and benzimidazole nuclei were examined, which showed excellent compatibility with present oxidative annulation. The substitution of methyl group (electron-donating) on benzimidazole aryl ring with **1b**, gave **3ba** in 84% yield. In contrast, substitution with electron-withdrawing group such as nitro in the case of **1c** gave **3ca** in 60% yield, and bromo **1d** gave **3da** in 74% yield, which indicated electron donating groups have better compatibility than electron-withdrawing groups for this annulation. Similarly, various substitutions on coumarin nuclei were also subjected to optimized conditions with the same alkenes and gave corresponding compounds in good yields.

4.1.2. Plausible Reaction Mechanism

I proposed a plausible catalytic cycle for [4+2] oxidative annulation, as shown in **Scheme 4.2**. Initially, substrate **1a** reacts with $Pd(OAc)_2$ and gives intermediate A, followed by intramolecular C-H activation of resulting Intermediate **A** and forms a five-membered palladacycle to give complex **B**. Subsequently, coordination of alkene gives complex **C** which

readily converts into seven-membered cyclic palladium complex **D** migratory insertion. Followed by reductive elimination to afford annulated compound **3aa**.

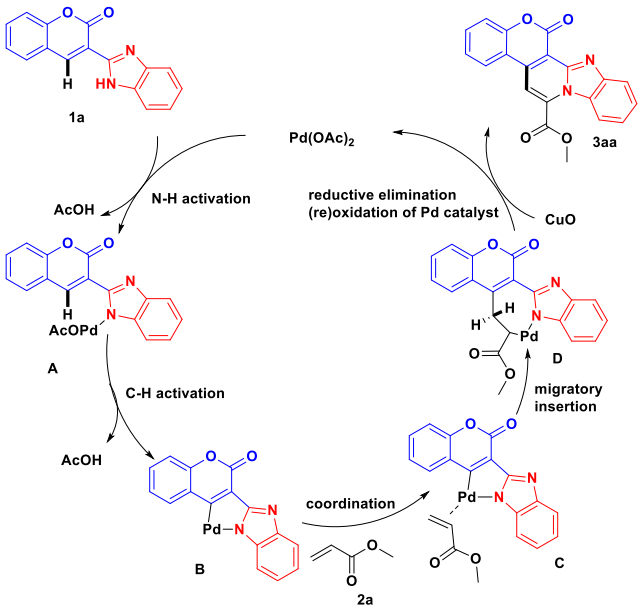

Scheme 4.2. A plausible Mechanism of oxidative annulation

4.2. Characterization

All ^{1}H and ^{13}C NMR characterization were performed on Jeol ECS 400 NMR spectrometer, operated at 400 MHz for ^{1}H nuclei and 100 MHz for ^{13}C nuclei, taking $CDCl_3$ as the solvent and further characterized by Electrospray ionization high resolution mass spectrometry was performed on a Bruker micrOTOF spectrometer.

4.3. Photophysical Studies

With these versatile annulated molecules in hand, I then turned around to decipher the photophysical properties of **3aa-3hc** by recording their UV-vis and emission spectra in MeCN. Absorption maxima on substitution have no significant effect and lie in the range of 315 nm to 340 nm. In contrast, emission maxima showed a broad range between 440 nm and 492 nm. Parent compound **3aa** showed an emission maximum at 460 nm with Stokes shift 8500 cm^{-1}, having a quantum yield of 0.40. The substitution of different alkenes on 3aa showed a bathochromic shift in emission maxima from 450 nm to 470 nm for compounds **3aa-3af**. Compound **3gb** showed emission maxima at 492 nm with a higher quantum yield (0.70) than other derivatives. Relative quantum yields[14] were determined with reference to hymecromone ($\Phi_F = 0.74$). Fascinated by bathochromic shift, I investigated the solvent effect of compound **3gb** by recording their emission maxima in different polar and non-polar solvents. Interestingly, compound **3gb** showed positive emission solvatochromism in the range from 410 nm in toluene to 550 nm in methanol.

4.4. Conclusion

Here, I have developed a protocol to access polycyclic aromatic hydrocarbons of imidazo[1,2-*a*]chromeno[3,4-*c*]pyridine by palladium-catalyzed oxidative annulation of 3-(1*H*-benzo[*d*]imidazol-2-yl)-2*H*-chromen-2-one with alkenes using benzimidazole as a directing group. This transformation involves C4-H, N-H functionalization, and cyclization of the coumarin-benzimidazole hybrids. Owing to the unique significance of polycyclic aromatic hydrocarbons, their photophysical properties have been well elucidated with improved quantum yields.

5. Chapter 5: Evaluation of Anticancer Activity of C-H Functionalized Compounds

5.1. Cytotoxicity Studies

All C-H functionalized compounds have been screened for cytotoxicity against NCI 60 human cancer cell lines. It was found that conjugates of coumarin-quinazolinone are the most active compounds of the library, with the range of growth inhibition -66 to 99.17. The

compound having bromo substitution on the coumarin nucleus at the C5 position and functionalized by methyl vinyl ketone has been selected for five dose assays. This compound was most sensitive against a full panel of leukemia and breast cancer cell lines.

5.2. DNA Binding Studies

For a qualitative determination of the interaction between the compound and ct-DNA, the binding constant (K_b) was calculated using the Benesi-Hildebrand equation and found to be 5.51×10^4 M^{-1}. Fluorescence emission spectroscopy confirmed the quenching mechanism in compound **7dh (from chapter 2)** and ct-DNA interactions. Competitive displacement assay for the ethidium bromide also suggested that compound (*E*)-2-(6-bromo-2-oxo-2*H*-chromen-3-yl)-2-methyl-5-(3-oxobut-1-en-1-yl)-2,3-dihydroquinazolin-4(1*H*)-one (**7dh)** interacted through partial intercalation.

5.3. Protein Binding Studies

HSA binding studies: UV-vis absorption spectroscopy gave strong interaction and the binding constant (K_b) was calculated to be 2.26×10^5 M^{-1} using the Benesi-Hildebrand plot. Results of fluorescence emission spectroscopy revealed that the binding process was static, spontaneous, and exothermic in nature. Synchronous fluorescence spectroscopic studies revealed that Trp residue contribute equally to the quenching of the HSA emission where HSA undergoes conformational changes around Trp residues upon binding to compound **7dh**.

5.4. Conclusion

I have successfully screened C-H functionalized compounds for their anticancer activity against NCI 60-human cancer cell lines. Compounds of coumarin-quinazolinone conjugates showed better activity and **7dh** was also used for five doses against all 60 cell lines. Further, various preliminary interaction studies were performed using compound **7dh** with ct-DNA and HSA to examine the mode of action. Based on these interaction studies, compound **7dh** was found to intercalate with ct-DNA and showed cytotoxicity against leukemia cancer cell lines.

6. References

1. Ferro, A., Peleteiro, B., Malvezzi, M., Bosetti, C., Bertuccio, P., Levi, F., Negri, E., La Vecchia, C., and Lunet, N. *Eur. J. Cancer.*, **2014**, *50*, 1330-1344.

2. Lilja, H., Vickers, A. J., Sjoberg, D., Johansson, R., Granfors, T., Johansson, M., Pettersson, K., Scardino, P. T., Hallmans, G., and Stattin, P. *J. Clin. Oncol*., **2014**, *32*, 5081-5082.

3. Collins, I., and Workman, P. *Nat. Chem. Biol.*, **2006**, *2***,** 689-700.

4. Siegel, R. L., Miller, K. D., and Jemal. *CA Cancer. J. Clin*., **2016**, *66*, 7-30.

5. Alexander, J. L. *Nat. Rev. Gastroenterol. Hepatol* **2017,** *14* (6), 356-365.

6. Hopkins, A. L. *Nat. Chemi. Biol*. **2008,** *4* (11), 682-690.

7. Guillemard, L., Kaplaneris, N., Ackermann, L., and Johansson, M.J. *Nat.Rev Chem*. **2021**, *5*, 522–545.

8. Bairy, G., Das, S., Begam, H.M., and Jana, R. *Org. Lett*. **2018**, *20*, 7107-7112.

9. Wu, S., Wang, Z., Ma, D., Chen, C., and Zhu, B. *Org. Chem. Front.*, **2020**, *7*, 1158-1163.

10. (a) Neog, K., Borah, A., and Gogoi, P. *J. Org. Chem.*, **2016**, *81*, 11971-11977. (b) Sharma, K., Neog, K., and Gogoi, P. *Org. Lett.*, **2019**, *22*, 73-77.

11. Chen, S. Q., Li, X. R., Li, C. J., Fan, J., Liu, Z. W., and Shi, X. Y. *Org. Lett*. **2020**, *22*, 259-1264.

12. Götzinger, A. C., Theßeling, F. A., Hoppe, C., and Müller, T. J. *J. Org. Chem.*, **2016**, *81*, 10328-10338.

List of Publications

- Singla, D., and Paul, K. Ru(II)-catalyzed regioselective C(5)-H functionalization of Quinazolinone-coumarin conjugates: synthesis and photophysical studies. *J. Org. Chem.* 2022, **87**, 10673
- Singla, D., and Paul, K. One-Pot Cascade Access to Ru(II)-Catalyzed Regioselective C(sp^2)-H Activation/Alkenylation of chromeno[4,3-*c*]pyrazol-4-ones and their Emission Solvatochromic Studies. *J. Org. Chem.* 2022, **87**, 16436-16448
- Singla, D., Luxami, V., and Paul, K. Eosin-Y mediated C-H functionalization: C-S, C-C bond formation. *Org. Chem. Front.*, 2023, **10**, 237-267
- Singla, D., and Paul, K. Pd(II)-Catalyzed Benzimidazole Assisted [4+2] Oxidative Annulation of 3-(1*H*-benzo[*d*]imidazol-2-yl)-2*H*-chromen-2-one: Access to imidazo[1,2-*a*]chromeno[3,4-*c*]pyridine. (Communicated)

Other publication

- Palta, A., Singla, D., Paul, K., and Luxami, V. Design and Synthesis of Fluorescent Reagent for Selective Amine recoginisation in Aqueous Medium: A Chemo Sensing Ensemble for Dopamine. (Communicated)

Conferences and Workshops

- Dinesh Singla, Chemical Science symposium (2022): Sustainable synthesis and catalysis: Organised by the Royal Society of Chemistry at Thomas Graham House, Milton Road Science Park, Cambridge, CB4 0WF, UK
- Dinesh Singla, International Symposium (2022) on "Recent advances in Self assembled Materials and Supramolecular Chemistry." at Guru Nanak Dev University (GNDU), Amritsar, Punjab. (Best Poster award by the American Chemical Society (ACS) at International Symposium 2022)
- Dinesh Singla, DST-SERB Sponsored Workshop on "Computational Drug Design using Molecular Docking and Virtual Screening" held at Thapar Institute of Engineering and Technology, Patiala on 27-29 April, **2018**